DTIC

GEOMORPHOLOGICAL CHANNEL AND BANK ASSESSMENT OF THE MISSOURI RIVER - FORT PECK DAM TO PONCA STATE PARK

Final Technical Report

By

Chris Bromley, Colin Thorne, and Chester Watson

September 2000

EUROPEAN RESEARCH OFFICE OF THE U.S. ARMY
London, England

Contract No.N68171-99-M-6313

Requisition No. W90C2K-8799-EN01

Department of Geography
University of Nottingham
University Park
Nottingham
NG7 2RD
UK

CONTENTS

BACKGROUND

In July 1999 the US Army Research Office (London) commissioned the University of Nottingham, UK to support and assist the staff of the US Army Corps of Engineers, Waterways Experiment Station (now ERDC) in studying plans to undertake stabilisation works along the Missouri River to alleviate problems of bank erosion. These works are authorised under Section 33 of the Water Resources Development Act (1988) and may include both structural and non-structural measures. In Spring 2000, the original contract was modified to support additional work concentrated on comparison of bed, bank and bar sediment size distributions.

In selecting the engineering approaches and designs for bank stabilisation measures, design engineers require information on the cumulative effects of stabilisation measures on channel form, sedimentary features and the ecological habitats that they provide to fish and wildlife. Of particular concern are the possible impacts of bank stabilisation works on medial sand bars in the Missouri River and the nesting sites that these bars provide for the Least Tern and the Piped Plover.

This report details findings of the project performed jointly by the University of Nottingham and Colorado State University. These findings will feed into Environmental Impact Studies for the proposed works which are being conducted by the US Army Corps of Engineers through providing information on the morphology and sediment dynamics of the channel. The information contained herein will also form the basis for prediction of future morphological response of the system by river engineers and managers with USACE ERDC and District staff.

The project involved conducting field reconnaissance and detailed channel surveys, executing morphological assessments and making predictions of morphological response. The report deals with each of these aspects in turn.

TECHNICAL REPORT

I Missouri River Field Reconnaissance

The PI, co-PI and a team from WES spent a five-day period reconnoitring the four study reaches in order to become familiar with the banks and the in-channel morphology of the river. As a result of this, a short report recommending an approach to the study was written by the PI and sent to staff at WES. It was recommended that geomorphologically distinct sub-reaches be identified within each of the four main reaches, based on their geology, planform sinuosity and degree of stability or instability, be this natural or artificial. The Brice channel classification system for categorising the degree of channel sinuosity was advocated for this purpose. Identification of these sub-reaches was recommended in order to supply the basis for determination of channel response to any future stabilisation works.

Another product of this reconnaissance trip was a series of thoroughly annotated aerial photographs showing the heights and extent of eroding areas of bank line, the types of terrace deposits that were being eroded and the dominant types of failure mechanisms causing the erosion. These notes were later used in a preliminary assessment of bank stability.

II Study Approach and Report Structure

The USACE has identified four reaches of the Missouri River, covering a total of 362 miles, in Montana, North Dakota, South Dakota and Nebraska that required investigation. These reaches are from Fort Peck Dam to the Yellowstone River (189 miles), Garrison Dam to Lake Oahe (79 miles), Fort Randall Dam to the Niobrara River (36 miles) and Gavins Point Dam to Ponca (58 miles). The dams on the four study reaches were closed in 1937, 1953, 1952 and 1955, respectively. Dam closure alters the flow of sediment and water downstream of the dam in a dramatic fashion and in so doing initiates a system wide catalogue of geomorphological changes.

The strategy for detailed field studies, sampling programs and morphological analyses was established at a joint meeting between project staff and USACE staff at Vicksburg in September 1999. The meeting built on the results of the river reconnaissance to identify the precise geomorphological issues that should be addressed. These included the relationship between bar and island location and the location of the sediment supply and establishing the connectivity between the two; the relationships of bar and island evolution to channel geometry, tributary inputs and the presence or absence of bank stabilisation works; and what sections of the main reaches are aggradational, degradational or transitionary and at what rates are these processes progressing.

It was decided that a combined quantitative-qualitative approach to predicting future channel morphology should be taken, since it was felt that either one on their own would be insufficient to provide all the required information. For example, numerical models and a total sediment budget would allow the effect of bank stabilisation on sediment transport to be ascertained and thus allow inferences about the resultant changes in morphology to be made. Using aerial photographs from differing time periods would enable the historical channel changes to be identified qualitatively and, in digital form, would also provide a basis for determining rates of erosion and deposition. The main methodological components of the geomorphic assessment were identified as:

- literature review;
- review of archive data and past reports for the Upper Missouri River concerning bank erosion, aggradation/degradation and sedimentological studies;
- specific gage analysis to document historical changes in water elevations for selected discharges at gauging stations along the mainstem and tributaries;
- historical bank erosion analysis;
- particle size analysis of field samples.

Finally, the field sampling program to support the particle size analysis was designed. Because the reconnaissance trip showed that much of the bank material was of a similar type, it was decided to sample the banks along the full length of each of the main reaches. This would produce full reach coverage at density sufficient to provide a good representation of the bank materials present. Only banks that were actively eroding over distances greater than 500 feet were sampled since these are the only ones potentially contributing significantly to bar and island formation. At each of the

bank sampling locations, the individual facies were to be sampled separately in order to identify the grade distributions of the various materials. The separate bar and island facies were also to be sampled based on several criteria such as sediment type; vegetation type; their relative elevation above the water level; whether they were downstream of tributaries, eroding banks or stabilised banks; whether they were in aggradational or degradational areas; and whether they were active species habitat. In so doing, bars and islands in all the potentially distinct geomorphological sub-reaches were designated as sample sites.

The structure of this report reflects the main study topics and consists of a series of self-contained elements dealing with:

- Part III Literature Review;
- Part IV Specific Gauge Analysis;
- Part V Historical Bank Erosion Analysis;
- Part VI Geomorphic Reach Classification
- Part VII Particle Size Analysis of Field Samples.

III Literature Review

Introduction

Under Section 33 of the Water Resources Development Act (1988), the U.S. Army Corps of Engineers (USACE) is authorised to undertake bank stabilisation works along the Missouri River in order to alleviate problems of bank erosion. These works may utilise both structural and non-structural measures. The projects constructed under this authority, as well as other non-Federal stabilisation efforts along the river, have created concern about the overall cumulative impacts of bank stabilisation on fish and wildlife resources along the Upper Missouri River. The USACE Omaha District is currently conducting a range of environmental impact assessments (EIAs) for the Section 33 Programme.

One principle component of the EIAs is a determination of what geomorphological impacts any further bank stabilisation works will have on the habitats within the Upper Missouri. More specifically, this study is looking to establish how the sediment budget and channel morphology will change in response to reduced sediment input from eroding bank sources as a result of any future stabilisation works. The investigation is looking at the four open water reaches of the Upper Missouri River in Montana, North Dakota, South Dakota and Nebraska. These are from Fort Peck Dam to the Yellowstone River (189 miles), Garrison Dam to Lake Oahe (79 miles), Fort Randall Dam to the Niobrara River (36 miles) and Gavins Point Dam to Ponca (58 miles).

The effect of dams

Whenever a dam is built on a river it initiates a wide ranging and complex series of geomorphological changes to the downstream river system and these changes have been extensively documented in the literature (e.g. Rasid, 1977; Petts, 1979; Petts and Lewin, 1979; Petts, 1980; Petts, 1982; Biedenharn, 1983; Williams and Wolman, 1984; Chien, 1985; Xu, 1990; Sherrard and Erskine, 1991; Sear, 1995). The primary effects of dams are to reduce the peak discharges and the sediment supply. Reducing the peak discharges tends to induce greater bank stability by deposition of sediment at the channel margins to form berms. The channel also adopts a smaller size due to the smaller channel forming discharge and this has the effect of lowering the base level of any tributaries to the main channel. As a result these channels begin to degrade as a knickzone migrates upstream and the supply of sediment to the main channel increases. However, channel boundary materials allowing the tendency towards bank stability is frequently superseded by the release of sediment-starved water from the reservoir, which causes much bed degradation and thus leads to widespread bank erosion by mass wasting processes. Degradation of the bed also lowers the tributary base level and thus reinforces their degradation and this, along with the sediment from the eroding banks, eventually leads to aggradation further downstream (Watson *et al*, 1999). In his work on the Hanjiang River in China, Xu (1997) divided the river downstream from a dam on a heavily sediment-laden river into degradational, transitional and aggradational reaches, thus highlighting the spatial distribution of the aforementioned processes. As the zone of degradation migrates downstream away

from the dam, the boundaries between these three zones also migrate downstream until the river has once again re-established a position of dynamic equilibrium.

Although it is not possible to accurately predict precisely how a river system will respond to the presence of a dam due to the complex nature of the interactions involved (Watson *et al*, 1999), a considerable number of reports detailing the changes that have occurred in the four study reaches of the Upper Missouri River have been written or commissioned by the USACE. Some, such as McCombs-Knutson Associates (1984); River Pro's (1985, 1986); Darby and Thorne (1996); HDR Engineering (1998); Simons, *et al* (1999) look at bank erosion issues, whilst Pokrefke, *et al* (1998) undertook a more wide ranging assessment of channel degradation in response to the presence of the dams, and the implications of these effects for a change in operating regime of the four dams. Other reports examine the changing downstream trends in channel variables such as bed material grain size distributions, average bed elevations, thalweg elevations, water surface profiles, stage trends and channel geometry, in order to elucidate the impact of each of the dams (USACE, 1986; Dangberg *et al*, 1988a, 1988b; USAEDNMRR, 1994; Midwest International, 1997). As expected, these parameters all show that degradation is most intense immediately downstream from the dam and, in the Garrison and Gavins Point Reaches, continues throughout the full extent of the reaches. The Fort Peck Reach has a zone of degradation and aggradation (USACE, 1994a), whilst in the Fort Randall Reach these two zones are separated by a transitional area.

One of the few reports to try and predict future channel changes is that of WEST Consultants (1998). Using HEC-2 and HEC-6 modelling they project average bed elevations and water surface elevations for the Fort Randall Reach from 1995 to 2045 under low, medium and high flow scenarios. The results show that degradation continues to occur immediately downstream of the dam whilst aggradation continues in the area around the Niobrara River confluence. Both the degradation and the aggradation are most intensive under the high flow scenario. The aggradation at the downstream end of this reach is largely a function of the delta that has been formed at the confluence of the Missouri and Niobrara Rivers, due to the Missouri's inability to remove all the sediment deposited by the Niobrara. Because of the problems caused by this excessive aggradation, the area upstream and downstream of the delta along the Missouri River and also upstream along the Niobrara River has been extensively studied (Resource Consultants and Engineers, 1992a, 1992b; Resource Consultants and Engineers, 1993; Resource Consultants and Engineers and Boyle Engineering, 1993; USACE, 1994b; USACE, 1997).

Mid-channel bars and islands

There is a large body of literature relating to mid-channel bars and islands, much of which is in relation to gravel-bed, braided rivers (e.g. Smith, 1974; Hein and Walker, 1977; Ashmore, 1982, 1991, 1993; Church and Jones, 1982; Fujita, 1989; Brierley, 1991; Bridge, 1993). Nevertheless, it is still relevant to this study, despite the Upper Missouri having a straight to meandering planform and having a high proportion of sand in its bed and banks. Hooke (1986) in her study of the meandering River Dane, whose sedimentology ranges from sand to cobbles, states that despite the channel not being truly braided the development and sedimentology of the medial bars is comparable to that of individual braid bars. Germanoski and Schumm (1993) note that

observations of bar-forming processes in sand and gravel-bed channels indicate that both form and processes in the flume and in natural braided rivers, of wide-ranging size, are kinematically and geometrically similar.

One of the classic papers on the development of a central channel bar is that of Leopold and Wolman (1957). Based on observations of both natural rivers and flume studies they found that initially, a short submerged central bar is deposited during a high flow. The head of the bar is composed of the coarse fraction of the bedload that is caused to accumulate by some local condition. As the water depth over the bar decreases the velocity stays the same or increases and this leads to finer particles moving over the top of the bar and depositing on its downstream end. Once the bar has reached a certain size the anabranches become unstable and begin to cut laterally into the riverbank. The anabranches also deepen and this may cause the bar to emerge as a subaerial bar or island. The above process may repeat itself in the anabranches and thus lead to the development of a braided pattern. As flow velocities decrease on the insides of the original anabranches the bar may grow laterally. If and when vegetation becomes established on the exposed bar, this will promote more deposition of fines and, in turn, development of more vegetation. Ultimately this leads to the development of a stable island. Coleman (1969) identified a very similar process of braid bar development in the Brahmaputra River, whilst Thorne, *et al* (1993) state that islands in the Brahmaputra are built by the amalgamation of groups of braid bars. This latter observation is supported by the flume work of Germanoski and Schumm (1993), who showed that braid bar size increases in degrading gravel-bed streams due to incision of the main channel, the drying out of the smaller anabranches between the braid bars and the subsequent coalescence of these bars.

Lane (1995) provides a more wide-ranging consideration of bar development in a braided system and identifies five mechanisms, which are not mutually exclusive, of formation. The first, the deposition of a central bar, is as described by Leopold and Wolman, but Lane goes one step further and states that deposition is induced at the local scale by one or a combination of decreasing discharge, increased upstream sediment inputs and variations in channel geometry. Reach-scale variations in channel geometry can also result in the second method of formation of a central braid bar: a transverse bar conversion. When the ratio of water depth to D_{90} is greater than 2-3, the pools at sites of flow convergence are likely to scour. If flow divergence, and therefore velocity reduction, occurs further downstream then some of the scoured material may be deposited as a lobe, which can trap further bedload and grow to a sufficient size to initiate bank erosion. These are both examples of depositional bar building processes. A key erosional process is chute cutoff, which requires a pre-existing set of one or more alternate bars. When flow is diverted across one of these bars, the sudden increase in velocity as it moves off the end of the bar can increase the value of bed shear stress to above its critical value, which causes headward incision. Eventually this completely separates the bar from the bank. Multiple dissections of a lobe are caused either by a highly sediment deficient flow moving over the bar, or the erosion of a previously aggraded bar head by a low flow which can still generate sufficient shear stress to do so. The final mechanism of bar formation is avulsion. This can be triggered by ponding behind a bar head, bank erosion in curved anabranches or aggradation and eventual blocking of a single anabranch.

Ashworth (1996) conducted a series of flume studies to investigate the formation of mid-channel bars immediately downstream from the junction between two tributary channels. He proposed the following five stage model for bar development: (1) development of confluence scour with flow convergence and maximum velocity in the channel centre; (2) exceedance of the local transport capacity and initial stalling of coarse sediment in the channel thalweg downstream of the scour; (3) bar growth through entrapment of all sizes of bedload; (4) change from velocity maximum to minimum and flow convergence to divergence when the bar height is between 40 per cent and 60 per cent of the thalweg depth, but with a mean of around 55% per cent; (5) broadening of the bar top platform, a drop in local competence and bankwards migration of the two distributaries whose cross-section and velocity remains approximately constant.

Despite all the research that has been undertaken into the development of the mid-channel bar/braided stream pattern two key areas of uncertainty still remain. Firstly, what initiates bar deposition and, secondly, what is the source of the material that builds the bars? Various suggestions have been put forward to answer the first point. Leopold and Wolman (1957) simply stated that the coarse fraction of the bedload was deposited in mid-channel at a location where the local flow competence was insufficient to transport it. Ashmore (1991, 1993) suggests that the initial deposition of material is due to the slowing down of a thin bedload sheet, possibly only one grain thick, which has been transported downstream as a discrete morphological unit. Ashworth (1996), on the other hand, considers local exceedance of the transport capacity and sediment accumulation in the channel centre by strongly convergent flows, to be a more likely cause of the initial deposition. In his flume experiments, exceedance of the transport capacity was caused by a rapid increase in sediment supply from scour at the junction between two artificially stabilised tributary channels at the head of the flume. Both Ashworth (1996) and Davoren and Mosley (1986) consider this confluence-diffluence unit to be of fundamental importance in the building of a mid-channel bar. Hooke (1986), in her work on the River Dane, states that the initial deposition is of coarse material on a riffle and may be caused by reversals of velocity and shear stress in pools and riffles as flows increase.

The second question is equally problematical to answer. The only papers uncovered for this study that links the sediments within a mid-channel bar directly to their source are those of Xu (1996, 1997). In his study of the middle Hanjiang River, a sand-bed, unstable, braided channel with a width:depth ratio of 209 to 239, he identified 20 minerals found in sediment samples from the channel. He then plotted the percentage of each mineral found in the mid-channel bar material against the percentage found in the three possible sources: the banks, the bed of the Hanjiang River upstream of the bars and an upstream tributary, and found that the banks supplied the majority of the bar materials. The correlation coefficient for the bar-bank plot was 0.94, whilst those for the bar-bed and bar-tributary plots were 0.89 and 0.51 respectively. Based on these plots, Xu used the following index to determine the degree of importance of each mineral source:

$$I = \sum(M_{s,i} - M_{bar,i})^2$$

Where $M_{bar,i}$ is the percentage of the ith mineral in the bars, and $M_{s,i}$ the percentage of the same mineral in one of the three material sources. The smaller the I value the

larger the contribution of the material source to bar formation. As calculated for the bank, the bed of the Hanjiang River and the tributary, the I values are 73.83, 336.37 and 984.58 respectively, thus showing even more conclusively that bank material is the major source of material for mid-channel bar building in the Hanjiang River.

Although these results appear conclusive for the middle Hanjiang River, the important question to ask is to what extent are they representative of all other rivers that contain mid-channel bars or a braided planform? Carson and Griffiths (1987), in their work on gravel-bed rivers, state that most braid-bar material comes from bank erosion and bartail trimmings as opposed to bed scour, whilst Hooke (1986) states that the major cause of mid-channel bar development on the River Dane is the rapid erosion of low resistance banks in steep sections and in bends. She goes on to say that mid-channel depositions from other causes, e.g. tributary inputs or due to a channel obstruction, can usually be identified due to differences in bar morphology, sedimentology and development sequence. Other than these papers, however, no further reference to this issue has been found in the literature.

A further question that arises from the previous two, and for which no specific mention has been found in the literature, relates to the source of the material that is deposited at the very beginning of bar development. The flume studies of Ashworth (1996) imply strongly that the initial deposition of material downstream of the confluence of the two tributaries, is of material scoured from the bed at this confluence. Hooke (1986) also states that scoured bed material is generally not transported very far downstream from the point of scour before being deposited. If this is the case, and assuming that bank material does provide the bulk of the material in the bar, then the contribution of the scoured bed material is just as important as the bank material in the formation of a mid-channel bar.

Bank stabilisation and sediment supply

One final area of importance to consider for this study, and unfortunately one where literature again appears to be scarce, is the effect that any further bank stabilisation measures will have on the sediment supply to the channel and, hence, how this will affect the bar and island morphology. This consideration becomes especially important for the Upper Missouri River if it is established that the bars and islands are composed primarily of material from eroding banks. Pokrefke, *et al* (1998) undertook to predict how any future increases in bank stabilisation would affect erosion rates in the four reaches. For the Fort Peck, Garrison and Fort Randall reaches they found that an exponential relationship exists between increasing amounts of bank stabilisation and decreasing rates of bank erosion, whilst in the Gavins Point Reach this relationship is linear. In part this is due to the fact that the first three reaches are much closer to a position of dynamic equilibrium than the Gavins Point Reach and so are stabilising naturally anyway. In a famous series of laboratory flume experiments, Friedkin (1945) investigated the effects of bank stabilisation on a meandering sand channel. In one experiment he stabilised three meander bends in the middle of a meandering section of channel, and observed the development of a mid-channel bar in the crossing after the first unstabilised bend downstream of the three stabilised ones. This indicates that bedload from above the stabilised reach passed straight through the three bends and deposited downstream of them as soon as the hydraulic conditions once again allowed this.

References

Ashmore, P.E. (1982), Laboratory modelling of gravel, braided stream morphology, *Earth Surface Processes and Landforms*, 7, 201-225.

Ashmore, P.E. (1991), How do gravel-bed rivers braid?, *Canadian Journal of Earth Sciences*, 28, 326-341.

Ashmore, P.E. (1993), Anabranch confluence kinetics and sedimentation processes in gravel-braided streams. In Best, J.L. and Bristow, C.S. (eds), *Braided Rivers*, Geological Society Special Publication No. 75, 129-146.

Ashworth, P.J. (1996), Mid-channel bar growth and its relationship to local flow strength and direction, *Earth Surface Processes and Landforms*, 21(2), 103-123.

Biedenharn, D.S. (1983), Channel response on the Little Tallahatchie River downstream of Sardis Dam, *Proceedings of the Rivers 1983 Conference*, ASCE, New Orleans, LA.

Bridge, J.S. (1993), The interaction between channel geometry, water flow, sediment transport and deposition in braided rivers. In Best, J.L. and Bristow, C.S. (eds), *Braided Rivers*, Geological Society Special Publication No. 75, 13-71.

Brierley,G.J. (1991), Bar sedimentology of the squamish river, British Columbia - definition and application of morphostratigraphic units, *Journal of Sedimentary Petrology*, 61(2), 211-225.

Chien, N. (1985), Changes in river regime after the construction of upstream reservoirs, *Earth Surface Processes and Landforms*, 10, 143-160.

Carson, M.A. and Griffiths, G.A. (1987), Bedload transport in gravel channels, *Journal of Hydrology (NZ)*, 26, 1-151.

Church, M. and Jones, D. (1982), Channel bars in gravel-bed rivers. In Hey, R.D., Bathurst, J.C. and Thorne, C.R. (eds), *Gravel-bed Rivers*, Wiley, Chichester, 291-324.

Colemen (1969), Brahmaputra River: channel processes and sedimentation, *Sedimentary Geology*, 3, 129-239.

Dangberg, D. & Assoc. and River Pro's (1988a), Missouri River, Fort Peck Dam: Downstream Degradation/Aggradation and Sediment Trends Study. USACE, Omaha District.

Dangberg, D. & Assoc. and River Pro's (1988b), Missouri River: Fort Randall Dam – Downstream degradation/aggradation and sediment trends study. USACE Omaha District

Darby, S.E. and Thorne, C.R. (1996), Bank stability analysis for the upper Missouri River. Unpublished report submitted to US Army Engineers Waterways Experiment Station, Vicksburg, MS.

Davoren, A. and Mosley, M.P. (1986), Observations of bedload movement, bar development and sediment supply in the braided Ohau River, *Earth Surface Processes and Landforms*, 11, 643-652.

Friedkin, J.F. (1945), A Laboratory Study of the Meandering of Alluvial Rivers, Waterways Experiment Station, U.S. Army Corps of Engineers.

Fujita, Y. (1989), Bar and channel formation in braided streams. In Ikeda, S. and Parker, G. (eds), *River Meandering*, American Geophysical Union, Water Resources Monograph 12, 417-462.

Germanoski, D. and Schumm, S.A.(1993), Changes in braided river morphology resulting from aggradation and degradation, *Journal of Geology*, 101(4) 451-466.

HDR Engineering (1998), Missouri River Streambank Erosion Assessment – Fort Randall Dam to the Niobrara River. USACE, Omaha District.

Hein, F.J. and Walker, R.G. (1977), Bar evolution and development of stratification in the gravelly, braided, Kicking Horse River, British Columbia, *Canadian Journal of Earth Sciences*, 14(4), 562-570.

Hooke, J.M. (1986), The significance of mid-channel bars in an active meandering river, *Sedimentology*, 33(6), 839-850.

Lane, S. (1995), The dynamics of dynamic river channels, *Geography*, 80(2), 147-162.

Leopold, L.B. and Wolman, M.G. (1957), River channel patterns – braided, meandering and straight. *U.S. Geological Survey Professional Paper* 422-H, 84pp.

McCombs-Knutson Associates (1984), Missouri River Bank Erosion Study: Fort Peck Dam to the Yellowstone River, July 1975 to August 1983. USACE, Omaha District.

Midwest International, Inc. (1997), Fort Peck Project, Montana: Downstream Channel and Sediment Trends Study. USACE, Omaha District.

Petts, G.E. (1979), Complex response of river channel morphology subsequent to reservoir construction, *Progress in Physical Geography*, 3, 329-362.

Petts, G.E. (1980), Morphological changes of river channels consequent upon headwater impoundment, *Journal of the Institute of Water Engineers and Scientists*, 34, 374-382.

Petts, G.E. (1982), Channel changes in regulated rivers. In Adlam, B.H., Fenn, C.R. and Morris, L. (eds), *Papers in Earth Studies*, Norwich, Geobooks, pp.117-143.

Petts, G.E. and Lewin J. (1979), Physical effects of reservoirs on river systems. In Hollis. G.E. (ed) *Man's impact on the hydrological cycle in the United Kingdom*, 79-92.

Pokrefke, T.J., Abraham, D.A., Hoffman, P.H., Thomas, W.A., Darby, S.E. and Thorne, C.R. (1998), Cumulative Erosion Impacts Analysis for the Missouri River Master Water Control Manual Review and Update Study, Technical Report CHL-98-7, USACE.

Rasid, H. (1977), The effects of regime regulation by the Gardner Dam on downstream geomorphic processes in the South Saskatchewan River, *Canadian Geographer*, 23, 140-158.

Resource Consultants and Engineers, (1992a), needs full reference

Resource Consultants and Engineers, (1992b), needs full reference

Resource Consultants and Engineers, (1993), needs full reference

Resource Consultants and Engineers and Boyle Engineering, (1993), needs full reference

River Pro's (1985), Missouri River Bank Erosion Study: Fort Randall Dam to the Niobrara River. USACE, Omaha District.

River Pro's (1986), Missouri National Recreational River, Gavins Point Dam to Ponca, Nebraska: Streambank erosion rate study, April 1978 to August 1985. USACE, Omaha District.

Sear, D.A. (1995), Morphological and sedimentological changes in a gravel-bed river following 12 years of flow regulation for hydropower, *Regulated Rivers: Research and Management*, 10, 247-264.

Sherrard, J.J. and Erskine, W.D. (1991), Complex response of sand bed streams to upstream impoundment, *Regulated Rivers: Research and Management*, 6, 53-70.

Simon, A., Shields, F.D., Ettema, R., Alonso, C., Garsjo, M.M., Curini, A. and Steffen, L. (1999), Channel Erosion on the Missouri River, Montana, between Fort Peck Dam and the North Dakota Border, USDA.

Smith, N.D. (1974), Sedimentology and bar formation in the upper Kicking Horse River, a braided meltwater system, *Journal of Geology*, 82, 205-223.

Thorne, C.R., Russell, A.P.G. and Alam, M.K. (1993), Planform pattern and channel evolution of the Brahmaputra River, Bangladesh. In Best, J.L. and Bristow, C.S. (eds), *Braided Rivers*, Geological Society Special Publication No. 75, 257-276.

USACE (1986), Missouri River Streambank Erosion Study, Fort Peck Dam, Montana, to the Yellowstone River, N. Dakota. USACE, Omaha District.

USACE (1994a), needs full reference

USACE (1994b), needs full reference

USACE (1997), needs full reference

U.S. Army Engineer Division, Northwestern, Missouri River Region (1994), Missouri River Master Water Control Manual, Review and Update, Draft Environmental Impact Statement, Volume 5: Aggradation, Degradation and Water Quality Conditions. Omaha District, USACE.

Watson, C.C, Biedenharn, D.S. and Scott, S.H. (1999), Channel Rehabilitation: Processes, Design and Implementation. Draft, July, 1999. U.S. Army Engineer Research and Development Centre, Vicksburg, Mississippi.

WEST Consultants, Inc. (1998) Final Report. Missouri River: Fort Randall Dam to Gavins Point Dam and Ponca Creek Aggradation Assessment. USACE, Omaha District.

Williams, G.P. and Wolman, M.G. (1984), Downstream effects of dams on alluvial rivers, *U.S. Geological Survey Professional Paper 1286*.

Xu, J. (1990), An experimental study of complex response in river channel adjustment downstream from a reservoir, *Earth Surface Processes and Landforms*, 15, 43-53.

Xu, J. (1996), Wandering braided river channel pattern developed under quasi-equilibrium: An example from the Hanjiang river, China, *Journal of Hydrology*, 181(1-4), 85-103.

Xu, J. (1997), Evolution of mid-channel bars in a braided river and complex response to reservoir construction: an example from the middle Hanjiang River, China. *Earth Surface Processes and Landforms* 22, 953-965.

IV Specific Gauge Analysis

Introduction

Specific gauge analysis is a simple but highly effective technique for inferring the changes in channel morphology (especially bed elevation) that occur in response to one or more disturbing factors on the fluvial system. Blench (1966) (cited in Watson, *et al.* 1999) wrote:

> *'There is no single sufficient test whether a channel is in-regime. However, for rivers, the most powerful single test is to plot curves of "specific gauge" against time; if the curves neither rise nor fall consistently the channel is in-regime in the vicinity of the gauging site for most practical purposes.'*

A specific gauge record is a plot of stage against time for a particular discharge at a gauging station. The first step in its construction is to plot stage as a function of discharge for each year in the period of record being analysed. A regression line is then added to each plot to represent the rating curve for that year and the equation for the rating curve is used to calculate the stages for a range of discharges between the maximum and minimum values observed during that year. These stages are then plotted against time to develop the specific gauge record. It is desirable to have as wide a range of discharges as possible on the specific gauge plot because low and high flows may behave in very different ways (Watson, *et al.* 1999). Frequently, however, it is not possible to include the highest and lowest selected discharges because there may only be a few years when these flows actually occurred and, consequently, there are an insufficient number of points from which to develop a coherent time series.

Specific gauge plots are generally used to *infer* the aggradational or degradational trends of the river bed, but what they actually represent is a change in elevation in the water surface, rather than the bed. Whilst it is true that changes in bed elevation must affect the water surface elevation, this is not the only factor which can do so (Watson, *et al.* 1999). Width change through bank deposition or erosion can also cause stage to rise or fall, for example, while the stage for a given discharge can also rise in response to the presence of channel ice or a debris jam. In light of the fact that stage changes may be driven by several different causative factors, care must be taken when interpreting a specific gauge record.

Data Processing and Analysis

The specific gauge analysis of the Missouri River performed in this study is based on data obtained from two sources. The most complete source of at-a-station data are the USGS 9-207 forms that contain details of the measured stages and discharges for each USGS station for the period of operation of that station. These data are collected approximately six to eight times a year and, because they list the actual measurements of both stage and discharge obtained in the field, they are the most complete available measurements. The second source is USACE (1994), which contains specific gauge plots for <u>all</u> of the stations in the four reaches being studied and thus provides more comprehensive spatial coverage at reach scale than that of the 9-207 stations. The data taken from these plots, however, are slightly less complete because not all the stations

record both measured stages and discharges. The missing data must be obtained from the rating curves constructed for each station. Furthermore, the rating curves are extrapolated beyond the range of measured data in both directions, depending on whether the year in question was particularly wet or dry. The most consistently reliable stage plots from this source are probably those for 20,000 cfs. Those for 10,000 cfs and 30,000 cfs are also fairly reliable, but the plot for 40,000 cfs will only be of high accuracy during years that experienced prolonged, high discharges (Garrison, *pers. comm.* 1999). Particular care must therefore be applied when interpreting the specific gauge plots for 40,000 cfs.

Prior to using the information on the 9-207 forms it was necessary to remove any potentially misleading data. For example, during the winter some stage measurements are affected by ice, while others are affected by large amounts of in-channel debris. These data cannot be used to infer changes in bed level from stage changes. For certain years of record this left too few data points to construct a meaningful stage-discharge curve and so two years of data were combined to produce a single plot. Where this was necessary it is clearly labelled on the specific gauge graph.

For gauging stations where data were available from both sources they were combined onto a single graph. This produces a longer period of record because the 9-207 data generally only extends back to the mid- to late-1970s, while the data from USACE (1994) frequently extends back to the 1960s or the 1950s – very near to the time when the dams in the Garrison, Fort Randall and Gavins Point reaches were constructed. The USACE (1994) data are used to derive stage records for discharges of 10,000 cfs; 20,000 cfs; 30,000 cfs and 40,000 cfs, while the discharges from the 9-207 stations are generally less well rounded figures.

The initial analysis presented here considers each reach individually. First, temporal trends for the individual gauging stations are discussed. These records are then used to describe the reach-scale trends. Finally, the trends observed in this analysis are compared to those observed in analyses of other channel parameters, such as average bed elevation, thalweg elevation, hydraulic geometry and grain size distribution. The aim is to gain an overall understanding of how the channel has evolved through time and, thus, to determine as accurately as possible, how close the morphology of each reach is to a state of dynamic equilibrium.

In describing the reach-scale trends, the stage data are presented as a summary graph of the total change in bed elevation over the period of record because it was felt that a first-order, quantitative approach to interpreting the reach-scale trends would be more objective than simply comparing the consecutive plots visually. The data for these graphs are listed in Appendix A.

The summary graphs for each reach are examined alongside the individual specific gauge plots and the data in the tables in Appendix A to ensure as accurate an interpretation as possible.

Fort Peck Reach

Mainstem gauging stations

These gauging station plots are based entirely or in part on rating curve data. Because the measurements used to construct the rating curves were updated only infrequently, it was necessary to interpolate between stage points, sometimes over long periods of time, to obtain the periods of record shown. This results in the plots having a less natural appearance than those based on measured data (Garrison, *pers. comm.* 1999).

The locations of the gauging stations used in the study are mapped in Figure 1. The specific gauge plots for all the gauging stations can be found in Appendix B (Figures B1-B10).

Gauge No. 1 (2.61 miles downstream from Ft Peck dam), MT – RM 1768.9
Stage lowering is evident at all discharges although the maximum value of about 0.8 ft over the 25 year period is relatively small (Fig. B1). Local bed degradation around this gauge may have been limited by bedrock controls or gravel layers.

7 Mile Gauge (Missouri River below Fort Peck Dam), MT – RM 1763.5
This site experienced much greater stage lowering than Gauge No. 1, with a maximum of 4 ft occurring for a discharge of 20,000 cfs between 1950 and 1984 (Fig. B2). For both 10,000 cfs and 20,000 cfs the fastest rate of stage lowering occurred between 1950 and 1958.

West Frazer Pump Plant, MT – RM 1751.3
This is the first gauge site in this reach where stages appear to have responded differently at different discharges (Fig. B4). At 10,000 cfs the stage shows a steady decrease in elevation, by about 3.2 ft, over the entire period of record (1950-1984). At 20,000 cfs there was virtually no change in elevation from 1950 to 1958 and then a steady decrease, by just less than 3 ft, from 1958 to 1984. At 30,000 cfs, however, the stage level rose by 0.4 ft from 1950 to 1958 before decreasing at a steady rate, by about 4.7 ft, up to 1984. Hence, as at 7 Mile Gauge, 1958 again appears to have been a pivotal year in the record.

East Frazer Pump Plant, MT – RM 1736.6
From 1950 to 1958 stages for all three discharges decreased markedly (Fig. B5). After 1958, the stage rose by 1 ft for a discharge of 10,000 cfs and by about 0.4 ft for 20,000 cfs. In contrast, the stage for 30,000 cfs continued to decrease, but at a much reduced rate, achieving only about 0.25 ft of lowering by 1984. 1958 was again a pivotal year in the records.

Oswego, MT – RM 1727.6
At this station throughout the period of record (1950 to 1966), stages lowered steadily at all discharges, with the amounts of overall lowering ranging from 0.7 ft for 10,000 cfs, to 1.4 ft for 30,000 cfs (Fig. B6). Unlike the stations upstream, there were no changes in these trends around 1958.

Missouri River near Wolf Point, MT – RM 1701.22
This is the first gauge site that combines data from both the 9-207 and USACE (1994) sources and two differences are immediately noticeable (Fig. B7). First, the 9-207 data do not cover as great a range of discharges as those from USACE (1994). This is because of the aforementioned need to remove the highest and lowest discharge values where no actual measurements took place in a given year. Second, data from

the USACE provide a much smoother line than those from the 9-207 sources. This reflects the lack of regular updating of the data used to create the plots and, as a result, the fact that more interpolation is needed between temporally-spaced data points than for frequently measured data (Garrison, *pers. comm.*, 1999).

Despite the differences in data used to create this chart there appears to be good agreement between the trends based on measured data (10,000 line) and rating curve data (10,000 II line) for the 10,000 cfs discharge. These lines overlap for the years 1976-1984 and it can be seen that for 1981 and 1984 the two show almost perfect agreement. The greatest discrepancy occurs in 1980 and is approximately 0.7 ft. This is a significant difference compared to the stage differences that occurred over the period of record and it highlights the desirability of using *measured* data wherever possible. Nevertheless, the salient feature is the general finding that the same amount of stage lowering is shown by both plots over the overlap period, albeit with slightly different absolute stage values.

The plots for 10,000 II cfs, 20,000 II cfs and 30,000 II cfs all show that a general lowering trend resulted in 3 ft of stage decrease from 1950-1984. For the first two discharges, the rate of stage reduction decreased around 1958 whilst for 30,000 cfs stages actually increased a little at that time. There then followed a period of near stability before renewed stage lowering from 1975 to 1984.

The 10,000 cfs plot, based on 9-207 data, continues through to 1999. The record shows that stage elevations were steady between the mid-1980s and mid-1990s, but may have begun decreasing again since 1996. This finding is supported by plots for 7,500 and 14,000 cfs which also suggest that stage elevations have begun to decrease following a decade of stability. However, it is too early to judge if renewed lowering in the late 1990s represents a significant trend or a short-term fluctuation.

Missouri River near Culbertson, MT – RM 1620.76
The two data sources again share a common discharge at 10,000 cfs and, although there is no period of overlap, the measured data for 10,000 cfs and the rating curve data (10,000 II) concur (Fig. B9). For 10,000 II cfs and 20,000 II cfs, stages decreased up to 1958, but then they began an 8-year period of stage increase, resulting in 1.0 to 1.5 ft of stage rise. For 30,000 II 1958 marked a slowing of the rate of stage lowering.

Recent trends in the measured data for 10,000 and 7,500 cfs reveal that stage lowering may be continuing to the present day in the this reach. This would suggest that morphological adjustments are not yet complete.

Tributary gauging stations

Milk River at Nashua, MT – (joins Missouri River at RM 1761.6)
The plot for 225 cfs shows stages to be unchanged during the period of record, suggesting that the channel was stable during the period 1978-1998 (Fig. B3). The plots for 1,500 cfs and 3,500 cfs also suggest overall stability, although there is wider scatter. This scatter is probably a function of event-related scour and fill related to these higher flows.

Poplar River near Poplar, MT - (joins Missouri River at RM 1678.9)
The discharge of 1 cfs should be discounted from the analysis because it is too low to be reliable (Fig. B8). The plots for 70 cfs and 400 cfs suggest a slight upward trend in stages that resulted in about 0.6 ft of stage rise between 1984/85 and 1999.

Yellowstone River near Sidney, MT - (joins Missouri River at RM 1582)
The plots for all three discharges indicate that the channel has been broadly stable over the period 1976 to 1998/99, although there may be a very slight upward trend after 1984 (Fig. B10). Also, for the two higher discharges, the records between 1993 and 1998/99 could indicate that some cyclical adjustments occurred in channel morphology.

Overall trends in the Fort Peck Reach

Figure 2 shows the overall changes in stage for each discharge at each gauging station in the reach. Most of the stations show substantial amounts of stage lowering, especially for the higher discharges. This finding suggests that there has been net degradation over the study period.

It was noted in the introduction that the greatest uncertainties are associated with gauge records for highest and lowest discharges, and that those for the mid-range discharges are the most reliable. In this context, the record for 20,000 cfs may best represent reach-scale morphological adjustment over the study period. Figure 2 reveals that, with the exception of Gauge No.1 (immediately downstream of the dam), the amount of stage lowering decreases with increasing distance downstream for the mainstem stations. This is consistent with the hypothesis that stage lowering represents reach-scale morphological response due to bed degradation downstream of the dam. As noted earlier, the limited degree of channel incision around Gauge No.1 may be explained by the presence of gravel and bed rock beneath the bed in the vicinity of that particular gauge.

Degradation at the station near Wolf Point perhaps shows rather more degradation than expected in comparison to the records immediately upstream at East Frazer Pump Plant and Oswago. The reason may be the local absence of a gravel layer beneath the bed, which allows greater degradation than upstream. This station is located at RM 1701.22 which places it just upstream of the area between river miles 1697 and 1636 where Danberg *et al.* (1988a) report that absence of the gravel layer has allowed the thalweg to lower more markedly than elsewhere (Table 1).

Comparison of the stage records for the tributaries is complicated by the fact that the data represent widely differing discharges and periods of record. Despite this, some salient points arise from the data. Low flows in the tributaries (represented by 225 cfs, 70 cfs, and 9000 cfs for the Milk, Poplar and Yellowstone Rivers, respectively) all display net stage rises over the period of record, but this may be attributed to siltation during conditions when the tributaries are ponded by flows in the mainstem. Of greater morphological significance is the finding that mid-range and high discharges in the Milk River show 1 ft of stage lowering while the equivalent flows in the Yellowstone River display only 0.2 feet of lowering. The confluence of the Milk River with the Missouri is only 7.5 miles below the dam, while that of the Yellowstone is 189 miles from the dam. Hence, this reduction in stage lowering in

tributaries with increasing distance downstream of the dam is consistent with the distribution of degradation at the mainstem stations. It should be noted, however, that the limited amount of stage reduction due to channel incision in the Yellowstone River may also have been influenced by the proximity of the gauge to Lake Sakakawea, whose backwater effects may reduce the capacity of the flow to degrade the bed. In contrast, the record for 400 cfs in the Poplar River indicates net aggradation, suggesting perhaps that the degradation has not occurred in the middle of the study reach.

Taken together with the results for the mainstem, the records for the tributaries suggest that stage lowering is driven by reach-scale degradation downstream of the dam, but that the spatial distribution of bed level change may be complicated by the presence or absence of coarse substrate or bed rock materials. There is, in fact, some evidence of aggradation in the middle of the reach, between the gauges near Wolf Point and Culbertson.

Comparison to Results of Earlier Studies

Other studies have investigated the trends in various channel parameters in response to closure of the dam and these are summarised in Table 1. The table shows that bed material grain size distribution, hydraulic geometry, average bed elevation and thalweg elevation have all been studied along the entire length of the reach, with the results used to infer where and to what extent aggradation or degradation has occurred.

It may be inferred from the summary information in Table 1 that has degradation occurred between the dam and a point around river miles 1717 to 1707. While degradation is identified downstream as far as RM 1636, it is limited to zones where absence of gravel in the bed limits the degree of armouring. The downstream limit of widespread degradation is indicated by a solid line in Figure 1, just downstream of Wolf Point (but upstream of gauge station No.6). The hydraulic geometry and thalweg elevation data suggest that two areas of aggradation may exist, the first downstream from the 1717/1707 point and the second downstream of RM 1697. This finding is consistent with the specific gauge record for the Poplar River (confluence at RM 1678.9) which displays net aggradation.

The largest grain sizes are found in upstream sections and the studies report increases in grain size with time as selective entrainment and armouring have progressed. The smaller grain size and coarsening trend downstream and are consistent with the hypothesis that selective transport and deposition have occurred over the period of record.

Table 1: Summary Table of Fort Peck Reach Aggradation/Degradation Characteristics - RM 1771-1582

Variable	1960 RM	Agg/ Deg	Description	Source
Grain Size	1771-1582	D & A	Largest in upstream segments but increasing in amount in all segments until 1978, then decreasing slightly.	Midwest (1977)
Hydraulic	1771-1757	D	In the period 1936-1978 degradation has	Dangberg

Geometry			been occurring at progressively slower rates.	(1988a)
Hydraulic Geometry	1757-1717/1707	D	In the period 1936-1978 there has been less degradation and it has been occurring at a much slower rate.	Dangberg (1988a)
Hydraulic Geometry	1717/1707-1582	A	The period 1936-1978 shows aggradation increasing with distance downstream.	Dangberg (1988a)
Average Bed Elev.	1771-1766	D	Bed lowering has revealed a gravel layer and armouring is occurring.	Dangberg (1988a)
Thalweg Elevation	1771-1766	Stable	No significant lowering of the thalweg.	Dangberg (1988a)
Thalweg Elevation	1766-1714	D	Slow thalweg lowering.	Dangberg (1988a)
Thalweg Elevation	1697-1636	D	Thalweg lowering where the gravel layer is absent, but none when the gravel layer is present.	Dangberg (1988a)
Thalweg Elevation	1697-1580	A	Rate of thalweg lowering decreases with distance downstream.	Dangberg (1988a)

While the information in Table 1 is broadly consistent with the results of the specific gauge analysis, it cannot be used to specify accurately the RM limits to zones where either degradation or aggradation has dominated due to lack of good spatial resolution in the data.

Conclusions

It may be inferred from the specific gauge records that degradation has occurred throughout the reach, but that the degree of bed lowering decreases with increasing distance from the dam and degradation is spatially discontinuous downstream of a point between RM 1717 and 1707. The relatively large degree of degradation for the station near Wolf Point (RM 1701.2), may be explained by the local absence of a gravel layer. There is evidence from previous studies of aggradation along the mainstem between about RM 1700 and 1580, and this is consistent with aggradational trend in the specific gauge record for the Poplar River tributary, which confluences with the Missouri River at RM 1678.9.

It is difficult to draw any firm conclusions regarding temporal variation in rates of morphological change through degradation or aggradation because only the plots for Wolf Point and Culbertson (figures B7 and B9) have data extending up to the present day. At both sites, stages continue to decrease up to the present, suggesting that morphological adjustments are not yet complete.

Garrison Reach

Mainstem gauging stations

All the mainstem gauging stations except the one at Bismarck (figure B19) are based on rating curve data. Despite this they have a good degree of detail because the measurements have been updated every one to two years, eliminating the need for interpolation between stages over long periods of time (Garrison, *pers. comm.* 1999).

The locations of the gauging stations used in the study are mapped in Figure 3. The specific gauge plots for all the gauging stations can be found in Appendix B (Figs. B11-B20).

Missouri River near Stanton, ND – RM 1378.4
The plots for 10,000 cfs, 20,000 cfs and 30,000 cfs are very similar, which increases confidence that stage changes may be attributed to long-term morphological changes in the channel (Fig. B11). There was a period of intense stage lowering from 1950 to 1970, resulting in 6 to 7 ft of stage decrease. Between 1970 and 1976 there was apparently a hiatus, followed by a very sudden drop in stages, by 2 to 4 ft, in 1977. After 1977, stage lowering continued at a much slower rate, resulting in a further 1 to 1.5 ft of decrease in stages up to 1997. The recent records suggest that stage lowering is continuing and that morphological adjustments may be on-going.

Missouri River near Fort Clark, ND – RM 1366.65
The trends are very similar for all three discharges (Fig. B13). Stages display an overall lowering trend with the 10,000 cfs the stage decreasing by 5.3 ft; the 20,000 cfs stage decreasing by 7 ft and the 30,000 cfs stage decreasing by 6.8 ft over the period of record (1960-1997). The rate of stage lowering was fastest in the 1960s, but slowed after the mid-1980s and stages appeared to have approached equilibrium in the early 1990s. However, renewed lowering can be identified in the records for the late-1990s, indicating that morphological adjustments may be continuing.

Missouri River near Hensler, ND – RM 1362
The trends for all three discharges are very similar for the study period, 1959-1997 (Fig. B14). Rates of stage lowering decrease with time, especially after 1977. At 10,000 cfs the overall decrease in stage elevation is 3.8 ft. The equivalent figures for 20,000 cfs and 30,000 cfs are 4.5 and 5.8 ft, respectively. At this gauge, stages appear to have been stable since the mid-1980s, although there is some evidence of renewed lowering since 1995. It is too early to determine if the recent downward trend represents a sustained trend of morphological change or a short-term adjustment.

Missouri River near Washburn, ND – RM 1354.7
The trends for all three discharges again appear to be very similar over the period of record, 1955-1997 (Fig. B15). Rates of stage lowering decrease with time. Overall, the stage decrease at 10,000 cfs is 4.4 ft, while at 20,000 cfs and 30,000 cfs, stages decrease by about 5.0 ft. At this gauge, stages appear to have been stable between the early-1980s and the mid-1990s, although there is clear evidence of renewed lowering since 1995. It is, however, still too early to determine if the recent downward trend represents a sustained trend of morphological change or a short-term adjustment.

Missouri River near Price, ND – RM 1338
All three plots show a lowering trend throughout the period of record, 1960-1986 however, the decrease in stages is less marked than at the gauges upstream. At 10,000 cfs the stage decreased by up to 2.6 ft, at 20,000 cfs by 2.5 ft and at 30,000 cfs by 2.1 ft. Rates of lowering tend to decrease with time, and there was hardly any reduction in stages during the 1980s. As the record at the Price station ends in 1986, it is not possible to establish whether the renewed stage lowering apparent at the other mainstem stations has occurred here.

Missouri River at Bismark, ND – RM 1314.2
Usable data were available for only a short period of record at this station. Nevertheless, the stage records for 16,500 cfs and 24,300 cfs, clearly reveal an increasing trend between the late-1980s and the late-1990s. Overall, stages rose by about 0.2 ft and 0.25 ft, respectively. Very recently, there is some evidence that the period of increasing stages may have ended and that stages may have fallen by about 0.5 ft. It is, however, much too early to determine if recent stage fluctuations represent trends of morphological change or a short-term adjustments.

Tributary gauging stations

Knife River near Hazen - (joins Missouri River at RM 1375.5)
Measured data are available only for a short period from this gauge. Fig. B12 shows the records for 13 years of stage data at 50 cfs and 10 years at 750 cfs. Stages for the lower discharge have been stable bed although the discharge is too small to be of great morphological significance. Stages for the higher discharge indicate a cyclical behaviour with perhaps 1.0 ft of net lowering during the 1990s.

Turtle Creek above Washburn, ND – (joins Missouri River at RM 1351.9)
In Fig. B16, stages for 6 cfs vary widely but should probably be discounted because this flow is too small to be of morphological significance. The record for 85 cfs only covers the period 1993-1999, which is too short a time to support meaningful conclusions. However, the few data that are available for this station, suggest that stages have not changed in any systematic fashion during the 1990s.

Burnt Creek near Bismark, ND – (joins Missouri River at RM 1316.2)
Data availability is also severely limited for Burnt Creek (Fig. B18). The short records for 10 cfs and 100 cfs are consistent with each other in suggesting that stage changes have produced no clear trend during the 1990s. However, the period of record is simply too short to support firm conclusions.

Heart River near Mandan, ND – (joins Missouri River at RM 1311.2)
The period of record on this tributary is also too short to establish long-term trends. The plot for 20 cfs should be discounted because this is too small a discharge to be morphologically significant. The records for 200 cfs and 1,200 cfs indicate that stages were steady during the first half of the 1990s but suggest that they have been more variable since 1995. It is too early to decide whether this activity has any wide morphological significance.

Reach-scale trends

Figure 4 shows the overall changes in stage elevations for all the stations with sufficiently long periods of record to merit inclusion in the reach-scale analysis. Plots of stages corresponding to 10,000 cfs, 20,000 cfs and 30,000 cfs for five stations along the mainstem Missouri River all indicate substantial stage lowering. They further reveal that the amount of stage lowering generally decreases with distance downstream from the dam at all three discharges. These findings suggest that there has been net degradation at the reach-scale over the study period.

The exceptions to this general trend of a decrease in the amount of stage lowering with downstream distance are the stages for 10,000 and 20,000 cfs at the gauge near Washburn, which are 0.6 feet and 0.5 feet respectively *higher* than the corresponding stages at the gauge immediately upstream, near Hensler. These exceptions may be explained by examination of Table A2, which reveals that the period of record at Washburn extends back 4 more years than that at Hensler. It is likely that stage lowering occurred at both stations during 1955-59, but that it is absent from the shorter record for Hensler. The data for the gauge at Bismark only represent changes during the last 10 to 12 years. This may explain why the amounts of stage decrease recorded there are very small.

Data from tributaries other than the Knife River have been excluded from Fig. 4, because the periods of record were too short to yield reliable indications of longer-term trends. The results for the Knife River suggest that the channel has degraded, while the absolute amount of lowering is proportionately smaller than that that in the much larger, mainstream Missouri River.

Comparison to Results of Earlier Studies

Other studies have investigated the trends in various channel parameters in response to closure of the dam and these are summarised in Table 2. The table shows that bed material grain size distribution, average bed elevation and thalweg elevation have all been studied along the entire length of the reach, with the results used to infer where and to what extent aggradation or degradation has occurred. The spatial distribution of degradation shown in Fig. 4 corresponds with the pattern of degradation inferred from various other channel parameters, which are summarised in Table 2.

According to USASCE (1994), average bed elevations have decreased by 8 ft due to degradation over a 27 year period at RM 1384, while thalweg elevations have decreased by a similar amount in the 10 miles immediately downstream of the dam. About 10.5 ft of degradation has been observed at the gauge at RM 1378.4 over a 47 year period. Direct comparison for specific locations between the results compiled herein and the findings earlier studies is rarely possible. However, ASCE (1994) report that the average bed elevation at RM 1337 decreased by over 2 ft due to bed degradation between 1958 and 1985, while the present study established that stages lowered by up to 2.5 ft at RM 1338 between 1960 and 1986.

Table 2: Summary Table of Garrison Reach Aggradation/Degradation Characteristics - RM 1389.9-1311

Variable	Agg./Deg.	Description	1960 RM	Source
TE	D	Over 8 ft of degradation has occurred in the 8-10 miles downstream from the dam since closure.	1389.9-1381.9/1379.9	USACE (1994)
ABE	D	Almost continues degradation from 1958 to 1985, ranging from about 8 ft near RM 1384 to just over 2 ft at RM 1337.	1389.9-1337	USACE (1994)
GS	D	The D_{50} grain size increases with time from 1958-1985 between river miles 1389.9 and 1335. From 1958-1964 grain size increases by about 0.16mm	1389.9-1335	USACE (1994)

		at RM 1386 and by about 0.03mm at RM 1340. From 1964-1985 the increase is 3.81mm at RM 1386 and 0.09mm at RM 1340.		

TE = Thalweg Elevation
ABE = Average Bed Elevation
GS = Grain Size

The results reported by USACE (1994) reveal that bed material coarsened substantially between river miles 1389.9 and 1335 during the period 1958-1985. Theoretically, it is expected that bed material coarsening occurs in a degrading channel due to selective entrainment of finer grains during bed scour events which drives the armouring process. Hence, the D_{50} grain size trend in the reach is also consistent with the finding of this study.

Conclusions

Consistency between the measurements of channel bed elevation and grain size parameters reported previously and the specific gauge analysis reported here, increases the degree confidence that can be placed on the results.

It may be inferred from the specific gauge records that degradation has occurred throughout the reach, and that the degree of bed lowering decreases with increasing distance from the dam in a spatially coherent manner. These findings are consistent with the general theory on degradation driven by the closure of a large dam. It is difficult to draw any firm conclusions regarding morphological response in the tributaries due to lack of long-term specific gauge records suitable for analysis. Available data for the tributaries suggest that during the 1990s stages have varied but shown no marked trends.

Trends of temporal variation in the rate of degradation at mainstem gauging stations are consistent between sites. The plots for Stanton, Fort Clark, Hensler and Washburn (Figs. B11, B13, B14 and B15), all reveal an overall decrease in the rate of degradation with time. The record for the station near Price (Fig. B17) is shorter and ends in 1986, making it less useful for examining time trends in the rate of stage lowering. However, the trends at Price are consistent with those at the other stations for the 1960s, 1970s and early 1980s.

All the mainstem stations with records extending to the present exhibit lowering of stages in the late 1990s. This establishes that morphological adjustments are definitely on-going. It is, however, impossible to say whether recent stage lowering is a short-term fluctuation or represents a renewed period of degradation. The fact that stage lowering in the late 1990s is common to all the mainstem sites establishes that degradation at that reach-scale is the probable cause (rather than local morphological adjustments), but it will not be possible to establish whether there is a sustained degradational trend until about 2005.

The results of the specific gauge analysis up to 1995 would suggest that morphological response of the reach to closure of the dam was essentially complete and that the river was close to a condition of dynamic equilibrium. Recent stage lowering throughout the reach must cast some doubt on this conclusion, but it will be

another five years or so before it can be determined whether the present degradational trend is driven by a short-term adjustment or marks a renewed period of sustained morphological change.

Fort Randall Reach

All the specific gauge analyses for gauging stations in this reach are based on rating curve data and, as in Garrison Reach, supply a good degree of detailed information. This is the case because the measurements have been updated every one to two years and, eliminating the need to interpolate between stages over long periods of time (Garrison, *pers. comm.* 1999).

The locations of the gauging stations discussed below are mapped in Figure 5. The specific gauge plots for all the gauging stations can be found in Appendix B (Figs. B21-B27).

Mainstem gauging stations

Fort Randall Dam Gauge, SD – RM 879.98
The plots of stage at the three discharges are almost identical in both pattern and the lowering trend that they exhibit (Fig. B21). In order of increasing discharge they reveal 5.3 ft, 5.2 ft and 5 ft of stage decrease over the period of record, 1953-1986. From 1975-1986 there is a step-like pattern evident in all three plots. In the period after the mid-1970s, the trends are stepped. A period of stable stage elevations in the late-1970s was followed by further stage decrease in the early 1980s before renewed stability in the late 1980s. The record ceases in 1986, making it impossible to determine whether stage stability has continue to the present day, or whether further adjustments have occurred.

Missouri River below Greenwood, SD – RM 865.04
The stage records at this station are generally similar to one another (Fig. B22). The overall trend of the records suggests a predominantly lowering trend, although there is more variability than at the Fort Randall Dam Gauge upstream. In the period 1966-1973 the lowest three discharges indicate stage lowering, by perhaps 1 to 2 ft, but this is not reflected in the stage for 40,000 cfs. For the period 1974-1981 the records suggest that stages were relative stable, but further stage lowering, by perhaps 0.5 to 1 ft occurred during the 1980s. In interpreting these records it should be borne in mind that the plot for 40,000 cfs contains a higher proportion of data points extrapolated beyond the range of measured data for various years. This introduces uncertainty and could explain the wider scatter displayed by the data points for this discharge.

Missouri River Gauge at RM 853.37
The period of record for this station is restricted to 1960-1972, reducing the utility of the results to identify long-term channel adjustments (Fig. B23). The plots all suggest that stages followed an overall upward trend, to produce a net rise of about 1 ft over the study period. The time distribution is non-uniform however, with most of the stage rise occurring in the early 1960 and then stages staying almost constant or falling slightly during the mid to late-1960s and early 1970s.

Missouri River near Verdel, NE – RM 845.91

The specific gauge plots constructed for three discharges at this station show similar patterns (Fig. B25). Stages varied widely with no consistent trend during the period 1964 to 1977, but began to rise steadily in 1977. By 1985 stages had risen between about 2 ft. This rising trend may be associated with backwater effects driven by sedimentation at the delta of the Niobrara River where it confluences with the Missouri River just downstream of this gauging station. While incremental growth of the delta is known to have occurred, the strong linearity of the data from 1977 to 1985, especially when compared to the scatter in the preceding period, suggests a high degree of data interpolation. It is likely that actual changes in bed elevation have not been as regular as they appear in Fig. B25.

Missouri River near Niobrara, NE – RM 842.45
The three discharge plots for this station have almost identical patterns, with an overall upward trend for the period of record, 1956-1985 (Fig. B27). During this period, stages rose by between about 5 to 5.5 ft. The rising trend was strongest during the early part of the record, 1957-1960, but slowed during the early to mid-1960s. Stages fell during the late 1960s and early-1970s before beginning a renewed upward trend in 1972. With one fall, between 1975-77, the upward trend was then sustained up to the end of the record in 1985, resulting in about 2 to 2.5 ft of net stage rise. However, the linear nature of the plot post 1977 suggests a high degree of data interpolation.

The general trend of rising stages may be explained by two factors. First, bed elevations at this station may have been affected by growth of the delta of the Niobrara River. Second, stages may be directly affected by the backwater from Lewis and Clark Lake, immediately downstream, and may also be indirectly affected by bed level rise due to siltation at the head of the lake.

Tributary gauging stations

Ponca Creek near Verdel, NE - (joins Missouri River at RM 848.9)
Generally similar patterns are displayed by all three discharges plotted for Ponca Creek (Fig. B24). The records reveal that there was rapid stage lowering during the early part of the period of record, between 1957 and the mid-1960s, leading to about 2.5 ft of stage decrease. In the mid-1960s a long period of net stage increase began, and this has continued to the present day, although the rising trends have been unsteady and are punctuated by shorter episodes of stage lowering. The overall net increase in stages between 1957 and 1997 is 1 to 2 ft. Ponca Creek is affected for a certain distance upstream by the backwater effects of the delta at the mouth of the Niobrara River. Some fraction of the net stage rise may thus be explained by backwater effects behind the Niobrara delta.

Niobrara River near Verdel, NE - (joins Missouri River at RM 844)
The most noticeable feature of the specific gauge record for Verdel is a rapid drop in stages by about 1.3 ft between 1983 and 1987. Prior to 1983 stages had displayed a slight rising tendency although there was a fair amount of variability from year to year. After 1987 the records for all three discharges reveal a rising tendency but, because of data scatter, it is difficult to determine whether this is a marked trend.

The two periods of rising stages are probably driven by sedimentation on the delta at the Niobrara River's confluence with the Missouri, either because bed aggradation or an increasing backwater effect at the gauge. The cause of the decline in stages between 1983 and 1987 is less obvious. It could be due to the channel retrenching into the delta as part of the natural cycle of deposition and erosion, it might be the response of the Niobrara River to degradation in the Missouri mainstem, or it might be associated with some local influence on hydrodynamics of flow at the gauge site.

Reach-scale trends

Figure 6 reveals a coherent distribution of overall stage changes along the reach, suggesting progression from degradation immediately downstream of the dam to somewhere around River Mile 860, and the aggradation along the remainder of the reach. However, in interpreting the overall record, it should be borne in mind that the data in Figure 6 represent different periods of record. The years of record at the mainstem gauging stations (from upstream to downstream) are:

Fort Randall Dam - 33
Greenwood - 20/21
RM 853.37 - 12
Verdel - 21
Niobrara – 29

Thus, although the distribution of degradation from the dam and beyond Greenwood appears to show diminishing bed lowering with distance from the dam, this is at least partly explained by the shorter record at Greenwood. Similarly, the increase in the lengths of record from RM 853.37, to Verdel and then to Niobrara could at least partly explain the apparent increase the degree of aggradation. Notwithstanding these caveats, the distribution of stage changes along the mainstem gauging stations is consistent enough for a reasonable degree of confidence to be placed in the pattern displayed in Figure 6.

The overall stage change for the gauge on Ponca Creek is consistent with the results for the mainstem in showing net aggradation during the 40-year period of record. Conversely, net change for the Niobrara River is stage lowering, which appears to contradict the aggradational change in the mainstem. However, it should be remembered that all the stage lowering at the Niobrara (figure B26) occurred during a short (four year) period, and that for the great majority of the period of record the trend was for slow aggradation.

Comparison to Results of Earlier Studies

Other studies have investigated the trends in various channel parameters in response to closure of the dam and these are summarised in Table 3. Studies of hydraulic geometry, water surface and average bed elevations all indicate that degradation has occurred between river miles 880 and 860 (USACE, 1997). Measured rates of erosion are consistent with this finding and suggest that degradation has been most intense between river miles 880 and 870. These results correspond with the identification in the present study of stage lowering due to degradation at the two upstream gauging stations in the reach.

The results of previous studies reveal that no temporal trend in average bed elevation is discernible between river miles 860 and 853. Dangberg (1988b) interprets this as indicating that the reach between RM 860 and RM 855 is a transition zone between degradation upstream and aggradation downstream. This interpretation is supported by the stage records reported in the present study for the gauge below Greenwood (net degradation) and that at RM 853.37 (net aggradation), which bracket the transition zone reported by Dangberg (1988b).

Table 3: Summary Table of Fort Randall Aggradation/Degradation Characteristics - RM 880-844

Variables	Agg/Deg	Description	1960 RM	Source
HG	D	Lowering thalweg, increasing cross-sectional area, increased bank top width	880-860	Dangberg (1988b)
ABE	D	Lowers at all cross-sections except RM 865	880-860	Dangberg (1988b)
ABE	T	No discernible trend	860-853	Dangberg (1988b)
ABE	A	Trends show both increasing and decreasing elevations, probably due to reworking of Niobrara sediments. The overall trend is likely to be aggradation	853-844	Dangberg (1988b)
ABE	D	Lowest elevation reached 30-40 years into the simulation, 2025-2035. Predicted degradation is greatest under the high flow scenario and lowest under the low flow scenario	880-863.5	WEST (1998)
ER	D	High erosion rate from 1953-1984	880-870	Dangberg (1988b)
ER	D	Decreasing erosion rate for period 1953-1984	870-844	Dangberg (1988b)
WSE	D	Water surface elevations adjusted to a common discharge show a decrease in elevation downstream of the dam	880-860	USACE (1997)
WSE	A	Water surface profiles downstream of this point rise through time. Maximum rise (5 ft) at Niobrara confluence. Magnitude and timing of these trends corresponds to observed stage trends at mainstem gauges	860-844	USACE (1997)
SUM	D	Degradation zone	880-860	Dangberg (1988b)
SUM	T	Transition zone	860-855	Dangberg (1988b)
SUM	A	Aggradation zone	855-844	Dangberg (1988b)

HG = Hydraulic Geometry
ABE = Average Bed Elevation
ER = Erosion Rate
WSE = Water Surface Elevation
SUM = Summary of reported trends

Past studies of average bed elevation show that aggradation has been the dominant channel change between RM 853 and RM 844. This is consistent with the net change established in this study, although the stage records for individual mainstem stations reveal that the overall aggradational trends has been punctuated by shorter periods of degradation (see, Figures B23, B25 and B27). Dangberg (1988b) concluded that

short-term fluctuations in stage and bed level are probably associated with reworking of the sediment deposits in the Niobrara River and the Missouri around the Niobrara confluence. The overall rise in water surface elevations reported for the mainstem between RM 860 and RM 844 occurs at the downstream limit (RM 844) and is of the order of 5 ft . This finding coincides with the specific gauge analysis reported herein for the Missouri near Niobrara (RM 842.45) which likewise shows 5.0 to 5.5 ft of increase in stages over the period 1956-85.

Conclusions

The zones of net degradation, transition and net aggradation identified on the basis of this and previous studies are indicated in Figure 5 by two solid lines across the Missouri River. The zone between the dam and the upstream line is that of degradation. The zone between the lines is the transition zone. The zone downstream of the second line is that of aggradation. This spatial distribution of channel change represents the morphological response expected downstream of a dam but, in fact, it would be incorrect to attribute the observed channel changes solely to closure of Fort Randall Dam. This is the case because morphological adjustments in lower half of this reach are strongly, and perhaps dominantly, affected by two other influences. First is the presence of Lewis and Clark Lake. Sedimentation at the head of this lake would be expected to drive local aggradation regardless of conditions in the upper half of the study reach. Second, the aggradational tendency at the head of Lewis and Clark Lake is massively enhanced by the introduction of a heavy sediment load from the Niobrara River at RM 844. The delta built by the Niobrara has a major influence on channel changes in the Missouri, both directly, through its impact on local bed levels, and indirectly, through supplying relatively coarse sediment that is deposited at the head of Lewis and Clark Lake. If the Niobrara were not present it is likely that the amount of aggradation would be smaller than that actually observed.

The specific gauge records for the upstream two gauging indicates that bed lowering in the degradational zone continued into the 1980s. Unfortunately, the records cease in the late-1980s, making it impossible to determine whether degradation has continue to the present day. WEST Consultants (1998) simulated average bed levels for a 50 year period, starting in 1995. They predicted that the degradation would continue in the first 20-miles downstream from the dam until sometime between 2025 and 2035.

There are no gauging stations in the transition zone, and the period of record at RM 853.37 is restricted to 1960-1972, reducing the utility of the results in identifying time trends in channel adjustment. The results for this period reveal that stages rose during the early 1960s but were steady or declined slightly during the mid to late-1960s and early 1970s. This might indicate that the transition zone has tended to migrate downstream with time as degradation in the zone below the dam has slowed and the supply of sediment to the transition zone has decreased.

In the aggradational zone, the record for Missouri River near Verdel (RM 845.91) does not begin until 1964. Stages varied widely with no consistent trend during the period 1964 to 1977, but began to rise steadily in 1977. The record for the Missouri River near Niobrara (RM 842.45) is more valuable because it begins in 1957. The early part of the record reveals a strong rising trend between 1957 and 1960 that slowed during the early to mid-1960s. Stages fell during the late 1960s and early-

1970s before beginning a renewed upward trend in 1972. However, the linear nature of the plots for both stations in the 1970s suggests a high degree of data interpolation. Unfortunately, records cease in the mid-1980s and so nothing can be deduced regarding recent and current trends of channel adjustment.

Two tributaries join the Missouri in the aggradational zone. The record for Ponca Creek near Verdel, which joins Missouri River at RM 848.9, reveals that there was rapid stage lowering between 1957 and the mid-1960s, followed by sustained and accelerating aggradation to the present day. The record for the Niobrara River near Verdel, which joins Missouri River at RM 844, reveals a slowly rising levels punctuated by a rapid drop in stages between 1983 and 1987. The record extends to the present day and also suggests that aggradation is on-going.

It appears that rising bed levels in the aggradational zone may be occurring due to the accumulation of sediment supplied from tributaries and delta formation at the head of Lewis and Clark Lake than morphological response to the closure of Fort Randall Dam. If confirmed this would suggest that aggradation will continue indefinitely although reworking of the Niobrara delta and lake head deposits mean that short-lived reductions in bed elevation may occur from time to time.

Taken together, the results presented herein suggest that:

1. degradation in response to the closure of Fort Randall Dam continues in the upper zone (extending from the dam to about RM 860) and has been predicted to persist until 2025 to 2035;
2. the zone of transition, identified by Dangberg (1988b), between RM 860 and RM 853 began to experience degradation in the late-1960s and may be migrating downstream;
3. on-going rises bed levels in the aggrading zone (downstream of RM 853) are primarily driven by the accumulation of sediment currently supplied by tributaries rather than morphological response to dam closure more than forty years ago.

On this basis it may be concluded that the Fort Randall Reach has not attained a condition of dynamic equilibrium and that it is unlikely to do so for at least two decades.

Gavins Point Reach

The data for these gauging stations are based entirely or in part on rating curve data except for those from Yankton (RM 805.8). The measurements used to construct the rating curves were only updated infrequently and hence it was necessary to interpolate between stage points, sometimes over long periods of time, in order to obtain the full periods of record shown. This results in the plots having a more unnatural appearance than those based on measured data (Garrison, *pers. comm.*, 1999).

The locations of the gauging stations discussed below are mapped in Figure 7. The specific gauge plots can be found in Appendix B (Figures B28-B33).

Mainstem gauging stations

Missouri River at Yankton, SD – RM 805.8

Stages for both discharges have decreased throughout the period of record, 1973-1995 (Fig. B28). The rate of lowering has been unsteady and this has produced a stepped pattern. At 20,000 cfs the stage decreases by a total of 4.4 ft and at 27,500 cfs it decreases by just less than 5 ft. The period of record did not begin until 1973 and so no data are available prior to that date but records indicate that stage lowering continued until as recently as 1995.

Missouri River near Gayville, SD – RM 796

Stages for all three discharges decreased over the period of record, 1956-1997 (fig. B30). The rate of lowering was slow between 1956 and 1967 but since 1967 it has been faster. The overall stage decrease is 4.2 ft at 20,000 cfs, 4.9 ft at 30,000 cfs and 5.1 ft at 40,000 cfs. During the early 1990s stages were almost constant but there has been renewed lowering since 1995.

Missouri River near Maskell, NE – RM 775.8

Stages for all four discharges decreased over the period of record, 1956-1997 (Fig. B31). The overall decrease in stages is 3.2 ft at 10,000 cfs, 4.9 ft at 20,000 cfs, 5.8 ft at 30,000 cfs and 6.1 ft at 40,000 cfs. Stages were almost steady in the early part of the period of record, 1955-1967. However, in 1967 there began a period of rapid stage lowering that persisted until the mid-1970s. There was then a recovery in water levels (1975-1978) that proved short-lived as stages fell again between 1978 and the present day. Stages were almost constant during the early 1990s, but there has been renewed and accelerated lowering since 1995.

Missouri River near Ponca, NE – RM 751

The period of record at this gauge (1974-1980) is too to be particularly useful (Fig. B33). The few available data suggest that stages decreased during the late-1970s, by perhaps 1 to 2 ft. However, the record is too short and data too sparse to be included in the graph of overall changes at the reach-scale.

Tributary gauging stations

James River near Yankton, SD – (joins Missouri River at RM 800)

The period of record for this station is only 13 years (1982-1995) which is really too short for a specific gauge analysis (Fig. B 29). Hence, the results obtained are only indicative. The points for 1,100 cfs and 2,600 cfs plots appear to decrease with time, although there is a wide degree of scatter that obscures the overall amount of stage lowering. The points for 300 cfs are less scattered and suggest that stages may have decreased about 1.2 ft between 1982 and 1993.

Vermillion River near Vermillion, SD – (joins Missouri River at RM 772)

The period of record for this station is only 16 years (1983-1999) which is really too short for a specific gauge analysis (Fig. B32). Hence, the results obtained are only indicative At 200 cfs the stage record indicate that water levels decreased by about 2 ft over the period of record. Data are sparse for 800 cfs and 1,700 cfs but that suggest about 4.7 ft and 6 ft of stage decrease may have occurred. The rate of stage lowering has been variable.

Reach-scale trends

Figure 8 reveals that there has been overall stage lowering throughout the Gavins Point Reach during the period of record. This indicates that the entire reach has experienced degradation since the 1950s. There are two reasons for this outcome. First, this reach does not have a dam at its downstream limit. Consequently, there are no backwater effects to drive sediment deposition. Second, it is relatively short, at 58 river miles. Consequently, it does not extend sufficiently far downstream to include the zone aggradation that would be expected to be found below a degrading reach.

The overall amounts of stage lowering at the mainstem stations are similar, and taken together they indicate that the bed has degraded by between 4 and 6 ft. In interpreting the overall record, however, it should be borne in mind that the data in Figure 8 represent different periods of record. The years of record at the mainstem gauging stations in Figure 8 are (from upstream to downstream):

Yankton – 22
Gayville – 42
Maskell - 42

It is probable that, had the Yankton gauge record extended back to 1956 (as at Gayville and Maskell), it would indicate a greater degree of incision than the other two stations.

The periods of record for the stations on tributaries to this reach are too short to draw anything but indicative conclusions. However, the 13-year record for the James River establishes that stages were decreasing during the 1980s in response to degradation in the mainstem. Similarly, the 16-year record for the Vermillion River (1983-1999) places the station within the zone affected by basal lowering in the mainstem as it too has experienced degradation by 4 to 6 ft.

Comparison to the Results of Earlier Studies

Other studies have investigated the trends in various channel parameters in response to closure of the dam and their results are summarised in Table 4. The results of these earlier studies support the finding of the specific gauge analysis performed in the present study that degradation has occurred throughout the study reach.

Table 4: Summary Table of Gavins Point Aggradation/Degradation Characteristics - RM 811-753

Variables	Agg/Deg	Description	1960 RM	Source
WSE	D	Greatest decrease in elevation occurs in the first 21 miles downstream of the dam, throughout the period 1956-1994, for the common discharge of 30,000 cfs	811-790	USACE (1997)
WSE	D	Elevations continue to decrease downstream of RM 790, but at a lower rate throughout the period 1956-1994, for the common discharge of 30,000 cfs	790-753	USACE (1997)

TE	D	Elevations at 10,000, 20,000 & 30,000 cfs were obtained. From 1956-1980 they decreased by a 7-8 ft for all discharges. For 1980-present they decreased by a further 1-2 ft	811-753	USACE (1986)
ABE	D	Bed elevations decreased throughout the reach	811-753	USACE (1986)
GS	D	Grain size coarsens with time. Size also slightly decreases in the downstream direction	811-795	USACE (1986)
GS	D	Very small decrease in grain size in the downstream direction	795-753	USACE (1986)

WSE = Water Surface Elevation ABE = Average Bed Elevation
TE = Thalweg Elevation GS = Grain Size

According to USACE (1997) thalweg elevations for a range of discharges decreased by 7-8 ft between 1956 and 1986. After that period, degradation continued but at a mush slower rate, to produce 1-2 ft of lowering between 1986 and the present. This suggests that degradation was somewhat more severe than would be inferred from Figure 8 (which suggests 4-6 ft of lowering between 1956 and 1997) However, it must be borne in mind that the USACE data refer to lowering of the thalweg rather than the water surface. USACE (1986) state that average bed elevations also decreased throughout the study reach though, unfortunately, they provide no measurements that could be used for direct comparison to the specific gauge record.

USACE (1997) report that reductions in the water surface elevation (for a discharge of 30,000 cfs) between 1956 and 1994 were greatest close to the Gavins Point Dam. Specifically, they report that reductions in WSE were higher between river miles 811 and 790 than between RM 790 and RM 753. This differs from the impression given by Figure 8, which shows very little difference in stage lowering at 30,000 cfs between Maskell (RM 775.8) and Gayville (RM 796). The figure for Yankton cannot be directly compared unfortunately as the specific gauge records only begins in 1974.

USACE (1986) report measurements of bed material size in the study reach. Their findings indicate that the grain size coarsened markedly in the upper part of the reach, close to the dam (RM 811 – RM 795) which is consistent with bed scour and selective entrainment due to degradation. Coarsening was present but was less marked further downstream (RM 795 – RM 753) suggesting that degradation extended throughout the reach but that the intensity of bed scouring decreased downstream.

Conclusions

The results of the specific gauge analysis and those of earlier studies clearly indicate that degradation has occurred throughout the Gavins Point Reach. The limited evidence available from gauging stations on the James and Vermillion Rivers suggest that degradation has also affected the tributaries in this reach.

Observations and records of thalweg and water surface elevations reported in past studies indicate that the rate and amount of degradation both decrease with distance downstream from the dam. This is neither corroborated or refuted by the findings of the specific gauge analysis, due to the short gauging record available at the Yankton gauge which prevents comparison of overall stage lowering close to the dam with data

for stations farther downstream. Measurements of bed material size indicate that coarsening with time has been most marked close to the dam and that bed material fines with distance downstream. All the available evidence is consistent with the conclusion that degradation in this reach has resulted from morphological response to closure of the dam.

Those specific gauge records that extend to the present all indicate that stages are continuing to decrease. For example, Figure B28 indicates that stage lowering was on-going when the record ceased in 1995, while Figures B30, B31 and B32 show stages lowering in 1997, following a period of relative stability in the early 1990s. It is unfortunate that the gauge record for the Missouri River near Ponca (figure B33) ends in 1980 as it would have been very useful to compare conditions at this downstream station (RM 751) with those upstream.

Taken together, the results presented herein suggest that degradation in response to the closure of Gavins Point Dam is continuing throughout the study reach. Short-term rates of incision vary cyclically, but show no sustained tendency to decrease through time. On this basis it may be concluded that the Fort Randall Reach has not attained a condition of dynamic equilibrium and that it is unlikely to do so in the near future.

References

Dangberg, D. & Assoc. and River Pro's (1988a), Missouri River, Fort Peck Dam: Downstream Degradation/Aggradation and Sediment Trends Study. USACE, Omaha District.

Dangberg, D. & Assoc. and River Pro's (1988b), Missouri River: Fort Randall Dam – Downstream degradation/aggradation and sediment trends study. USACE Omaha District

Midwest International, Inc. (1997), Fort Peck Project, Montana: Downstream Channel and Sediment Trends Study. USACE, Omaha District.

USACE (1986), Missouri River Streambank Erosion Study, Fort Peck Dam, Montana, to the Yellowstone River, N. Dakota. USACE, Omaha District.

U.S. Army Engineer Division, Northwestern, Missouri River Region (1994), Missouri River Master Water Control Manual, Review and Update, Draft Environmental Impact Statement, Volume 5: Aggradation, Degradation and Water Quality Conditions. Omaha District, USACE.

Watson, C.C, Biedenharn, D.S. and Scott, S.H. (1999), Channel Rehabilitation: Processes, Design and Implementation. Draft, July, 1999. U.S. Army Engineer Research and Development Centre, Vicksburg, Mississippi.

WEST Consultants, Inc. (1998) Final Report. Missouri River: Fort Randall Dam to Gavins Point Dam and Ponca Creek Aggradation Assessment. USACE, Omaha District.

Figure 1: Fort Peck Reach - Location of Gauging Stations

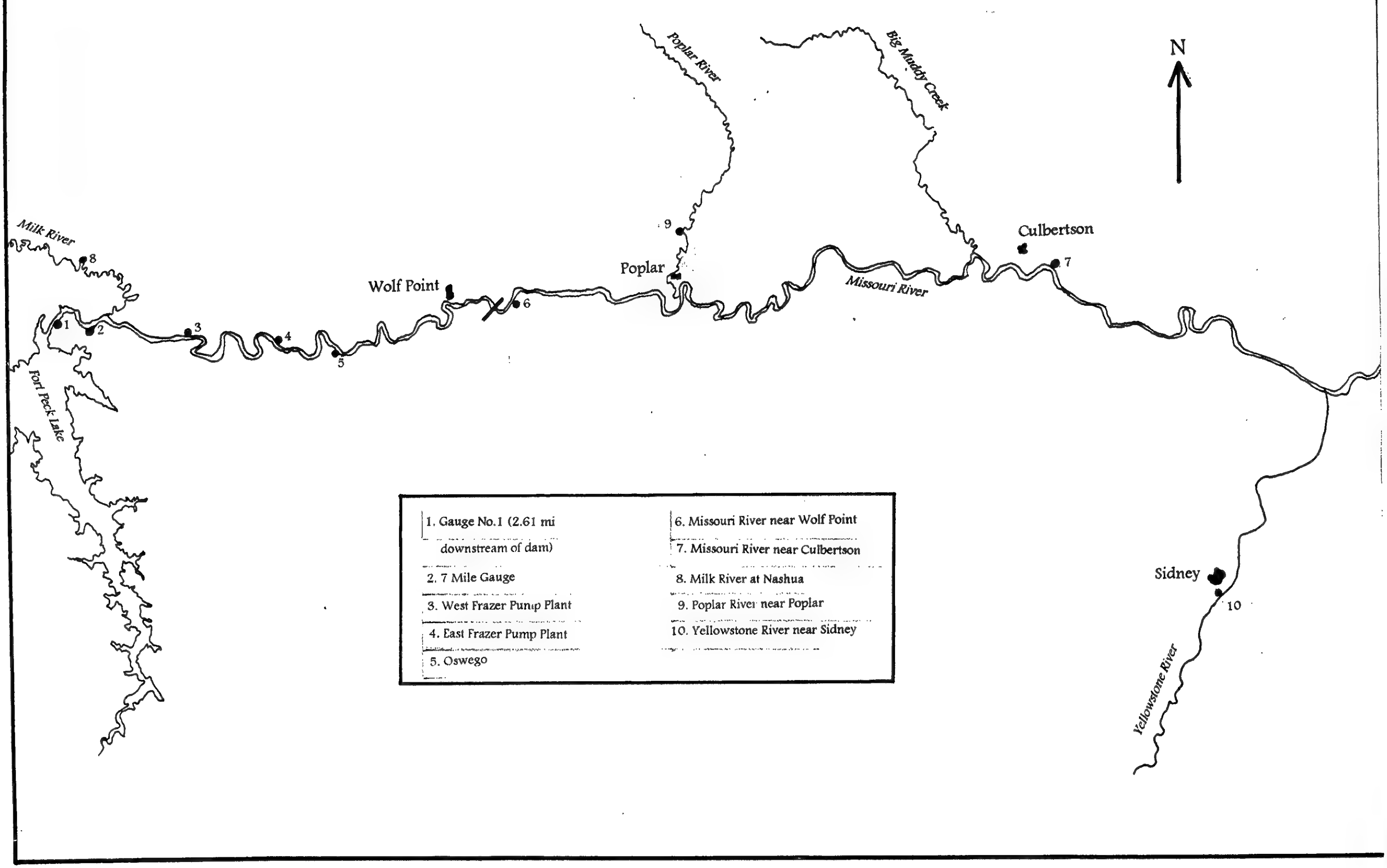

Figure 2: Summary of Specific Gauge Bed Elevation Changes in Fort Peck Reach, RM 1771-1582

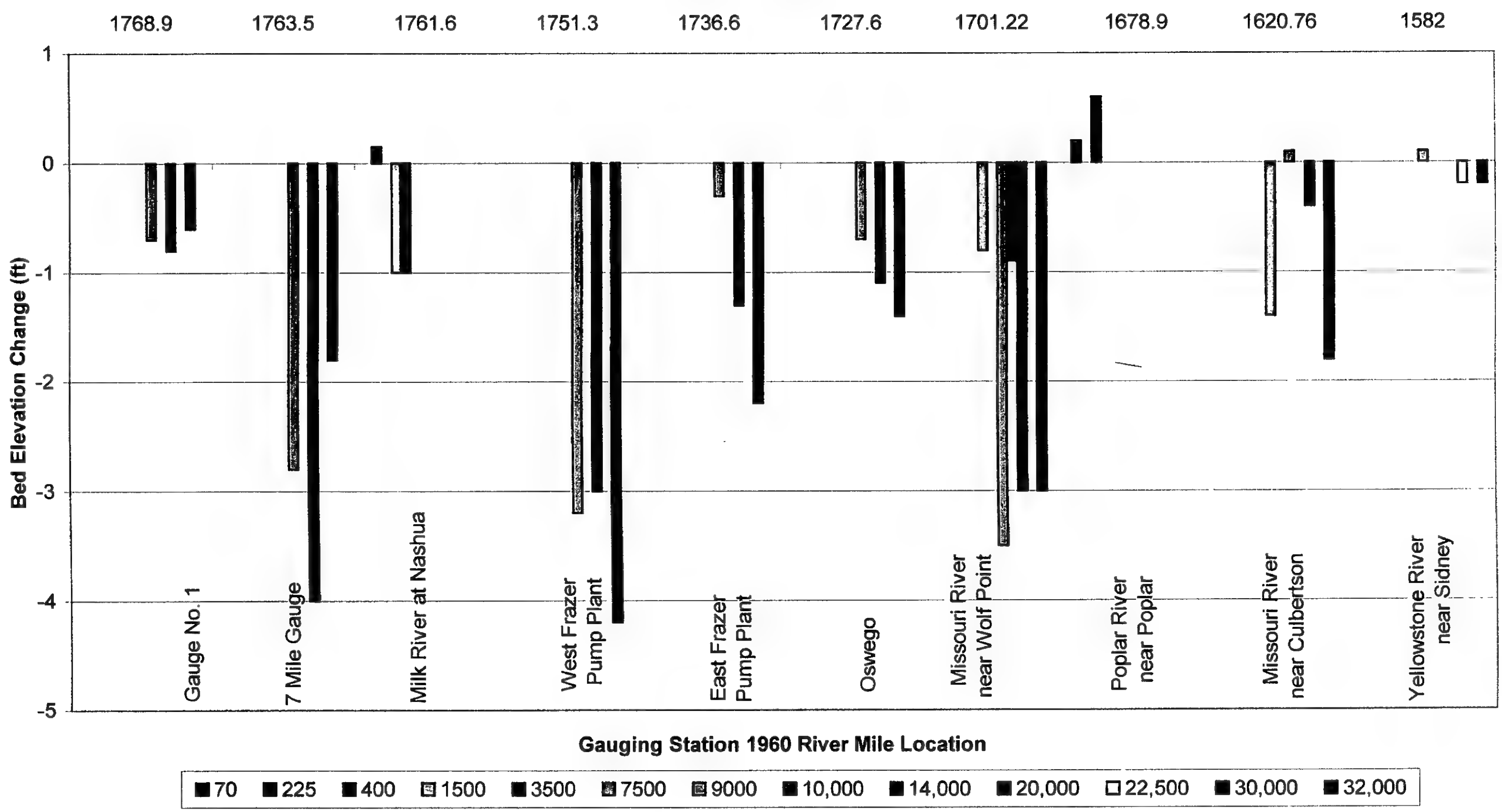

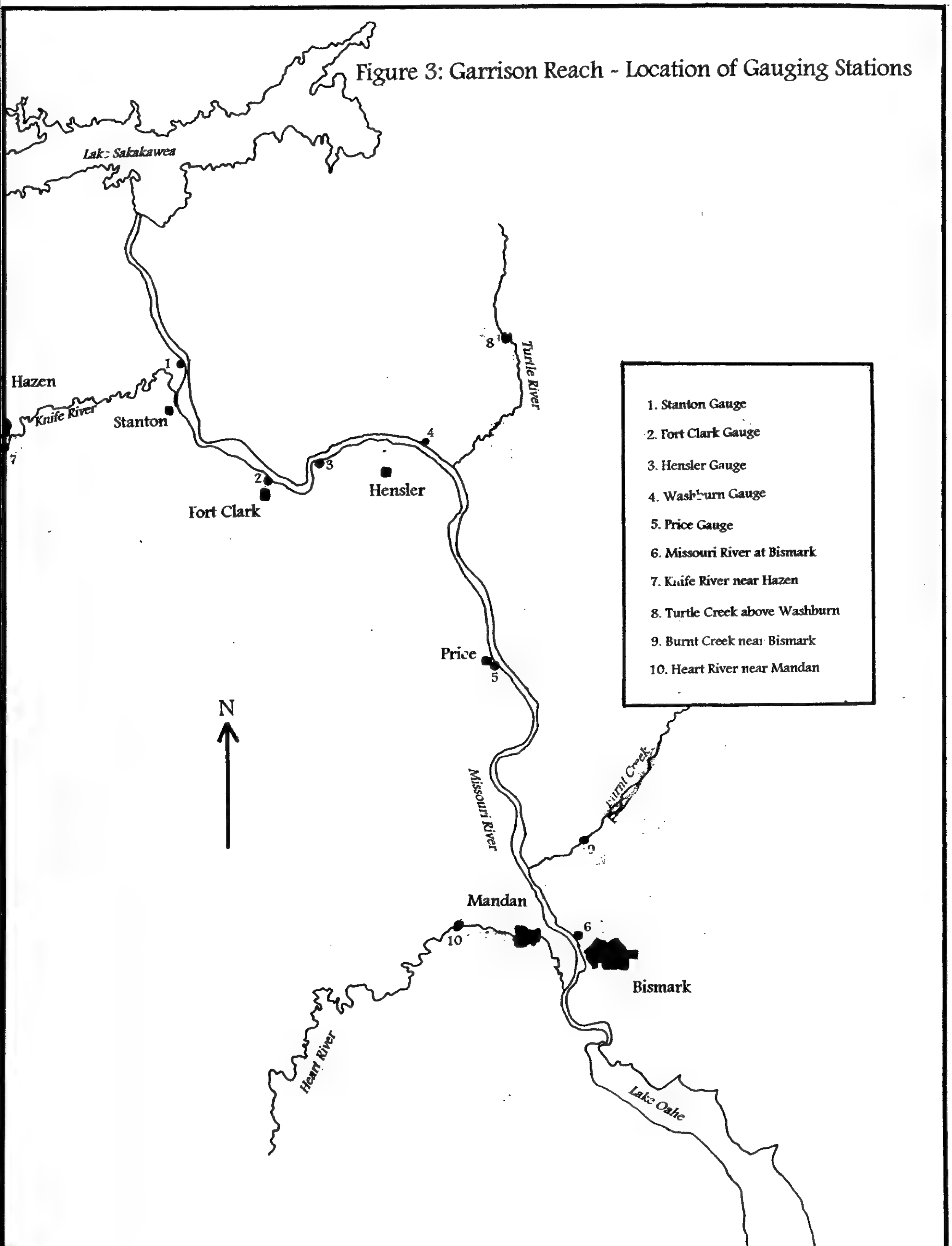

Figure 3: Garrison Reach - Location of Gauging Stations
Lake Sakakawea
Hazen
Knife River
Stanton
Fort Clark
Hensler
Turtle River
Price
Missouri River
Burnt Creek
Mandan
Bismark
Heart River
Lake Oahe
N
1. Stanton Gauge
2. Fort Clark Gauge
3. Hensler Gauge
4. Washburn Gauge
5. Price Gauge
6. Missouri River at Bismark
7. Knife River near Hazen
8. Turtle Creek above Washburn
9. Burnt Creek near Bismark
10. Heart River near Mandan

Figure 4: Summary of Specific Gauge Bed Elevation Changes in Garrison Reach

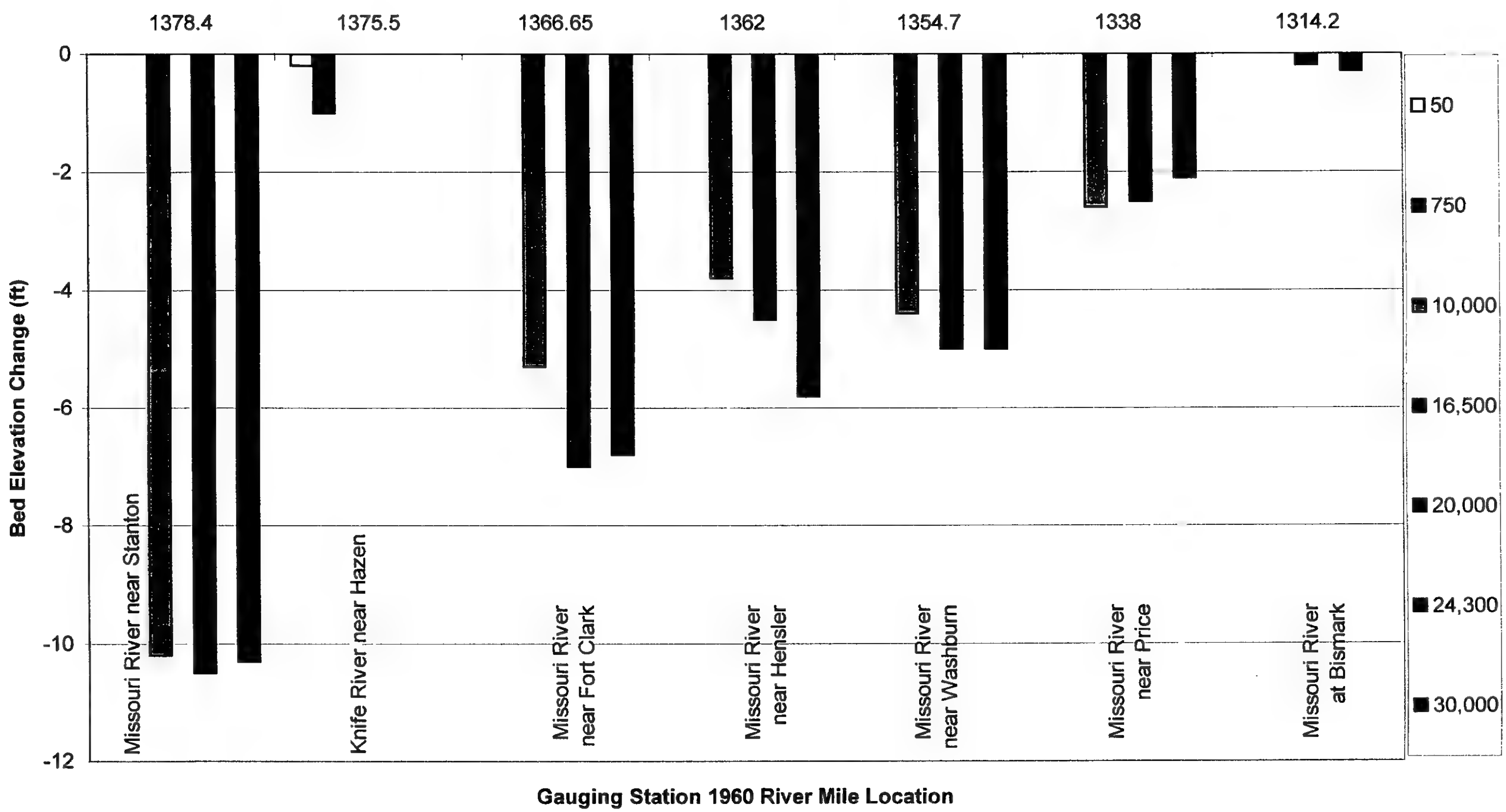

Figure 5: Fort Randall Reach ~ Location of Gauging Stations

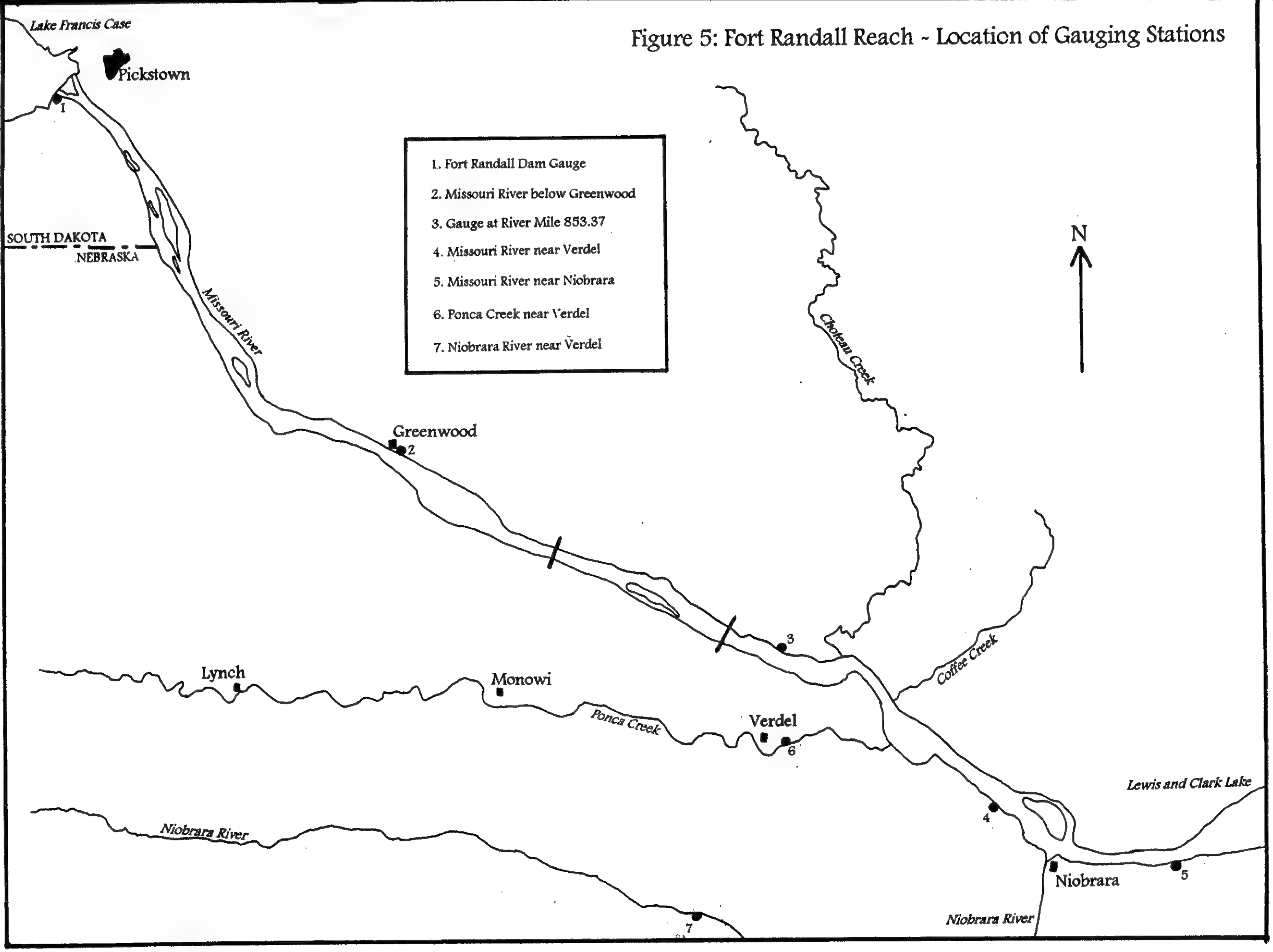

Figure 6: Summary of Specific Gauge Bed Elevation Changes in Fort Randall Reach

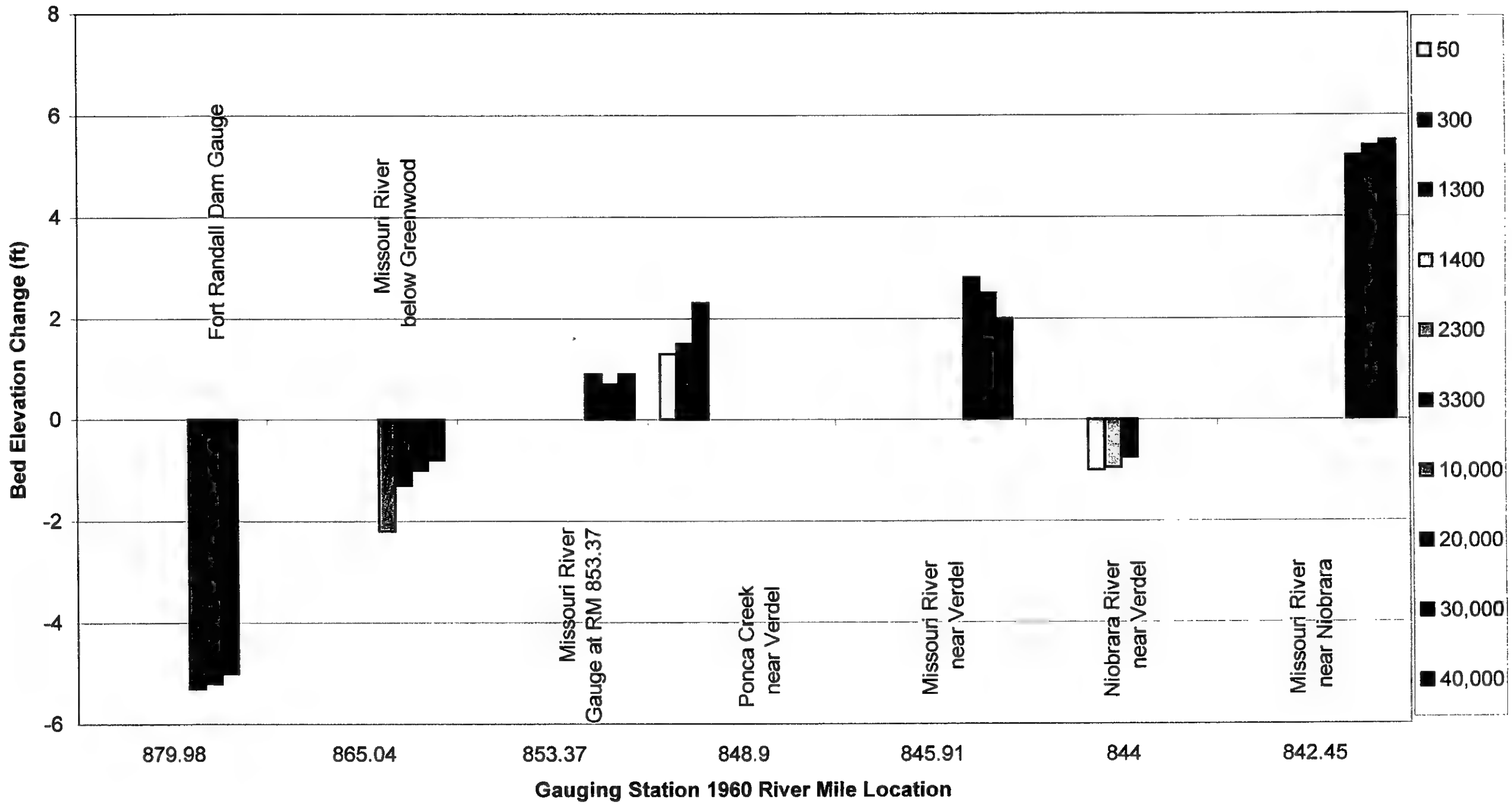

Figure 7: Gavins Point Reach - Location of Gauging Stations

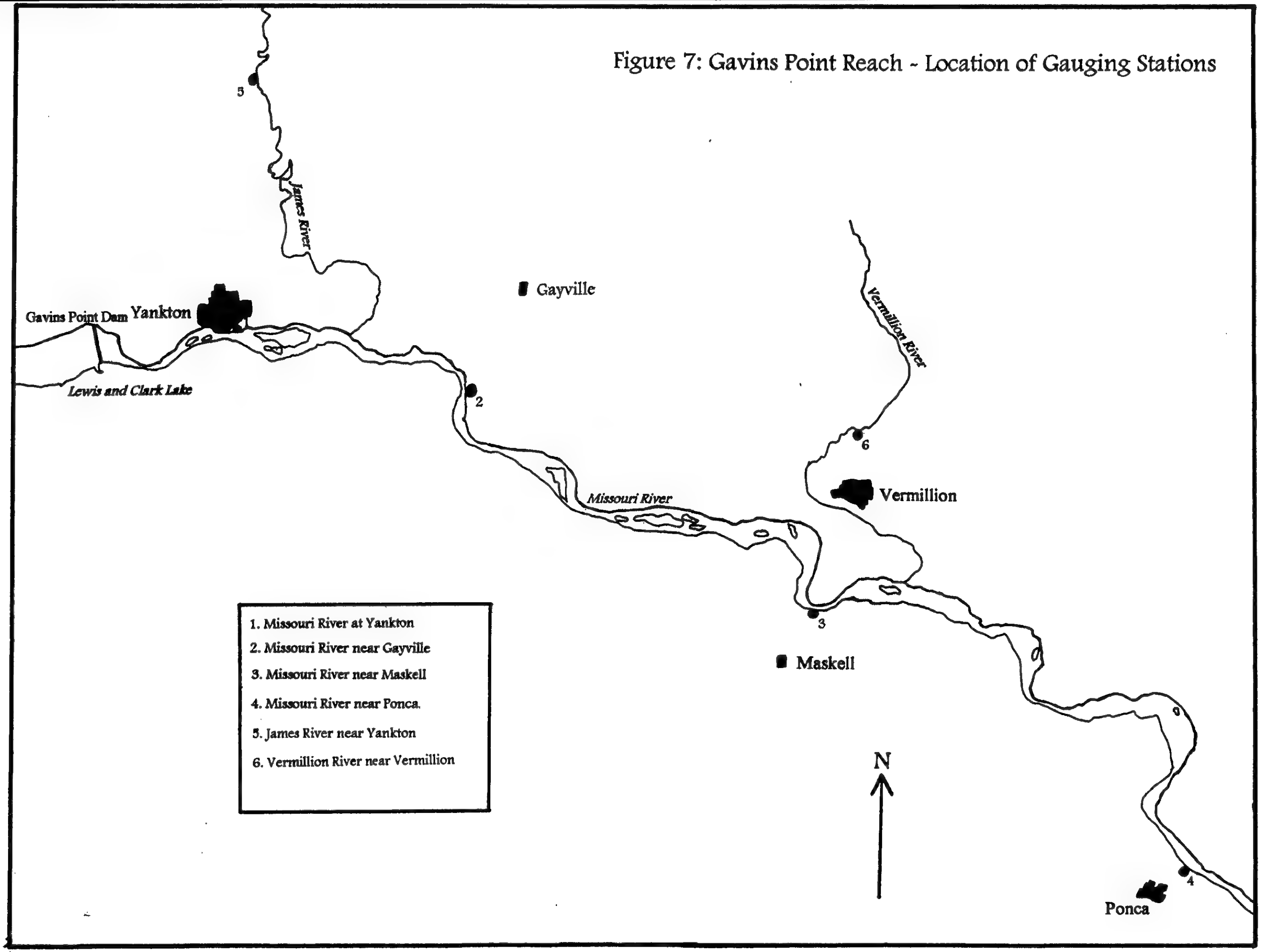

Figure 8: Summary of Specific Gauge Bed Elevation Changes in Gavins Point Reach

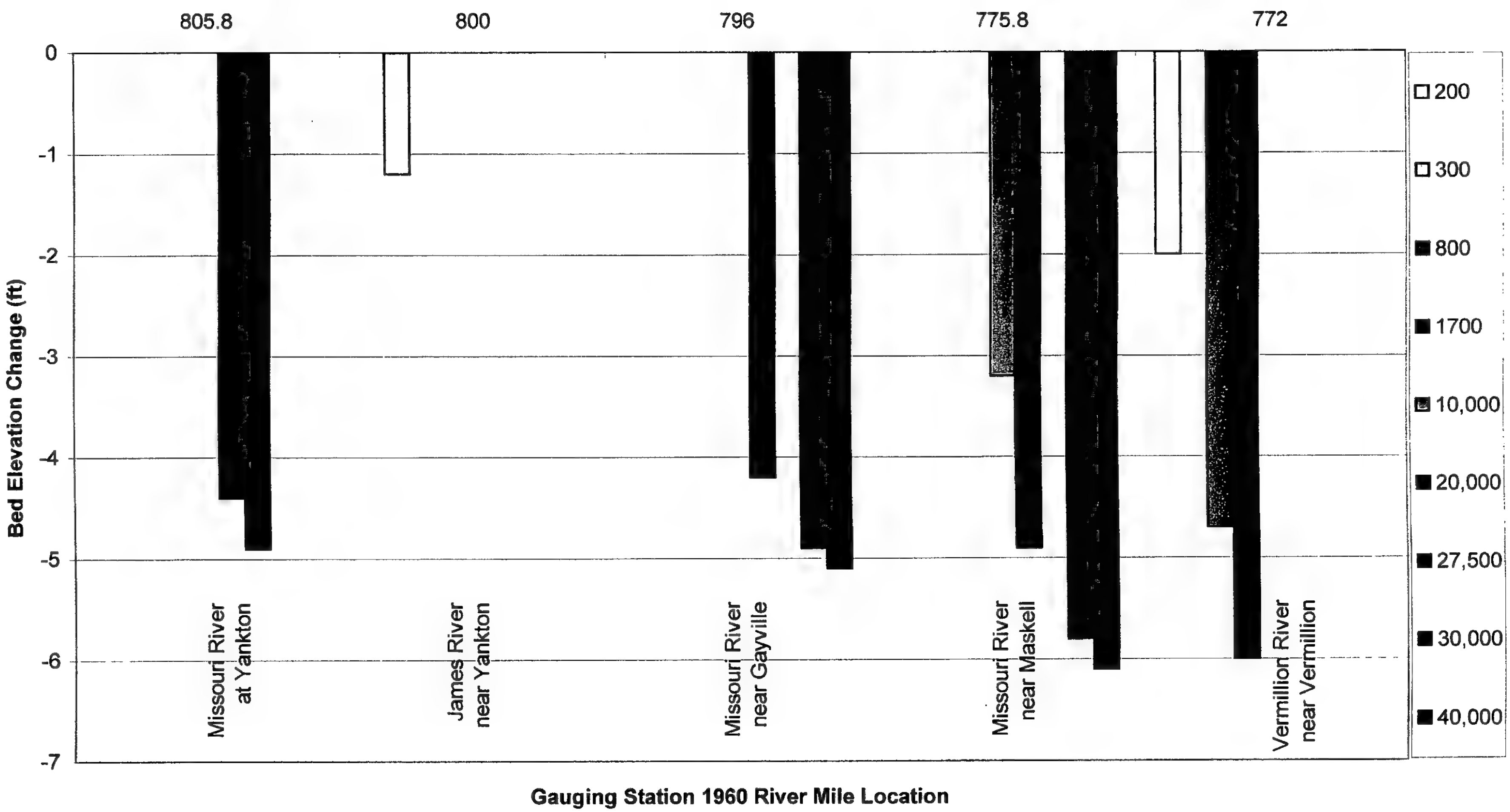

Table A1: Fort Peck Reach - Summary of Bed Elevation Change

Station Name	1960 River Mile	Discharge (cfs)	Total Change in Elevation (ft)	Years of Record
Gauge No.1	1768.9	10,000	-0.7	1950-1975
		20,000	-0.8	1950-1975
		30,000	-0.6	1950-1975
7 Mile Gauge	1763.5	10,000	-2.8	1950-1984
		20,000	-4.0	1950-1984
		30,000	-1.8	1950-1966
Milk River at Nashua	1761.6	225	0.15	1978-1998
		1500	-1.0	1984-1998
		3500	-1.0	1984-1998
West Frazer Pump Plant	1751.3	10,000	-3.2	1950-1984
		20,000	-3.0	1950-1984
		30,000	-4.2	1950-1984
East Frazer Pump Plant	1736.6	10,000	-0.3	1950-1984
		20,000	-1.3	1950-1984
		30,000	-2.2	1950-1984
Oswego	1727.6	10,000	-0.7	1950-1966
		20,000	-1.1	1950-1966
		30,000	-1.4	1950-1966
Missouri River near Wolf Point	1701.22	7500	-0.8	1977-1999
		10,000	-3.5	1950-1999
		14,000	-0.9	1975-1999
		20,000	-3.0	1950-1984
		30,000	-3.0	1950-1984
Poplar River near Poplar	1678.9	70	0.2	1984-1999
		400	0.6	1984-1999
Missouri River near Culbertson	1620.76	7500	-1.4	1985-1998
		10,000	0.1	1950-1998
		20,000	-0.4	1950-1984
		30,000	-1.8	1950-1984
Yellowstone River near Yellowstone	1582	9000	0.1	1976-1999
		22500	-0.2	1974-1999
		32000	-0.2	1974-1999

Table A2: Garrison Reach - Summary of Bed Elevation Change

Station Name	1960 River Mile	Discharge (cfs)	Total Change in Elevation (ft)	Years of Record
Missouri River near Stanton	1378.4	10,000	-10.2	1950-1997
		20,000	-10.5	1950-1997
		30,000	-10.3	1950-1997
Knife River near Hazen	1375.5	50	-0.2	1987-1999
		750	-1.0	1990-1999
Missouri River near Fort Clark	1366.65	10,000	-5.3	1960-1997
		20,000	-7.0	1960-1997
		30,000	-6.8	1960-1997
Missouri River near Hensler	1362	10,000	-3.8	1959-1997
		20,000	-4.5	1959-1997
		30,000	-5.8	1959-1997
Missouri River near Washburn	1354.7	10,000	-4.4	1955-1997
		20,000	-5.0	1955-1997
		30,000	-5.0	1955-1997
Missouri River near Price	1338	10,000	-2.6	1960-1986
		20,000	-2.5	1960-1986
		30,000	-2.1	1960-1986
Missouri River at Bismark	1314.2	16,500	-0.2	1987-1999
		24,300	-0.3	1989-1999

Table A3: Fort Randall Reach - Summary of Bed Elevation Change

Station Name	1960 River Mile	Discharge (cfs)	Total Change in Elevation (ft)	Years of Record
Fort Randall Dam Gauge	879.98	10,000	-5.3	1953-1986
		20,000	-5.2	1953-1986
		30,000	-5.0	1953-1986
Missouri River below Greenwood	865.04	10,000	-2.2	1966-1987
		20,000	-1.3	1967-1987
		30,000	-1.0	1966-1987
		40,000	-0.8	1967-1987
Missouri River Gauge at RM 853.37	853.37	20,000	0.9	1960-1972
		30,000	0.7	1960-1972
		40,000	0.9	1960-1972
Ponca Creek near Verdel	848.9	50	1.3	1957-1998
		300	1.5	1957-1998
		1300	2.3	1960-1998
Missouri River near Verdel	845.91	20,000	2.8	1964-1985
		30,000	2.5	1964-1985
		40,000	2.0	1964-1985
Niobrara River near Verdel	844	1400	-1.0	1958-1997
		2300	-0.95	1958-1997
		3300	-0.75	1958-1997
Missouri River near Niobrara	842.45	20,000	5.2	1956-1985
		30,000	5.4	1956-1985
		40,000	5.5	1956-1985

Table A4: Gavins Point Reach - Summary of Bed Elevation Change

Station Name	1960 River Mile	Discharge (cfs)	Total Change in Elevation (ft)	Years of Record
Missouri River at Yankton	805.8	20,000	-4.4	1973-1995
		27,500	-4.9	1973-1995
James River near Yankton	800	300	-1.2	1982-1993
Missouri River near Gayville	796	20,000	-4.2	1955-1997
		30,000	-4.9	1955-1997
		40,000	-5.1	1955-1997
Missouri River near Maskell	775.8	10,000	-3.2	1955-1995
		20,000	-4.9	1955-1997
		30,000	-5.8	1955-1997
		40,000	-6.1	1955-1997
Vermillion River near Vermillion	772	200	-2.0	1983-1999
		800	-4.7	1983-1999
		1700	-6.0	1983-1999

Appendix A: Summary Data on Bed Elevation Change

Appendix B: Specific Gauge Plots for Mainstem and Tributary Stations

Figure B1: Fort Peck Reach: Specific Gauge Record for Gauge No. 1 (2.61 mi downstream of dam), MT - RM 1768.9

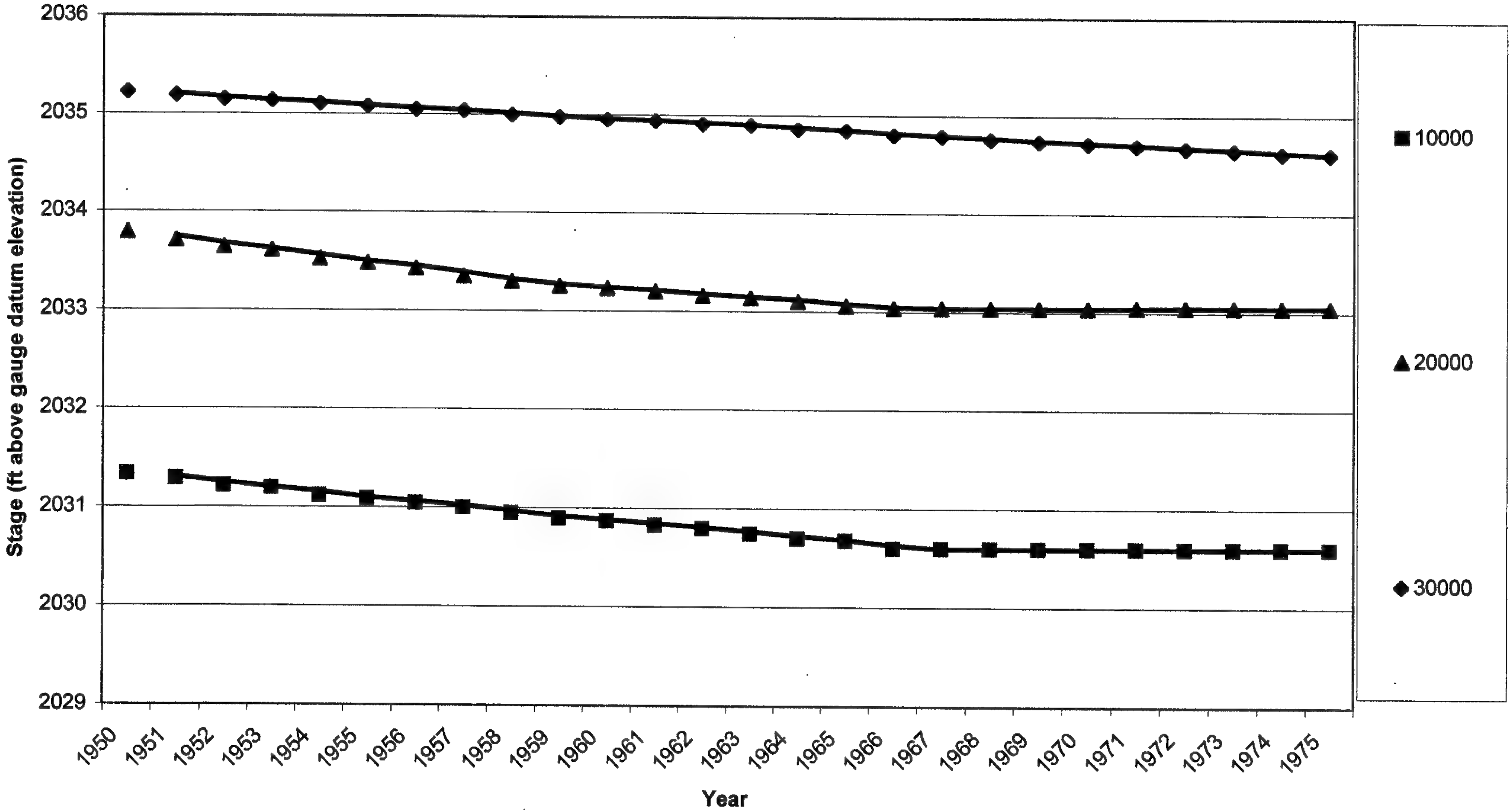

Figure B2: Fort Peck Reach: Specific Gauge Record for 7 Mile Gauge (Missouri River below Fort Peck Dam), MT - RM 1763.5

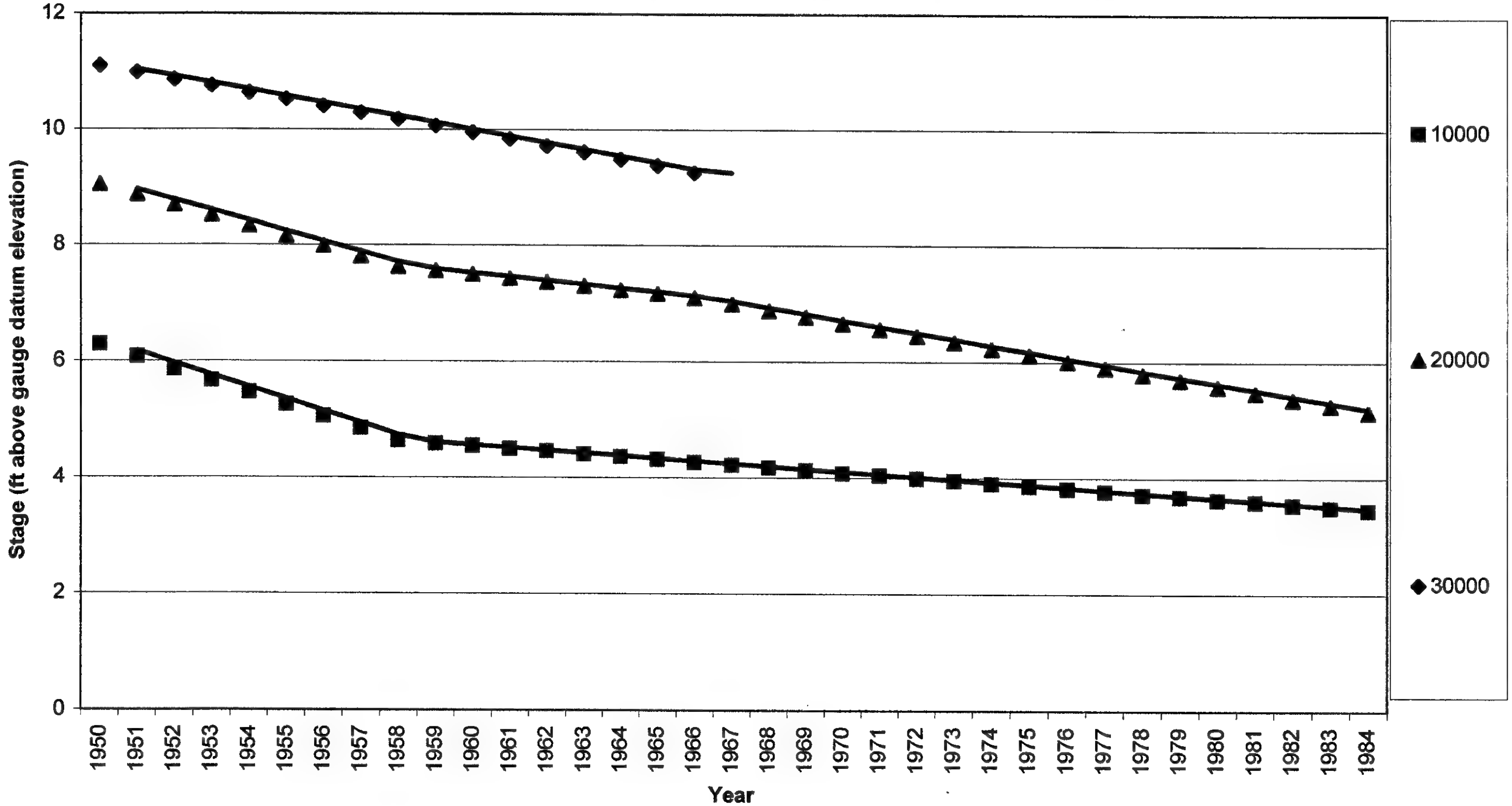

Figure B3: Fort Peck Reach: Specific Gauge Record for the Milk River at Nashua, MT - RM 1761.6

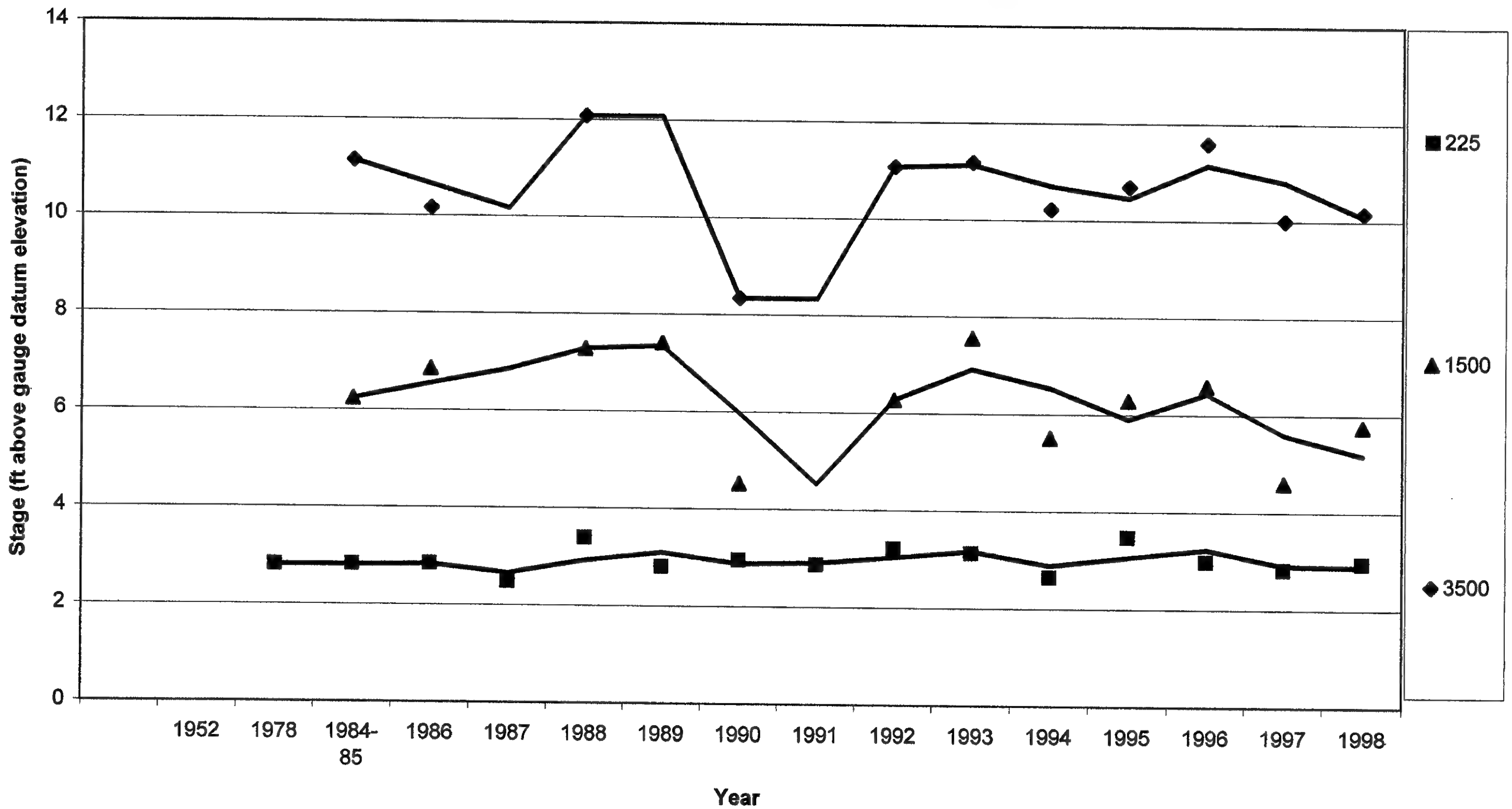

Figure B4: Fort Peck Reach: Specific Gauge Record for West Frazer Pump Plant, MT - RM 1751.3

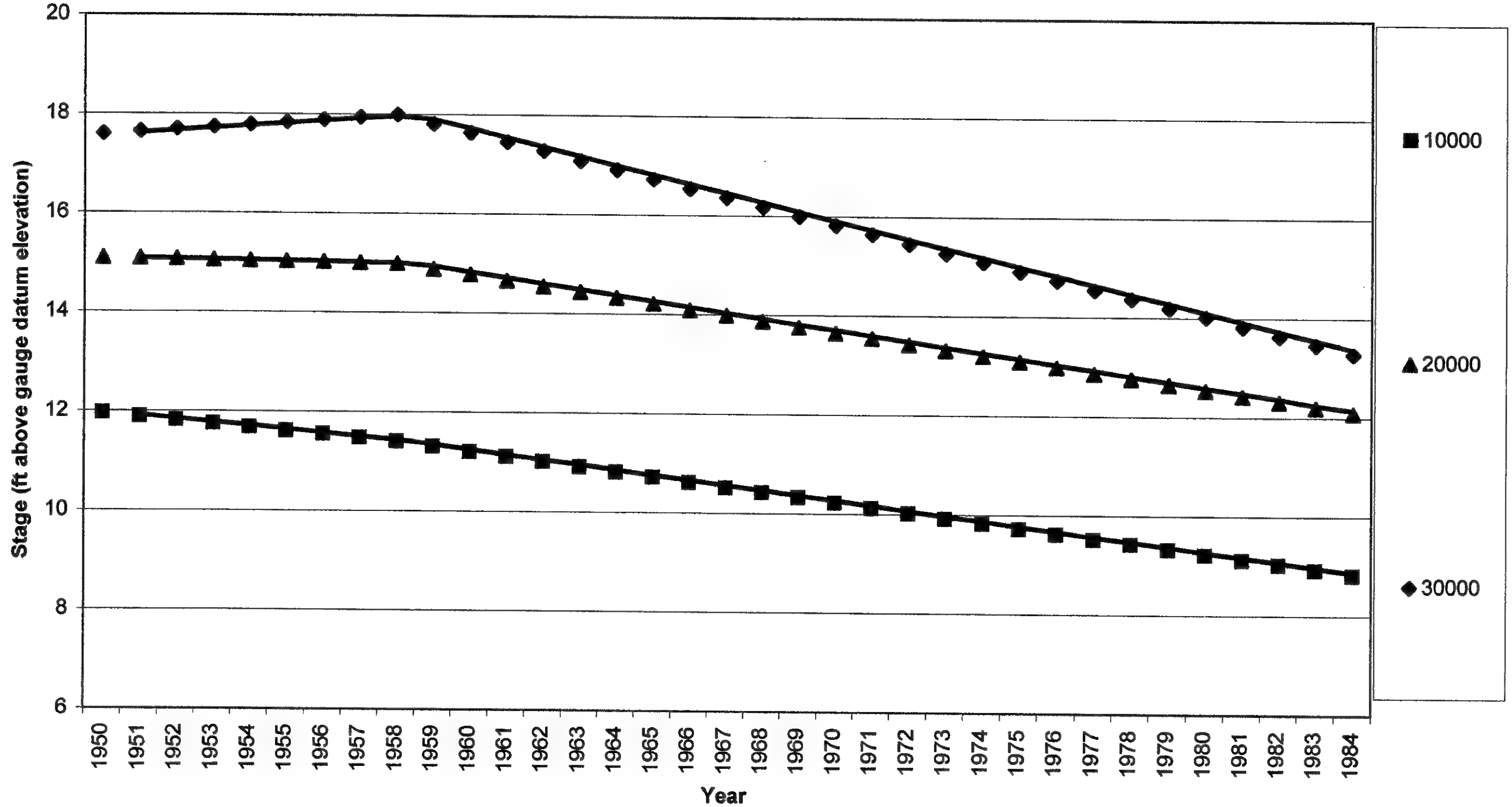

Figure B5: Fort Peck Reach: Specific Gauge Record for East Frazer Pump Plant, MT - RM 1736.6

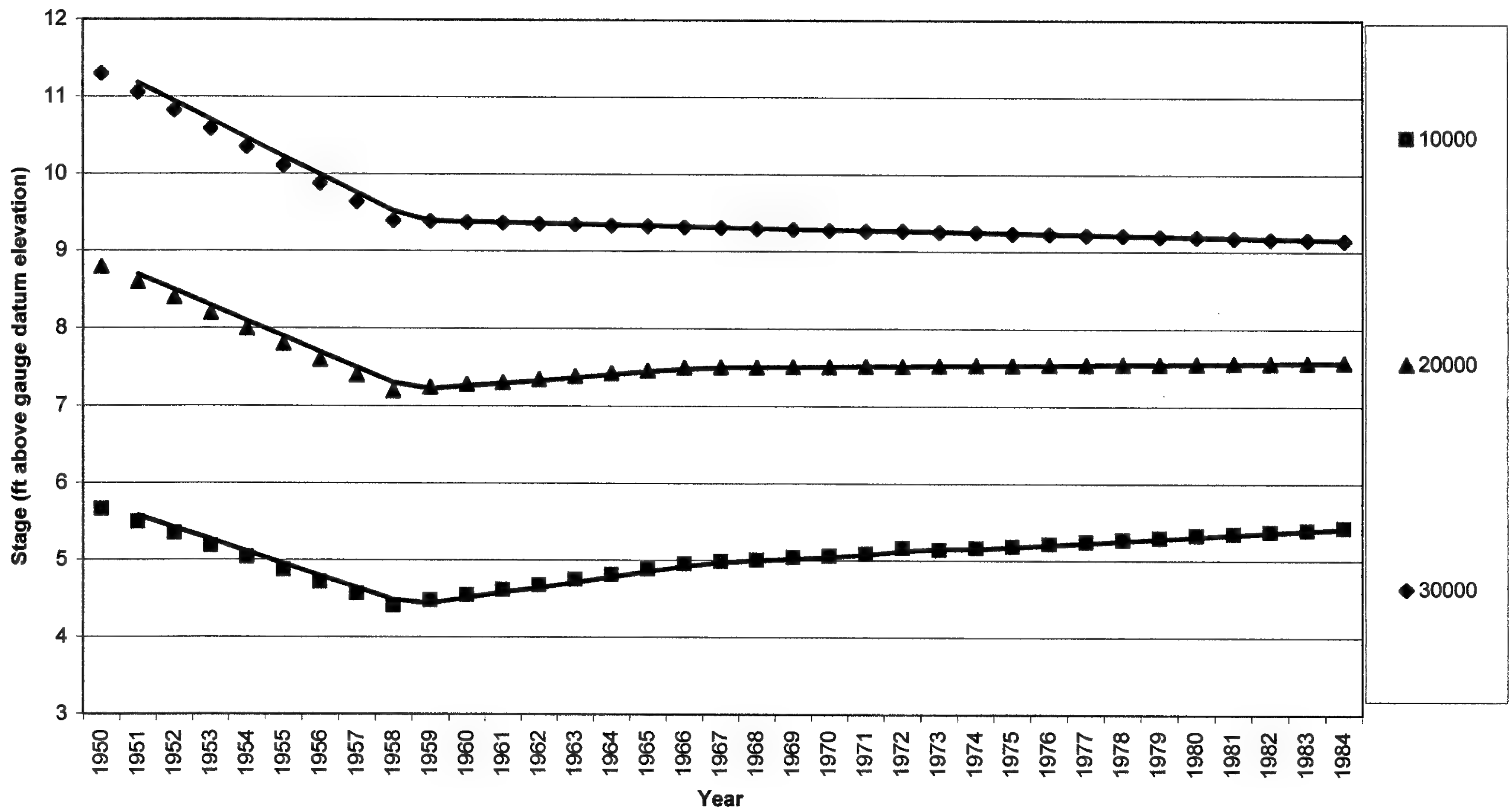

Figure B6: Fort Peck Reach: Specific Gauge Record for Oswego, MT - RM 1727.6

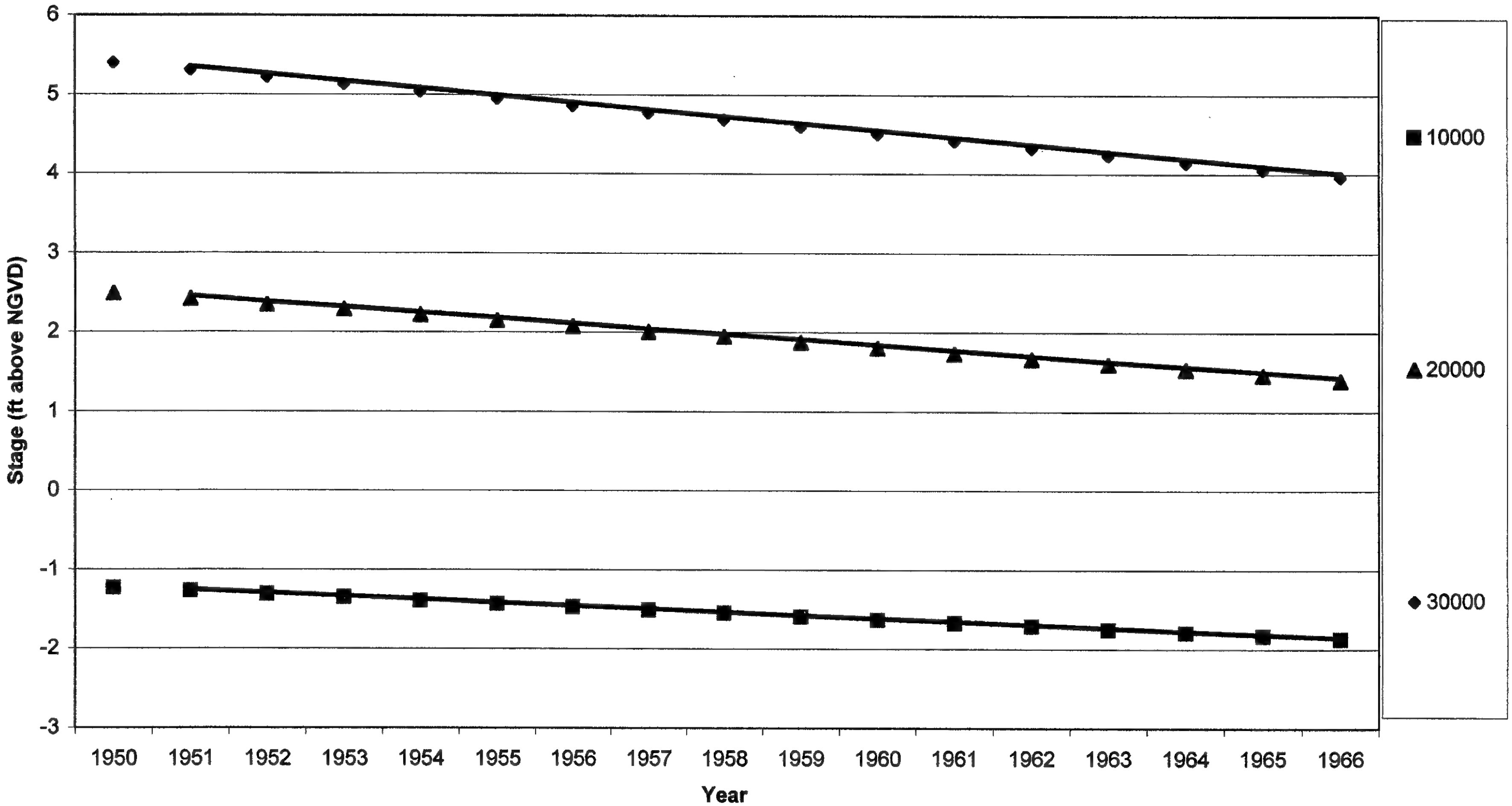

Figure B7: Fort Peck Reach: Specific Gauge Record for the Missouri River near Wolf Point, MT - RM 1701.22

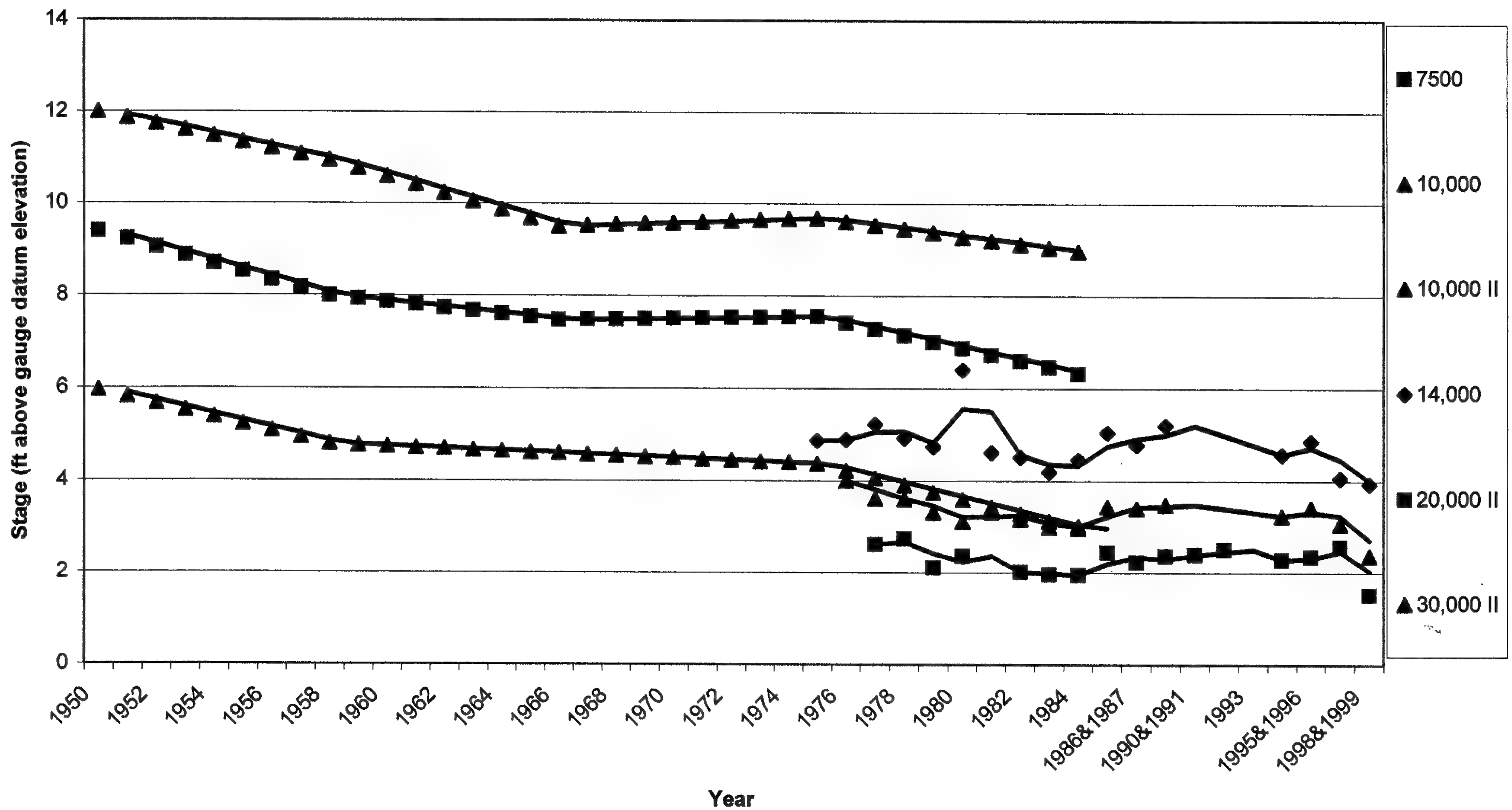

Figure B8: Fort Peck Reach: Specific Gauge Record for Poplar River near Poplar, MT - RM 1678.9

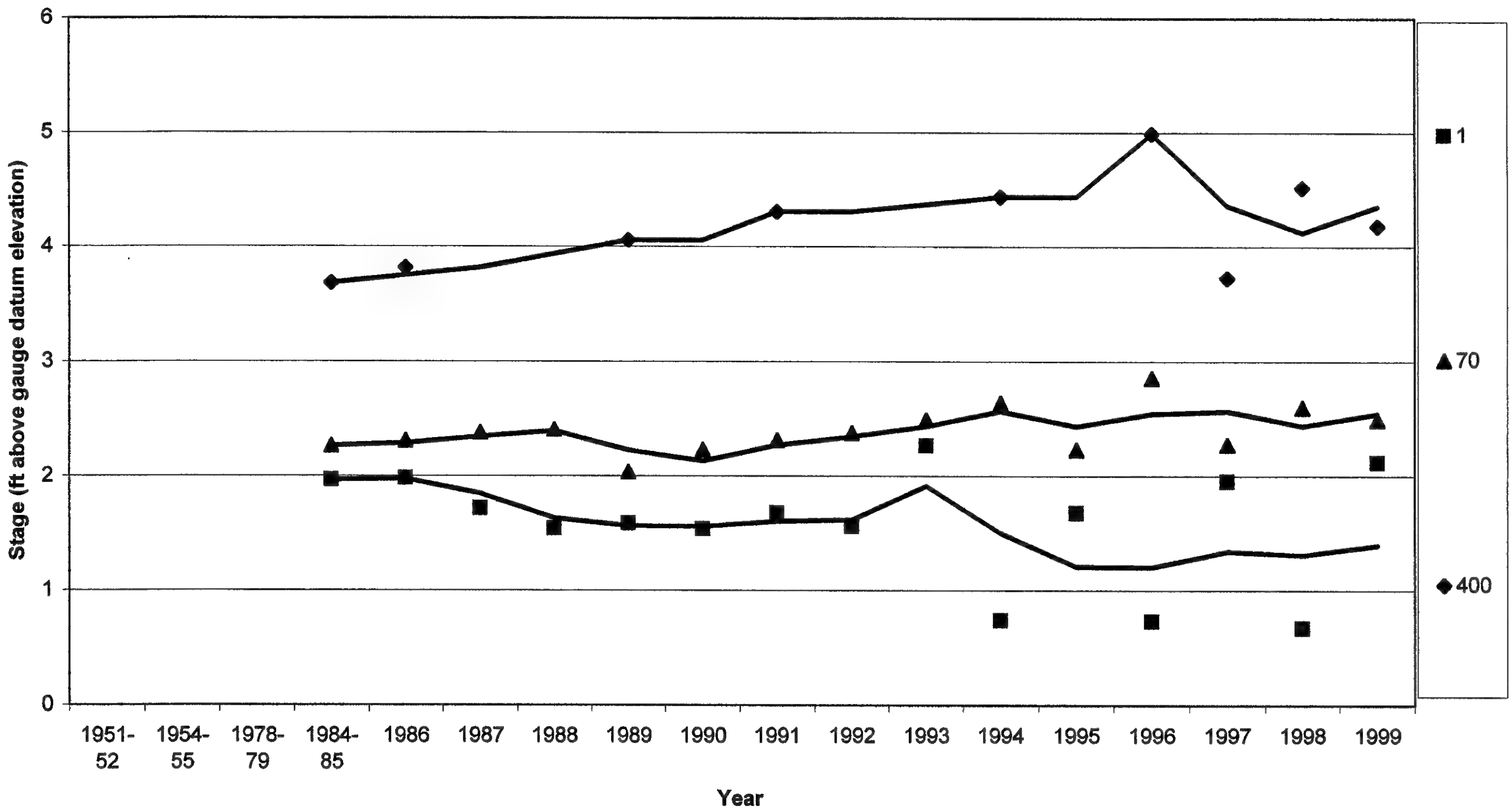

Figure B9: Fort Peck Reach: Specific Gauge Record for the Missouri River near Culbertson, MT - RM 1620.76

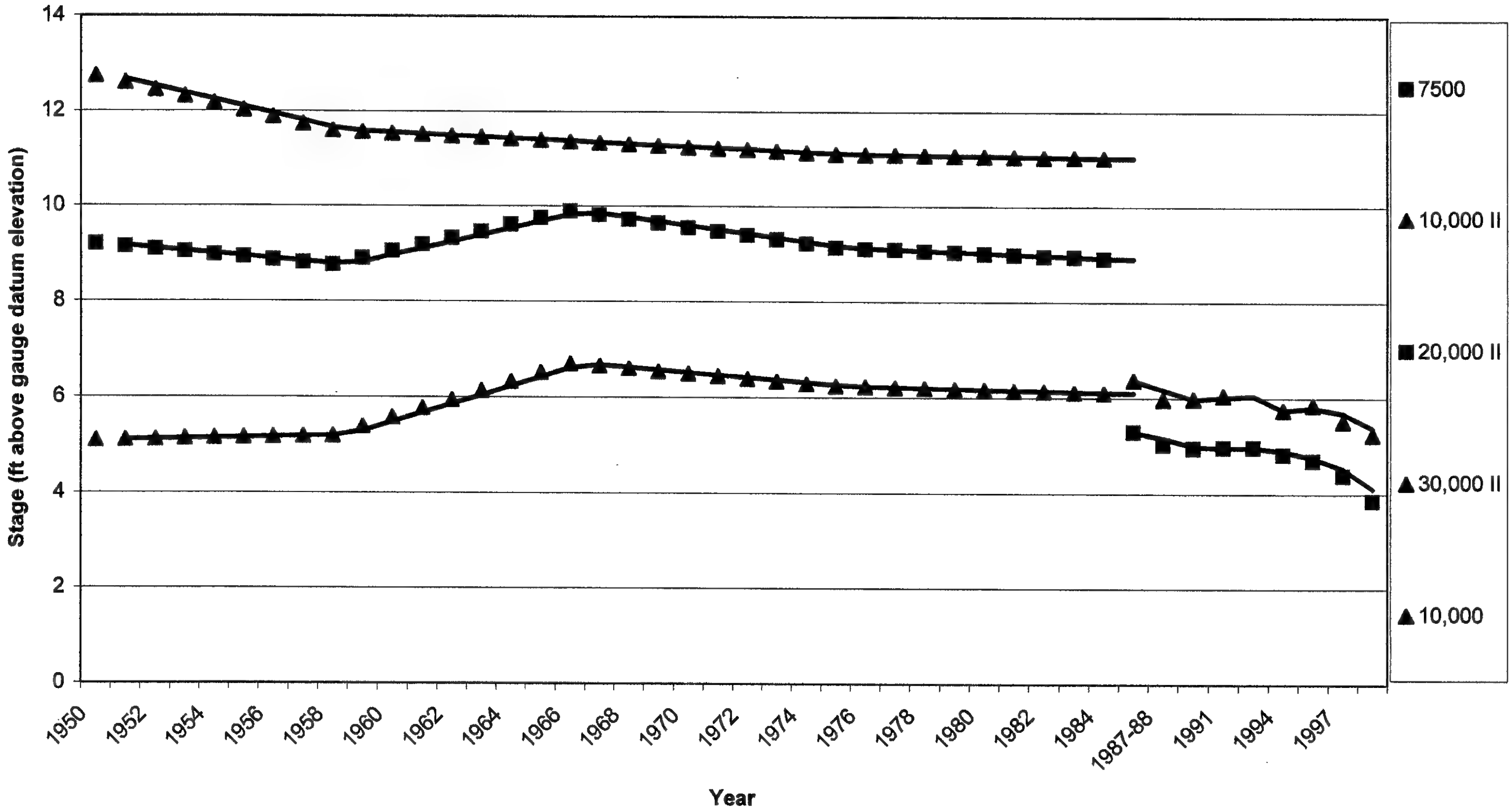

Figure 10: Fort Peck Reach: Specific Gauge Record for Yellowstone River near Sidney, MT - RM 1582

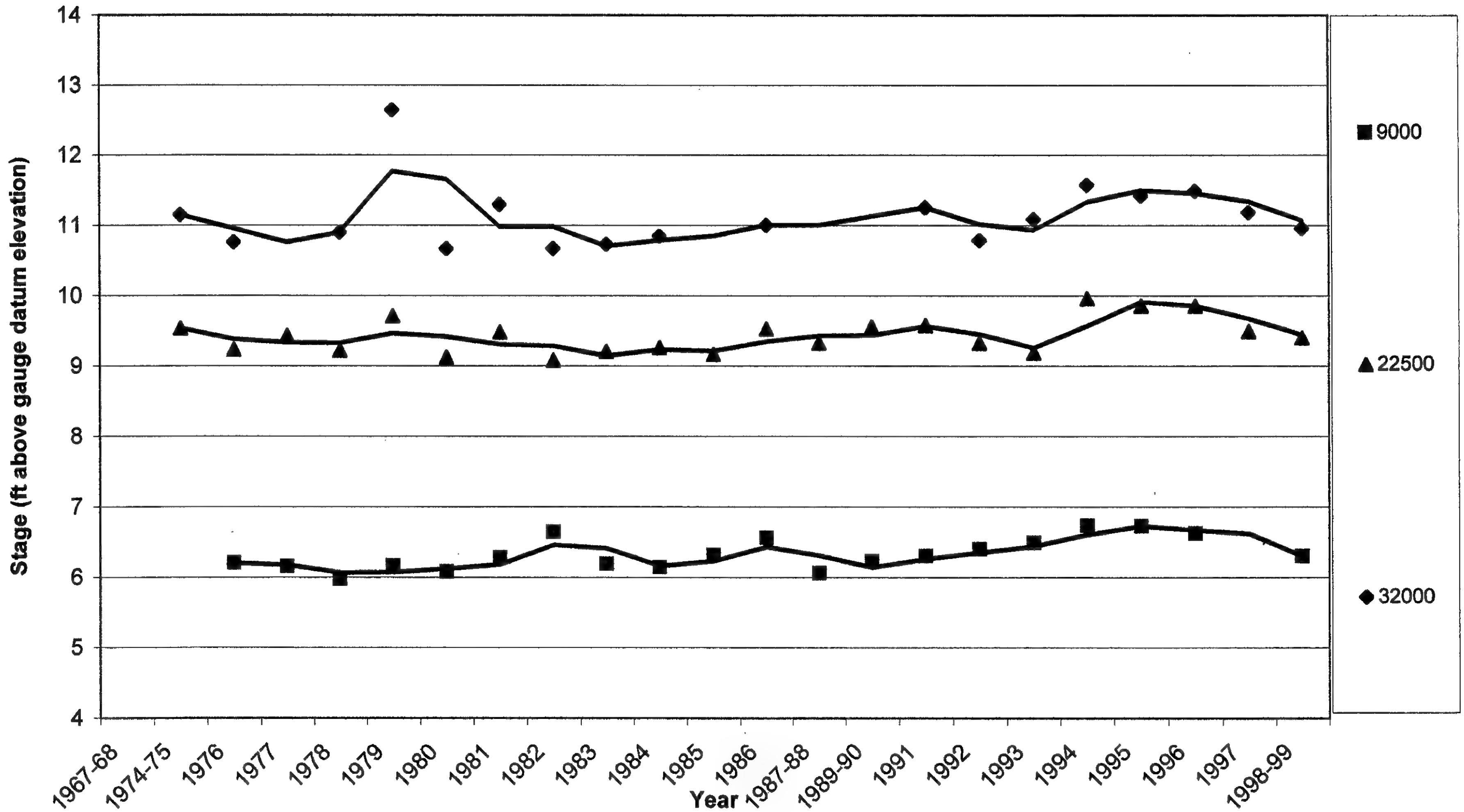

Figure B11: Garrison Reach: Specific Gauge Record for Stanton Gauge, ND - RM 1378.4

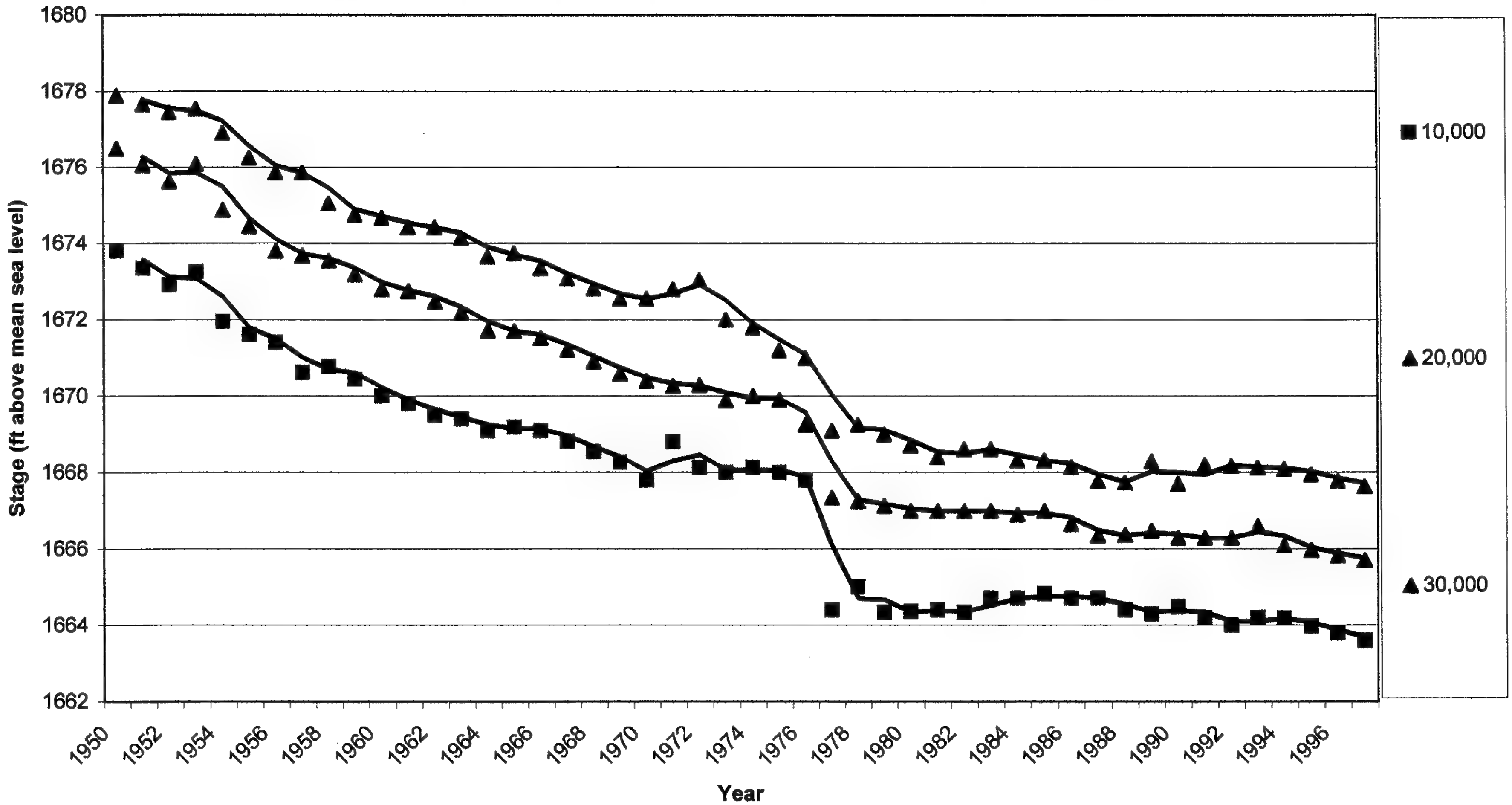

Figure B12: Garrison Reach: Specific Gauge Record for Knife River near Hazen, ND - RM 1375.5

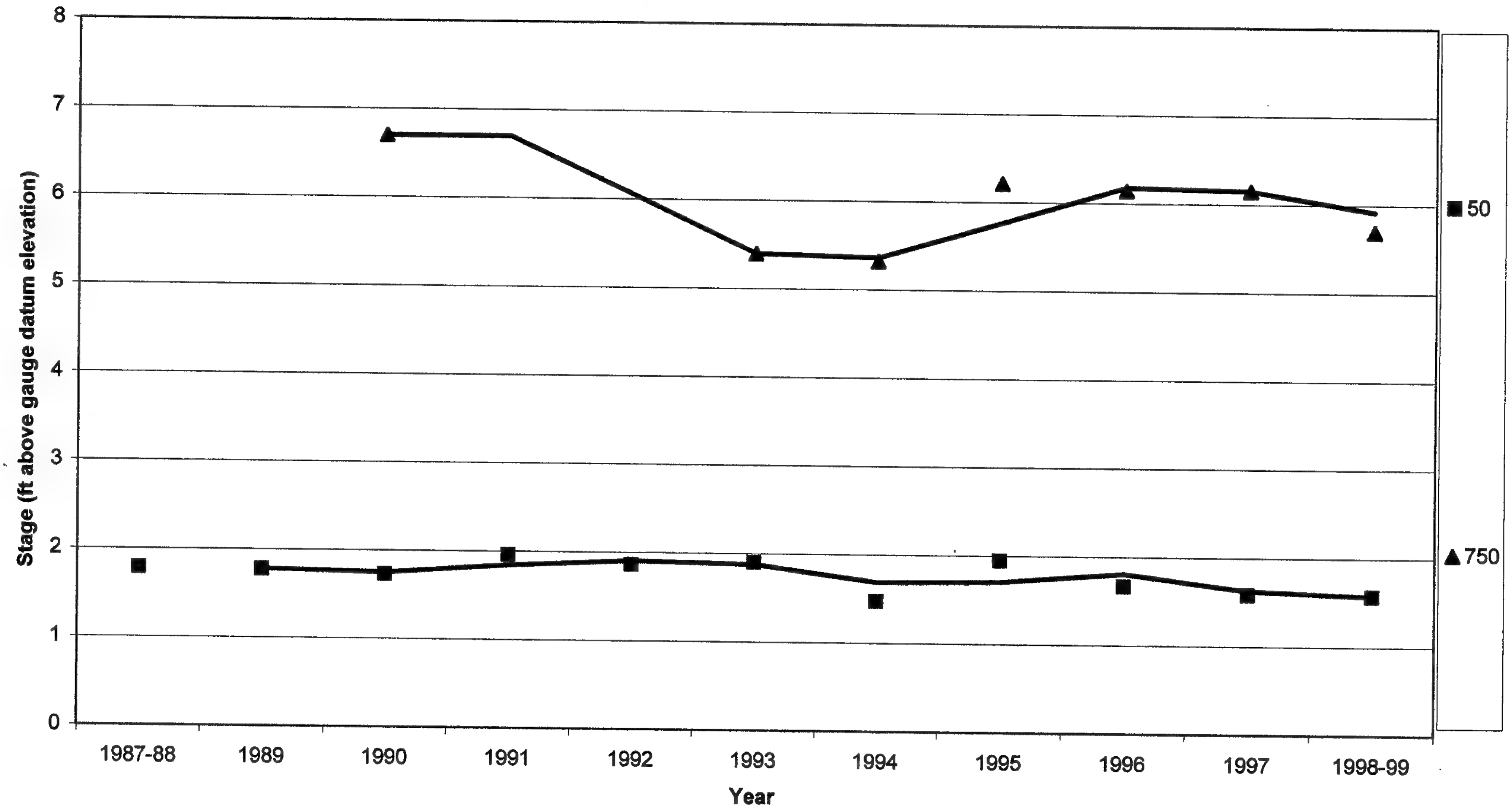

Figure B13: Garrison Reach: Specific Gauge Record for Fort Clark Gauge, ND - RM 1366.65

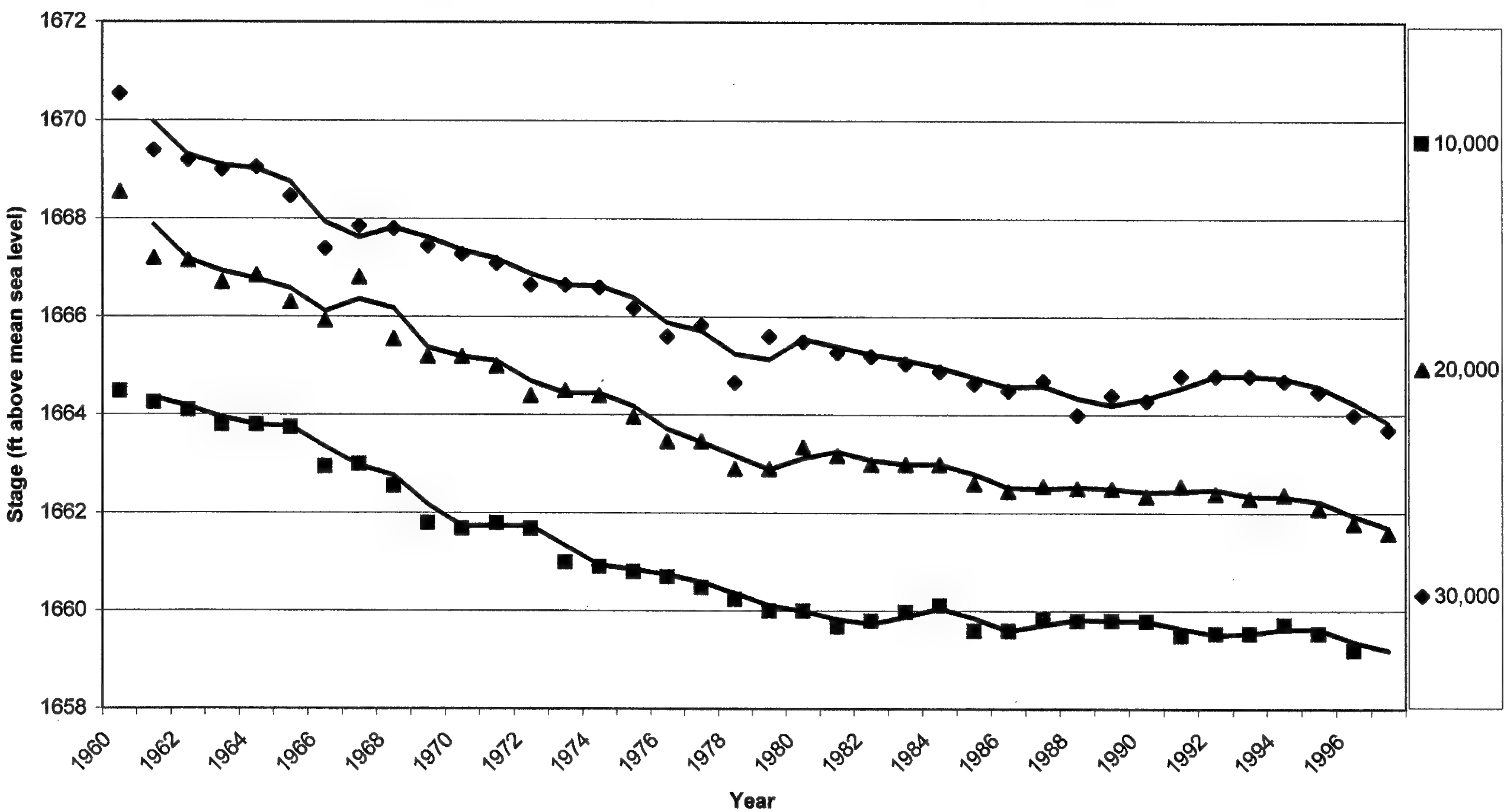

Figure B14: Garrison Reach: Specific Gauge Record for Hensler Gauge, ND - RM 1362

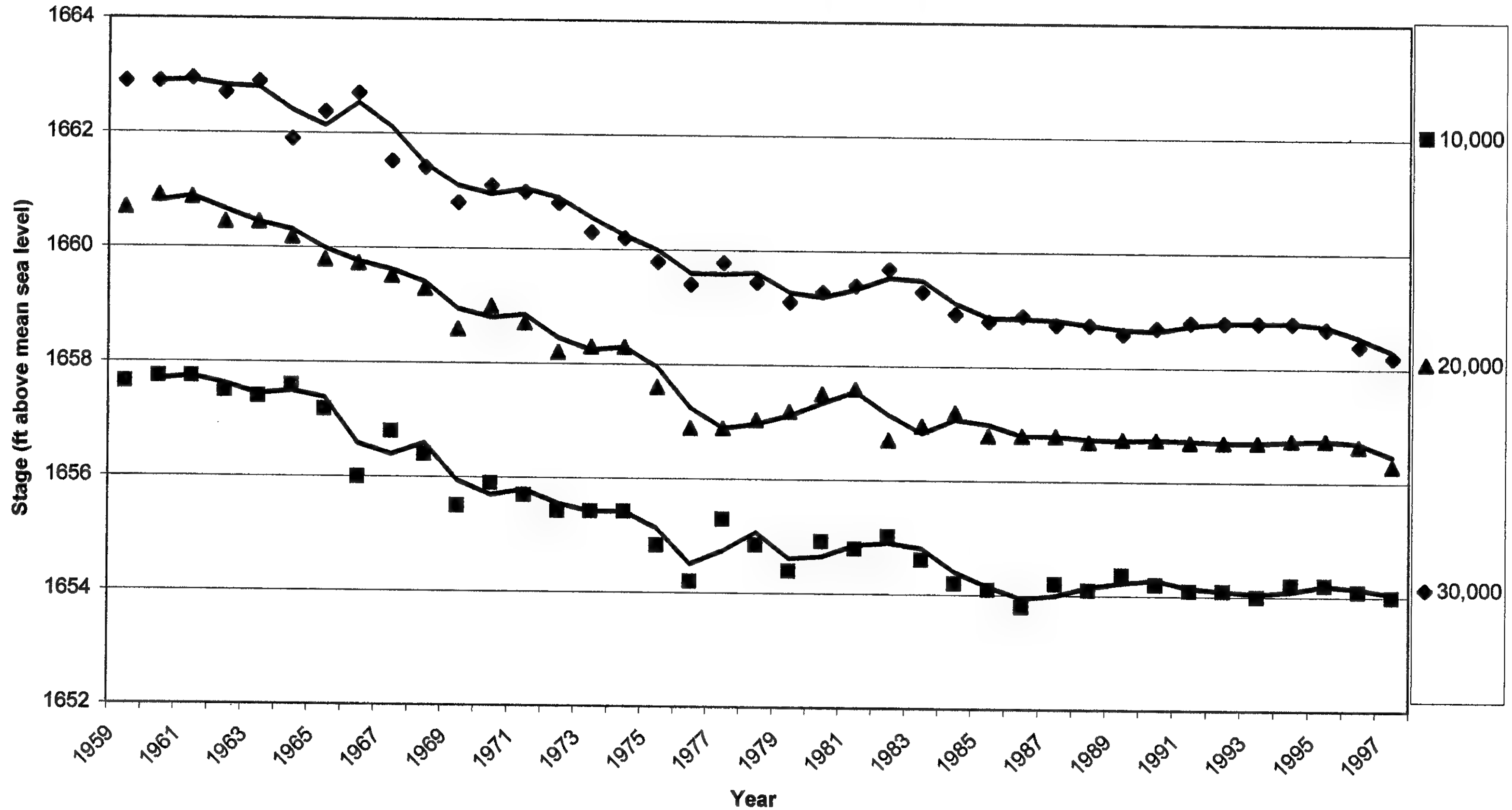

Figure B15: Garrison Reach: Specific Gauge Record for Washburn Gauge, ND - RM 1354.7

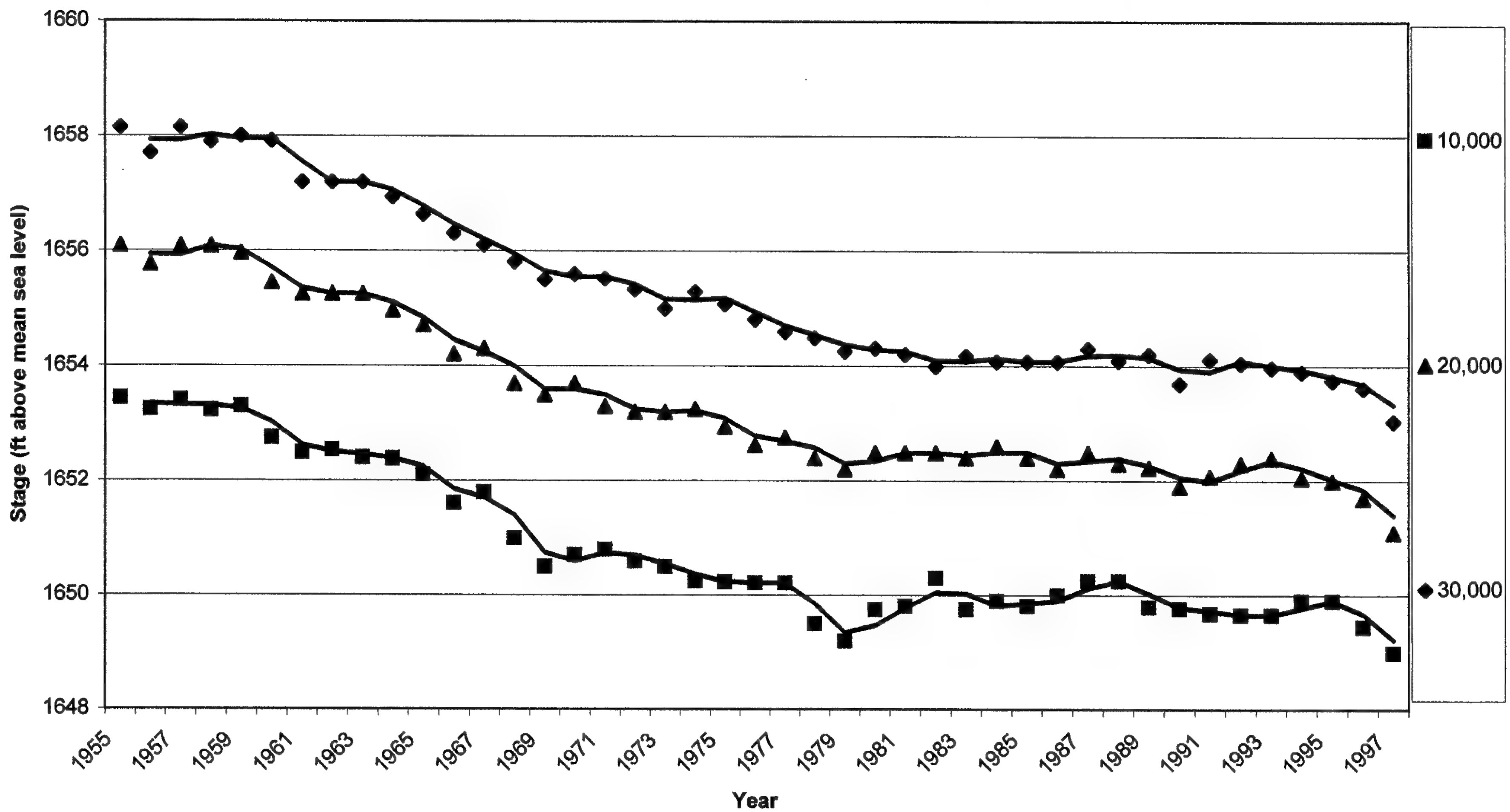

Figure B16: Garrison Reach: Specific Gauge Record for Turtle Creek above Washburn, ND - RM 1351.9

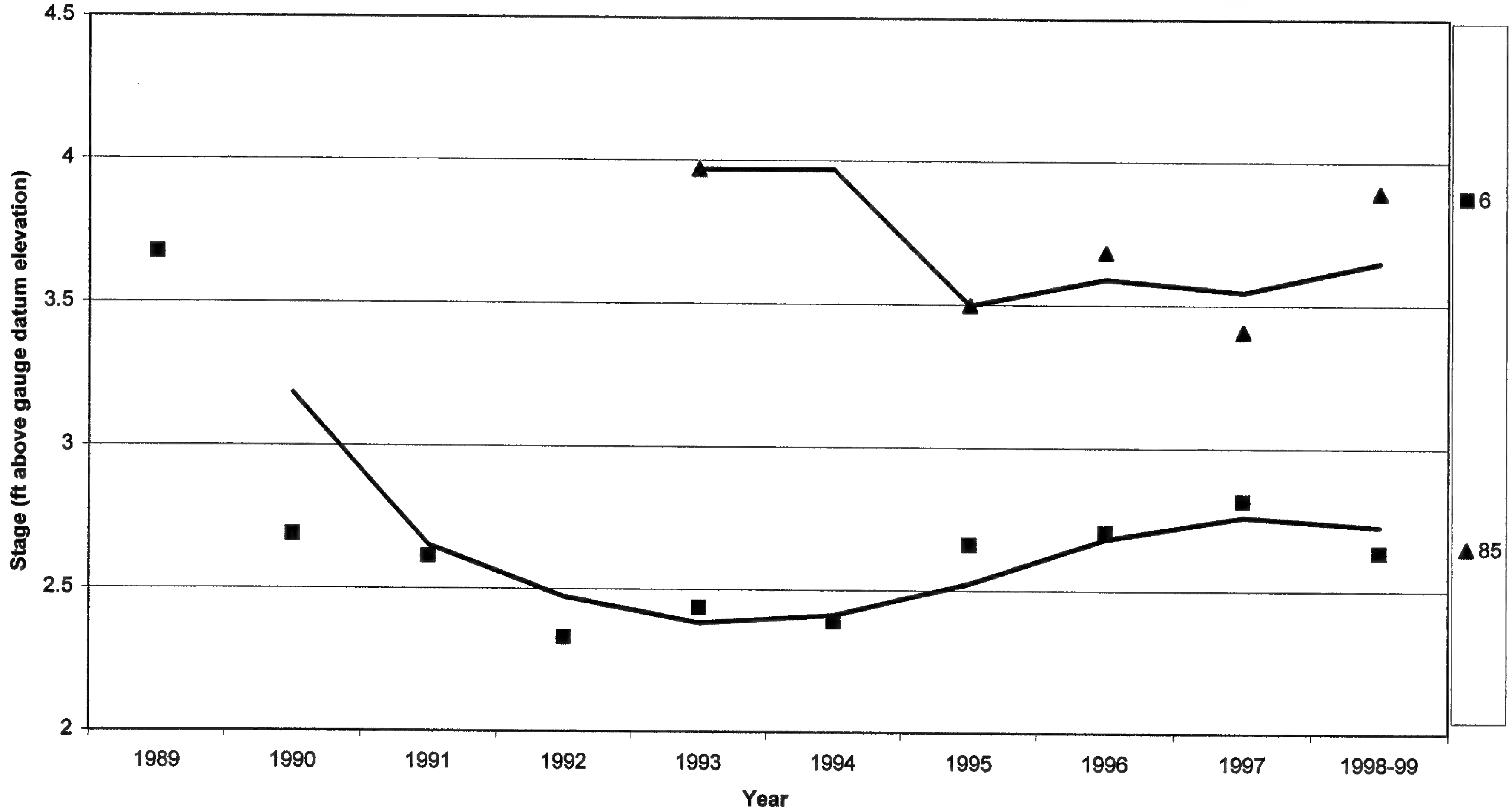

Figure B17: Garrison Reach: Specific Gauge Record for Price Gauge, ND - RM 1338

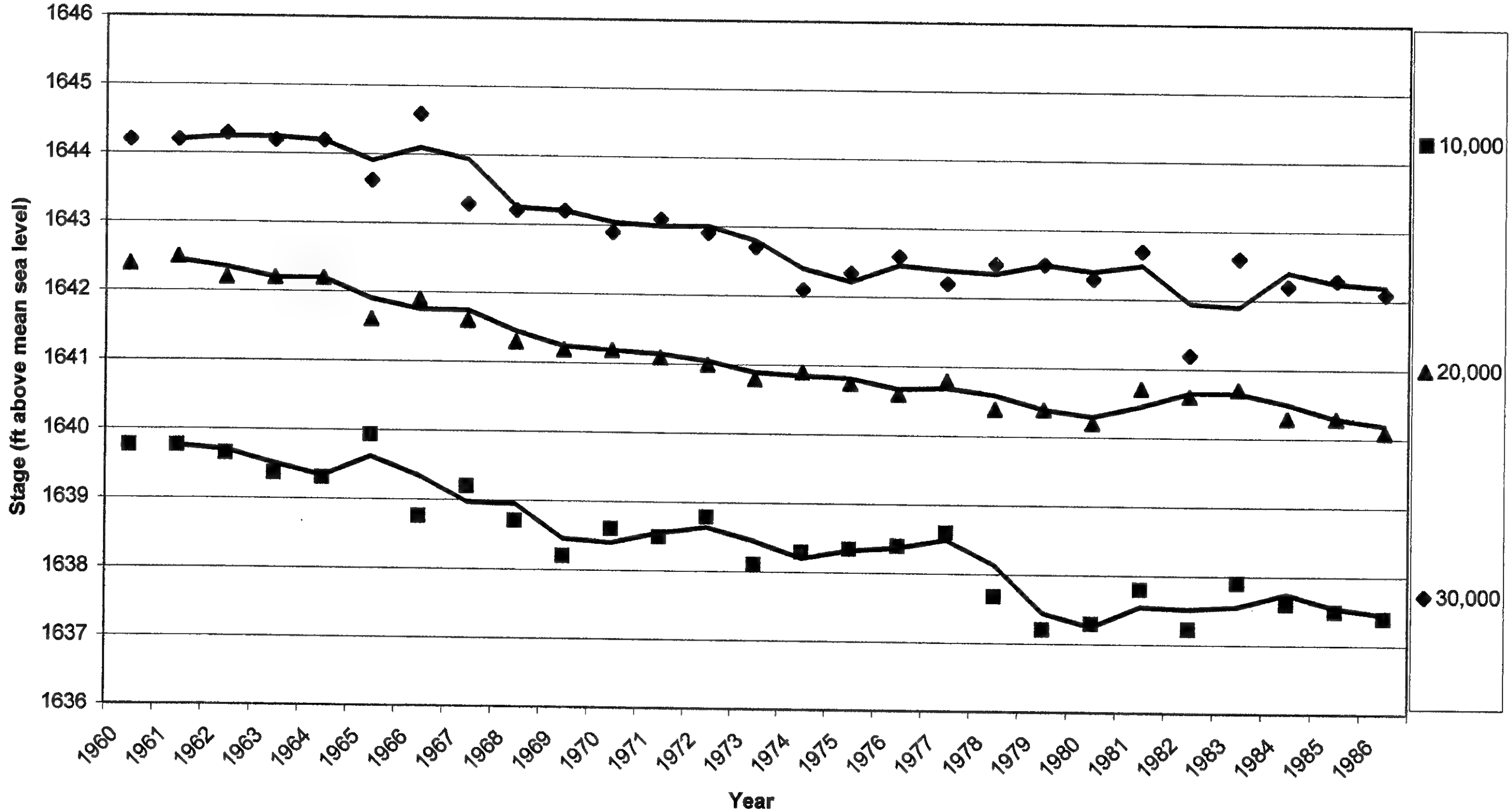

Figure B18: Garrison Reach: Specific Gauge Record for Burnt Creek near Bismarck, ND - RM 1316.2

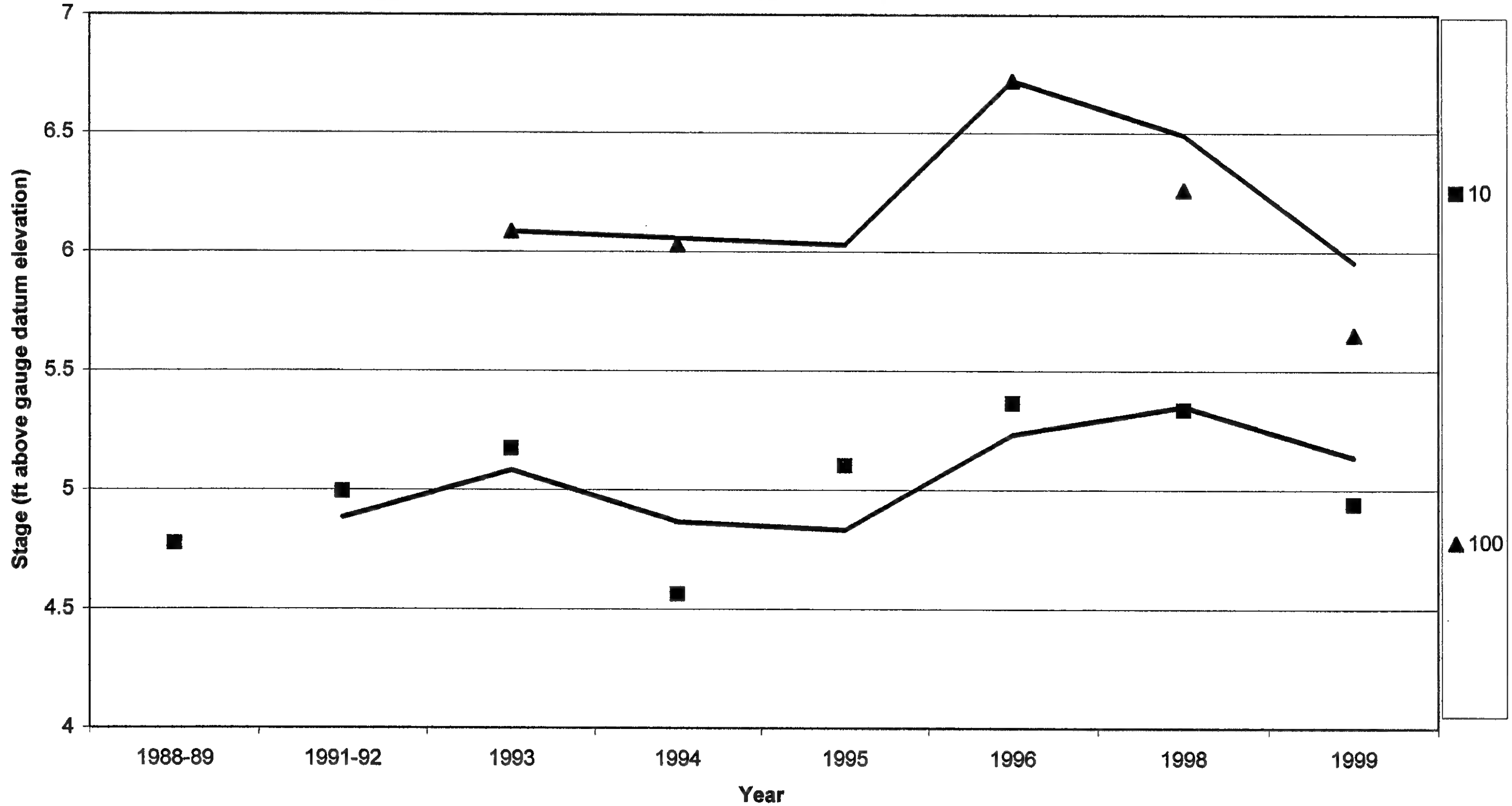

Figure B19: Garrison Reach: Specific Gauge Record for the Missouri River at Bismark, ND - RM 1314.2

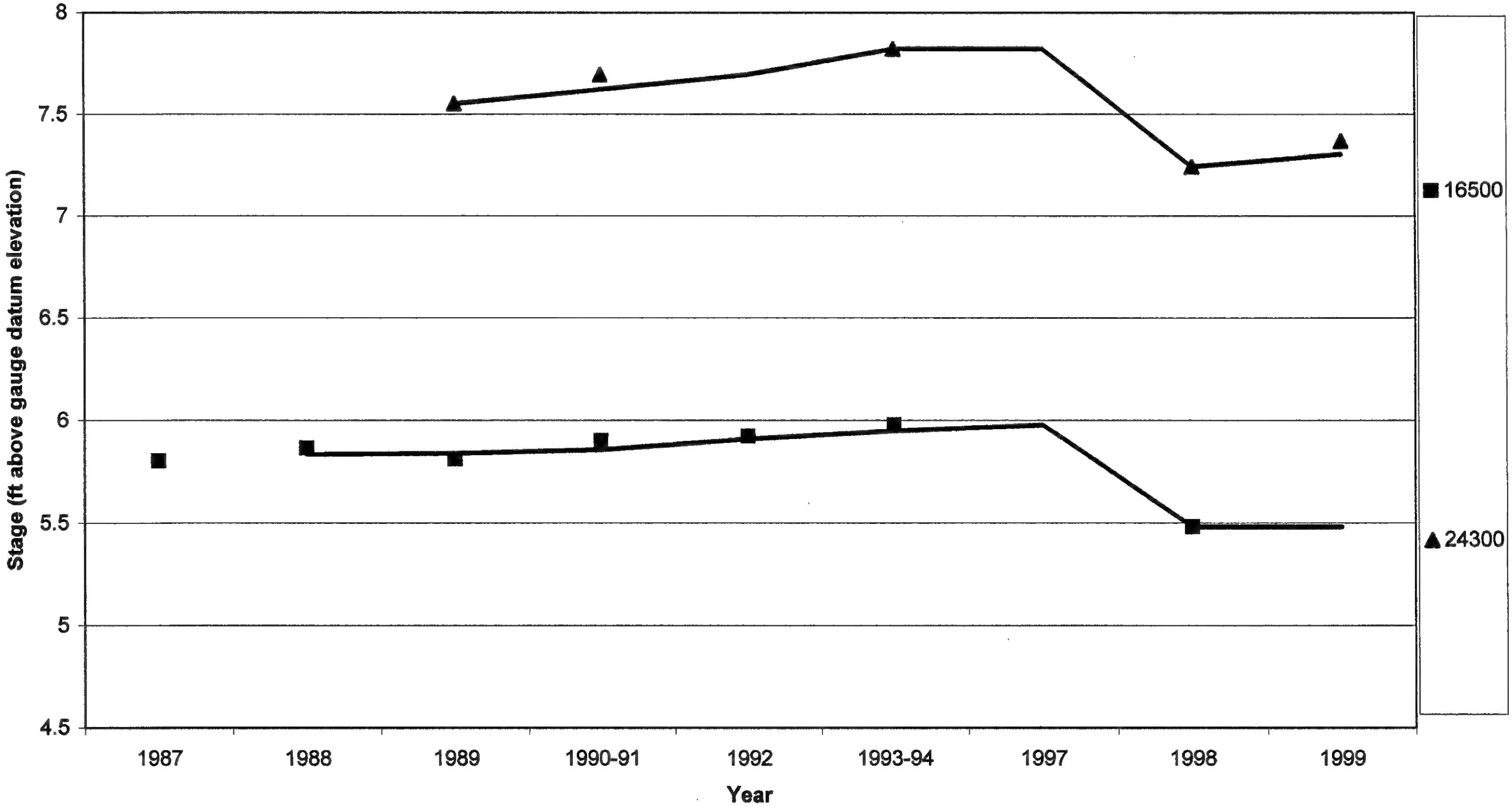

Figure 20: Garrison Reach: Specific Gauge Record for Heart River near Mandan, ND - RM 1311.2

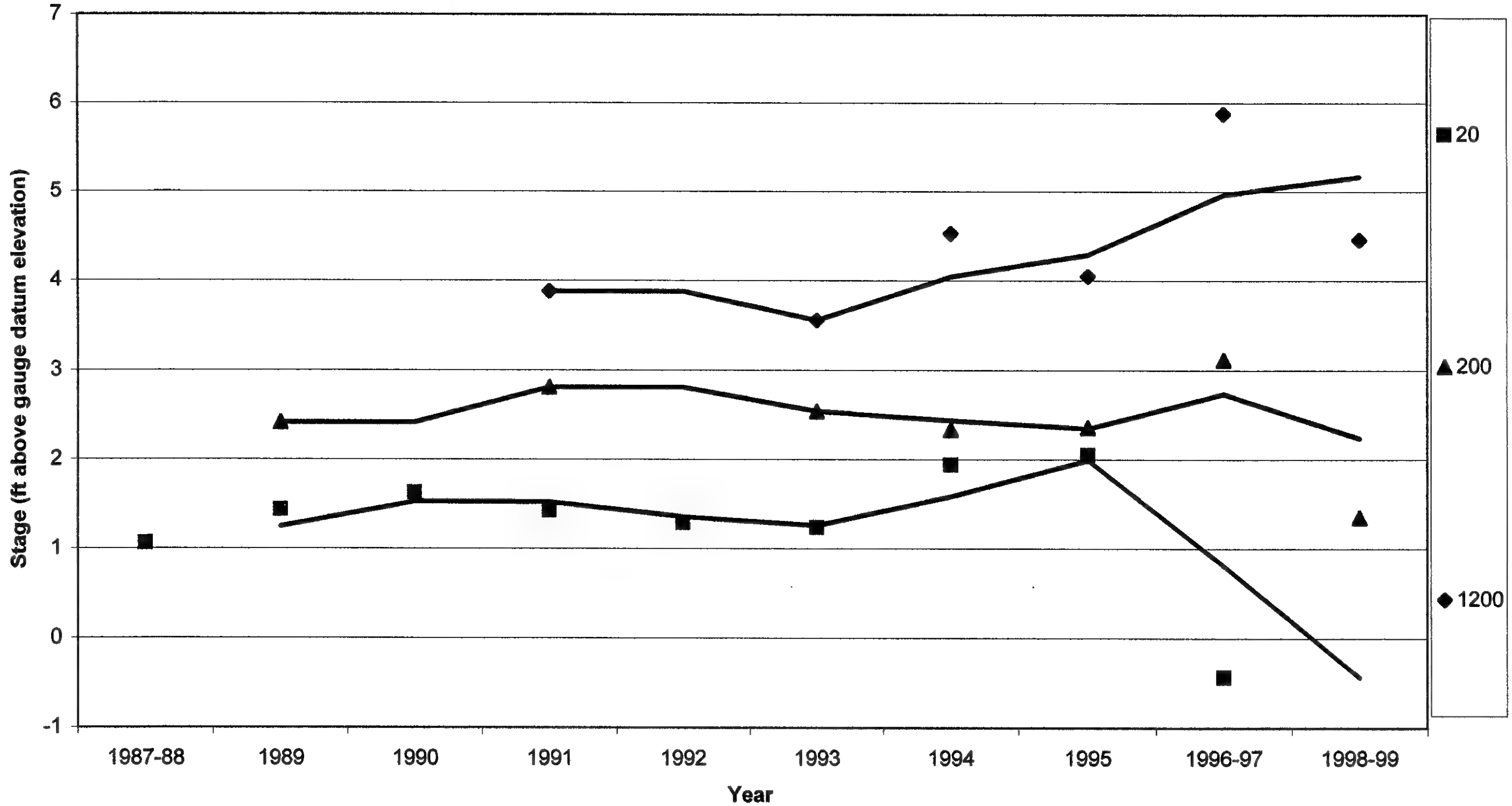

Figure B21: Fort Randall Reach: Fort Randall Dam Gauge, SD - RM 879.98

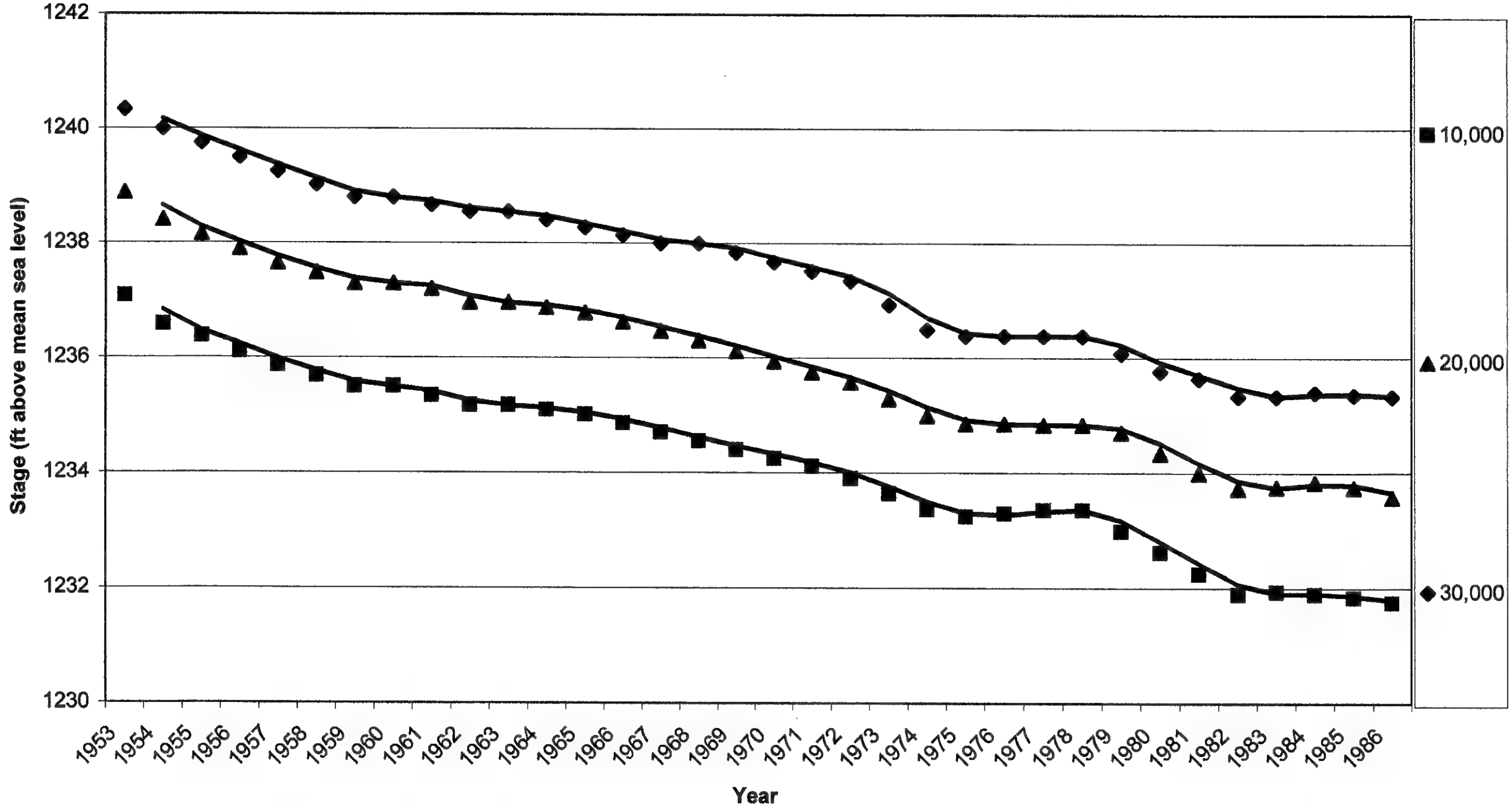

Figure B22: Fort Randall Reach: Specific Gauge Record for Missouri River below Greenwood, SD - RM 865.04

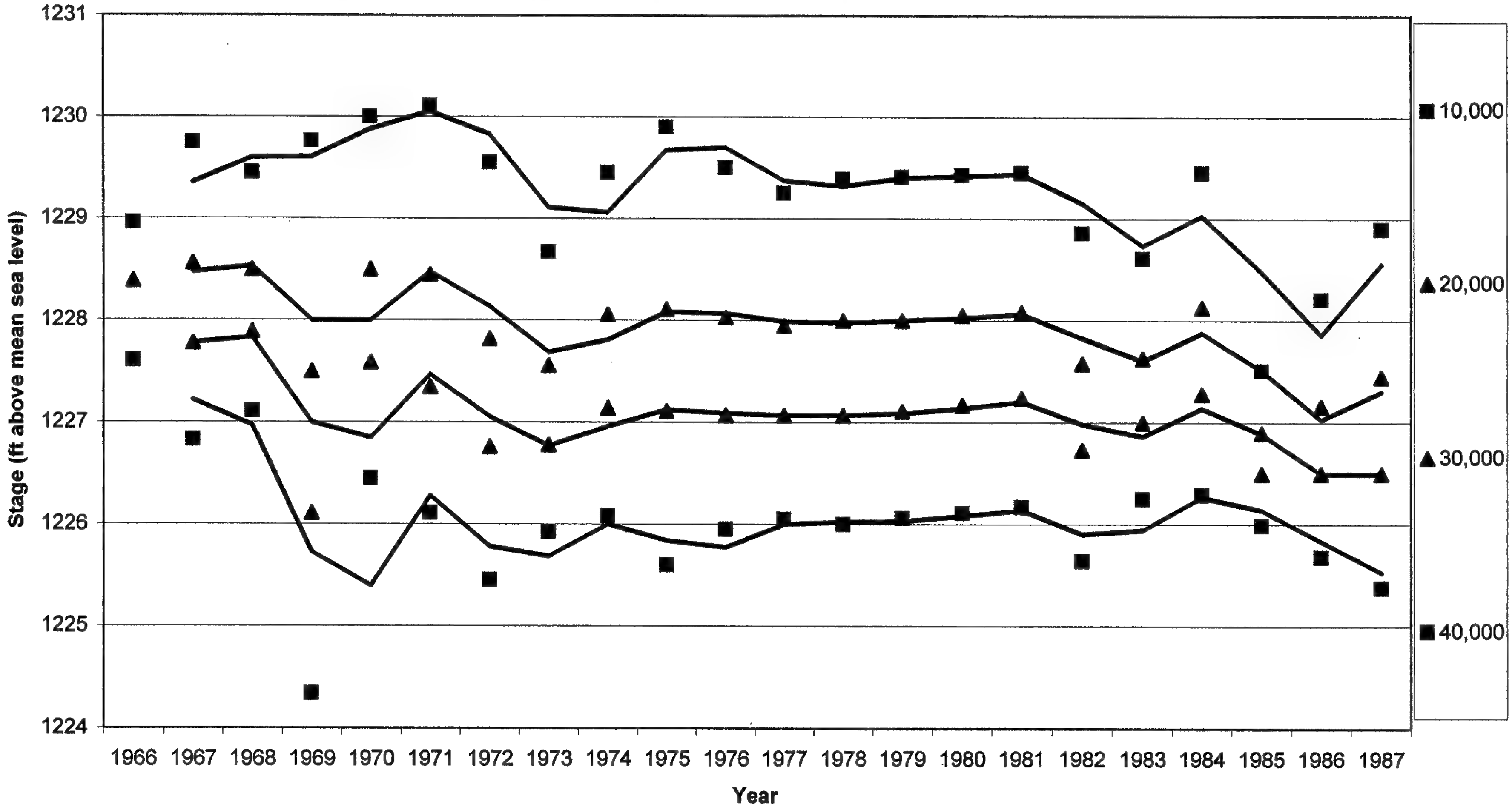

Figure B23: For Randall Reach: Specific Gauge Record for the Gauge at RM 853.37

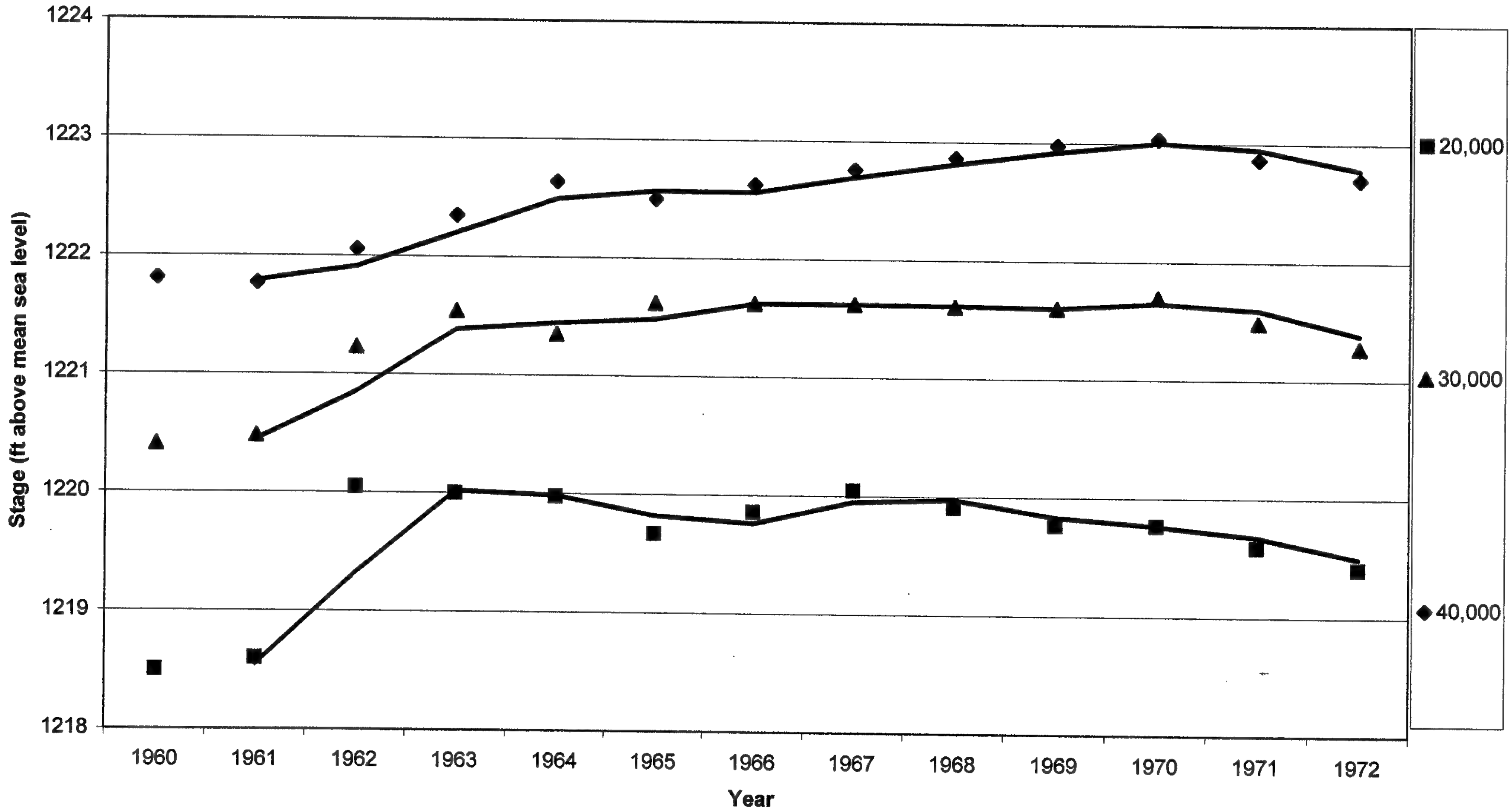

Figure B24: Fort Randall Reach: Specific Gauge Record for Ponca Creek near Verdel, NE - RM 848.9

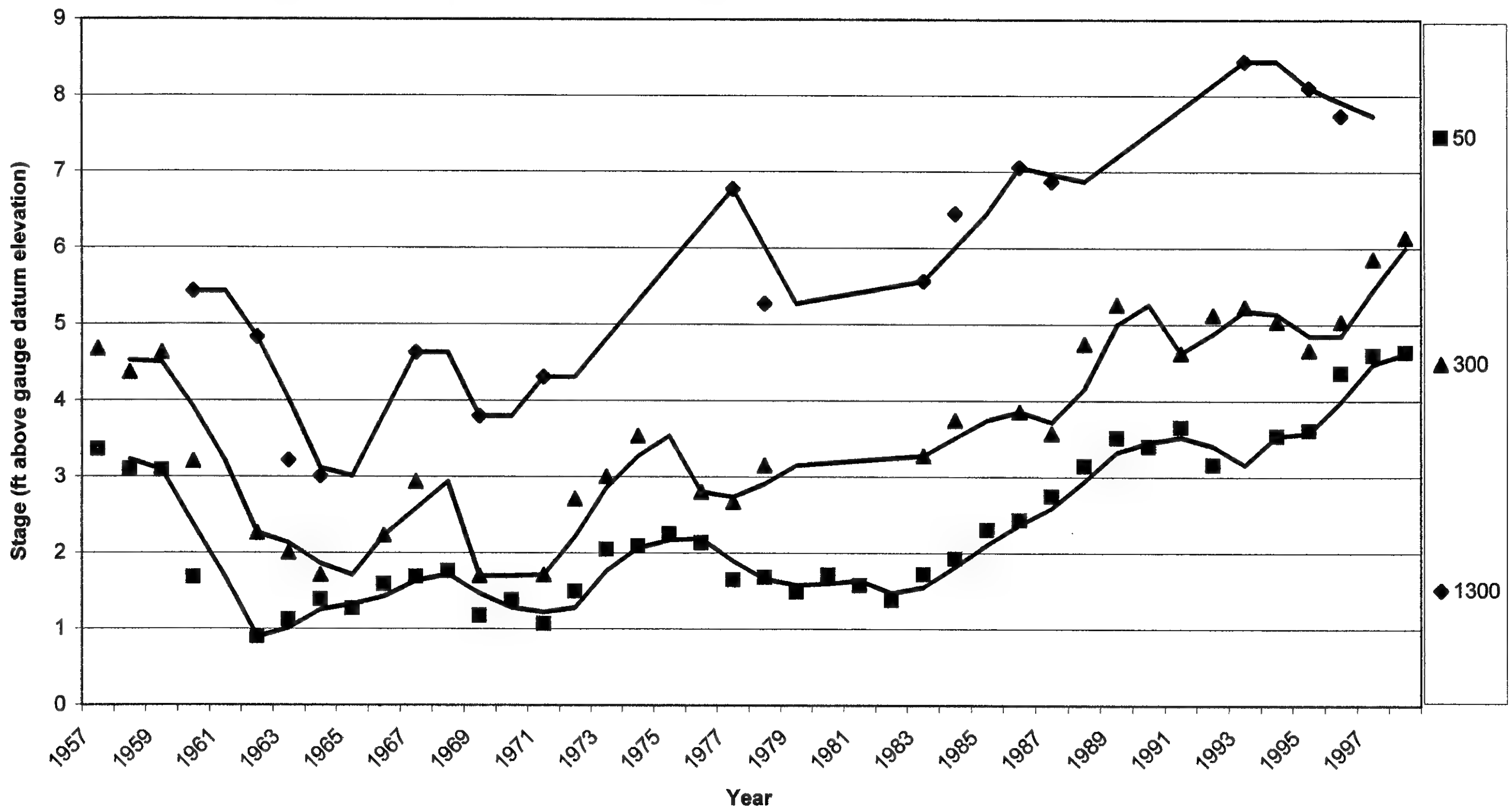

Figure B25: Fort Randall Reach: Specific Gauge Record for the Missouri River near Verdel, NE - RM 845.91

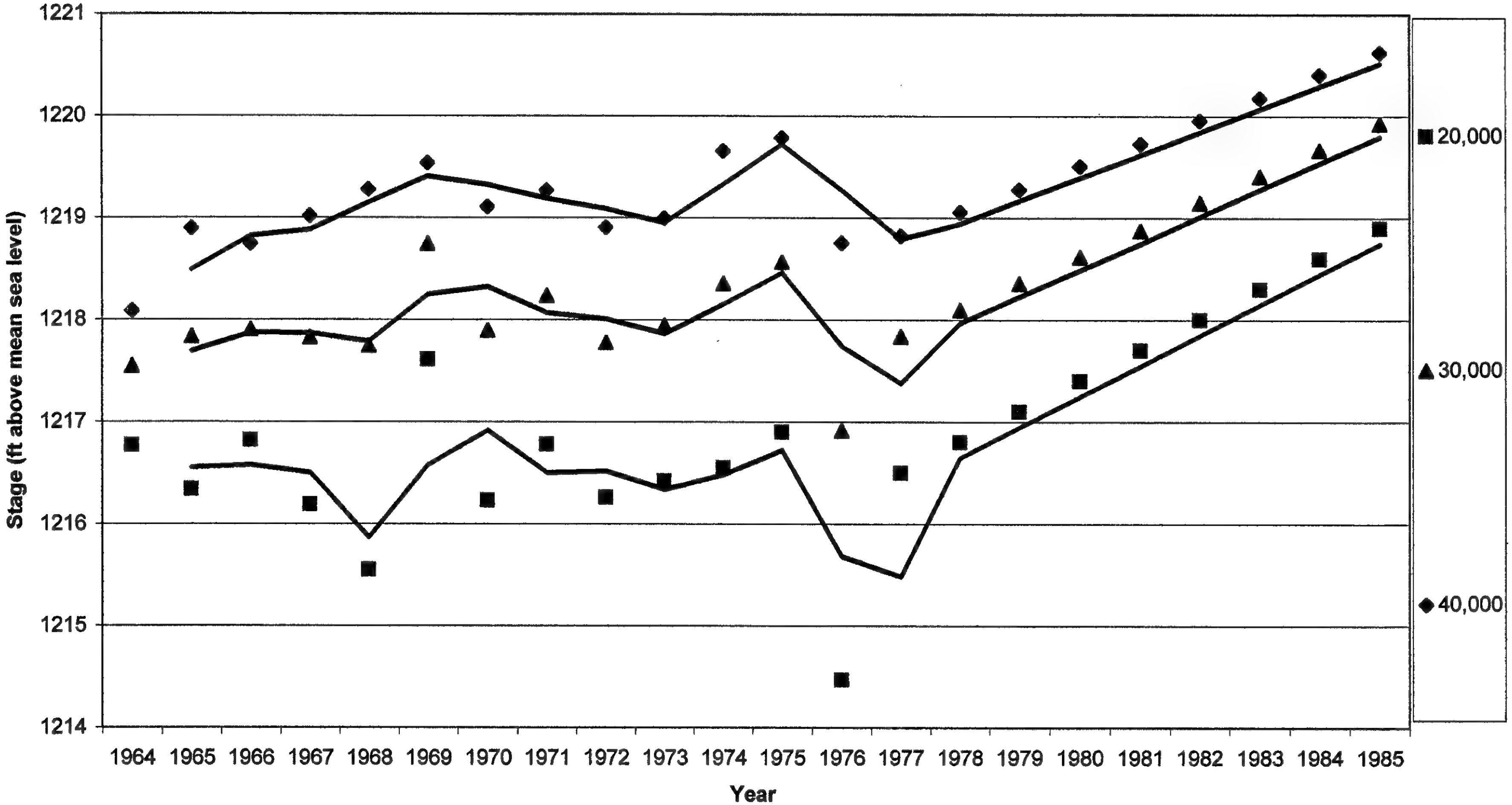

Figure B26: Fort Randall Reach: Specific Gauge Record for the Niobrara River near Verdel, NE - RM 844

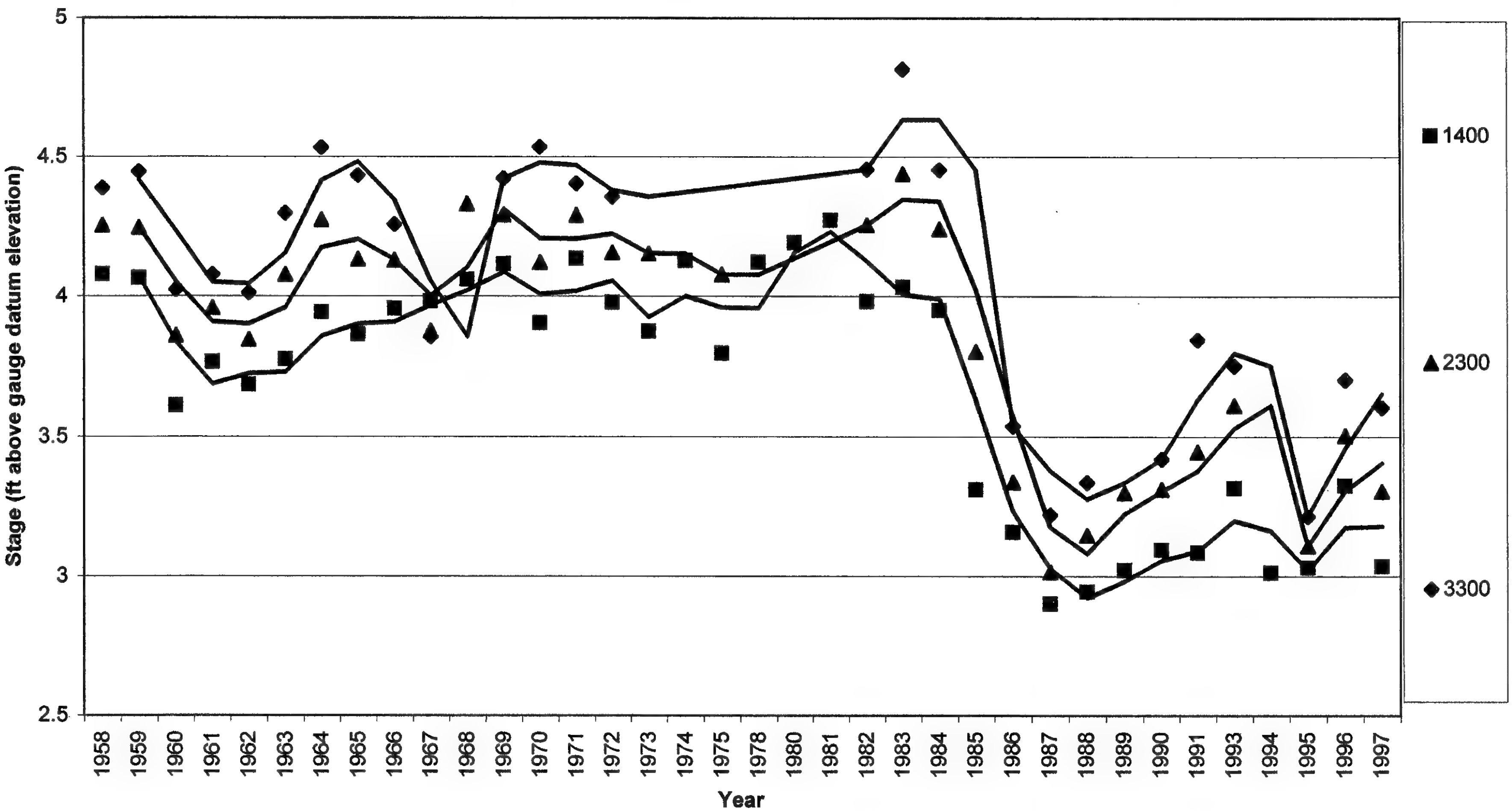

Figure B27: Fort Randall Reach: Specific Gauge Record for the Missouri River near Niobrara, NE - RM 842.45

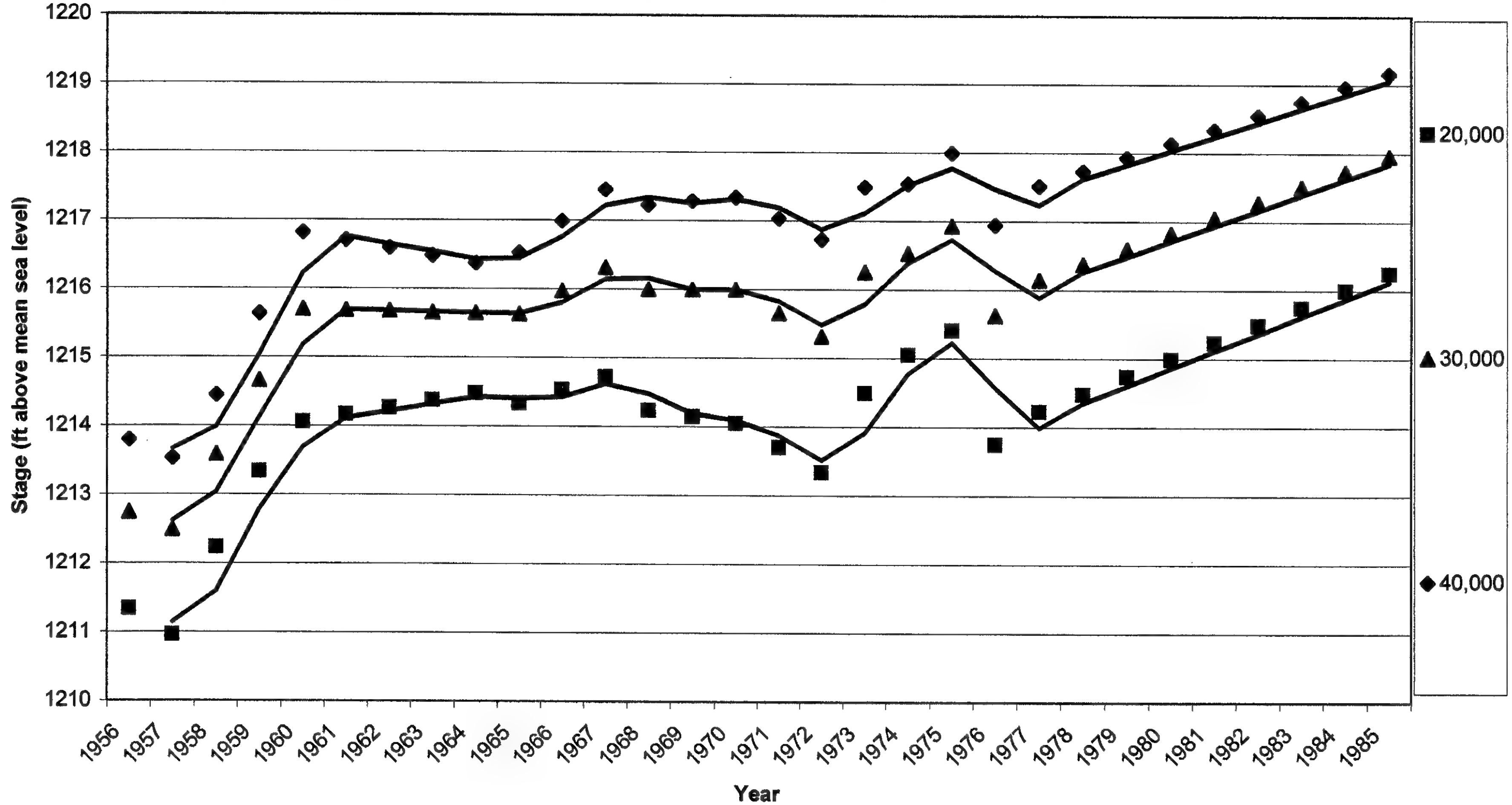

Figure B28: Gavins Point Reach: Specific Gauge Record for the Missouri River at Yankton, SD - RM 805.8

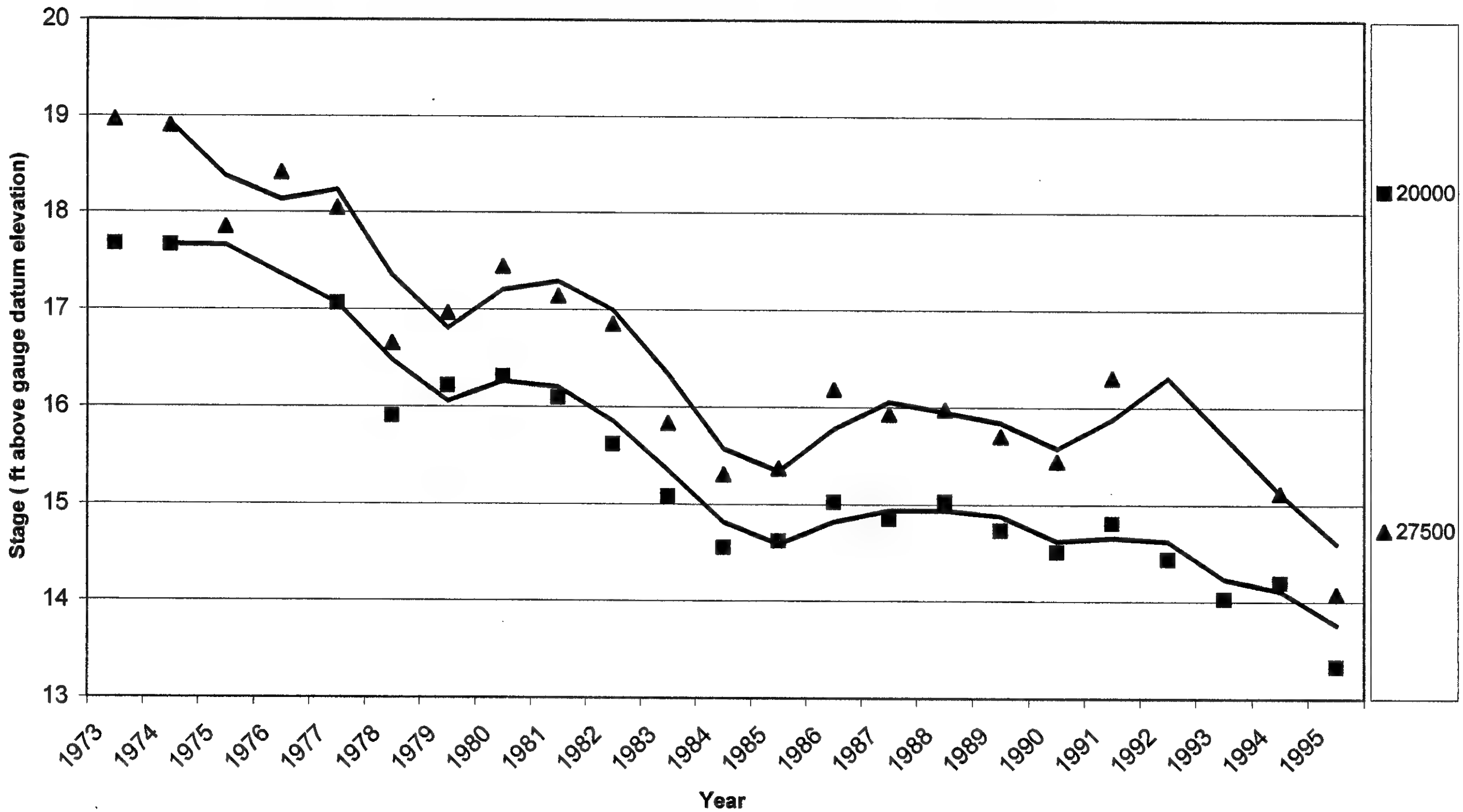

Figure B29: Specific Gauge Relationship for James River at Yankton, SD - RM 800

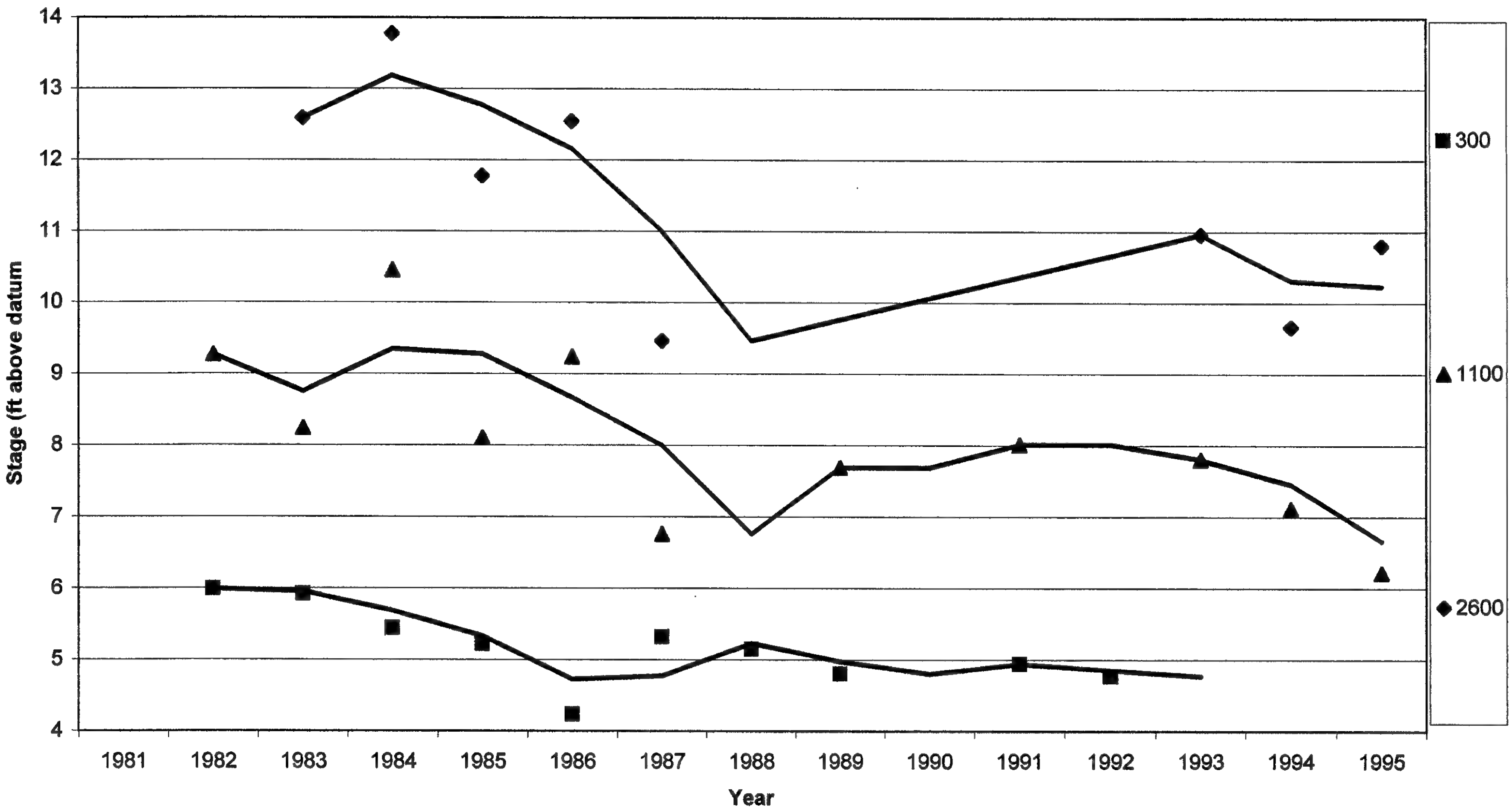

Figure B30: Gavins Point Reach: Specific Gauge Record for the Missouri River near Gayville, SD - RM 796

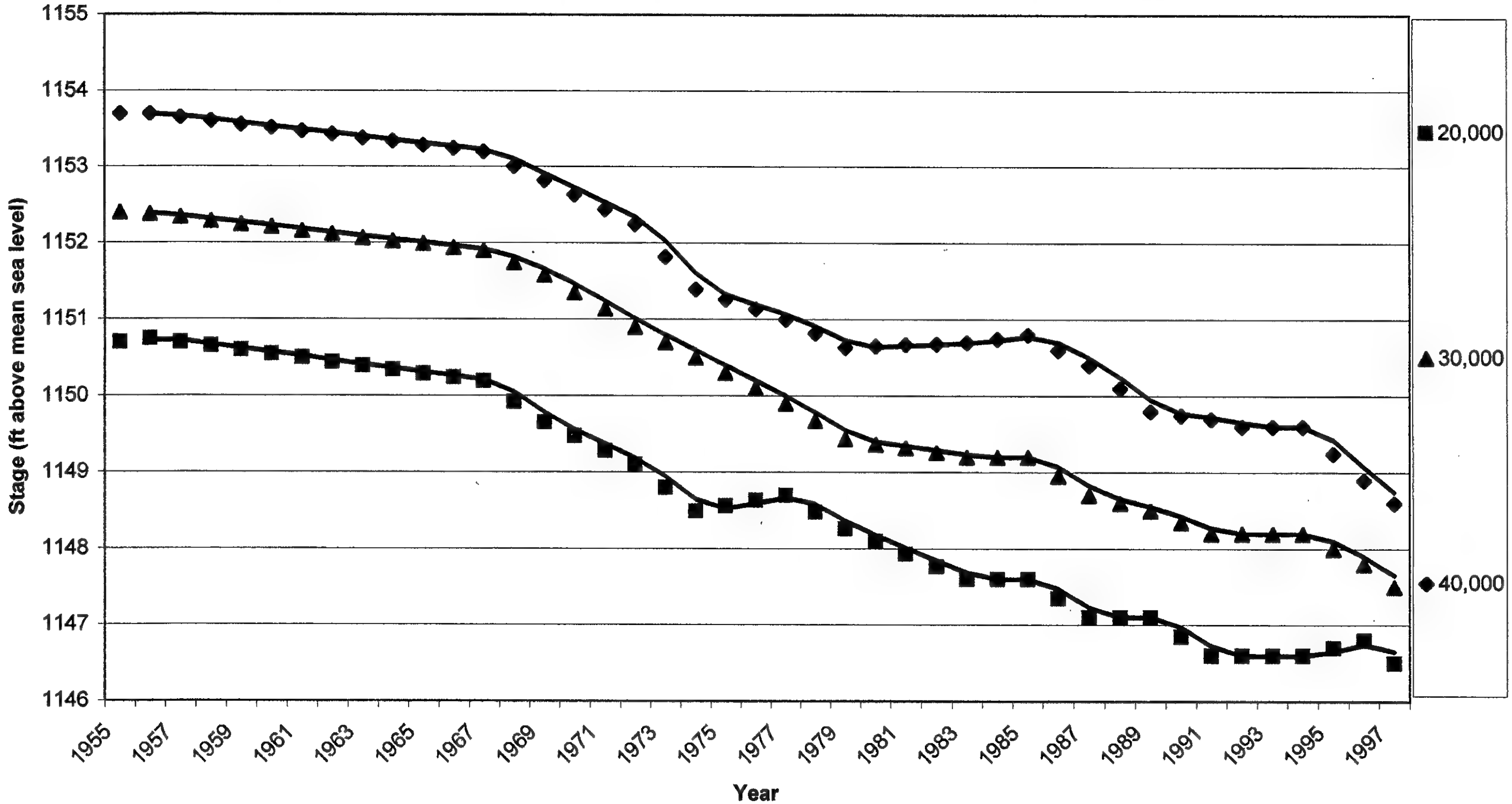

Figure B31: Gavins Point Reach: Specific Gauge Record for the Missouri River near Maskell, NE - RM 775.8

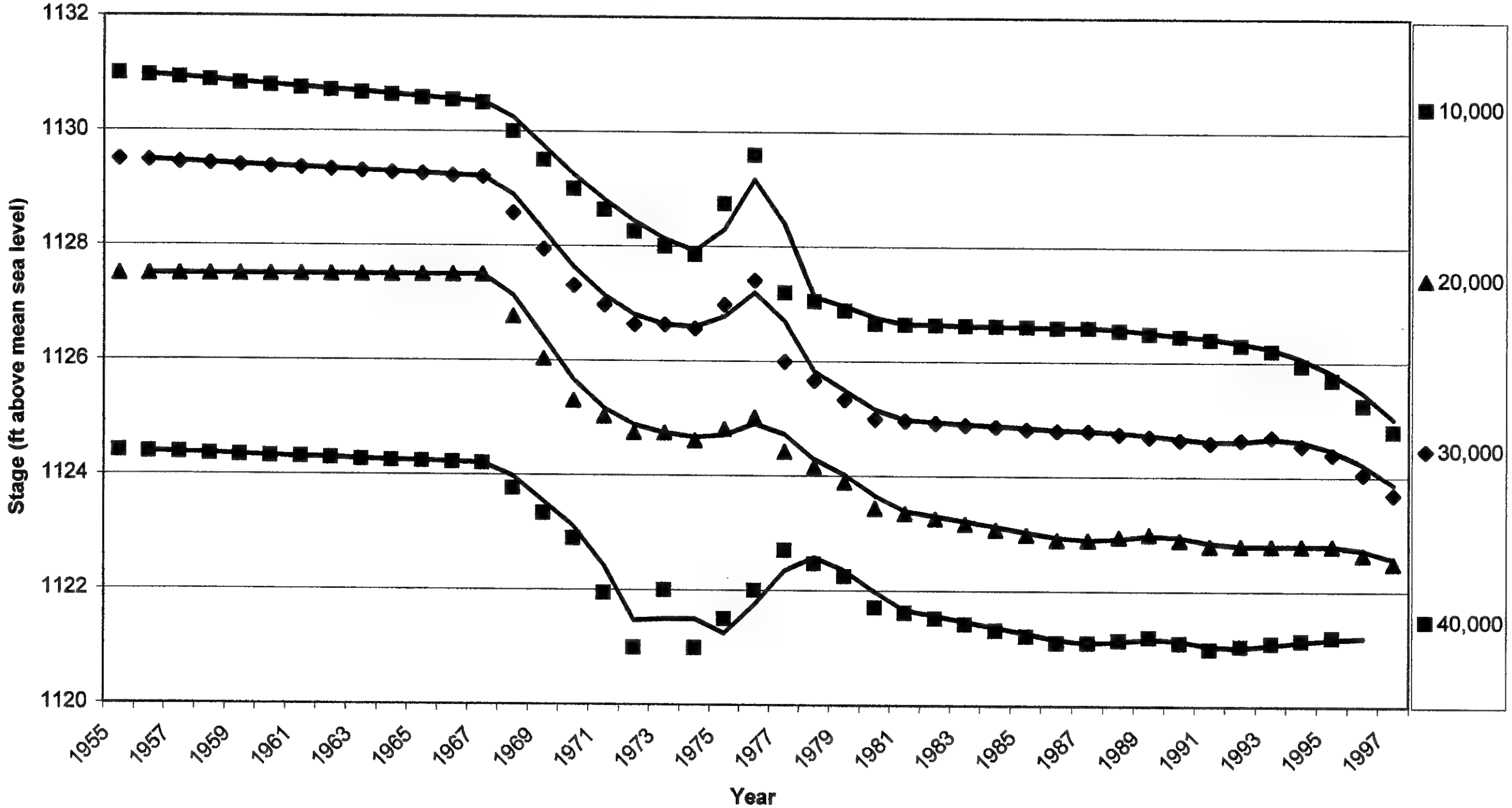

Figure B32: Specific Gauge Record for Vermillion River near Vermillion, SD - RM 772

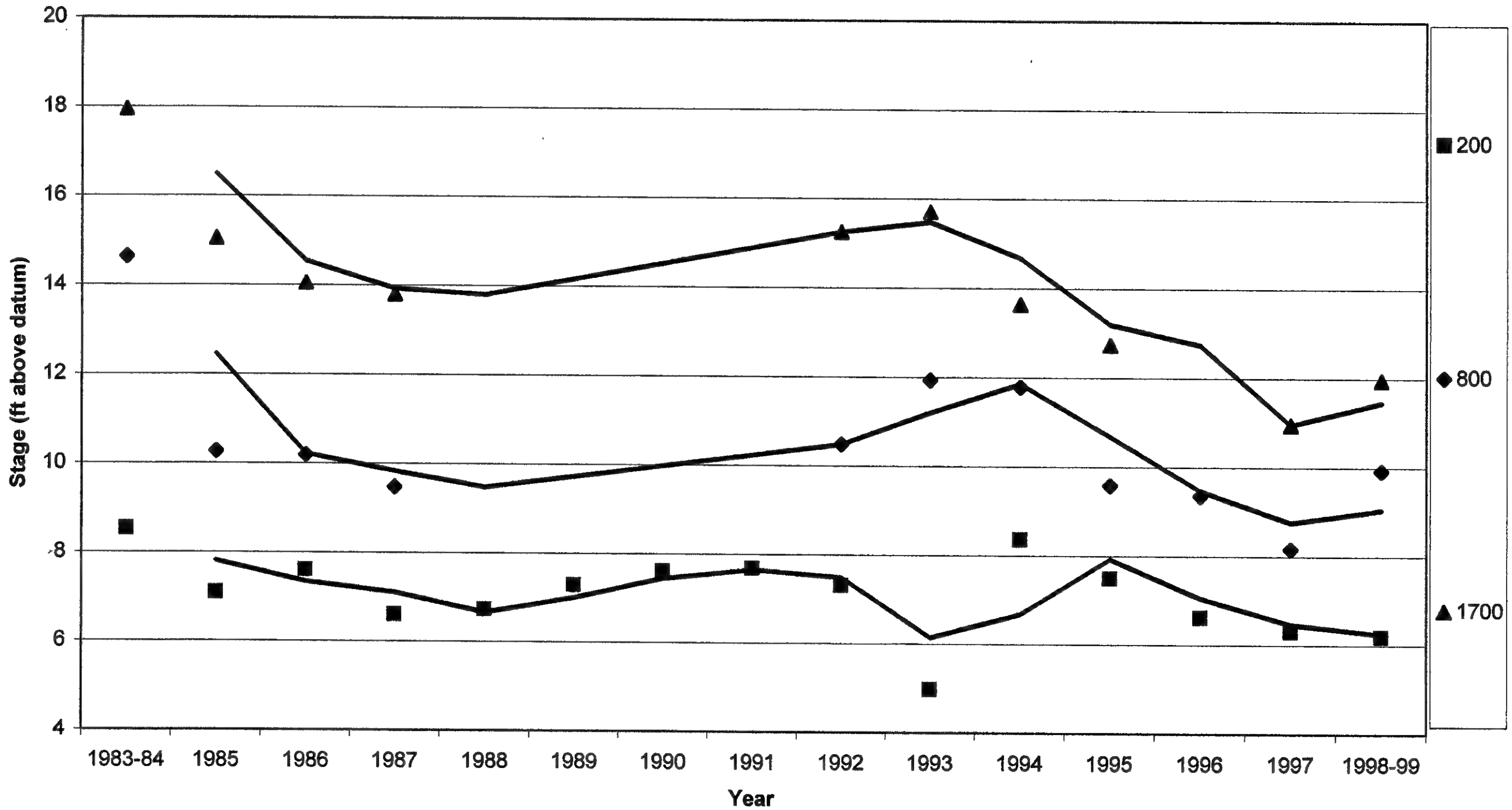

Figure B33: Gavins Point Reach: Specific Gauge Record for the Missouri River near Ponca, NE - RM 751

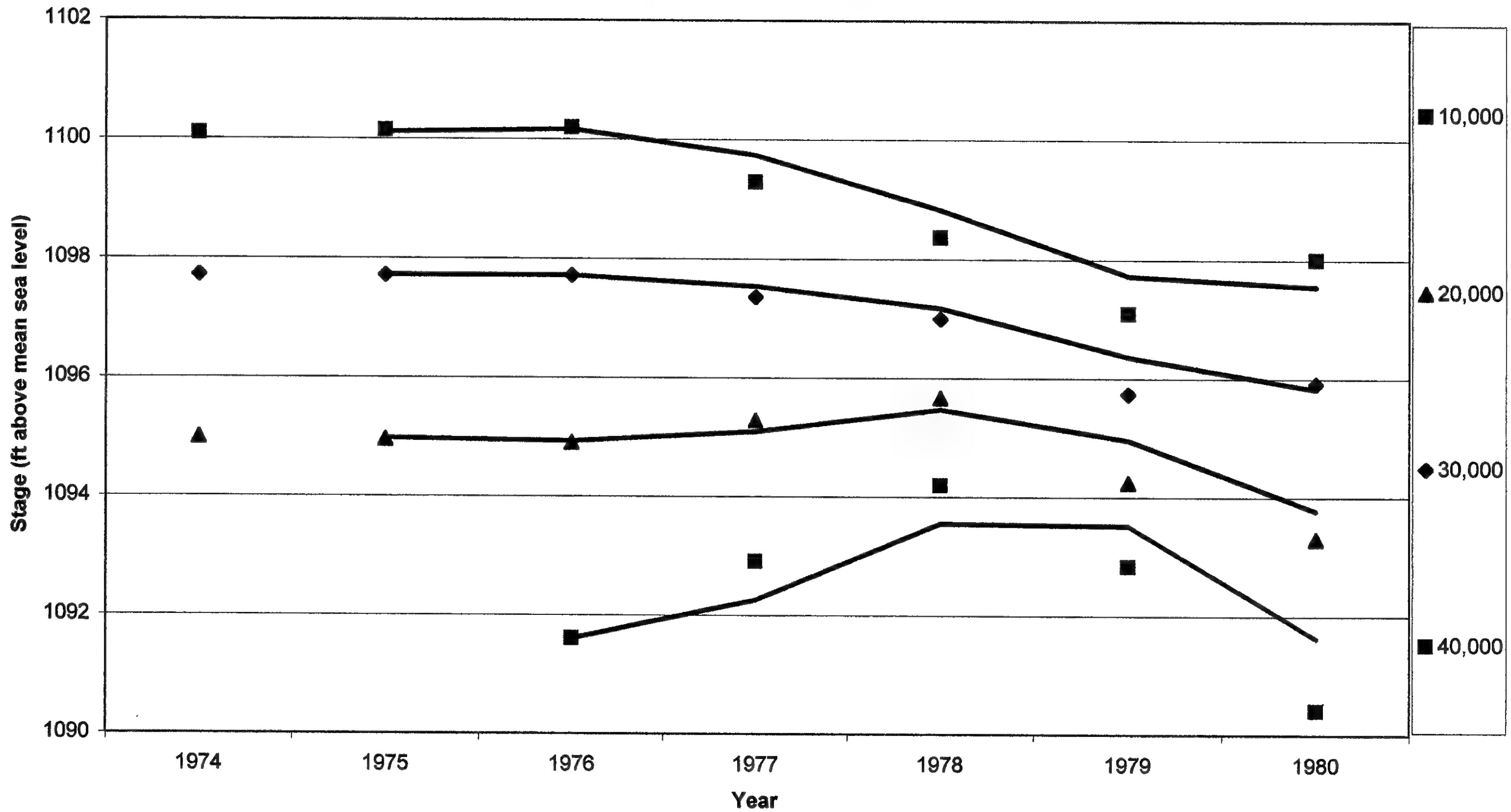

V Bank Erosion Study

Introduction

This section presents a preliminary analysis of the condition of banks in the Fort Peck, Garrison, Fort Randall and Gavins Point reaches of the River Missouri and is based on observations made during the reconnaissance trip undertaken in June 1999, as well as on data taken from the report by Pokrefke (1998). It is fully intended to update this report next financial year with a more accurate assessment of bank stability and erosion rates based on analysis of successive sets of digitised and overlain aerial photographs. Before proceeding however, it is necessary to discuss several aspects of the data used in this analysis in order to keep the results in perspective.

The erosion rates used to create figures 3, 6, 8 and 10 were obtained by multiplying the changes in cross-sectional area, for left and right banks and the bed, from one time period to the next, by the distance in 1960 river miles between adjacent cross-sections and then dividing the result by the number of years in the study period. The figures for cross-sectional area were taken from Pokrefke (1998). In turn, Pokrefke obtained these figures by applying a planform correction factor to the USACE cross-sectional areas to make them more representative of the planform of the entire reach as opposed simply to the planform of the five sub-reaches covered by the cross-sections. This planform correction factor was obtained by dividing the change in water-surface area for the entire reach, as determined in the USAEDNMRR (1994) study and obtained via aerial photography, by the USACE change in water-surface figures based on cross-sectional data, i.e. cross-sectional width multiplied by distance between adjacent cross-sections. This technique was applied to all reaches. In the case of Fort Peck Reach, however, the data against which the cross-sectional figures are compared come from the Darrel Dangberg and Associates and River Pros (1988) report, although these figures do not actually appear to be in the report. In his analysis, Pokrefke <u>assumes</u> that these figures are also based on aerial photography, although no reference to this is made in the Dangberg report. It is thus possible that the figures do not derive from such a source, in which case the technique has been applied erroneously and a potentially error has been introduced. Also, in itself, the planform correction technique may introduce or propagate errors since it is combining data from both cross-sectional and aerial photography sources. Thus a more accurate assessment of bank erosion rates based solely on digitized aerial photographs is needed. This work is currently scheduled to be undertaken in the first few months of the year 2000.

The data upon which figures 1a, 1b, 2, 4, 5, 7 and 9 are based come from the 1981 aerial photographs (currently in use at WES) that were annotated by Rebecca Seal during the reconnaissance trip. The approximate heights of the various depositional features, i.e. border fill (BF), channel fill (CF), post-dam terrace (PDT), old terrace (OT) and bluff lines (BL), that were eroding were noted in the field and used to develop a frequency distribution for the bank heights, of which figure 11 is an example. A very basic classification system was then produced by assigning a range of bank heights to each of the depositional features mentioned above and then using the median value of each range for plotting purposes. Thus BF features were postulated to be those that occurred between 0 and 5 feet high with a median height of 2.5 feet, CF features were between 5 and 10 feet high with a median height of 7.5 feet, PDT features were between 10 and 20 feet high with a median height of 15 feet, OT

features were between 20 and 50 feet high with a median height of 35 feet and the bluffs were said to be anything over 50 feet high and were thus assigned 50 feet as their representative value. Graphs such as figures 2 and 5 were then produced to show the frequency distribution and to what extent it was accurate, whilst figures 1a, 1b, 4, 7 and 9 were produced to show the distribution of left and right bank and bar and island erosion. The latter five figures especially were created in order to reveal some trends to the spatial distribution of the erosion and thus to provide some input to the identification of the geomorphologically similar reaches.

It must be borne in mind that the above is only a preliminary analysis of the data obtained in the field, which is susceptible to a certain degree of error. For example, it is difficult to accurately estimate eroding bank heights from a distance and in a sometimes difficult working environment, whilst at the same time correctly distinguishing between, say, post-dam terraces and older terraces, or between border fills and channel fills. Furthermore, it is highly unlikely that the areas of erosion observed in the field correspond to all the areas of historical erosion that are covered by data in the Pokrefke report and, also, the two data sources come from different time frames. Nevertheless, such an analysis was undertaken because it will help to interpret the results of the grain size distribution analysis of the field samples, pending the development of the digitised aerial photography resource discussed above. For example, there might be some correlation between old terrace deposits and a particular grain size distribution found in the bars and islands.

For each reach, the erosion and deposition that occurs along the left and right banks and the degradation and aggradation of the bed is compared for two consecutive time periods, e.g. 1955-1966 and 1966-1978 in the case of Fort Peck Reach. This will help in identifying any significant changes in channel process and morphology that have occurred over this time frame. It should be noted that where gaps appear in the plots on figures 3, 6, 8 and 10, this is due to an absence of cross-sectional data for one or the other of the survey dates involved. It should be noted on these four figures that the degradation and bank erosion are represented by the negative values on the ordinate. Finally, it should also be noted that the river miles (RMs) decrease in the downstream direction, thus the confluence of the Missouri River with the Mississippi River occurs at RM 0.

Fort Peck Reach RM 1771-1585

This reach is by far the most extensively eroding of all the four study reaches, with erosion frequently occurring in tandem along left and right banks. Darby and Thorne (1996) showed that in 1995, 57% of the banks were actively eroding by mass wasting processes. Examination of figures 1a and 1b shows that it is banks with a mean height of 15 feet that erode most consistently throughout the reach. Within this, the areas of greatest activity are located between RMs 1742-1680 and 1665-1606, with the right bank eroding more than the left. Twenty of these eroding bank sites are made up of old terrace type deposits with a further nine being formed of post-dam terrace deposits (figure 2). Erosion of banks with a mean height of 35 feet occurs most intensively between RM 1769-1738, whilst in the remainder of the reach it is more sporadic. This suggests that downstream of the zone between RM 1742 and 1738, either the lower banks are preferentially eroding or mean bank height decreases in the downstream direction. In view of the fact that banks with a mean height of 35 feet are still to be

found downstream of RMs 1742-1738, as shown by their less extensive erosion on figures 1a and 1b, it is likely that the lower banks are being preferentially eroded. And, as with the banks with a mean height of 15 feet, the right bank again appears to erode more than the left at 35 feet mean height (figures 1a &1b). Twenty-three of these sites are formed of old terrace deposits and nine of post-dam terrace deposits (figure 2). Erosion of banks with a mean height of 7.5 feet occurs most extensively from RM 1662-1590 and is more sporadic in the remainder of the reach. Erosion of bank lines with a mean height of 2.5 feet is even more sporadic than above but accounts for the majority of the eroding bars and islands, especially between RM 1724-1673. Erosion of the highest bluffs and terraces is too rare to show any obvious pattern.

Study of figure 3 shows that rates of bank erosion were lowest immediately downstream of the dam from RM 1771-1732. This is perhaps surprising given that the zone of most intense historical degradation was found immediately downstream of the dam (RM 1771-1757) but can probably be explained by a combination of the following. At certain locations, especially between RMs 1771 and 1757, *(Colin – I can't be any more specific than this in terms of river miles at the moment without the aerial photographs, which are being used in America)* the river impacts directly upon the bluffs which are composed of more erosion resistant material than other bank types, such as post-dam terraces or old terraces. Furthermore, at several locations where this occurs, the bed is eroded down to the gravel layer and becomes armored (USACE, 1986), thus precluding any further increases in bank height and therefore any further increases in bank instability. At least the first five miles downstream from the dam and possibly the following 52 miles have a continuous gravel layer in the bed (Dangberg *et al*, 1988a) which has resulted in armoring once degradation has reached this layer. Therefore, by preventing further increases in bank height, continuously high or even increasing erosion rates may be prevented. Another possibility is that since Fort Peck dam was closed in 1937 (USACE, 1994) the most intense period of erosion had already occurred in the immediate vicinity of the dam and had begun to migrate downstream, prior to the collection of cross-sectional data in 1955.

Erosion rates of about 73,000, 95,000 and 73,000 m3/yr occurred between RMs 1723-1720, 1720-1715 and 1707-1700 respectively along the right bank for the period 1955-1966, with the two 73,000 m3/yr readings increasing to 128,000 and 169,000 m3/yr respectively from 1966-1978. Along the left bank, rates of 110,000, 129,000 and 138,000 m3/yr occurred between RMs 1728-1724.5, 1695-1687.5 and 1682.5-1675 respectively during the period 1955-1966. Between 1966 and 1978 RMs 1728-1724.5 decreased to 67,000 m3/yr, RMs 1695-1687.5 stablised, whilst RMs 1682.5-1675 showed 87,000 m3/yr of deposition. These zones of erosion correspond very well to the erosion of banks with a mean height of 15 feet that occurs between RMs 1742-1680 (see above). 201,000 m3/yr of erosion occurred between RM 1608-1603 along the left bank from 1955-1966, but which decreased to 23,000 m3/yr from 1966-1978. Other peaks of erosion that developed during this time but which were not present from 1955-1966, were found between RMs 1653-1647, 1631-1625 and 1621-1617 and were of 78,000, 93,000 and 127,000 m3/yr respectively. A rate of 42,000 m3/yr along the right bank between RMs 1617-1612 increased to 90,000 m3/yr between 1966 and 1978. This is in the area where banks with a mean height of 7.5 feet and 15 feet are eroding the most and where aggradation is increasing towards the downstream end of the reach. Indeed, figure 3 shows that aggradation rates had been

increasing greatly downstream of RM 1625 during the period 1966-1978, to a maximum of 186,000 m3/yr from RM 1612-1607, whilst at the same location for the period 1955-1966 the bed was actually degrading at a rate of 19,000 m3/yr.

It is difficult to ascribe a precise cause to the increases in rates of erosion at the aforementioned sites. Unfortunately, no bed profiles show the precise locations of the gravel layer, but the D50 grain size distribution plot in USACE (1994) shows no place downstream of RM 1725 that had a D50 greater than 0.7mm for the period 1955-1984. It is therefore highly probable that in the areas nearer to the dam, e.g. RMs 1723-1720 and 1707-1700, the bed lacked a gravel layer and, as the degradation immediately below the dam migrated downstream, the bank height and angle increased due to fluvial undercutting and pore-water pressure related bank failures near the base of the bank. In so doing, they crossed their threshold of stability as determined by the shear strength of the bank material and several other characteristics (Simon, *et al*, 1999). This would place such banks in stages III and IV of Simon's (1989) model of channel evolution. But the increased erosion rates could also simply be caused by the changing angles of flow impingement upon the banks, for example as caused by meander migration or the appearance of transient mid-channel bars. This could also explain why some of the erosion rates decreased, i.e. as the area of greatest flow-imparted shear stresses moves to another point along the bank the section of bank previously under attack is allowed some respite.

In some places the aggradation may be the cause of the erosion. For example, the 127,000 m3/yr of erosion that occurred from RM 1621-1617 in the period 1966-1978 is immediately adjacent to the section of bed that aggraded at a rate of 55,000 m3/yr over the same period. The suggestion is thus that a bar or island developed and attained sufficient size to significantly deflect the current onto the left bank and cause it to erode. Unfortunately, the aerial photographs are not currently available to verify this hypothesis. A similar possibility exists for the bed and left bank between RMs 1612 and 1607.

Garrison Reach RM 1390-1311

Figure 4 shows that bank erosion in this reach is also overwhelmingly along banks with a mean height of 15 feet, with three distinct zones of activity between RMs 1389-1369, 1366-1352 and 1348-1331. Right bank erosion is dominant in the first two of these zones whilst left bank erosion predominates in the third. Figure 5 shows that post-dam terraces are the principal deposits being eroded at this height with 11 recorded sites of activity. From RM 1354 to the end of the reach right bank erosion is much less common. Bar and island erosion is concentrated downstream of RM 1350 along banks with a mean height of 2.5 feet. Erosion of banks with a mean height of 7.5 and 35 feet is very sporadic and is mainly of the left bank, whilst erosion of bluffs greater than 50 feet is restricted to one small area of the right bank immediately downstream of the dam at RM 1389. Figure 5 shows that there is also bluff line erosion at a mean height of 35 feet at four locations.

Examination of figure 6 shows that for the period 1956/58-1976 the right bank experienced erosion rates of 54,000 m3/yr between RMs 1381.5-1380.5 and 1377.5-1376.5. These increased and decreased respectively to 63,000 and 42,000 m3/yr for the period 1976-1985. The left bank eroded at a rate of 66,000 m3/yr between RM 1380.5-1379.5 from 1956/58-1976 and then at a mean rate of 92,000 m3/yr between

1976 and 1985. These areas correspond very well to the region of eroding banks with a mean height of 15 feet between RM 1389-1369 mentioned above. Several other stretches of right bank erosion correspond well to the zones from RMs 1366-1352 and from 1348-1331 mentioned above. From 1956/58-1976, 87,000 m3/yr of erosion occurred between RMs 1345 and 1343, although this changed to 36,000 m3/yr of deposition from 1976-1985. During this latter period, erosion rates of 59,000; 100,000; 61,000 and 123,000 m3/yr occurred respectively between RMs 1362.5-1361, 1354-1351.5, 1341.5-1340 and 1338-1337. Figure 4, based on the 1999 reconnaissance survey, does not show the sections of right bank from RMs 1354-1351.5 and 1341.5-1340 currently experiencing erosion and, as mentioned in the introduction, this highlights the problem of working with data from two different time-frames.

A very prominent zone of activity occurred along the left bank and bed between RM 1352 and 1349. Here, the bank was eroding at a rate of 200,000 m3/yr from 1956/58-1976 whilst the bed was aggrading at a rate of 136,000 m3/yr. Over the nine years from 1976-1985, however, the bed degraded at a mean rate of 169,000 m3/yr whilst the bank experienced deposition of 82,000 m3/yr. The section of bank between RMs 1352-1349 is on the outside of a right hand bend which contains several large bars and islands in the right hand side of the channel, as shown on the October 1981 aerial photograph. One possible explanation for this is that from 1956/58-1976 the high left bank erosion rate was due to the natural scour of the bed and bank toe associated with the outer bend of a meander, amplified by a further concentration of flow due to the presence of the bar and island complex. At the same time, though, a net rate of aggradation was occurring due to growth of the bars and islands. Then, from 1976-1985, and maybe as a result of excessive bar and island growth, the thalweg was deflected away from the left bank and into another section of the channel, thus causing a net rate of degradation and allowing deposition to occur in the vicinity of the left bank. Although Turtle Creek is immediately upstream of the reach in question, it is only a small tributary and its added discharge was unlikely to have been the primary cause of the high erosion rate.

Fort Randall Reach RM 880-844

The results of this analysis are incomplete since this was the first reach to be reconnoitered and the system of annotating the aerial photographs with bank heights and the extent of erosion had not yet been fully implemented. This is evident by comparing figure 8, which shows almost continuous erosion or deposition along both left and right banks from RM 879-845, to figure 7, which shows a much more incomplete record of erosion.

Examination of figure 7 reveals that left bank erosion appeared to dominate throughout the reach, with only three locations experiencing right bank erosion. From RM 871-862 erosion was concentrated along banks with a mean height of 15 feet, whilst between RMs 862.5-849 erosion alternated between the 2.5 and 7.5 feet high banks. Erosion of banks with mean heights of 35 and 50 feet was very isolated. When figure 8 is examined, however, we soon see that, historically at least, erosion occurs with similar frequency along both banks. Along the right bank erosion rates of 23,000; 37,000; 25,000 and 53,000 m3/yr occurred from 1954-1975 for RMs 875-872, 865-863.5, 854.5-853 and 851-849 respectively. For the period 1975-1985, erosion rates of

40,000 and 29,000 m3/yr were observed for RMs 870-868 and 865-863.5. For the period 1954-1975 left bank erosion occurred from RMs 870-868, 853-851 and 847.5-845 at rates of 265,000, 72,000 and 25,000 m3/yr. From 1975-1985 erosion occurred from RMs 867-865 and 847.5-845 at rates of 45,000 and 76,000 m3/yr respectively. The erosion rate of 265,000 m3/yr may be explained by the growth of a large bar/island complex, stretching from RM 870.3-868 (see aerial photograph, June 1982 *-being used at WES*), concentrating the flow against the left bank and thus greatly increasing the shear stresses being imposed upon it.

Downstream of RM 855, identifying the mechanisms responsible for the observed effects in the reach becomes much more complicated because of the delta being built at the mouth of the Niobrara River and the resulting backwater effects. The left bank erosion between RMs 853 and 851 from 1954-1975 may have been caused by the discharges from Basil Creek and Choteau Creek, both left bank tributaries, whose input remained concentrated along the left bank between RMs 853 and 851.3 by a very large bar and island complex (aerial photograph, June 1982). The small amount of aggradation that took place along this section of bank from 1975-1985 is probably due to a combination of the current being deflected away from the left bank and infilling of the channel between the bar and island complex and the bank. Between 1975 and 1985 the left bank erosion from RMs 847.5-845 was probably caused by bar growth along the right bank, as mentioned above (aerial photograph, June 1982), fed by sediment input from Ponca Creek, which concentrated flow against the left bank and caused increased scour. Figure 8 seems to support this assertion since the lines depicting left bank erosion and right bank deposition have an almost symmetrical relationship.

These patterns of bank erosion and deposition were all underscored by net aggradation upstream of the Niobrara River confluence from RM 853-844 for the period 1954-1975, which culminated in a mean aggradation rate of 81,000 m3/yr between RMs 847.5-845. For the period 1975-1985, however, from RM 851-844 the bed ranged from 101,000 m3/yr of degradation to 59,000 m3/yr of aggradation and this suggests that the Niobrara River delta was experiencing significant reworking during the time frame in question.

The 265,000 m3/yr of erosion from RM 870-868 aside, it is evident that the bank erosion rates are considerably lower in this reach than in the other three. This is unusual because this reach is the shortest of the four and the erosional and degradational effects of the dam would be expected to dominate throughout most of its extent. Downstream of RM 855 the lack of more intensive bank erosion may be due in part to the presence of the Niobrara Delta imparting stabilising backwater effects and, a little further downstream, the presence of Lewis and Clark Lake doing the same. This backwater effect is shown in USACE (1994) by the adjusted water surface profile downstream of RM 860 increasing steadily in elevation by about six feet between 1954 and 1985. Upstream of RM 855, a zone stretching only 25 miles downstream from the dam, the lower erosion rates may be a function of the bank materials, although in view of the absence of bank material sample data it is not yet possible to verify this statement.

Gavins Point Reach RM 811-753

Inspection of figure 9 shows that the mean height of eroding banks tends to decrease in a step-like manner in the downstream direction. From RM 809-793 erosion occurs mainly along banks with a mean height of 15 feet. Downstream of this range it is principally the right bank that erodes sporadically at this height. For banks with a mean height of 7.5 feet there is a low density of eroding bank line between RMs 791-773 and also erosion from RM 764-756.5. Overall at this height there is a greater proportion of eroding left bank that at 15 feet. Erosion of banks with a mean height of 2.5 feet is concentrated in the downstream end of the reach between RM 774.5-754. The greatest concentration of eroding bars and islands occurs at this height along with the lowest proportion of eroding right bank. Generally speaking, left bank erosion increases in the downstream direction and as the mean bank height decreases, whilst right bank erosion occurs throughout the reach but decreases as bank heights decrease.

Figure 10 shows that there was a great deal of instability in both the bed and banks from 1960-1986, making this reach the most intensively eroding of the four. This is probably because there is no dam downstream of the reach to impart stabilizing backwater effects. The left bank shows more instability from 1960-1974 than for 1974-1986, with erosion rates of 112,000; 61,000; 56,000; 71,000; 318,000; 306,000 and 217,000 m3/yr occurring from RMs 808-807, 804-802, 801-800 798-797, 778.5-777, 774-771.5 and 761.5-758 respectively. Along the right bank both time periods show several peaks of extremely high erosion rates. From 1960-1974 rates of 317,000; 98,000; 101,000; 141,000 and 733,000 m3/yr were observed from RMs 804-802, 797-795.5, 780-778.5, 771.5-769 and 761.5-758 respectively. From 1974-1986 rates of 185,000; 187,000; 148,000; 88,000; 271,000; 283,000 and 206,000 m3/yr occurred respectively from RMs 804-802, 797-795.5, 792.5-790.5, 786-784.5, 782-780, 776-774 and 761.5-758. Slightly greater fluctuations occur between the maximums of erosion and deposition downstream of about RM 780, but apart from this there is no significant relationship between the locations of bank erosion and the erosion of banks of a certain height.

The bed also shows some high rates of degradation, notably 160,000; 114,000; 117,000; 320,000 and 537,000 m3/yr from RMs 790.5-789, 784.5-782, 780-778.5, 769-762.5 and 756-753 respectively from 1960-1974. From 1974-1986 the greatest points of degradation occur between RMs 782-780, 774-771.5, 769-762.5 and 756-753 with rates of degradation of 104,000; 321,000; 312,000 and 233,000 m3/yr. The fluctuation between rates of degradation from point to point appears to increase downstream from around RM 790, with the largest fluctuations occurring downstream of RM 774. This may partially be due to the input of the Vermillion River at RM 772.

Summary

Over the period of study, Fort Peck Reach is the most extensively eroding of the four reaches, with virtually no river mile unaffected by erosion of one or both banks, and with the greatest number of erosion sites occurring along banks with a mean height of 15 feet. Old terrace followed by post-dam terrace are the principal bank types affected. It also has some of the highest rates of erosion, surpassed only by those in Gavins Point Reach, although bed armoring immediately downstream of the dam may have reduced some previously high erosion rates.

Erosion of banks in Garrison Reach is concentrated along those with a mean height of 15 feet, which are mostly post-dam terraces, although there are no really high rates of erosion in this reach as compared to the rates in other reaches. From RMs 1376-1365 there is quite a range of bed activity that is not reciprocated by activity along the banks, thus suggesting a greater bank stability, either natural or artificial.

Fort Randall Reach has the lowest rates of bank erosion of all four reaches and is dominated in its downstream end by backwater effects caused by the delta at the mouth of the Niobrara River. This may prevent bank erosion rates being as high as they might otherwise be in the immediate upstream areas, by reducing the overall velocity of the flow as it approaches the delta. Erosion in this section of the reach is probably caused by tributary discharge and bar and island growth concentrating flow against the banks. Reworking of the delta may also cause the point of bank attack to switch relatively rapidly. Field observations of the extent of left and right bank erosion and of bank heights were not very thorough and should thus be treated with caution. Upstream of the zone affected by the delta, the erosional bank morphology generally associated with the area downstream from a dam is not as evident as it perhaps should be and this suggests some stabilising factors in the bank material. Field sample data results are still awaited to verify this.

Gavins Point is the most unstable and intensively eroding of the reaches, having by far the highest rates of both left and right bank erosion and also bed degradation. This is almost certainly due to there being no dam at the downstream end of the reach to impart stabilizing or aggradational tendencies upstream.

References

Dangberg, D. & Assoc. and River Pro's (1988), Missouri River, Fort Peck Dam: Downstream Degradation/Aggradation and Sediment Trends Study. USACE, Omaha District.

Darby, S.E. and Thorne, C.R. (1996), Bank Stability Analysis for the Upper Missouri River, Unpublished Report submitted to the European Research Office, London.

Pokrefke, T.J., Abraham, D.A., Hoffman, P.H., Thomas, W.A., Darby, S.E. and Thorne, C.R. (1998), Cumulative Erosion Impacts Analysis for the Missouri River Master Water Control Manual Review and Update Study, Technical Report CHL-98-7, USACE.

Simon, A. (1989), A model of channel response in disturbed alluvial channels, *Earth Surface Processes and Landforms,* 14, 11-26.

Simon, A., Shields, F.D., Ettema, R., Alonso, C., Garsjo, M.M., Curini, A. and Steffen, L. (1999), Channel Erosion on the Missouri River, Montana, between Fort Peck Dam and the North Dakota Border. USDA.

USACE (1986), Missouri River Streambank Erosion Study, Fort Peck Dam, Montana, to the Yellowstone River, N. Dakota. USACE, Omaha District.

U.S. Army Engineer Division, Northwestern, Missouri River Region (1994), Missouri River Master Water Control Manual, Review and Update, Draft Environmental Impact Statement, Volume 5: Aggradation, Degradation and Water Quality Conditions. Omaha District, USACE.

Figure 1a: Summary of Fort Peck Reach Bank Line Erosion and Height (a)

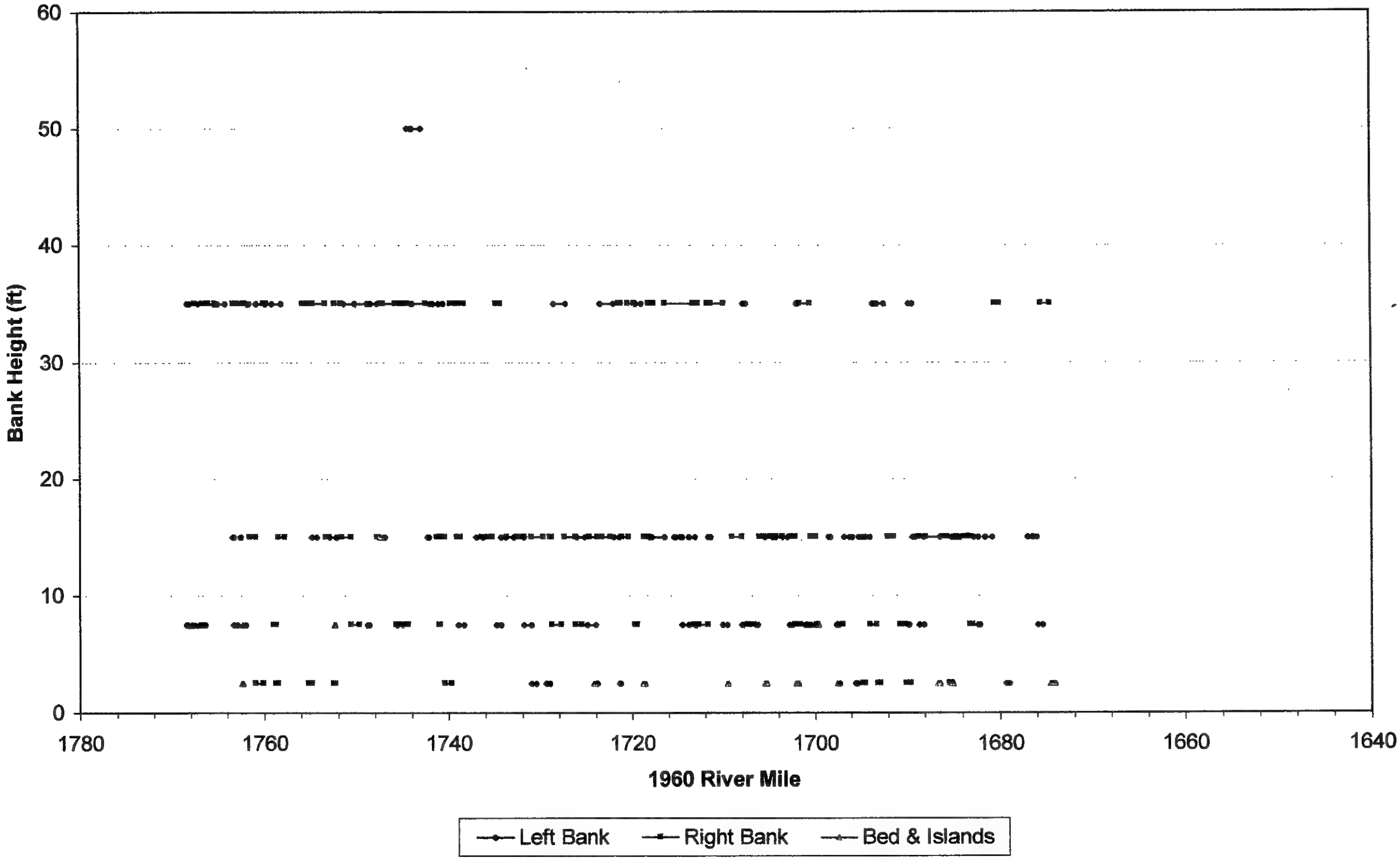

Figure 1b: Summary of Fort Peck Reach Bank Line Erosion and Height (b)

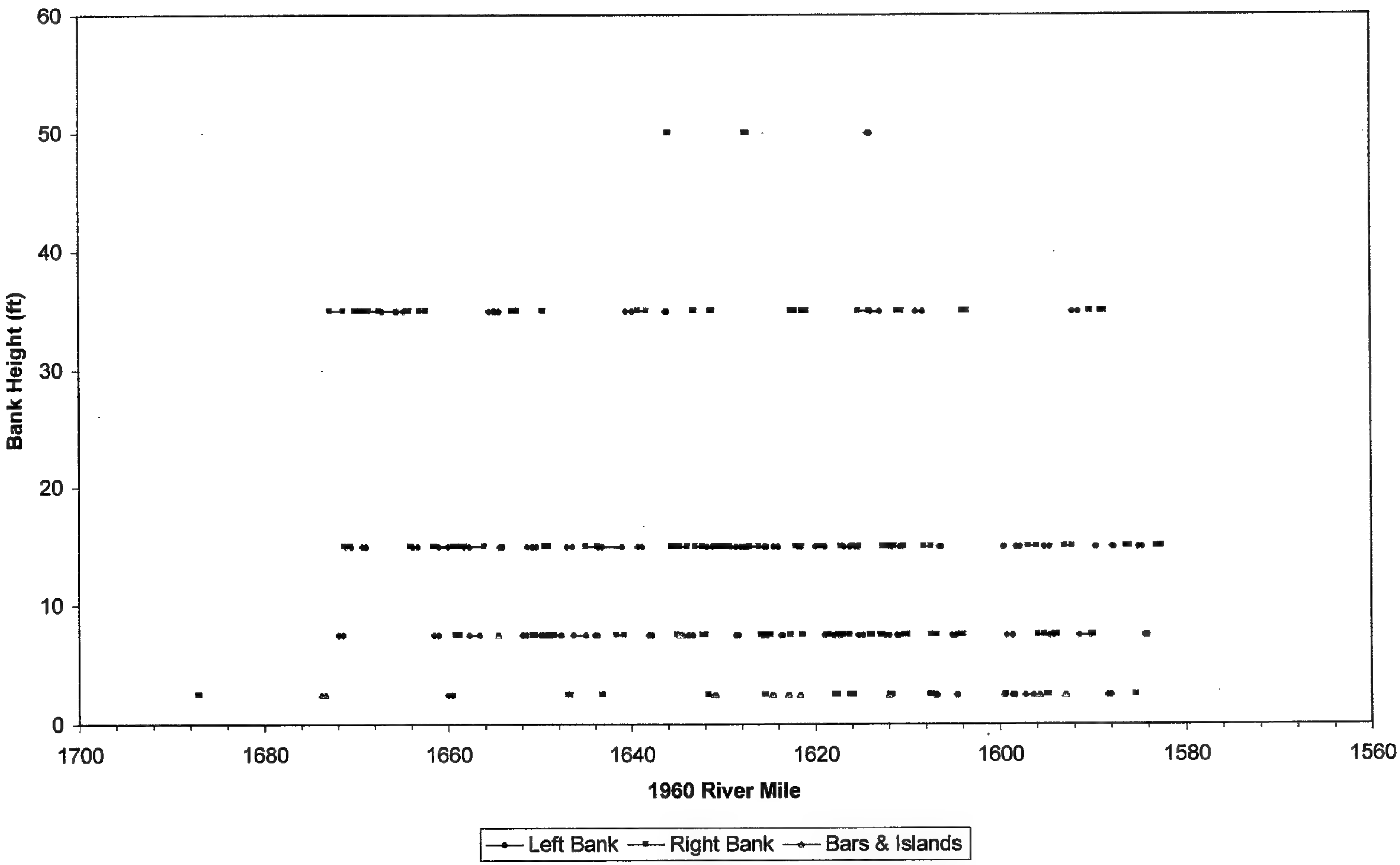

Figure 2: Fort Peck Reach frequency analysis of bank heights based on the overlay bank height classification scheme

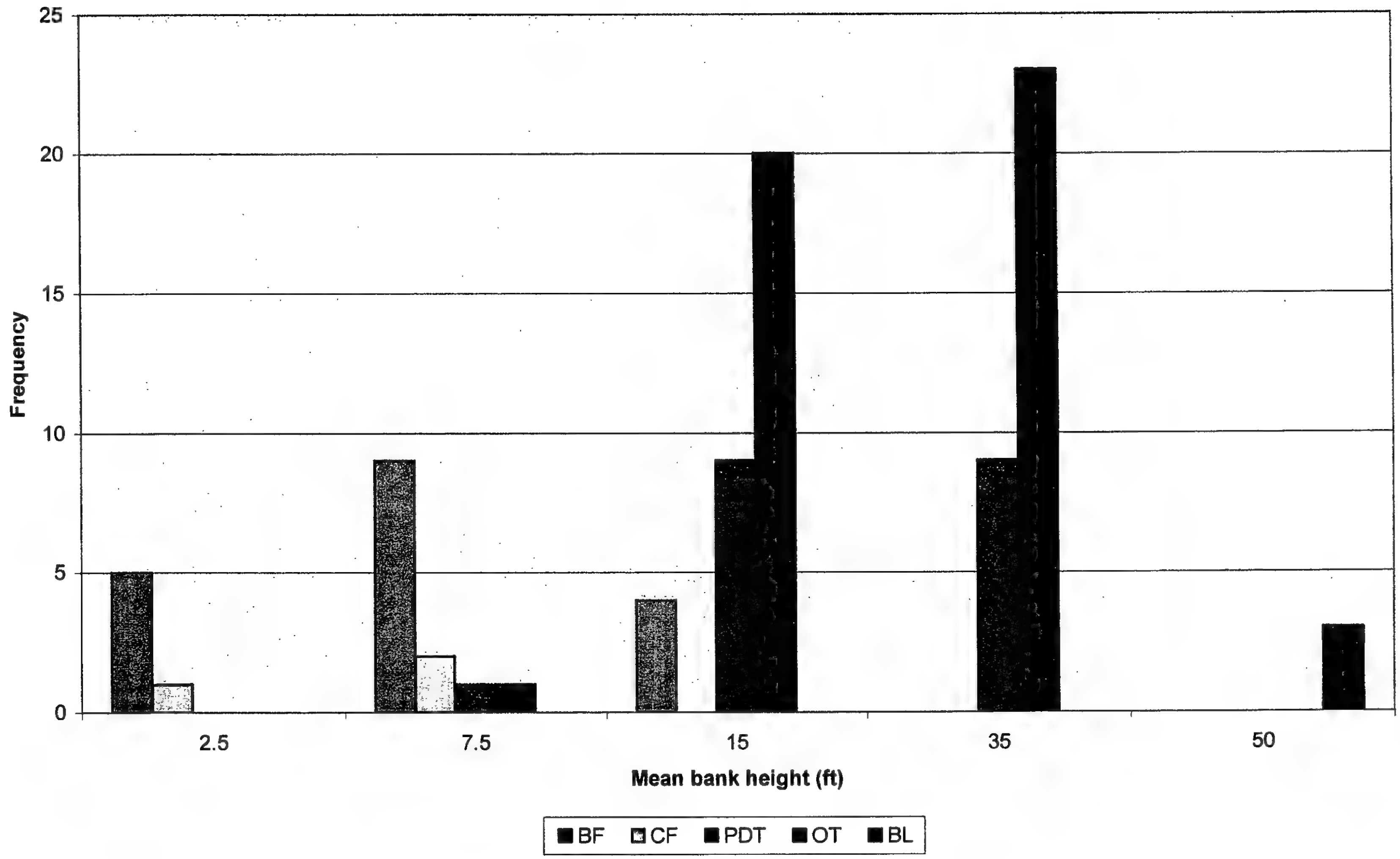

Figure 3: Fort Peck Reach
Comparison of Left Bank Erosion Rates

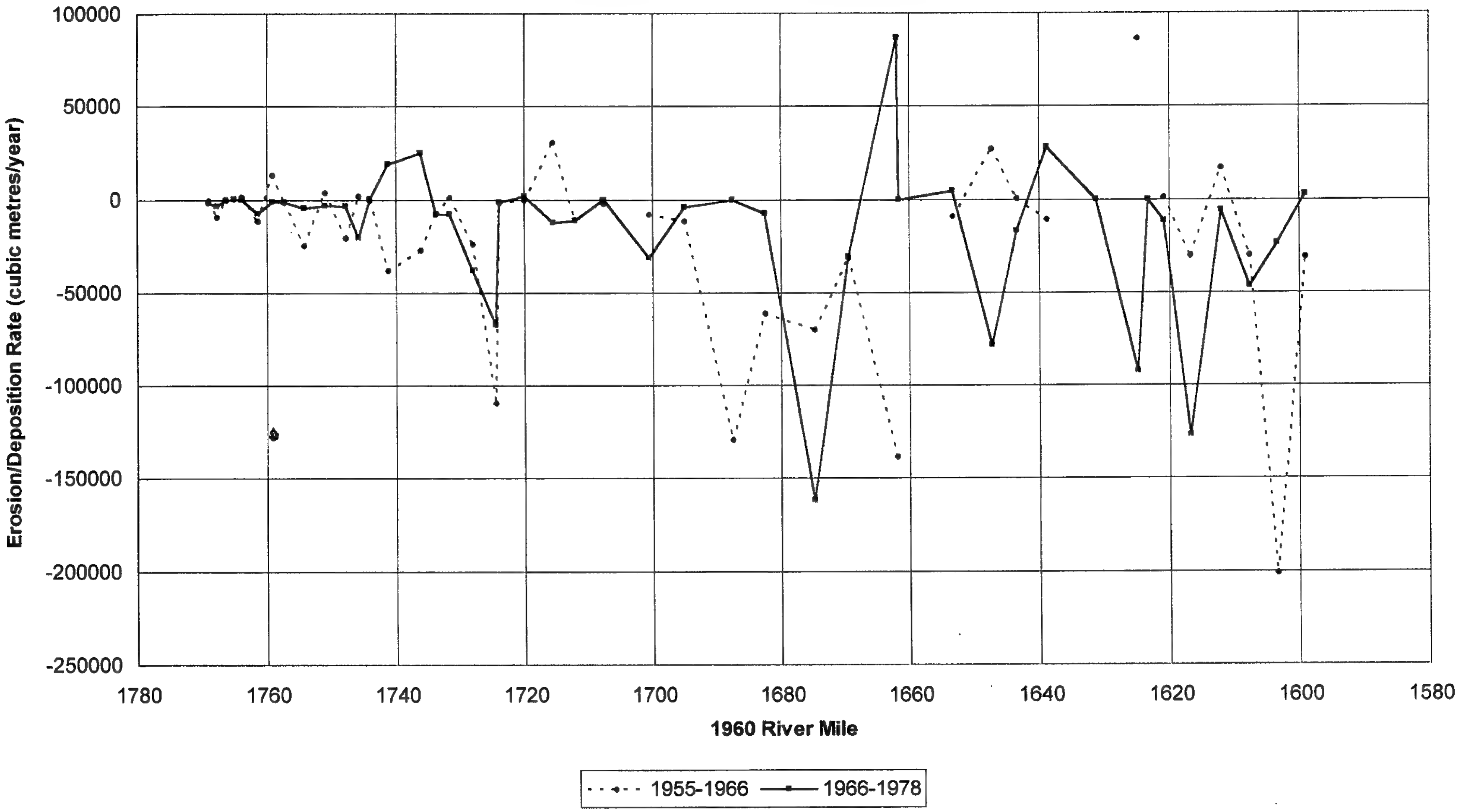

Figure 4: Summary of Garrison Reach Bank Line Erosion and Heights

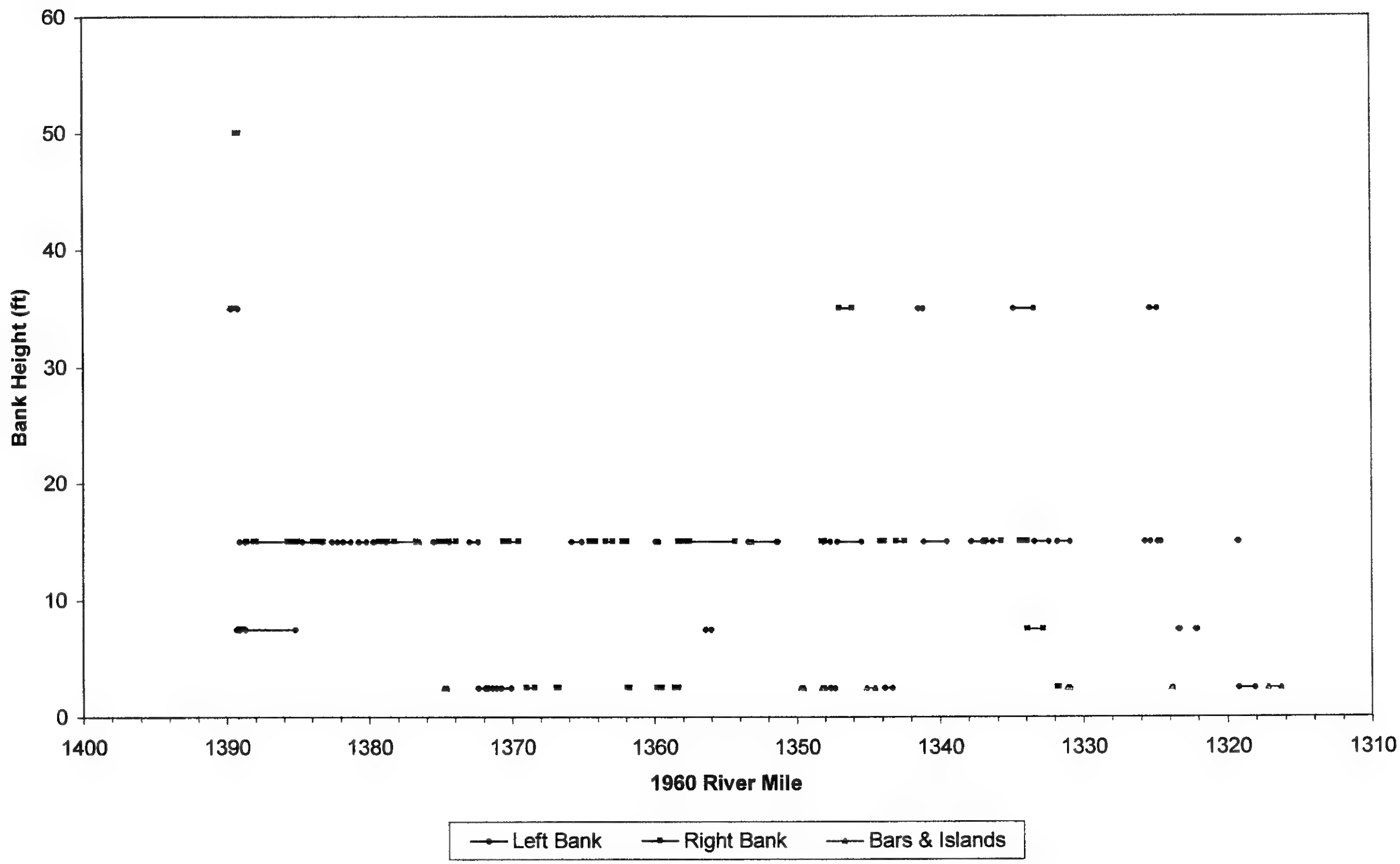

Figure 5: Garrison Reach frequency analysis of bank heights based on the overlay bank height classification scheme

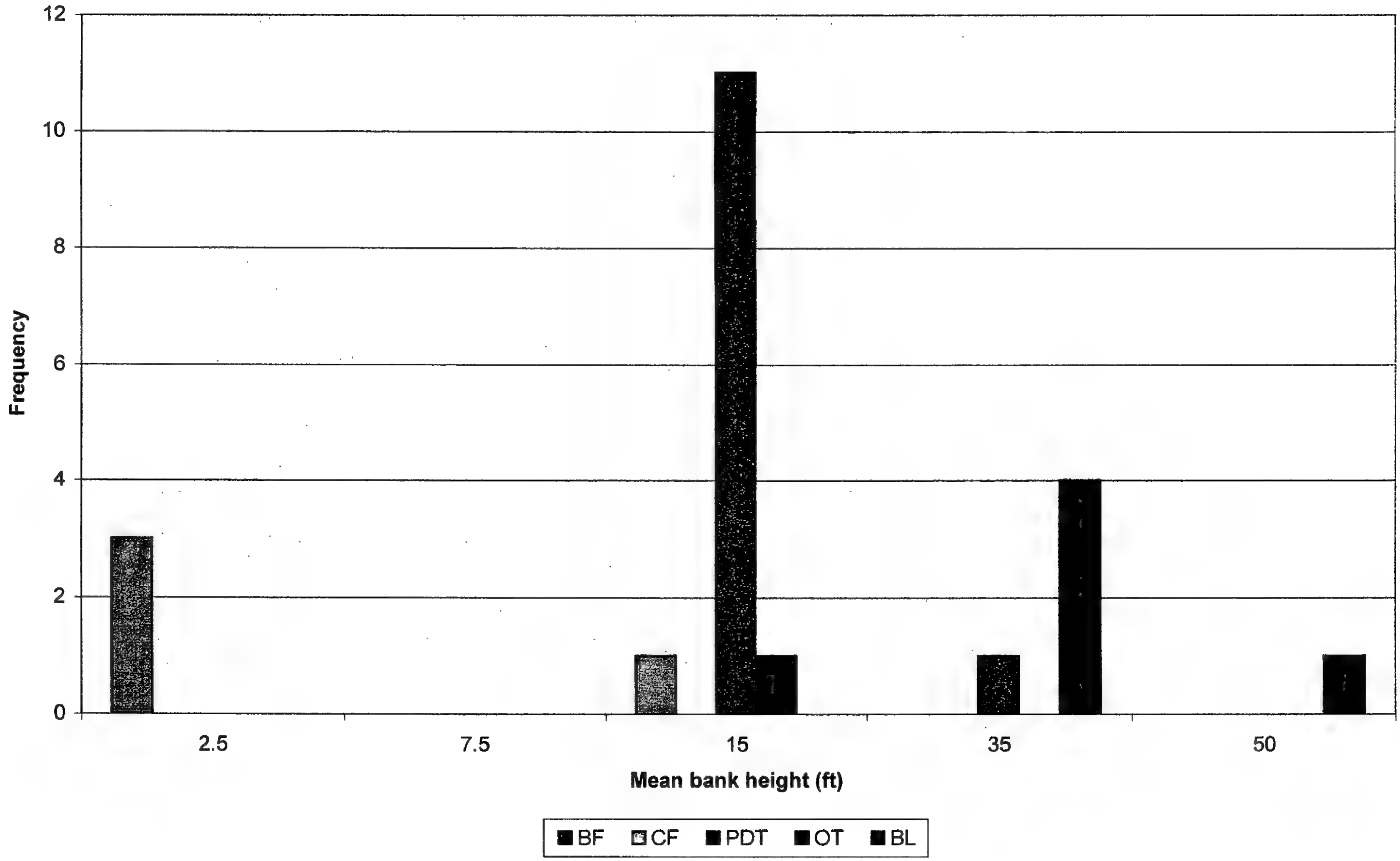

Figure 6: Garrison Reach
Comparison of Left Bank Erosion Rates

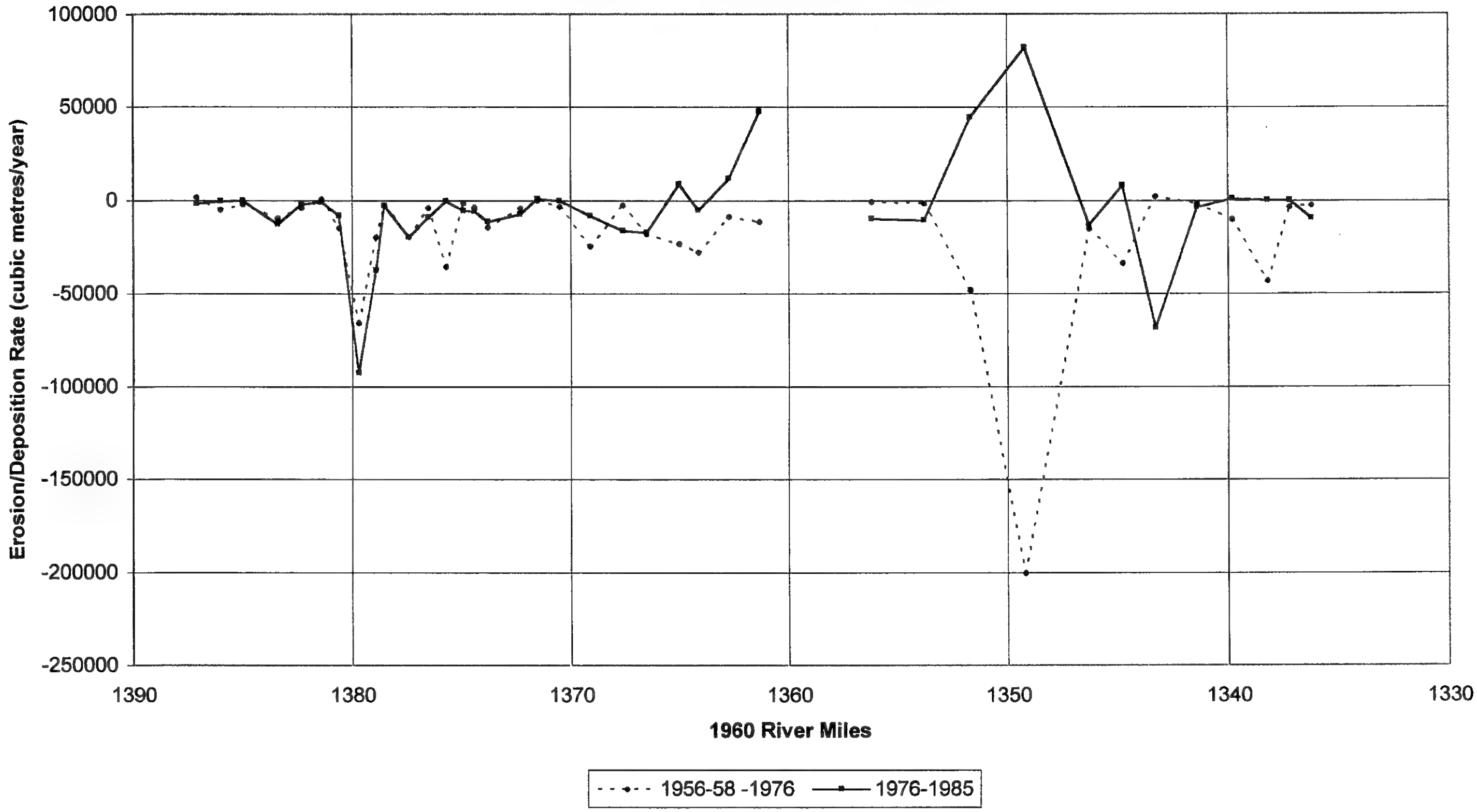

Figure 7: Summary of Fort Randall Reach Bank Line Erosion and Height

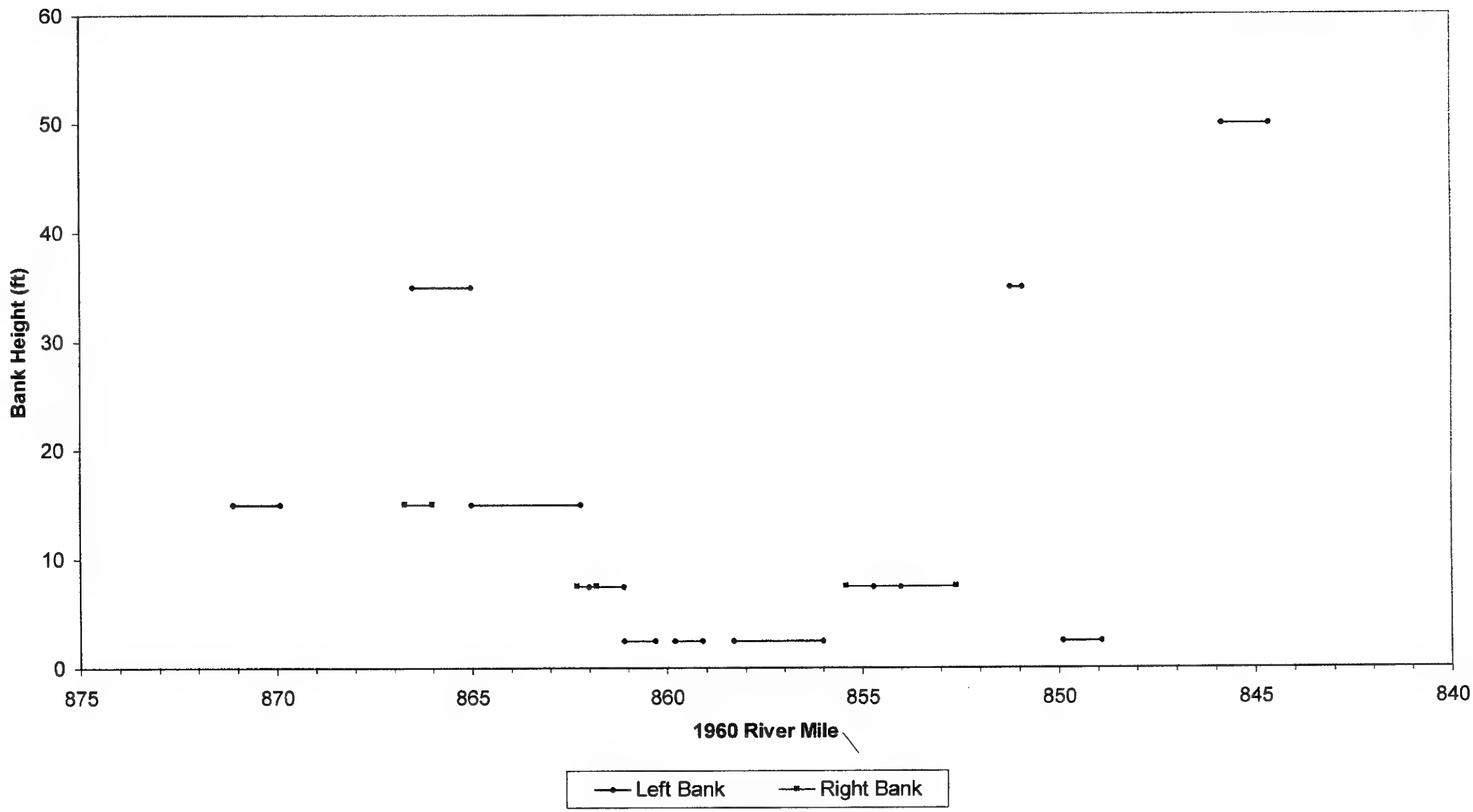

Figure 8: Fort Randall Reach
Comparison of Left Bank Erosion Rates

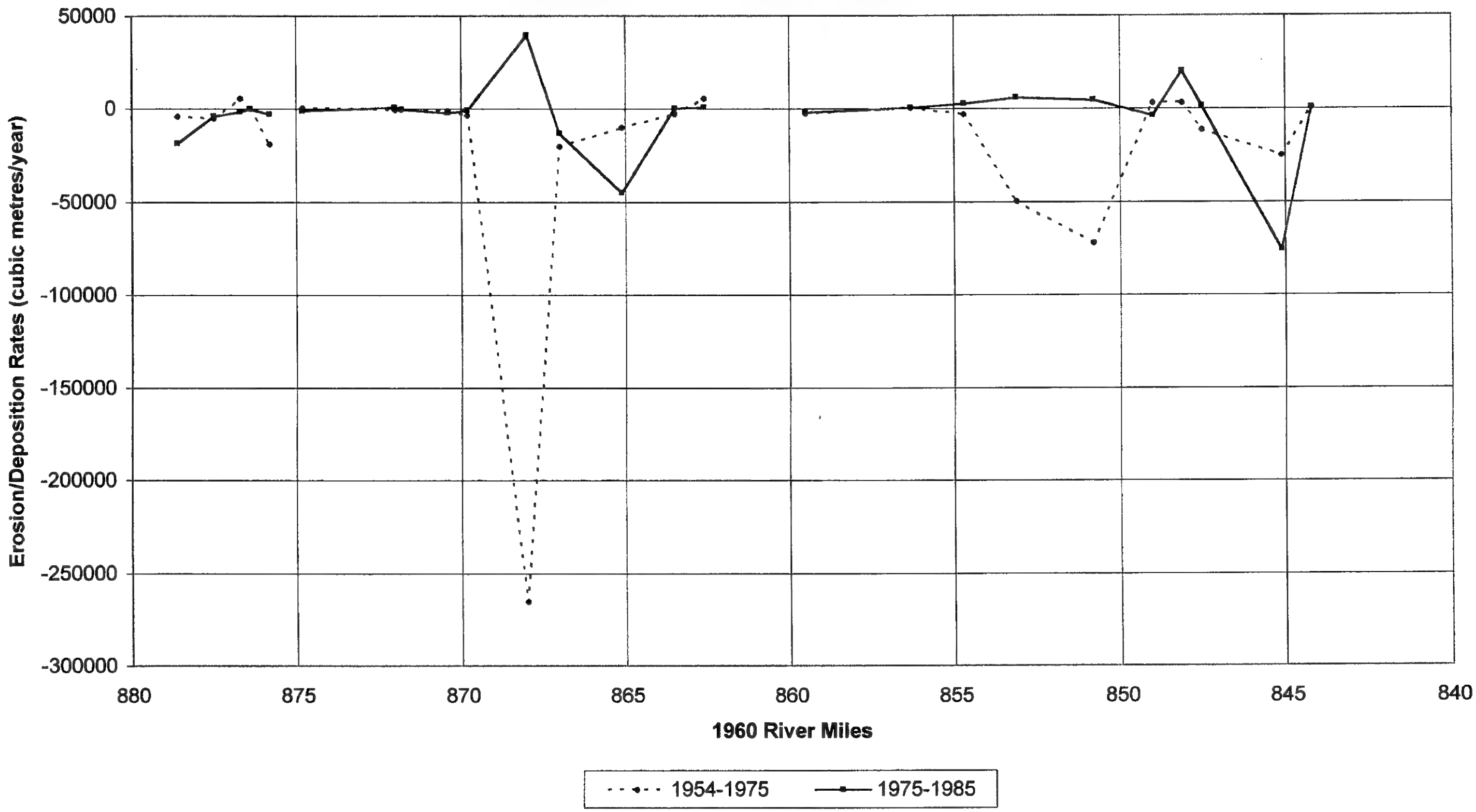

Figure 9: Summary of Gavins Point Reach Bank Line Erosion and Heights

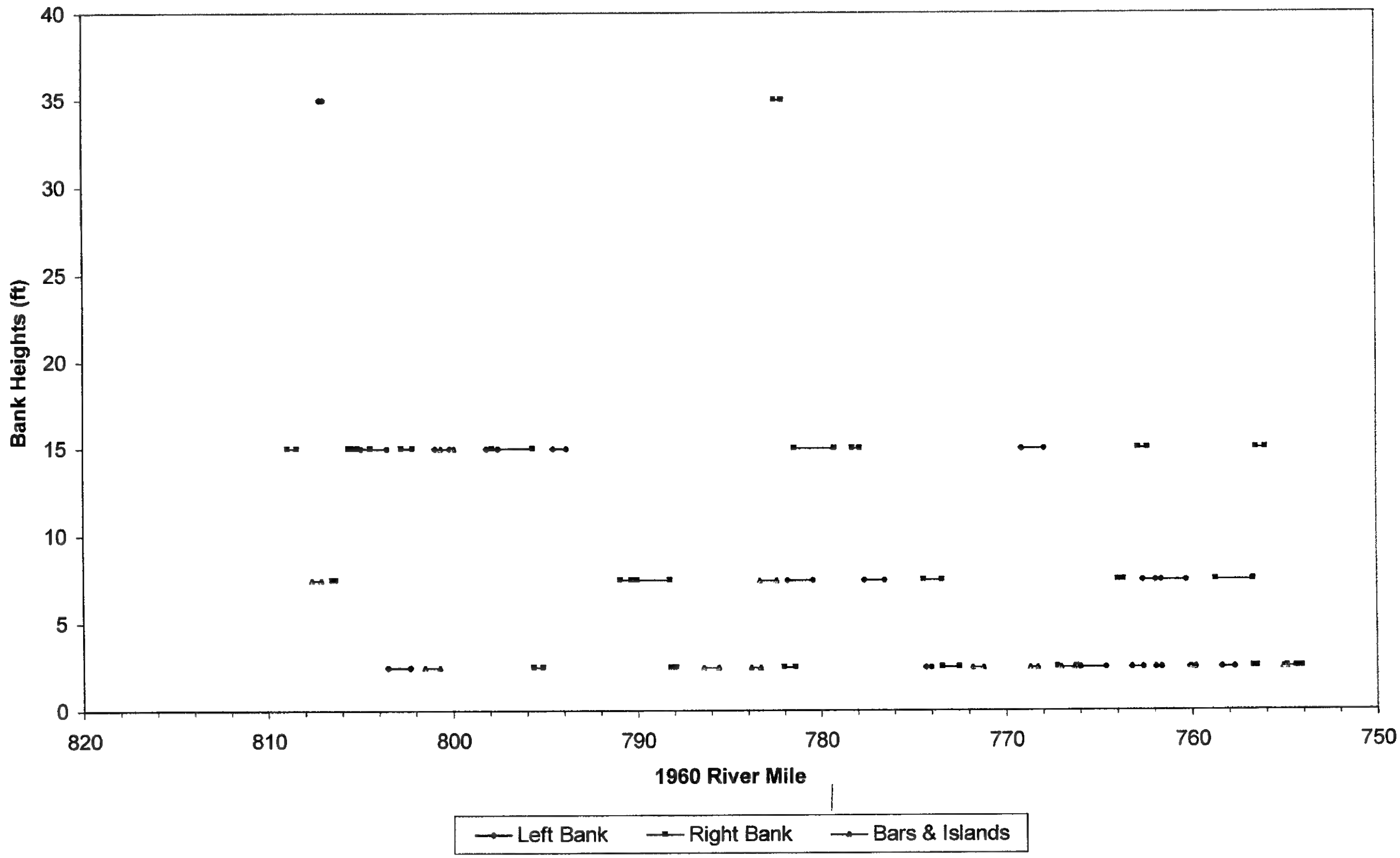

Figure 10: Gavins Point Reach
Comparison of Left Bank Erosion Rates

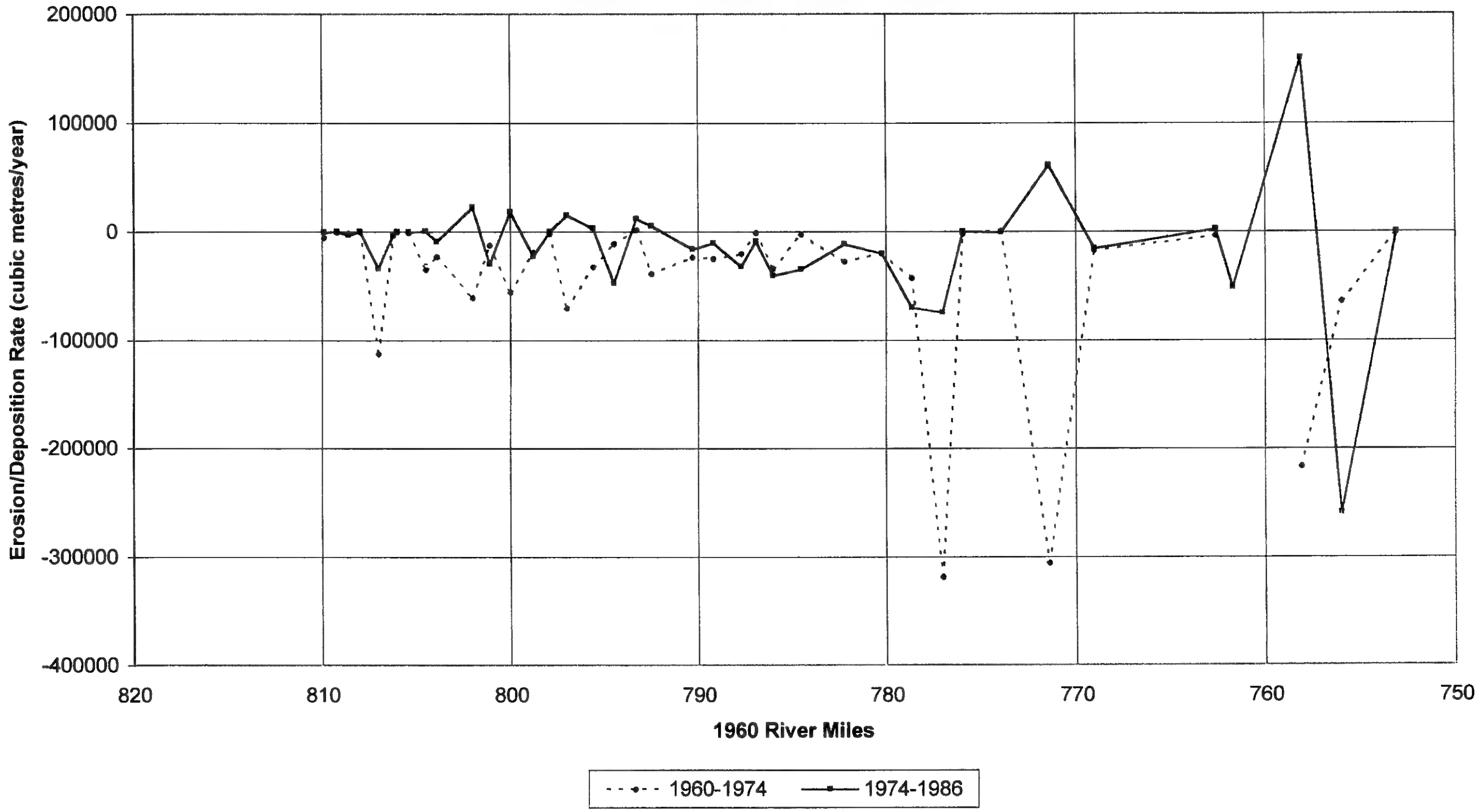

Figure 11: Frequency analysis of bank types in the Fort Peck Dam Reach

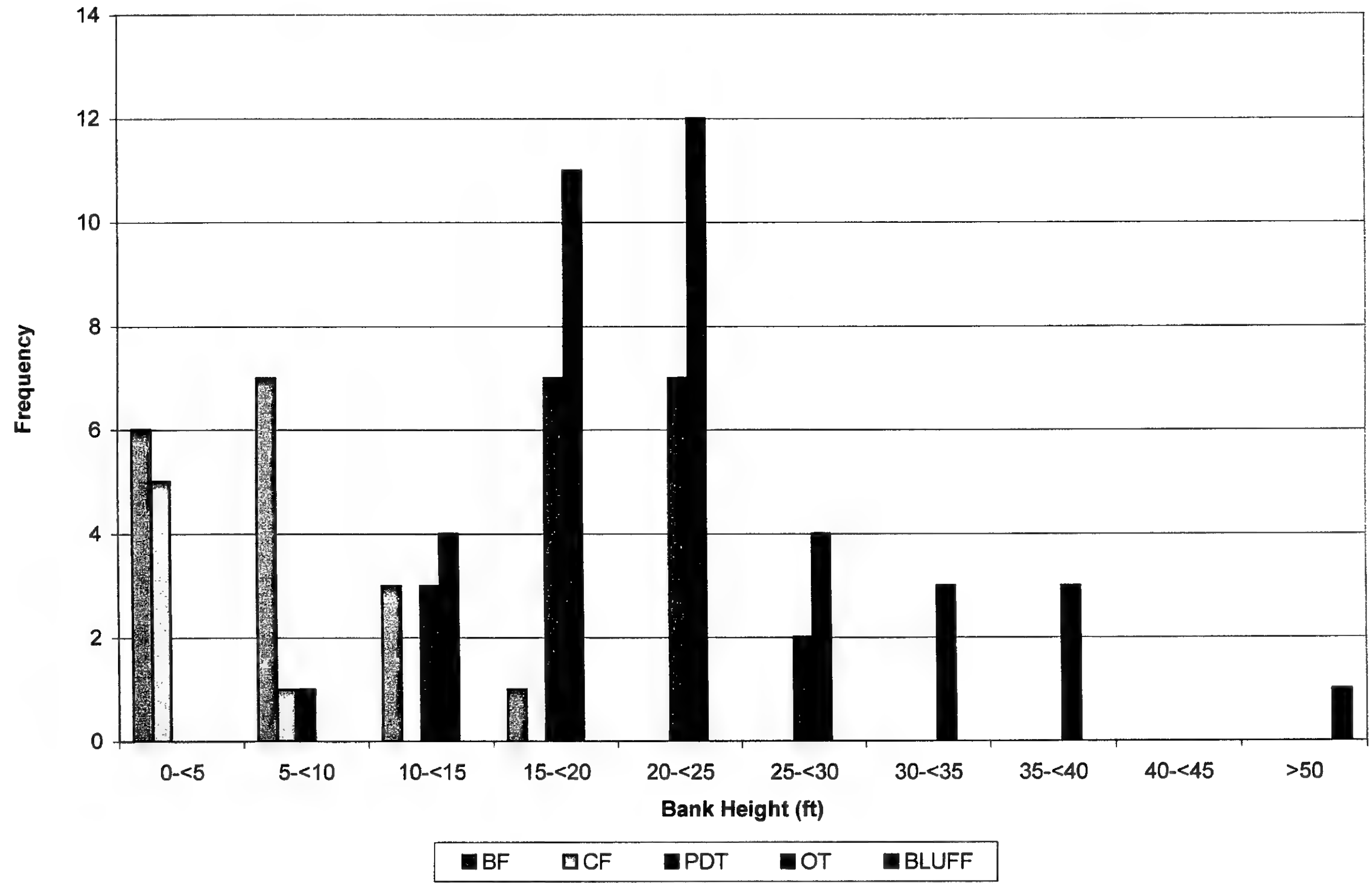

Part VI Geomorphic Reach Classification

River channel classification

River channel classification is undertaken because it presents a means of reducing a complex system into a series of more easily understandable units, which in turn facilitates further study and the organization of management options. A distinction needs to be made between schemes that *classify* rivers and schemes that *characterize* them. The former involves a subdivision of the river channel into discrete reaches according to designated criteria whereas the latter concurrently uses multiple criteria that allow the formation of statistically distinct groupings. There are a wide variety of types of classification scheme. Morphological classifications proceed on the basis of the existing channel features, whereas other schemes classify on the basis of river channel adjustment by distinguishing active processes from the facets of the existing morphology. A third type of classification provides information about the conservation value of the river by noting the differences between the existing channel morphology and the morphology that would exist without the effects of human disturbances (Downs, 1995).

Both a classification and a characterization scheme are applied in this study. First, the four study reaches are characterized by identifying Geomorphologically Similar Reaches (GSRs) and, second, the river is classified according to the system developed by Brice (1975).

Geomorphologically Similar Reaches

Identification of GSRs involves breaking down each main reach into discrete sub-reaches based on similarities in form and process. Both quantitative and qualitative techniques are employed to synthesize data from a variety of sources. First, summary tables of data were compiled for the four reaches. These include information on whether the banks are eroding or accreting and the location of this activity (i.e. inside of the bend, outside of the bend or at a crossing); the results of Pokrefke *et al's* (1998) analysis into rates of erosion and deposition along both banks and the bed, (note that these data are included as working figures only and will be replaced when more accurate rates based on the digitized banklines are available); reach-scale trends of bed aggradation and degradation based on the findings of various workers (USACE, 1986, 1994, 1997; Dangberg *et al*, 1988a & b; Midwest International, 1997; and WEST Consultants, 1998); and on the solid and drift geology in which the river is located. These tables are presented in Appendix A. Second, the cross-sectional data for each reach was input to HEC-RAS and, by running the maximum mean monthly discharge, the bed slope, energy slope, velocity, width-depth ratio, hydraulic radius and conveyance were calculated. These parameters along with sinuosity, the locations of left and right bank revettements and the bar and island densities from Pokrefke (1998) were plotted and are presented as Figures B1 to B4 in Appendix B. Finally, aerial photograph mosaics from the mid-1980s and late-1990s were examined to see the variations in degrees of meandering and braiding. Taken together, these three sources were used to identify reaches that had similar planform and hydraulic properties and where similar processes appeared to be occurring. For instance, when a clear change from a meandering to a straighter and more braided planform was noticed on the photographic mosaics, the plots of the hydraulic variables would be

examined to see if any of the trend lines showed a significant change in pattern at a similar river mile location. This was frequently the case and so this location was chosen as a boundary to a GSR. It is important to note that a change in planform did not occur at the exact same location as changes in the hydraulic variables or a change in geology, but generally within a few river miles. This is because rivers are natural systems that exhibit a continuum of channel form that are a function of the driving variables and boundary conditions of the particular physiographic region in which they are located (Thorne, 1997). As a result, it is only natural to expect a certain degree of lag between the point when a particular driving variable begins to change and the point when a threshold is crossed that allows a change in form to occur. The selection of the precise location of the boundary to the GSR is thus subjective to a certain degree in that it represents the personal opinion of the workers involved as to what are the most significant factors for the project out of all the data being considered.

The Brice Classification

The Brice Classification describes the morphology of rivers or sections of rivers additively in terms of their degree and character of sinuosity, braiding and anabranching. Each of these three aspects of planform are assigned a number and letter code for the degree and character respectively, such that each reach can be described by a six letter code. For example, a river section assigned the code 1D2B3C would be described as having a sinuosity between 1 and 1.05 and be single phase, wider at bends with chutes common; be between 35% and 65% braided with mostly bars and islands; and have >65% anabranching with split channel, sub-parallel anabranches. A total of 3120 river types can be identified in this way.

The system was developed based on the morphological characteristics that were observed from aerial photographs of about 250 river reaches, mostly within the United States but from other parts of the world also, and occurring in climates ranging from arctic to equatorial. In addition to the photographs, large-scale topographic maps and gauging station data for 200 reaches were used to develop the classification.

Application of the classification

To apply the classification Brice developed a series of diagrams with accompanying verbal descriptions that describe the degrees of sinuosity, braiding and anabranching and their accompanying characteristics (Figure 1). The degree of sinuosity was calculated by dividing the channel centerline length by the straight-line valley length. When determining the character of the sinuosity, several of the options were frequently applicable to the reach in question and it was necessary to make a sometimes subjective judgment as to which of the characteristics were most common, or the most important for this project. For instance there might be irregular width variation in the reach (option 'e') but chutes might also be common (option 'd'). If it was felt that the presence of chutes was of greater significance to the morphology of the channel, option 'd' would be selected and the 'chutes common' aspect emphasized to highlight the fact that this was the reason for this particular selection. The degree of braiding is also a quantifiable property and was determined by measuring the proportion of total reach length that was divided by one or more bars and islands. The character of braiding was determined by looking at the relative numbers of bars and

islands present and, if necessary, the morphology of the islands. This was a much less contentious issue than selecting the character of sinuosity. The degree of anabranching was measured in the same way as the degree of braiding. Character of anabranching was determined by seeing which was the predominant type present in the reach. If two or more types were present then the character was described as composite (option 'e').

Problems with the classification

It soon became apparent when applying the classification that there were some major problems and ambiguities with the terminology as used by Brice in 1975 and the terminology as it is used today in 2000. He states that a reach is braided if the '*Width of individual bars and islands is less than three times total water width at "normal" discharge. In this size range, an island differs from a bar in that it is vegetated.*' And when considering whether or not anabranching is occurring he writes, '*...the term "anabranching" refers to the division of a river by individual islands whose width is greater than three times water width at "normal" discharge. Ground of such width between anabranches is called an island whether vegetated or not. As the division becomes more complex, such that the number of anabranches consistently exceeds three along the length of the reach, the river becomes an anabranched distributary system.*' (Brice, 1975; p3).

The selection of islands of three times water width as the distinguishing feature between braiding and anabranching is completely arbitrary (Bridge, 1993). Brice gives no explanation as to the reasons for selecting this figure and it is therefore assumed here to have no physical basis. Furthermore, why is Brice's anabranched distributary system not considered to be a braided system? Presumably, although this is not stated by Brice, each island of the anabranched distributary system must be greater than three times the width of the water surface at average discharge in order for the reach not to be considered braided. This leads to the question of where exactly should the measurement to determine the width of the bar/island be made? Should it be at the widest point only, or should measurements be taken at several cross-sections along the length of the feature and an average taken? Also, must the 'island' be a whole entity to actually be considered an island, or can it be dissected by small channels at higher discharges? Or, if dissected, would this mean that the reach is braided? In effect, the definitions given by Brice mean that an anabranched channel cannot be clearly distinguished from a braided channel. Also, the inconsistent definition of islands is problematic since it artificially separates depositional forms that may have a common genesis and geometry, the elements that determine whether or not a feature is vegetated or not being factors such as the length of time the sediment surface is exposed, the nature of the sediments, the local climate, and the types of vegetation available for colonization (Bridge, 1993).

These ambiguities were resolved in the following fashion. A braided channel is one where the channel itself is still very clearly a single-thread channel. One or both banks may be eroding and thus widening the channel adjacent to the bar and island deposits, and smaller channels may be dissecting and flowing around the bars and islands, but as soon as the water flows past these deposits it is still a single-thread channel. An anabranched system is one in which the channel exists as a multi-thread channel for a significant distance downstream, generally a minimum of 5 to 10 pre-division channel

widths. Also, the mechanism of deposit formation is not important for the purposes of the Brice classification and so bars and islands do not have to conform to the patterns of formation elucidated by, for example, Leopold and Wolman (1957). For instance, if a point bar or section of floodplain has recently been separated from its bank by a cutoff but is still clearly a single sedimentary feature, it would be classified as a chute cutoff and accounted for by options 'c' or 'd' in the character of sinuosity section of the classification. It would not subsequently be included in the assessment of the degree of braiding. If, however, the cutoff feature has experienced significant dissection it would be included in the quantification of the degree of braiding. Alternately, if the cutoff feature has not been dissected and is greater than approximately 5 to 10 times the channel width, that section of the reach would be classified as an anabranched channel system. Chuting and anabranching can thus co-exist since the former is one of the mechanisms of formation of the latter. Where sections of an anabranch exhibit braiding, i.e. the presence of bars or islands in one of the anabranches around a much larger island, only this section is measured and included in the degree of braiding. The entire anabranched reach is then measured and included in the degree of anabranching in the normal way. In view of the above it is thus possible for the Brice code for a particular reach to show very different values for degrees of braiding and degrees of anabranching (Thorne *Pers. Comm.*, 2000).

Results of the GSRs and Brice Classifications

The sub-reaches identified by the application of the two classification systems to the four main reaches are presented in Table 1 below. Tables C1 to C8 in Appendix C present the full results of the two classifications, including the numerical and written explanations to the code symbols for the Brice system, and the criteria used to delineate each of the GSRs. The Brice classification was applied to each of the main reaches in their entirety and then to sub-reaches that were identified where distinctions in Brice-type channel could be made.

Table 1: Sub-reaches identified under the two classification systems

Reach Number	Boundaries of GSRs (1960 River Miles)	Boundaries of Brice Reaches (1960 River Miles)	Brice Channel Type
Fort Peck Reach			
Entire Reach		1771-1582	3D2B0C
1	1766-1750	1766-1758	3B0D00
2	1750-1713	1758-1752	1E3D00
3	1713-1700	1752-1698	3D2B0C
4	1700-1686	1698-1686.3	2E3A00
5	1686-1654	1686.3-1653	3D3B1E
6	1654-1621.7	1653-1618	3E2B1E
7	1621.7-1605	1618-1605	2B3B00
8	1605-1582	1605-1582	3D2A00
Garrison Reach			
Entire Reach		1390-1311	2E2B0C
1	1390-1376	1390-1378	1B0000
2	1376-1363	1378-1368	1D2B1C
3	1363-1353	1368-1329	2E3A00
4	1353-1340	1329-1315	2D2B00
5	1340-1324.5		
6	1324.5-1311		

Fort Randall Reach			
Entire Reach		880-843	1D2B1E
1	880-873.9	880-854.1	1D1B1E
2	873.9-867.5	854.1-843	1D3B00
3	867.5-861.7		
4	861.7-854.5		
5	854.5-851		
6	851-844		
Gavins Point Reach			
Entire Reach		811-753	2D1B1E
1	811-796	811-798	1D1B1B
2	796-776.2	798-769	2D2B1D
3	776.2-764.7	769-753	2D1B0D
4	764.7-753.9		

References

Brice, J.C. (1975), Airphoto interpretation of the form and behaviour of alluvial rivers. Final report to the U.S. Army Research Office - Durham, Box CM, Duke Station, Durham, NC 27706, prepared under contract number DA-ARD-D-31-124-70-G89, Washington University, St. Louis, pp 1-10.

Bridge, J.S. (1993), The interaction between channel geometry, water flow, sediment transport and deposition in braided rivers. In Best, J.L. and Bristow, C.S. (eds), *Braided Rivers*, Geological Society Special Publication No. 75, 13-71.

Dangberg, D. & Assoc. and River Pro's (1988a), Missouri River, Fort Peck Dam: Downstream Degradation/Aggradation and Sediment Trends Study. USACE, Omaha District.

Dangberg, D. & Assoc. and River Pro's (1988b), Missouri River: Fort Randall Dam – Downstream degradation/aggradation and sediment trends study. USACE Omaha District

Downs, P.W. (1995), River Channel Classification for Channel Management purposes, in Changing River Channels, Gurnell, A.G. and Petts, G.E. (eds.), John Wiley and Sons Ltd.

Leopold, L.B. and Wolman, M.G. (1957), River channel patterns – braided, meandering and straight. *U.S. Geological Survey Professional Paper* 422-H, 84pp.

Midwest International, Inc. (1997), Fort Peck Project, Montana: Downstream Channel and Sediment Trends Study. USACE, Omaha District.

Pokrefke, T.J., Abraham, D.A., Hoffman, P.H., Thomas, W.A., Darby, S.E. and Thorne, C.R. (1998), Cumulative Erosion Impacts Analysis for the Missouri River Master Water Control Manual Review and Update Study, Technical Report CHL-98-7, USACE.

USACE (1986), Missouri River Streambank Erosion Study, Fort Peck Dam, Montana, to the Yellowstone River, N. Dakota. USACE, Omaha District.

U.S. Army Engineer Division, Northwestern, Missouri River Region (1994), Missouri River Master Water Control Manual, Review and Update, Draft Environmental Impact Statement, Volume 5: Aggradation, Degradation and Water Quality Conditions. Omaha District, USACE.

WEST Consultants, Inc. (1998) Final Report. Missouri River: Fort Randall Dam to Gavins Point Dam and Ponca Creek Aggradation Assessment. USACE, Omaha District.

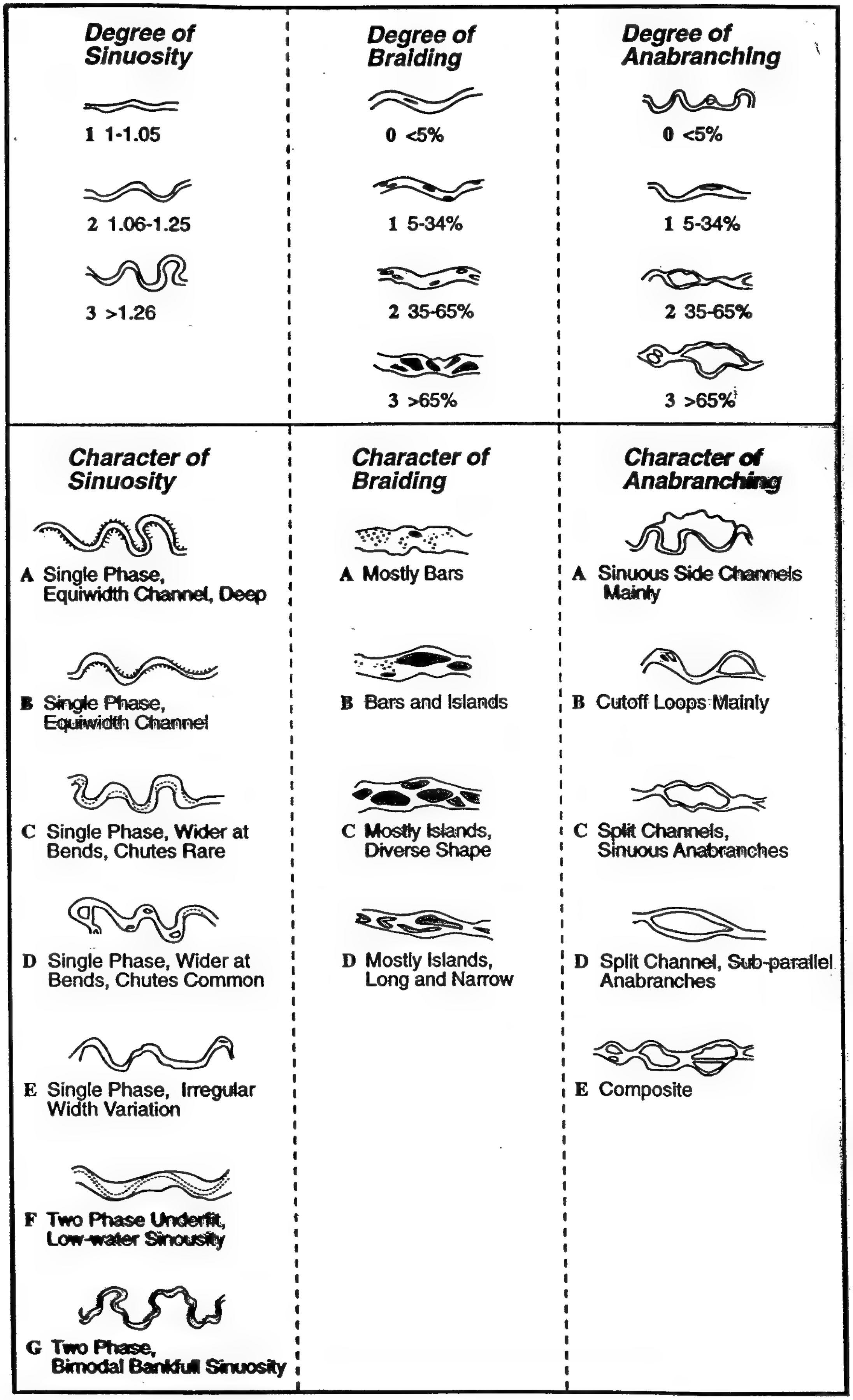

FIGURE 1: BRICE CLASSIFICATION

Appendix A

able A1: Fort Peck Reach summary table of channel characteristics to use as basis of channel stability assessment a

60 RM	Banks Eroding? (1999 recon. Trip)	Position on bend (1999 recon. Trip)	Erosion/ Deposition Rate (m3/yr) (Tompo Data, 1955-1966) Left Bank	Right Bank	Bed
1770.0	No				
1769.0	No		-353	1019	-2080
1767.7	L & R	crossing	-9241	-3110	-1467
1766.3	Deposition on R	inside	0	-1922	-2969
1765.1	Deposition on R	inside	685	-12429	-734
1763.9	No		1517	-33	-8351
1761.4	R	inside	-11383	9005	-2820
1759.2	No		13396	-419	-9360
1757.3	L = Dep. R = Eros.	crossing	-1110	-181	-28356
1754.3	L & R	crossing	-24466	-5953	-72745
1751.0	L & R	L = outside, R = inside	3902	-4799	-30007
1747.8	L & R	crossing	-20356	-913	696
1745.8	R	outside	2120	-6497	-60784
1744.0	L & R	L = outside, R = inside	-196	-8196	-1003
1741.2	R	outside	-37774	-13100	29982
1736.1	L & R	L = outside, R = inside	-26770	-8237	82231
1733.8	L = Eros. R = Dep.	L = inside, R = outside	-7634	-20089	58326
1731.7	L = Eros. R = Dep.	L = inside, R = outside	1420	9119	40481
1728.1	L & R	L = outside, R = inside	-23728	-55608	-22515
1724.5	L & R	crossing	-109558	-1174	38362
1723.9	L & R	crossing	-1452	0	
1720.0	R	inside	-106	-73259	-64300
1715.5	R	crossing	30705	-95172	24405
1712.1	R	inside	-10629	-1571	14696
1707.7	L	outside			
1707.6	L	outside	-1927	1450	3556
1707.5	L	outside			
1700.5	L & R	L = inside, R = outside	-7707	-73356	131014
1695.0	L & R	crossing	-11288	2018	-12933
1687.5	L	crossing	-129261	1937	204697
1682.5	L	inside	-60961	-2650	-1563
1674.8	R	outside	-69808	-123916	229203
1669.5	No		-31265	6051	-54821
1661.9	No		-138310	-6782	155162
1661.7	No				
1653.3	Deposition on R	outside	-8791	5252	-4795
1647.2	No		27444	9535	-156289
1643.4	No		671	-26806	-25257
1638.8	L & R	L = inside, R = outside	-10629	5502	-17882
1631.3	L	crossing			
1624.9	R	inside	86380	-136486	-47061
1623.3	No				
1620.9	L & R	L = outside, R = inside	1267	-12572	37910
1616.8	L & R	crossing	-30039	-17094	-15213
1612.0	L	inside	17159	-42277	82792
1607.7	R	crossing	-29807	2981	-19170
1603.4	R	inside	-200937	8416	111807
1599.0	L	outside	-30501	-28647	19317

Geomorphically Similar Reaches assessment (TABLE B1 CONT.)

Erosion/ Deposition Rate (m3/yr) (Tompo Data, 1968-1978)			Bed aggrading /degrading?
Left Bank	Right Bank	Bed	(Various sources)
			intense degradation
-1744	-386	-473	intense degradation
-3353	-3110	3790	intense degradation
0	-1605	-5006	intense degradation
374	-4635	-10735	intense degradation
209	239	-5741	intense degradation
-7226	2835	-51395	intense degradation
-905	-18475	-9594	intense degradation
-1136	6889	-13257	intense degradation
-4373	11213	39135	less intense degrad.
-2960	-1192	-46749	less intense degrad.
-3269	33850	4146	less intense degrad.
-20334	-1969	-19462	less intense degrad.
606	-6751	-13793	less intense degrad.
19396	-15965	7877	less intense degrad.
25105	-26867	-162208	less intense degrad.
-7621	-20105	2906	less intense degrad.
-7421	10729	-27212	less intense degrad.
-37808	-25354	10987	less intense degrad.
-67146	1435	-9419	less intense degrad.
-1233	0	-1757	less intense degrad.
1992	-128331	4519	less intense degrad.
-12167	-59600	-5102	less intense degrad.
-11014	-381	22875	less intense degrad.
0	0	0	aggradation
-506	1209	1378	aggradation
0	0	0	aggradation
-31049	-169199	-34101	aggradation
-3769	19804	-37827	aggradation
-93	-23081	-213710	aggradation
-7413	-1620	31335	aggradation
-162134	10073	-74256	aggradation
-30574	-27669	23310	aggradation
86752	3956	-96360	aggradation
0	0	0	aggradation
4919	19048	-37468	aggradation
-78282	1292	-380	aggradation
-16713	21069	-5918	aggradation
28141	-3439	-745	aggradation
0	0	0	aggradation
-92578	109882	-52868	aggradation
0	0	0	aggradation
-11256	8636	-12269	aggradation
-126927	22819	54665	aggradation
-5622	-89887	-23862	aggradation
-46450	536	185800	aggradation
-23412	30967	-9322	aggradation
2851	-8717	-4989	aggradation

Table A2: Garrison Reach summary table of channel characteristics to use as basis of channel stability assessment and Geomor

1960 RM	Banks Eroding? (1999 recon. Trip)	Position on bend (1999 recon. Trip)	Erosion/ Deposition Rate (m3/yr) (Tompo Data, 1956/58-1976) Left Bank	Right Bank	Bed	Erosion/ Deposition Rate (m3/yr) (Tompo Data, 1976-1985) Left Bank	Right Bank	Bed	Bed aggrading /degrading? (Various sources)
1388.3	L & R	L = inside, R = outside							Degradation
1387.1	L & R	L = inside, R = outside	1722	-1731	-62141	-1635	1894	-35464	Degradation
1386.0	L & R	crossing	-4769	-41856	-26216	-439	-6103	-2302	Degradation
1385.0	R	inside	-1951	336	-53698	50	-1379	-15450	Degradation
1383.4	L	outside	-9485	-24831	-97985	-12546	-5794	-36867	Degradation
1382.3	L = Eros. R = Dep.	L = inside, R = outside	-3906	-6463	-69535	-1919	2522	-38247	Degradation
1381.4	L = Eros. R = Bluff.	L = inside, R = outside	794	444	-35639	-867	-4022	-673	Degradation
1380.6	Erosion on L	inside	-14903	-53873	-24179	-8094	-63354	7389	Degradation
1379.7	Bluff on R	outside	-65673	-7986	-22337	-92444	-7012	15714	Degradation
1378.9	L	outside	-19572	-1411	-25377	-37311	-79	-7651	Degradation
1378.5	L = Dep. R = Eros.	L = outside, R = inside	-2347	3889	1131	-2656	3019	7302	Degradation
1377.4	L = Dep. R = Eros.	L = inside, R = outside	-19333	-9553	-20421	-19592	-8149	4354	Degradation
1376.5	Deposition on L	inside	-3795	-54296	-11337	-8911	-42252	-6160	Degradation
1375.7	No		-35333	-7033	-38000	-173	0	0	Degradation
1374.9	L	inside	-981	-8498	-27756	-5396	-5675	-85149	Degradation
1374.4	R	crossing	-3499	-13636	-28759	-5698	-17460	-282	Degradation
1373.8	No		-14304	-15170	-22234	-11213	2223	-41126	Degradation
1372.3	R	outside	-4149	3902	-54161	-7376	0	-3538	Degradation
1371.5	L	outside	341	-3020	-65726	1023	306	-52217	Degradation
1370.5	L	crossing	-3125	1682	-92212	0	0	-17	Degradation
1369.1	No		-24344	1172	-59195	-8047	279	-149011	Degradation
1367.6	No		-2422	359	-163134	-16073	324	110565	Degradation
1366.5	No		-17885	-14111	-62562	-17232	-17707	31723	Degradation
1365.0	No		-23055	7132	-120848	8697	1969	-76326	Degradation
1364.1	No		-27599	-36628	-28070	-5233	14578	-3633	Degradation
1362.7	L	outside	-8582	-17311	-57521	11838	-58214	-21002	Aggradation
1361.3	L	inside	-11209	-13679	-78589	47818	-58818	114637	Aggradation
1358.5	R	inside							Aggradation
1356.2	L & R	L = outside, R = inside	-656	-25471	-180873	-9786	44784	-27822	Aggradation
1353.8	No		-1399	-24096	-76593	-10566	-94771	-23284	Aggradation
1351.7	L & R	L = outside, R = inside	-48164	-40519	-33046	44375	-100229	-125800	Aggradation

phically Similar Reaches as

TABLE A2 (CONT.)

Bedrock Geology (Nalini's Report)
Shale and sandstone
Shale and sandstone
Shale and sandstone
Shale and sandstone
Shale and sandstone
Shale and sandstone
Shale and sandstone
Shale and sandstone
Bullion Creek Formation
Bullion Creek Formation
Bullion Creek Formation
Bullion Creek Formation
Bullion Creek Formation
Bullion Creek Formation
Bullion Creek Formation
Bullion Creek Formation
Bullion Creek Formation
Bullion Creek Formation
Bullion Creek Formation
Bullion Creek Formation
Shale, siltstone and sandstone
Shale, siltstone and sandstone
Shale, siltstone and sandstone
Shale, siltstone and sandstone
Shale, siltstone and sandstone
Shale, siltstone and sandstone
Shale, siltstone and sandstone
Shale, siltstone and sandstone
Shale, siltstone and sandstone
Shale, siltstone and sandstone
Shale, siltstone and sandstone

TABLE A2 (CONT)

1349.2	L & R	crossing	-200048	-26613	135963	81900	-42570	-168784	Aggradation
1346.3	L & R	L = inside, R = outside	-15002	-6439	-55499	-12815	-1493	-68507	Aggradation
1344.8	R	outside	-33629	9217	-4564	8173	1545	-24346	Aggradation
1343.3	L	crossing	2489	-86714	25298	-68377	35783	28507	Aggradation
1341.4	L	outside	-1378	-63761	-67525	-3535	32732	-46588	Aggradation
1339.8	L	outside	-9987	-54722	11554	930	-60922	27696	Aggradation
1338.2	No		-43155	-383	-21063	213	1967	-92685	Aggradation
1337.2	R	outside	-3162	15	-5607	116	-122650	42445	Aggradation
1336.2	R	crossing	-2385	-1682	-32056	-9552	-4037	27178	Aggradation

TABLE A2 (CONT.)

Shale, siltstone and sandstone
Shale, siltstone and sandstone
Bullion Creek Formation
Bullion Creek Formation
Bullion Creek Formation
Shale, siltstone and sandstone
Shale, siltstone and sandstone
Shale, siltstone and sandstone
Shale, siltstone and sandstone

Table A3: Fort Randall Reach summary table of channel characteristics to use as basis of channel stability assessment and Geomorph

1960 RM	Banks Eroding? (1999 recon. Trip)	Position on bend (1999 recon. Trip)	Erosion/ Deposition Rate (m3/yr) (Tompo Data, 1954-1975)			Erosion/ Deposition Rate (m3/yr) (Tompo Data, 1975-1985)			Bed aggrading /degrading? (Various sources)
			Left Bank	Right Bank	Bed	Left Bank	Right Bank	Bed	
879.3	No								Degradation
878.6	No		-3902	-4027	4421	-18284	-4553	-17447	Degradation
877.5	L	outside	-5067	-1065	-59575	-3798	-470	-12993	Degradation
876.7	L	crossing	5827	-3605	-44740	-1481	-575	-7940	Degradation
876.4	No		513	-4146	-16062	53	-2424	-5395	Degradation
875.8	No		-18604	-6561	-70399	-2704	-26	-46135	Degradation
875.2	No								Degradation
874.8	No		649	-10130	-37116	-1045	-3548	-5459	Degradation
872.0	No		-379	-22866	-114706	977	-13675	26673	Degradation
871.8	No		-238	-5334	-9209	-68	2610	-2943	Degradation
870.4	No		-1067	11971	-65337	-1924	8672	-13626	Degradation
869.8	No		-3477	3554	-27835	-564	-4618	-10739	Degradation
868.0	No		-265151	13008	55042	39676	-40048	-25246	Degradation
867.0	No		-20020	-15428	-68448	-12986	456	15222	Degradation
865.1	L	crossing	-9699	676	-57194	-44857	460	-45966	Degradation
863.5	L	crossing	-2438	-36703	17087	262	-29265	-86370	Degradation
862.6	L	crossing	5805	-8926	-14770	1051	-4082	-29597	Degradation
861.5	L	inside							Degradation
859.5	L	crossing	-2179	-11947	-40796	-1680	-4955	22128	Transition
856.3	No		706	-3759	-40599	570	1914	-52948	Transition
854.7	L & R	crossing	-2905	-14684	13841	2677	-11881	-74136	Aggradation
853.1	R	crossing	-49393	-24526	-11676	5946	-2893	1185	Aggradation
850.8	No		-72067	-868	78143	4765	-884	-100839	Aggradation
849.0	L	crossing	3306	-53427	95180	-3627	20902	-38049	Aggradation
848.1	No		3294	1397	23555	20184	372	11233	Aggradation
847.5	No		-11085	-3370	22756	1337	-2999	9872	Aggradation
845.1	L	crossing	-24725	22282	80805	-75679	21274	54628	Aggradation
844.2	No		788	-12405	26714	775	-11880	59066	Aggradation

ically Similar Reaches assessment (TABLE A3 CONT.)

Bedrock Geology (Nalini's report)	
Northeastern side of river	**Southwestern side of river**
Shale (overlain with glacial till & loess)	Cretaceous Pierre Shale overlain by silt, sandstone & clay
Shale (overlain with glacial till & loess)	Cretaceous Pierre Shale overlain by silt, sandstone & clay
Shale (overlain with glacial till & loess)	Cretaceous Pierre Shale overlain by silt, sandstone & clay
Shale (overlain with glacial till & loess)	Cretaceous Pierre Shale overlain by silt, sandstone & clay
Shale (overlain with glacial till & loess)	Cretaceous Pierre Shale overlain by silt, sandstone & clay
Shale (overlain with glacial till & loess)	Cretaceous Pierre Shale overlain by silt, sandstone & clay
Shale (overlain with glacial till & loess)	Cretaceous Pierre Shale overlain by silt, sandstone & clay
Shale (overlain with glacial till & loess)	Cretaceous Pierre Shale overlain by silt, sandstone & clay
Shale (overlain with glacial till & loess)	Cretaceous Pierre Shale overlain by silt, sandstone & clay
Shale (overlain with glacial till & loess)	Cretaceous Pierre Shale overlain by silt, sandstone & clay
Shale (overlain with glacial till & loess)	Cretaceous Pierre Shale overlain by silt, sandstone & clay
Shale (overlain with glacial till & loess)	Cretaceous Pierre Shale overlain by silt, sandstone & clay
Shale (overlain with glacial till & loess)	Cretaceous Pierre Shale overlain by silt, sandstone & clay
Shale (overlain with glacial till & loess)	Cretaceous Pierre Shale overlain by silt, sandstone & clay
Shale (overlain with glacial till & loess)	Cretaceous Pierre Shale overlain by silt, sandstone & clay
Shale (overlain with glacial till & loess)	Cretaceous Pierre Shale overlain by silt, sandstone & clay
Shale (overlain with glacial till & loess)	Cretaceous Pierre Shale overlain by silt, sandstone & clay
Shale (overlain with glacial till & loess)	Cretaceous Pierre Shale overlain by silt, sandstone & clay
Shale (overlain with glacial till & loess)	Cretaceous Pierre Shale overlain by silt, sandstone & clay
Shale (overlain with glacial till & loess)	Cretaceous Pierre Shale overlain by silt, sandstone & clay
Shale (overlain with glacial till & loess)	Cretaceous Pierre Shale overlain by silt, sandstone & clay
Shale (overlain with glacial till & loess)	Cretaceous Pierre Shale overlain by silt, sandstone & clay
Shale (overlain with glacial till & loess)	Cretaceous Pierre Shale overlain by silt, sandstone & clay
Shale (overlain with glacial till & loess)	Cretaceous Pierre Shale overlain by silt, sandstone & clay
Shale (overlain with glacial till & loess)	Cretaceous Pierre Shale overlain by silt, sandstone & clay
Shale (overlain with glacial till & loess)	Cretaceous Pierre Shale overlain by silt, sandstone & clay
Shale (overlain with glacial till & loess)	Cretaceous Pierre Shale overlain by silt, sandstone & clay
Shale (overlain with glacial till & loess)	Cretaceous Pierre Shale overlain by silt, sandstone & clay

Table A4: Gavins Point Reach summary table of channel characteristics to use as basis of channe

1960 RM	Banks Eroding? (1999 recon. Trip)	Position on bend (1999 recon. Trip)	Erosion/ Deposition Rate (m3/yr) (Tompo Data, 1960-1974) Left Bank	Right Bank	Bed
810.7	No				
809.9	No		-5331	-1956	-35772
809.2	No		-643	-568	-44204
808.6	R	outside	-1519	-1153	-39670
808.0	No		0	-10445	-64192
807.0	L	outside	-112476	0	-12698
806.2	No		-3247	-325	-69365
806.0	No		-70	45	-8606
805.8	No				
805.4	R	outside	-692	-743	-21714
804.5	L & R	L = inside, R = outside	-34746	-19694	-9227
803.9	No		-23106	-449	-26605
802.0	No		-60548	-316723	64505
801.1	No		-12533	-129823	-7113
800.0	No		-55648	2537	-27101
798.8	No		-18916	-13174	-36755
797.9	L	outside	-1653	-8785	-40090
797.0	R	inside	-70520	-103161	41061
795.6	R	inside	-32205	-98320	-48726
794.5	L	crossing	-10843	-2021	-68464
793.3	No		1845	-12918	-20466
792.5	R	outside	-38711	-2102	19206
790.3	R	inside	-23307	-25069	-38179
789.2	R	inside	-24717	-787	-160376
787.7	R	outside	-20296	7064	5014
786.9	No		-1059	-2674	-8655
786.0	No		-33448	-25807	-10986
784.5	No		-2275	-23484	-12399
782.2	R	crossing	-27805	1474	-114144
780.2	R	crossing	-19757	-105706	39706
778.6	No		-42598	-101293	-146523
777.0	L	inside	-318403	-64795	58780
775.9	No		-1645	-39753	-23859
773.9	R	inside	983	-79221	-39899
771.4	No		-305594	14604	52543
769.0	L & R	L = inside, R = outside	-17531	-140662	-141405
762.6	L & R	L = inside, R = outside	-3486	-56388	-319872
761.7	L	crossing			
758.1	R	inside	-216606	-732900	-42483
756.0	No		-64119	-98185	-43262
753.1	No		0	-898	-536750

I stability assessment and Geomorphically Similar Reaches assessment TABLE A4 (CONT.)

Erosion/ Deposition Rate (m3/yr) (Tompo Data, 1974-1986) Left Bank	Right Bank	Bed	Bed aggrading/degrading? (Various sources)
			intense decrease in WSE
-632	137	-18719	intense decrease in WSE
0	-867	-2848	intense decrease in WSE
-3435	-948	-2371	intense decrease in WSE
0	820	-15411	intense decrease in WSE
-33961	0	9046	intense decrease in WSE
-2580	0	-29458	intense decrease in WSE
-56	62	-5718	intense decrease in WSE
			intense decrease in WSE
-568	-1294	-13217	intense decrease in WSE
682	-34746	-44809	intense decrease in WSE
-9214	320	-23004	intense decrease in WSE
22340	-185257	-12641	intense decrease in WSE
-29863	-11322	1788	intense decrease in WSE
18432	4041	-62273	intense decrease in WSE
-22388	-31910	-44969	intense decrease in WSE
-221	-433	-49105	intense decrease in WSE
15138	-87561	-18964	intense decrease in WSE
3095	-187310	61898	intense decrease in WSE
-47260	905	-37169	intense decrease in WSE
12046	14661	-47930	intense decrease in WSE
5545	-10398	-31466	intense decrease in WSE
-16164	-148135	-38273	intense decrease in WSE
-10385	0	-73680	less intense decrease in WSE
-31990	-9163	-80000	less intense decrease in WSE
-8783	-85	-25896	less intense decrease in WSE
-40417	-13908	-1836	less intense decrease in WSE
-34586	-88410	7769	less intense decrease in WSE
-11716	-2505	-56396	less intense decrease in WSE
-20206	-270982	-104125	less intense decrease in WSE
-69767	-13294	25665	less intense decrease in WSE
-74603	59293	-72416	less intense decrease in WSE
0	-6226	6567	less intense decrease in WSE
-491	-282964	48271	less intense decrease in WSE
61194	-18315	-321079	less intense decrease in WSE
-15763	-13712	-40497	less intense decrease in WSE
2256	-21598	-311807	less intense decrease in WSE
-51710	-92050	8679	less intense decrease in WSE
159590	-205918	97154	less intense decrease in WSE
-259368	-3342	-44944	less intense decrease in WSE
0	2478	-232682	less intense decrease in WSE

TABLE A4 (CONT.)

Bedrock Geology (Nalini's report)	
Northeastern side of river	Southwestern side of river
Sandstone and shale (covered with alluvium)	Carlisle Shale
Sandstone and shale (covered with alluvium)	Carlisle Shale
Sandstone and shale (covered with alluvium)	Carlisle Shale
Sandstone and shale (covered with alluvium)	Carlisle Shale
Sandstone and shale (covered with alluvium)	Carlisle Shale
Sandstone and shale (covered with alluvium)	Carlisle Shale
Sandstone and shale (covered with alluvium)	Carlisle Shale
Sandstone and shale (covered with alluvium)	Carlisle Shale
Sandstone and shale (covered with alluvium)	Carlisle Shale
Sandstone and shale (covered with alluvium)	Carlisle Shale
Sandstone and shale (covered with alluvium)	Carlisle Shale
Sandstone and shale (covered with alluvium)	Carlisle Shale
Sandstone and shale (covered with alluvium)	Carlisle Shale
Sandstone and shale (covered with alluvium)	Carlisle Shale
Sandstone and shale (covered with alluvium)	Carlisle Shale
Sandstone and shale (covered with alluvium)	Carlisle Shale
Sandstone and shale (covered with alluvium)	Carlisle Shale
Sandstone and shale (covered with alluvium)	Carlisle Shale
Sandstone and shale (covered with alluvium)	Carlisle Shale
Sandstone and shale (covered with alluvium)	Carlisle Shale
Sandstone and shale (covered with alluvium)	Carlisle Shale
Sandstone and shale (covered with alluvium)	Carlisle Shale
Sandstone and shale (covered with alluvium)	Carlisle Shale
Sandstone and shale (covered with alluvium)	Carlisle Shale
Sandstone and shale (covered with alluvium)	Carlisle Shale
Sandstone and shale (covered with alluvium)	Carlisle Shale
Sandstone and shale (covered with alluvium)	Carlisle Shale
Sandstone and shale (covered with alluvium)	Carlisle Shale
Sandstone and shale (covered with alluvium)	Carlisle Shale
Sandstone and shale (covered with alluvium)	Carlisle Shale
Sandstone and shale (covered with alluvium)	Carlisle Shale
Sandstone and shale (covered with alluvium)	Carlisle Shale
Sandstone and shale (covered with alluvium)	Carlisle Shale
Sandstone and shale (covered with alluvium)	Carlisle Shale
Sandstone and shale (covered with alluvium)	Carlisle Shale
Sandstone and shale (covered with alluvium)	Carlisle Shale
Sandstone and shale (covered with alluvium)	Carlisle Shale
Sandstone and shale (covered with alluvium)	Carlisle Shale
Sandstone and shale (covered with alluvium)	Carlisle Shale
Sandstone and shale (covered with alluvium)	Carlisle Shale
Sandstone and shale (covered with alluvium)	Shale and limestone

Appendix B

Figure B1: Fort Peck Reach - HEC-RAS calculated channel variables based on 1978 cross-sectional surveys

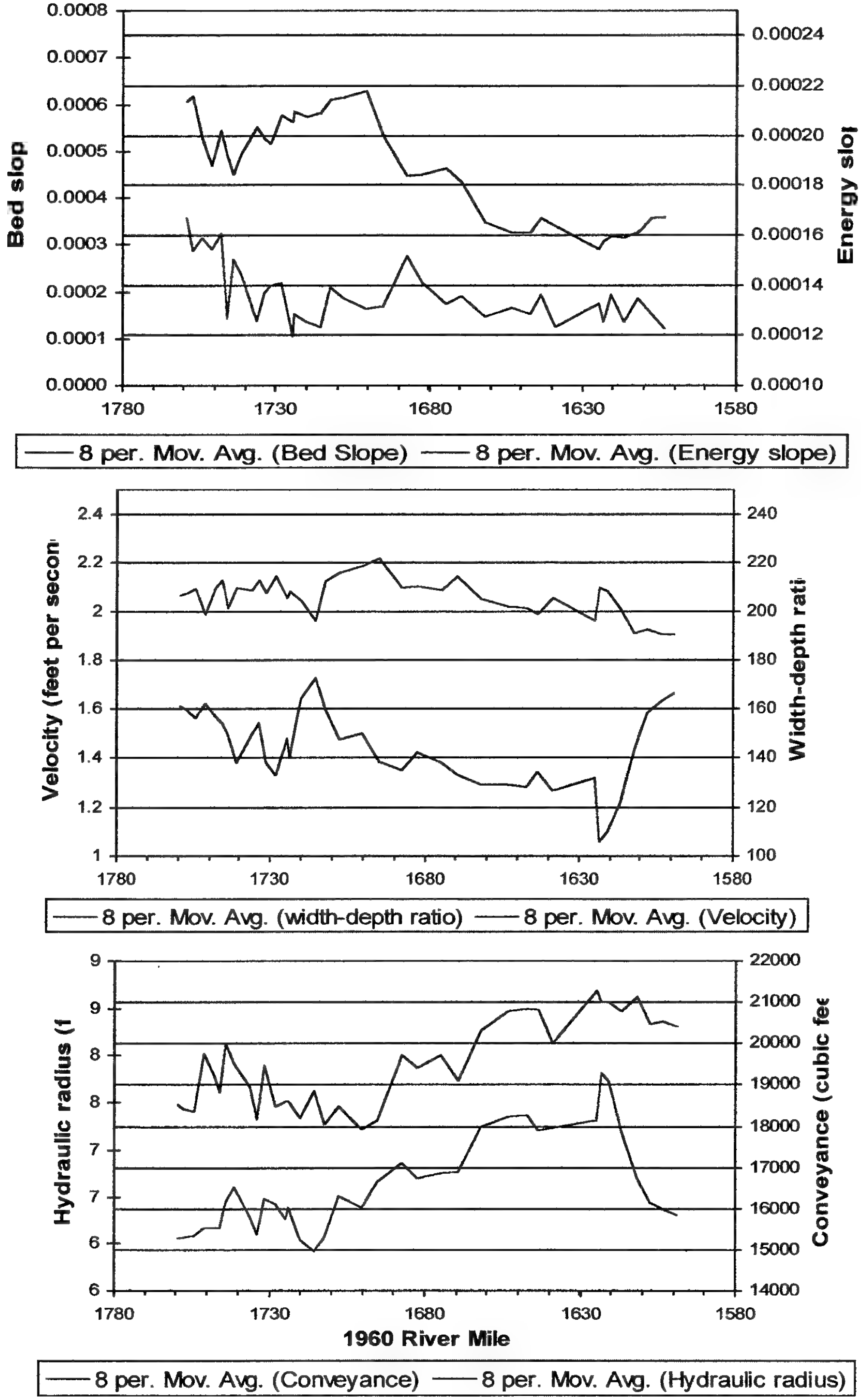

Figure B2: Garrison Reach - HEC-RAS calculated channel variables based on 1985 cross-sectional surveys

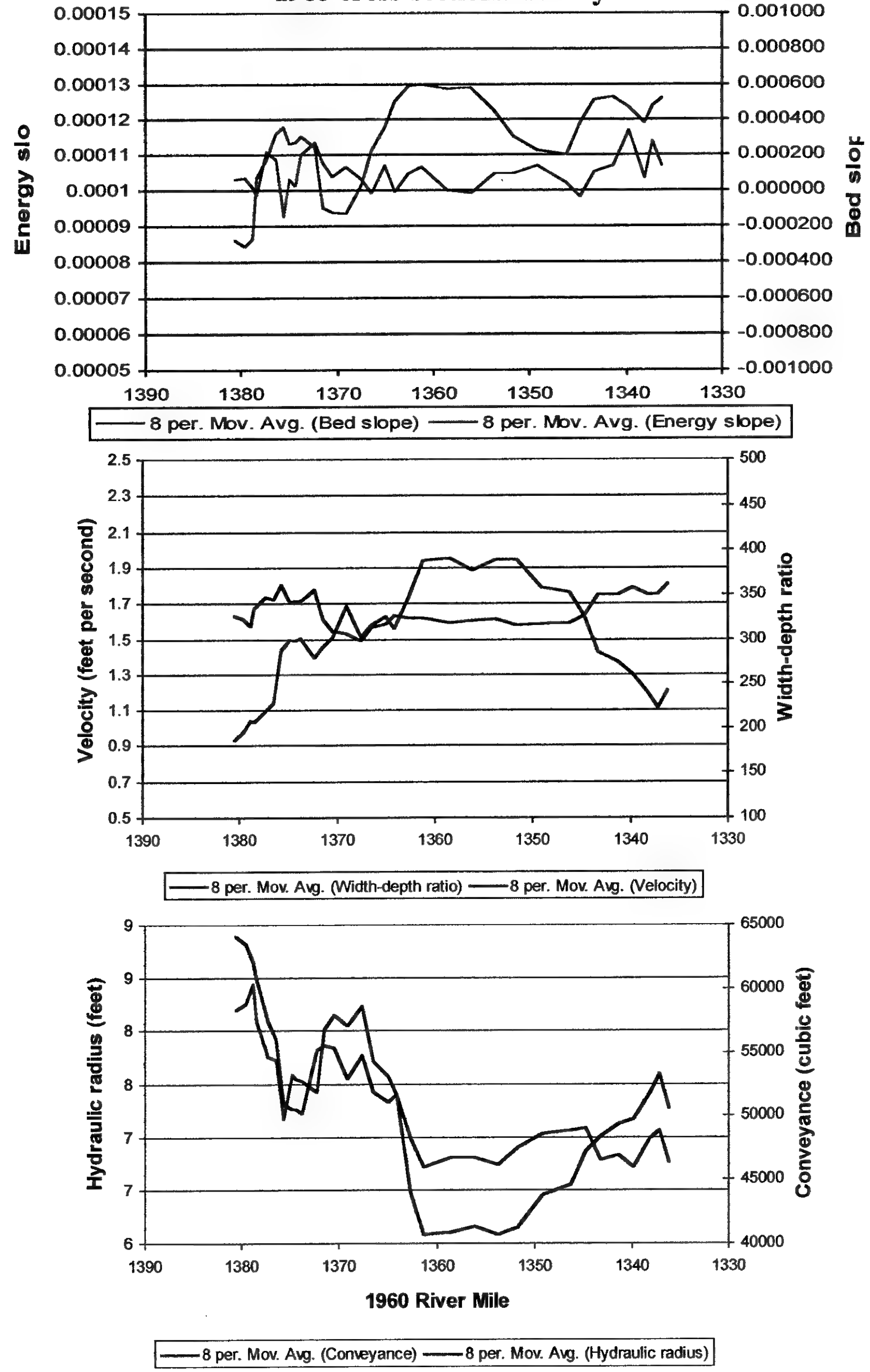

Figure B2 (cont.): Garrison Reach - Bar and island densities, channel sinuosity and bank revettements

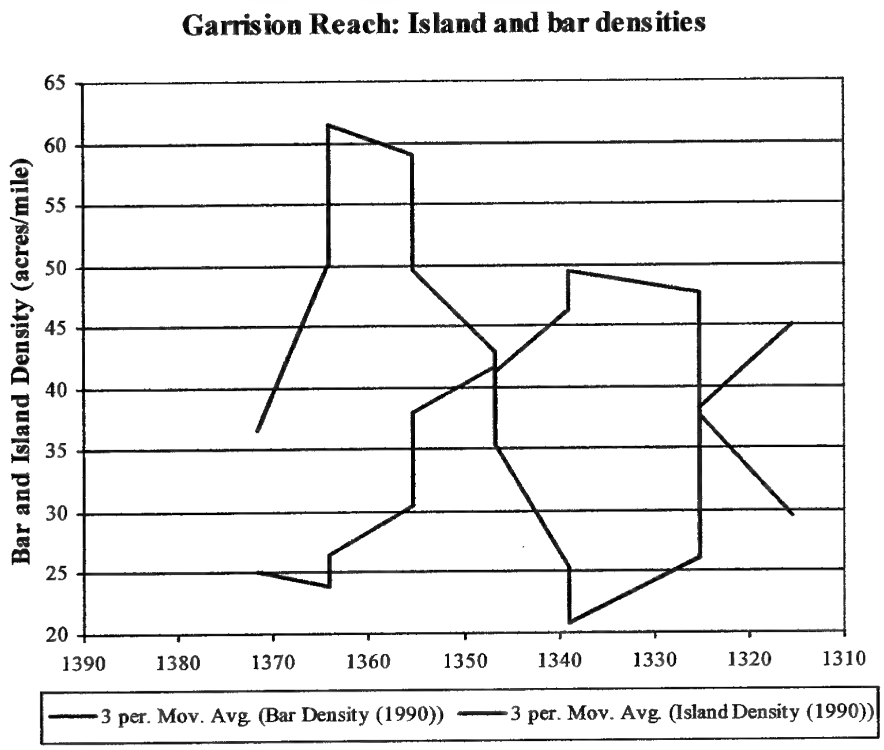

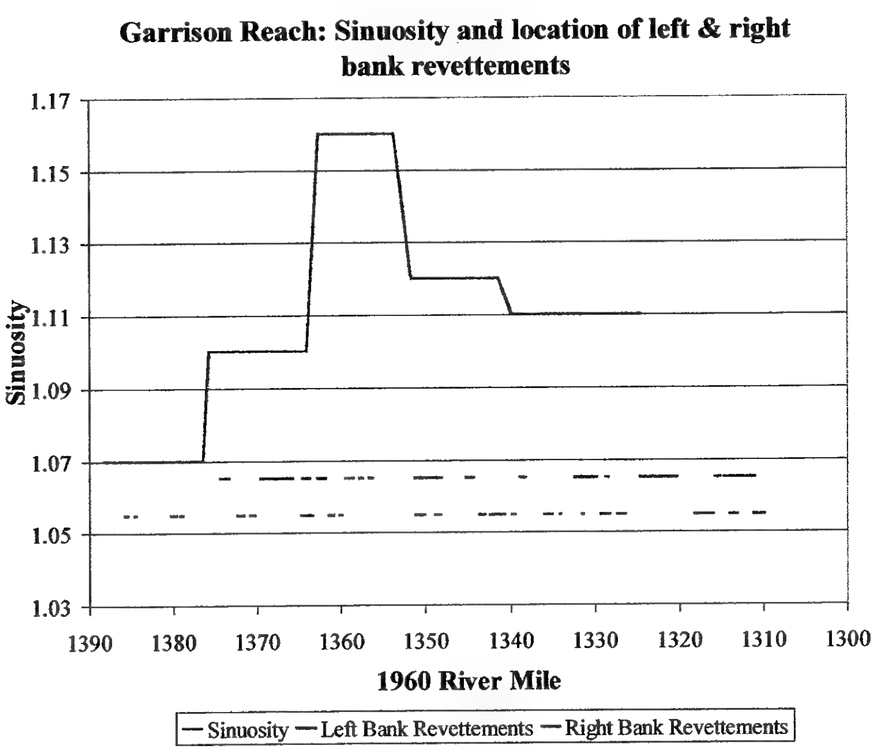

Figure B3: Fort Randall Reach: HEC-RAS calculated channel variables based on 1985 cross-sectional surveys

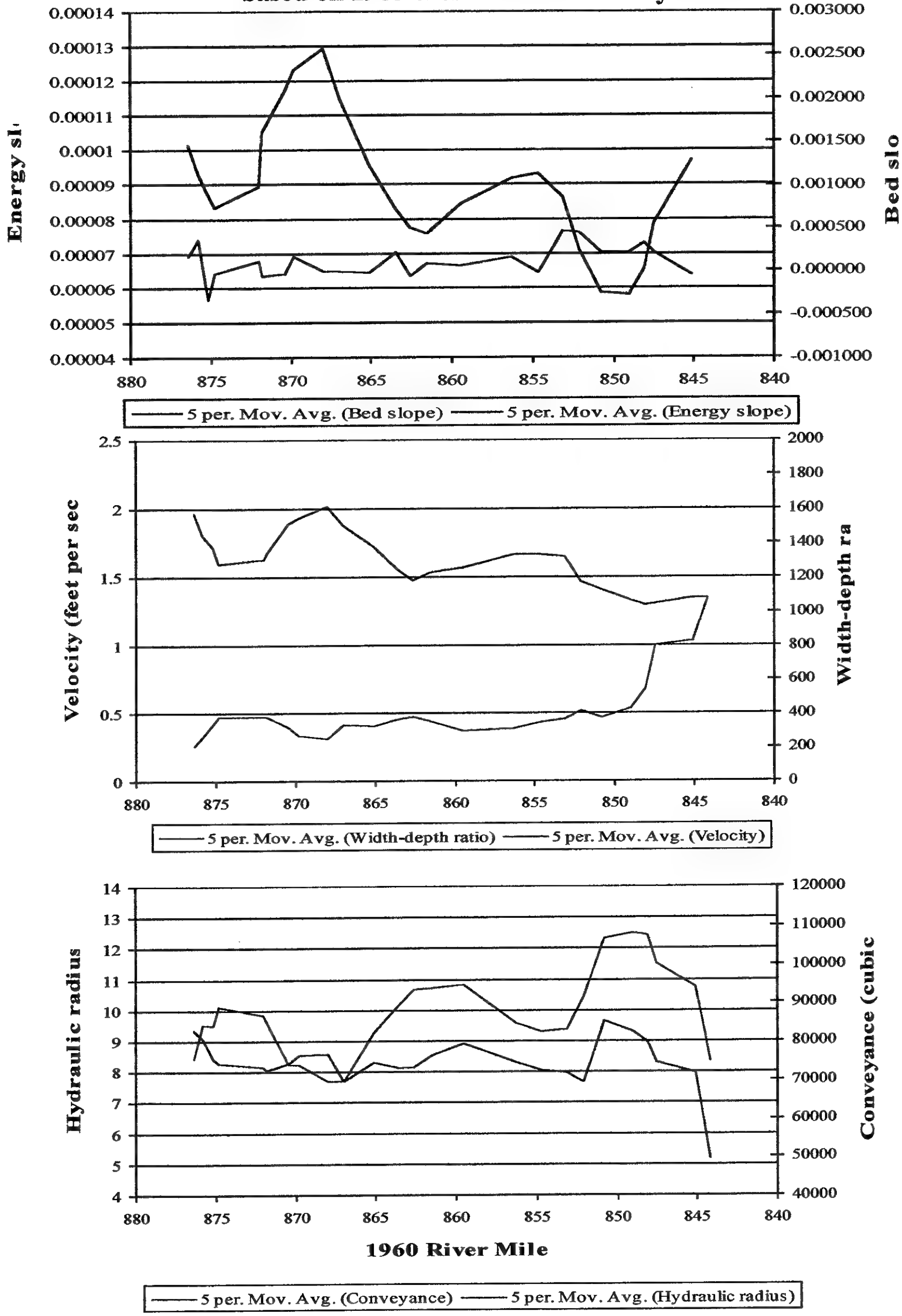

Figure B4: Gavins Point Reach - HEC-RAS calculated channel variables Based on 1986 cross-sectional surveys

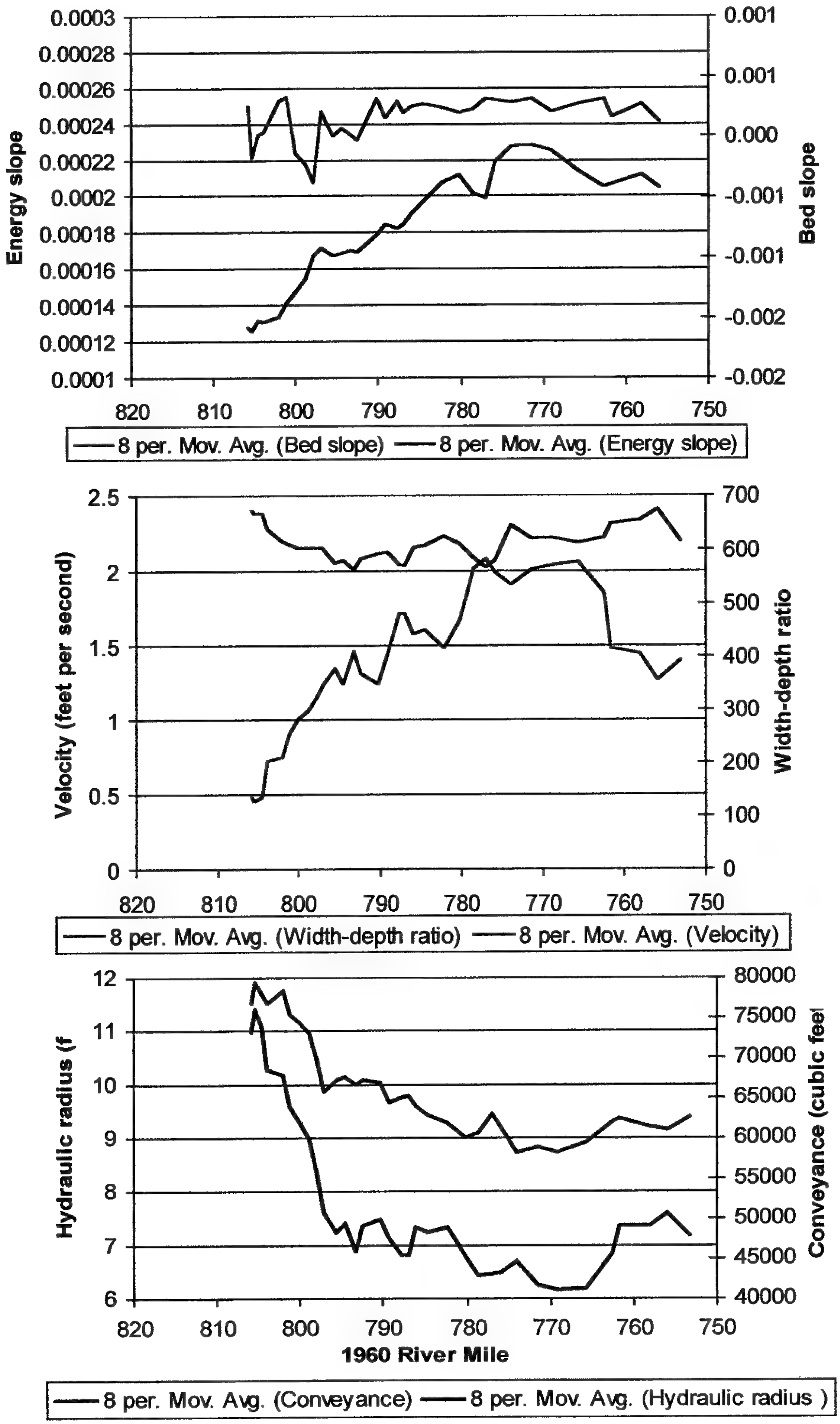

Figure B4 (cont.): Gavins Point Reach - Bar and island densities, channel sinuosity and bank revettements

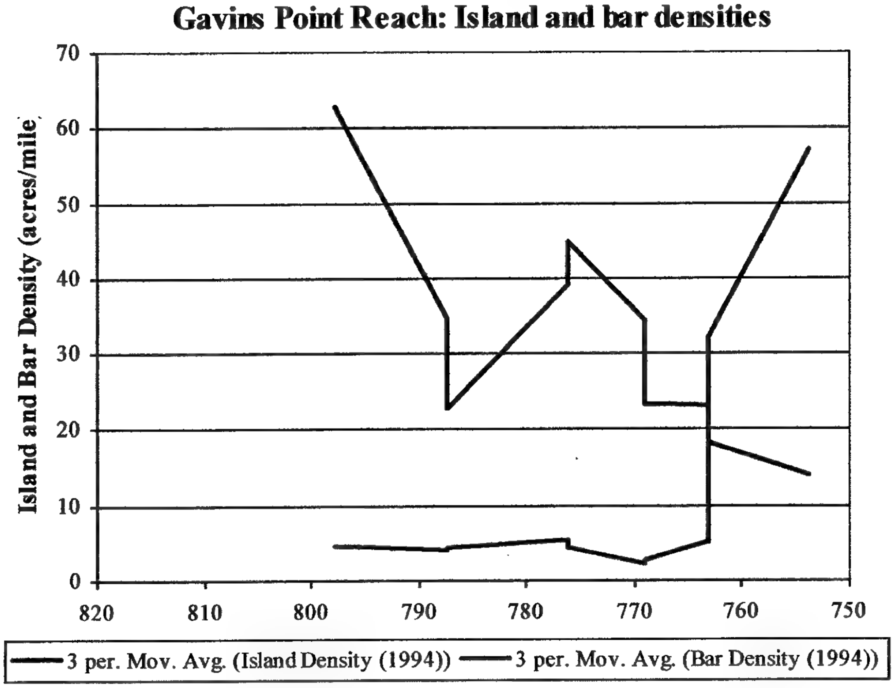

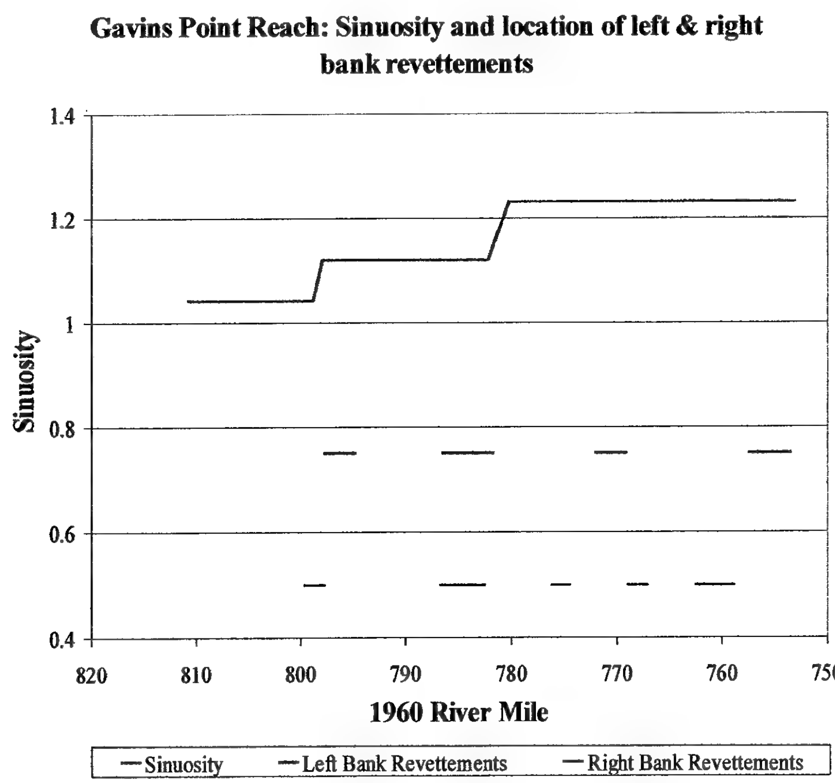

Appendix C

Table C1: Results of the Brice Classification for Fort Peck Reach

Reach	Degree of Sinuosity	Character of Sinuosity	Degree of Braiding	Character of Braiding	Degree of Anabranching	Character of Anabranching	Brice Channel Type
Entire Reach (RM 1771-1582)	1.43 (3)	Single phase, wider at bends, chutes common (D)	61% (2)	Bars & islands (B)	<5% (0)	Split channels, sinuous anabranches (C)	3D2B0C
1 (RM 1766-1758)	1.34 (3)	Single phase, equiwidth channel (B)	<5% (0)	Mostly islands, long and narrow (D)	0% (0)	None (0)	3B0D00
2 (RM 1758-1752)	1.04 (1)	Single phase, irregular width variation (E)	66% (3)	Mostly islands, long and narrow (D)	0% (0)	None (0)	1E3D00
3 (RM 1752-1698)	1.63 (3)	Single phase, wider at bends, chutes common (D)	48% (2)	Bars & islands (B)	<5% (0)	Split channels, sinuous anabranches (C)	3D2B0C
4 (RM 1698-1686.3)	1.07 (2)	Single phase, irregular width variation (E)	83% (3)	Mostly bars (A)	0% (0)	None (0)	2E3A00
5 (RM 1686.3-1653)	2.13 (3)	Single phase, wider at bends, **chutes common**[1] (but high width irregularity also) (D)	67% (3)	Bars & islands (B)	5% (1)	Composite (E)	3D3B1E
6 (RM 1653-1618)	1.39 (3)	Single phase, irregular width variation (with considerable number of chutes) (E)	60% (2)	Bars & islands (B)	8% (1)	Composite (E)	3E2B1E
7 (RM 1618-1605)	1.08 (2)	Single phase, equiwidth channel (with some gentle width irregularity) (B)	82% (3)	Bars & islands (B)	0% (0)	None (0)	2B3B00
8 (RM 1605-1582)	1.37 (3)	Single phase, wider at bends, chutes common (D)	41% (2)	Mainly bars (A)	0% (0)	None (0)	3D2A00

() Characters in parentheses are the Brice code designation for the observed parameter

[1] Text in bold indicates that the presence of this feature was the reason for the selection of this Brice category, even though the other parameters may not have been present.

Table C2: Results of the Brice Classification for Garrison Reach

Reach	Degree of Sinuosity	Character of Sinuosity	Degree of Braiding	Character of Braiding	Degree of Anabranching	Character of Anabranching	Brice Channel Type
Entire Reach (RM 1390-1311)	1.06 (2)	Single phase, irregular width variation (E)	35-65% (2)	Bars &islands (B)	<5% (0)	Split channels, sinuous anabranches (C)	2E2B0C
1 (RM 1390-1378)	1 - 1.05 (1)	Single phase, equiwidth channel (B)	<5%) (0)	None (0)	0% (0)	None (0)	1B0000
2 (RM 1378-1368)	1 - 1.05 (1)	Single phase, wider at bends, **chutes common** (D)	35-65% (2)	Bars & islands (B)	5 – 34% (1)	Split channels, sinuous anabranches (C)	1D2B1C
3 (RM 1368-1329)	1.06-1.25 (2)	Single phase, irregular width variation, (E)	>65% (3)	Mostly bars (A)	<5% (0)	None (0)	2E3A00
4 (RM 1329-1315)	1.06-1.25 (2)	Single phase, wider at bends, chutes common (D)	50% (2)	Bars &islands (B)	0% (0)	None (0)	2D2B00

Table C3: Results of the Brice Classification for Fort Randall Reach

Reach	Degree of Sinuosity	Character of Sinuosity	Degree of Braiding	Character of Braiding	Degree of Anabranching	Character of Anabranching	Brice Channel Type
Entire Reach (RM 880-843)	1.0 (1)	Single phase, wider at bends, **chutes common** (D)	35-65% (2)	Bars & islands (B)	5-34% (1)	Composite (E)	1D2B1E
1 (RM 880-854.1)	1.02 (1)	Single phase, wider at bends, **chutes common** (D)	5-34% (1)	Bars & islands (B)	5-34% (1)	Composite (E)	1D1B1E
2 (RM 854.1-843)	1.01 (1)	Single phase, wider at bends, **chutes common** (D)	>65% (3)	Bars & islands (B)	0% (0)	None (0)	1D3B00

Table C4: Results of the Brice Classification for Gavins Point Reach

Reach	Degree of Sinuosity	Character of Sinuosity	Degree of Braiding	Character of Braiding	Degree of Anabranching	Character of Anabranching	Brice Channel Type
Entire Reach (RM 811-753)	1.15 (2)	Single phase, wider at bends, **chutes common** (D)	5-34% (1)	Bars & islands (B)	5-34% (1)	Composite (E)	2D1B1E
1 (RM 811-798)	1.04 (1)	Single phase, wider at bends, **chutes common** (D)	5-34% (1)	Bars & islands (B)	5-34% (1)	Cutoff loops mainly (B)	1D1B1B
2 (RM 798-769)	1.06-1.25 (2)	Single phase, wider at bends, **chutes common** (D)	35-65% (2)	Bars & islands (B)	5-34% (1)	Split channel, sub-parallel anabranches (D)	2D2B1D
3 (RM 769-753)	1.06-1.25 (2)	Single phase, wider at bends, **chutes common** (D)*	5-34% (1)	Bars & islands (B)	<5% (0)	Split channel, sub-parallel anabranches (D)	2D1B0D

* But much bank protection is present in this reach and so the natural tendency might be towards more chutes, even though the planform appears to have an irregular width variation.

The results presented in Tables C5 to C8 below should be read in conjunction with the relevant tables and figures from Appendices A and B respectively.

Table C5: Geomorphologically Similar Reaches for Fort Peck Reach

GSR (1960 River Miles)	Criteria
1 (1766-1750)	A zone of adjustment downstream from the dam (intense degradation to RM 1757.3) along with extensive right bank bluff line control (RM 1764-1763.4; 1760.3-1759.8; 1757.7-1756.2); decreasing energy and bed slopes; increasing conveyance and hydraulic radius.
2 (1750-1713)	Greater planform sinuosity and larger meander arc lengths; less bluff line control (two right bank points of contact from RM 1748.75-1747.3 and 1731.7-1730.9) and evidence of greater meander migration across the floodplain – extensive scroll features are visible on the 1998 aerial mosaic; bed slope decreases to about RM 1725; velocity kinks down and hydraulic radius and w:d ratio both kink up at RM 1715; RM 1725-1715 appears to be transition zone between the meandering planform upstream of this 10-mile reach and the more braided planform downstream.
3 (1713-1700)	The meander migration is less intense than in the previous reach due to the less extensive scrolling visible on the 1998 aerial mosaics and there is a greater degree of braiding than in the previous reach; right bank bluff line contact occurs from RMs 1711.4 –1711.1 and 1701.6-1701.2; energy slope and conveyance both increase to RM 1700.
4 (1700-1686)	There is even less planform migration than in the previous reach (fewer scroll features on the floodplain in the 1998 aerial mosaic). Sinuosity is lower and the degree of braiding more intense than in the previous reach; right bank bluff line control occurs from RMs 1695.9-1694.7; 1692-1691.8 and 1688.6-1688.2; bed slope increases and w:d ratio decreases to RM 1688.
5 (1686-1654)	A highly sinuous planform due to active meandering across the floodplain, as evidenced by meander scroll topography on the 1998 aerial mosaics and the relative absence of bluff line control. The hydraulic variables show trends that continue through this reach and into reach 6 downstream. (From RM 1686-1625 bed slope, energy slope, velocity and w:d ratio all decrease, whilst conveyance and hydraulic radius both increase).
6 (1654-1621.7)	All six of the hydraulic variables continue the trends started in the previous reach but the meandering changes from active to passive due to probable geologic controls. Right bank bluff line contact occurs from RM 1653.7-1652.1; 1639.8-1639.3; 1635.85-11635.5; 1633.2-1633.05; 1627.3-1626.7; and 1622.7-1622.5. From RM 1625 the hydraulic variables show an abrupt change: the energy slope increase, a reversal of its previous trend; velocity increases rapidly then resumes its previous trend; w:d ratio decreases rapidly then increases; conveyance and hydraulic radius both decrease rapidly , also a reversal of their previous trends. These changes are possibly related to a channel constriction at RM 1624.8, but it should be noted that there have been many previous channel constrictions that have not initiated such drastic changes in the hydraulic variables). The sinuosity of this passively meandering reach decreases to 1.39 from the value of 2.13 for the actively meandering reach 5.
7 (1621.7-1605)	Sinuosity again shows a decrease, to a value of 1.08 and the reach is still exhibiting the characteristics of passive meandering. Bluff line control occurs along the right bank from RM 1617.9-1617.8 and 1612-1610.55, and along the left bank from RM1614.3-1613.8 and 1609-1608.15. No hydraulic variable data are available downstream of RM 1620 since no cross-sections exist beyond this point.
8 (1605-1582)	Sinuosity increases to 1.37. From RM 1605-1590 the floodplain is less constricted by bluffs and the channel is allowed to meander freely, to the extent that a very large cutoff has occurred at RM 1599.5. Bluffs constrict the valley for a few miles downstream of RM 1590 before again opening out around the confluence with the Yellowstone River.

Table C6: Geomorphologically Similar Reaches for Garrison Reach

GSR (1960 River Miles)	Criteria
1 (1390-1376)	The energy slope and w:d ratio show a rapid rate of increase to the downstream limit of this reach, whilst the conveyance and hydraulic radius both show a very rapid rate of decrease to the same point. The downstream limit to this reach is 0.5 miles upstream of the Knife River tributary and also marks the downstream limit of one of the 1999 field sampling reaches.
2 (1376-1363)	The planform initiates an abrupt and significant change in direction at RM 1373 and this may be due to the input of the Knife River 3 miles upstream; bed slope and hydraulic radius begin to decrease at RM 1373, whilst the w:d ratio shows a decreased rate of increase at this point; the energy slope decreases gradually from RM 1376 before decreasing rapidly at RM 1373.
3 (1363-1353)	Another abrupt change in planform occurs at RM 1363; somewhere between RM 1364.1 and 1362.7 the bed begins to aggrade; energy slope levels out at RM 1363 before beginning to drop off sharply at RM 1356; hydraulic radius drops sharply at RM 1363 whilst conveyance continues an already decreasing trend – both level off at RM 1361.25 and stay this way until approximately RM 1354; a small amount of left bank bluff line contact occurs from RM 1361.3-1361.1.
4 (1353-1340)	Significant bluff line control of meandering – on the right bank from RM 1347.9 to approximately 1346.9 and on the left bank from RM 1342.7-1342.6 and 1342.2-1341.6; extensive left and right bank protection from RM 1351.5-1348.1; w:d ratio decreases sharply and hydraulic radius increases sharply at RM 1353; bed and energy slope show considerable fluctuation in this reach; velocity remains equal until RM 1346 and then begins to increase steadily; the reach is heavily braided.
5 (1340-1324.5)	The bluff control is gone and the reach is again very heavily braided; bedrock changes from Bullion Creek Formation to shale, siltstone and sandstone at RM 1340; the hydraulic variable plots only extend to RM 1336, but there appears to be an abrupt change to several of the trends at RM 1337 – w:d ratio shows a sharp increase whilst both hydraulic radius and conveyance decrease sharply.
6 (1324.5-1311)	There are extensive sections of bank protection along both banks: on the left bank from RM 1324.6-1320.3 & 1315.7-1311 and on the right bank from RM 1321.9-1320.15; 1318.2-1315.9 & 1313.9-1313.1; the reach is still heavily braided although probably less so than reaches 4 and 5, but there are two large and heavily dissected bar & islands complexes from RM 1324.2-1322 and 1318.2-1316.

Table C7: Geomorphologically Similar Reaches for Fort Randall Reach

GSR (1960 River Miles)	Criteria
1 (880-873.9)	The channel experiences left bank bluff line control from RM 878.5-876 and there is a large bar/island complex from RM 876-874.4; energy & bed slope, velocity and hydraulic radius all decrease to RM 875, whilst w:d ratio and conveyance both increase to this point.
2 (873.9-867.5)	There is right bank bluff line control of the channel from RM 874-869.8; energy slope and velocity increase sharply from RM 872-868 whilst w:d ratio shows a gradual decrease over this distance; conveyance decreases considerably from RM 872-867.
3 (867.5-861.7)	The energy slope and velocity plots show a large decrease from RM 868-862.5 whilst conveyance shows a large increase over the same distance.
4 (861.7-854.5)	There is right bank bluff line control over the full extent of the reach, which is also a zone of transition between the dam–related degradation and aggradation; energy slope, velocity and w:d ratio all increase throughout most of this reach, whilst hydraulic radius and conveyance both decrease.
5 (854.5-851)	There is no bluff line control in this reach; energy slope decreases sharply to RM 851 whilst velocity also decreases through into the next downstream reach; bed slope fluctuates whilst w:d ratio increases gently; conveyance and hydraulic radius increase sharply from approximately RM 853.25-851 and 852.25-851 respectively; the upstream limit of this reach marks the approximate starting point of the zone of bed aggradation that is probably due to the backwater effect created by Lewis and Clark Lake at the downstream end of Fort Randall Reach and the delta that has been deposited at the confluence with the Niobrara River at RM 844; as a result of the backwater effect braiding is much more extensive than in the previous reaches.
6 (851-844)	There is left bank bluff line control from RM 851.2-850.5, although this bluff line extends well beyond the downstream limit of Fort Randall Reach and imposes the ultimate control on the direction of the channel. The present morphology of the channel is controlled by the backwater effects and the extensive deposition that has occurred as a result, and braiding and chuting are extensive throughout; energy slope decreases fractionally from RM 851-849 before increasing very sharply to RM 844; similarly, conveyance increases slightly before decreasing rapidly; over the same distance bed slope shows a fluctuating decreasing trend, whilst hydraulic radius decreases sharply and w:d ratio increases rapidly.

Table C8: Geomorphologically Similar Reaches for Gavins Point Reach

GSR (1960 River Miles)	Criteria
1 (811-796)	There is an abrupt planform change of direction at about RM 796; this reach corresponds closely to the reaches identified using the Brice system and based on sinuosity alone (both from RM 811-798); bed slope fluctuates considerably but energy slope and w:d ratio show a steady increase from RM 806-797 and RM 806-796 respectively; velocity decreases steadily to RM 796 while hydraulic radius decreases by a large amount to this point; conveyance also decreases significantly to RM 797; this section appears to be one in which the river is settling downstream from the disturbing effects of the dam.
2 (796-776.2)	There is a south-east-south-east stepwards progression of the planform in this reach that may be due to the presence of erosion-resistant materials (possibly Dakota Sandstone) in the left bank; there is a decreased rate of increase in the energy slope from RM 797-775 with a major downwards fluctuation around RM 777.5; there is also a decreased rate of increase in the w:d ratio from RM 796-777 but with more fluctuation about the mean than for the energy slope; both conveyance and hydraulic radius show a sharply decreased rate of increase throughout this reach and into the next one downstream, with the fluctuation in the trend of the latter matching well the fluctuation of the w:d ratio.
3 (776.2-764.7)	The river appears to deflect off right bank bluffs from RM 776.3-775.3, before gradually arcing back southwards towards the bluff line that re-commences along the right bank at RM 764.7. As in the previous reach this pattern may be aided by the presence of erosion resistant material (Dakota Sandstone?) along the left bank from approximately RM 767-766; most of the hydraulic variables maintain fairly constant values in this reach.
4 (764.7-753.9)	This reach is largely controlled by channel impingement on two sections of right bank bluff line, from RM 764.7-762 and 753.9 to beyond RM 751. Again, it is possible that erosion-resistant Dakota Sandstone is exerting a controlling influence in the left bank centered at about RM 758; w:d ratio decreases from RM 766.5-756; hydraulic radius increases steadily through the reach while conductivity increases from RM 766-756.

VII Particle Size Analysis

Introduction

To determine as accurately as possible the effects that any future bank stabilisation works will have on the in-channel morphology of the Upper Missouri River, it is necessary to develop a fully quantitative sediment budget for each of the four study reaches. This section details the first step in developing this budget, namely undertaking a quantitative analysis of the grain size distributions of sediment samples from the tributaries, the banks, the bed and the bars and islands of the Missouri River.

During the summer of 1999, a field team from Colorado State University (CSU) collected a total of 655 sediment samples from the four main study reaches of the Upper Missouri River. Over the course of the following year these samples were dry sieved to obtain the grain size distributions in the range between 0.063mm and 42mm. In order to ensure that accuracy was maintained, these data were entered twice into a master spreadsheet by two different people. Once complete, this spreadsheet formed the basis for the following analysis.

This section details the steps that were taken to analyze the data, presents the results of this process and discusses the implications of the findings. It concludes by outlining the steps needed to complete the sediment budget. These steps will be undertaken in the next phase of the study.

Methodology

The first stage of the analysis involved plotting percentile curves for each sample. Where more than one sample existed for a sampling location (referred to as waypoints), for example from several different sedimentary strata within a bank, all the points were plotted onto the same chart so that differences between the layers could be observed. These charts will form a useful reference tool if specific details need to be checked at a later date.

The next stage involved combining the individual sample data for all the waypoints where more than one sample was collected. To ensure that the relative proportion of material contributed from each sample in a multiple layer bank waypoint was accurately represented in the composite sample, it was necessary to multiply each individual size fraction in the sample by the fraction of the bank height occupied by that layer. This approach makes the assumption that the bank fails over its full height and that not just one particular stratum within the bank fails. When creating a composite particle size distribution from a number of individual samples from a tributary or arroyo bed for which no layer thickness is given, an arbitrary thickness value of 1 foot was allocated to each sample to ensure that they received equal weighting in the compositing process. Island or bar samples for which no percentage coverage or areal extents of the particular facies being sampled are recorded were also treated in exactly the same fashion. This makes it possible for one weighted percentile curve to be plotted for each waypoint and thus serve as the basis for the comparisons between bank and bar/island sediments. Although this method is not ideal, it is the

only way to transform the data into a usable form and therefore ensure that as many bar/island-potential sediment source comparisons as possible can be made.

The first series of bar/island to bank comparisons were made at the sampling reach (SR) scale. Sampling reaches are generally less than six river miles in length and were identified in order to isolate and investigate particular bar/island-bank, bar/island-tributary and bar/island-arroyo couplings. Where possible, the bar/island and bank data were composited so that only the necessary number curves were plotted. These then allowed a visual and qualitative assessment of the degree of particle size overlap to be made for each of the couplings.

The second series of comparisons involved examining the same pairings as above, but over a greater distance. This provides for the case of sediments that do not deposit on the nearest depositional form from their source, but travel further downstream before doing so, or of sediments that deposit near their source but are then remobilized by erosion of that feature. The bar/island grain size distributions from a particular sampling reach were thus compared to banks, tributaries and arroyos in the upstream 'Geomorphically Similar Reach' (GSR), which might vary in length from 3 to nearly 40 river miles. If a sampling reach was located near the upstream end of a GSR, the comparisons would be extended from the sampling reach through whatever remained of that GSR and over the full extent of the next GSR upstream, to ensure that a sufficient length of river was included in the analysis. Again, wherever possible, the data for the features being compared was composited such that as few weighted percentile curves as possible need be plotted. Table 1 shows the locations of all the habitat features, as well as the sampling reaches and GSRs. The identification of GSRs is discussed in detail in a separate report.

Table 1: Location of habitat bars and islands, sampling reaches and Geomorphically Similar Reaches

Habitat bar/island (1960 River Miles)	Sampling Reach (1960 River Miles)	Geomorphically Similar Reach (1960 River Miles)
Fort Peck Reach		
1712.5 (WP303)	1 (1761.65-1753)	1 (1766-1750)
1695.9 (WP187)	2 (1741.05-1737.7)	2 (1750-1713)
1685.4 (WP197)	3 (1730.8-1725)	3 (1713-1700)
1674.6 (WP211)	4 (1712.9-1711.8)	4 (1700-1686)
1659.1 (WP227)	5 (1707.3-1703.4)	5 (1686-1654)
1615.3 (WP167)	6 (1695.95-1692.7)	6 (1654-1621.7)
1595.1 (WP178)	7 (1681.4-1679.9)	7 (1621.7-1605)
	8 (1679.15-1674.3)	8 (1605-1582)
	9 (1663-1658.7)	
	10 (1651.2-1648.6)	
	11 (1646.1-1643.2)	
	12 (1631.2-1627.5)	
	13 (1618.1-1614.3)	
	14 (1608-1604.2)	
	15 (1598.35-1594.4)	
Garrison Reach		
1380 (WP97)	1 (1381.2-1376.2)	1 (1390-1376)
1370 (WP112)	2 (1376.1-1373.1)	2 (1376-1363)

1369.1 (WP114)	3 (1371.4-1366.4)	3 (1363-1353)
1361.5 (WP121)	4 (1362.65-1359.5)	4 (1353-1340)
1361.1 (WP122)	5 (1351.5-1346.7)	5 (1340-1324.5)
1348 (WP85)	6 (1335-1329.1)	6 (1324.5-1311)
1334.2 (WP132)	7 (1320-1315.7)	
1319.5 (WP143)		
Fort Randall Reach		
866.7 (WP70)	1 (876.7-873.85)	1 (880-873.9)
864.8 (WP69)	2 (867.6-864.5)	2 (873.9-867.5)
851.5 (WP556)	3 (858.5-854.5)	3 (867.5-861.7)
	4 (854.1-850.95)	4 (861.7-854.5)
	5 (847.45-846)	5 (854.5-851)
	6 (843.1-841)	6 (851-844)
Gavins Point Reach		
804.5 (WP6)	1 (804.8-800.5)	1 (811-796)
803.4 (WP7)	2 (800.3-793)	2 (796-776.2)
797 (WP16)	3 (782.8-779.3)	3 (776.2-764.7)
781.7 (WP25)	4 (779.3-775.7)	4 (764.7-753.9)
	5 (776-763.4)	

Before the principle grain size distribution analysis was undertaken, however, a first attempt was made to ascertain what effect the current bank revetments had had on the grain size distributions of the habitat and non-habitat bars and islands. Once all the individual waypoints had been composited, the aerial photographic mosaics were used to ascertain which bars and islands were located either within, or just downstream of, a zone of significant bank revetments on one or both banks of the Missouri. All the composited and weighted bar and island grain size distributions for each study reach were then plotted onto one graph, with the individual plots being colour-coded according to whether they were habitat or non-habitat and whether they were within the potential zone of influence of bank revetment or not. The four graphs are presented in Appendix A and the results are discussed in the next sub-section.

Results and Analysis

The results of the sampling reach-scale and GSR-scale analysis are presented graphically in Appendix A. Wherever appropriate, the plot showing the comparison between sampling reach and the upstream GSR is presented first and is then followed by the plot or plots representing the various couplings being investigated at the sampling reach-scale. This was done so that the effects on the sampling reach-scale comparisons of the compositing process to the GSR-scale could be readily compared. Additionally, a quantitative evaluation of the degree of overlap of the grain size distribution curves, and the range of grain sizes over which this comparison is being made are presented in Tables 2 to 5. In each case, the habitat or non-habitat bar or island is the point of reference to which the potential upstream sediment sources are compared. In the case of the habitat and non-habitat bars and islands, the percentage figure actually represents the total amount of material in the sample greater than 0.063mm in diameter. Thus, for example, in Table 2b, the GSR1 & SR1 comparison shows that 67.28% of the non-habitat bar material occurs in the range 0.063-4.75mm (and by implication 37.72% is finer than 0.063mm). The table also shows that 83.82% of the upstream bank material, 34.73% of the upstream tributary material and 55.07% of the upstream arroyo material occurs in the size range 0.063-4.75mm and can thus

potentially contribute to formation of the non-habitat bars. This means that 16.18%, 65.27% and 44.93% of these three samples respectively are finer than 0.063mm and/or coarser than 4.75mm.

Before proceeding with this analysis, however, the results of the first attempt to examine the effects of bank revetments are presented and discussed briefly.

Preliminary analysis of the effects of bank revetments on grain size distributions

Figures B1 to B4 in Appendix B show the effects that bank revetments have had on the grain size distributions of habitat and non-habitat bars and islands. In fact, only Garrison Reach and Gavins Point Reach (Figures B2 and B4) had revetments of a sufficient extent to make this analysis worthwhile. Nevertheless, plots were still drawn up for the Fort Peck and Fort Randall Reaches (Figures B1 and B3), since it will be informative for the main analysis in this report to see whether or not there are any differences in the grain size distributions of habitat and non-habitat bars and islands.

In Garrison Reach (Figure B2) it can be seen that there is no obvious difference between the habitat and non-habitat bars and islands in the zones influenced by and not influenced by bank revetments. The plots for these four categories are mostly of a very similar shape and occupy a similar position on the chart. This is also the case in the Fort Peck and Fort Randall Reaches (Figures B1 and B3) - the habitat plots are mingled randomly with the non-habitat plots and no distinct pattern is discernible. In the case of Gavins Point Reach (Figure B4) however, it can be seen that the habitat bars uninfluenced by bank revetments have a slightly coarser grain size distribution than those that are in close proximity to revetments. Unfortunately, this pattern is not replicated by the non-habitat bars and it is at best tenuous to draw any conclusions from these findings. Furthermore, the sample is too small (only two habitat none-bank-influenced and two habitat bank-influenced bars are present) for statistical comparison.

Nevertheless, these findings should be borne in mind when undertaking further analyses. It may be that once the channel perimeters and in-channel features have been digitised and combined with bank heights and the results of this report to produce some absolute values for the amounts of sediment moving through the system, that a more detailed evaluation of the effects of bank revetments will be possible.

Fort Peck Reach

GSR1 & SR1

The figures for this comparison (Figure A1 and Table 2b) have already been discussed in the example above and show that the upstream banks can potentially contribute a large proportion of material (83.82%) over the range 0.063-4.75mm to the formation of the non-habitat bars (0.063-4.75mm), as can the upstream arroyo (55.07% from 0.063-4.75mm). The relationship between the non-habitat bars and the upstream banks is shown to be even stronger at the sampling reach scale. Table 2a (and Figures A2 & A3) show that 98.73% and 97.89% respectively of the bank material in the 1st

and 2nd couplings within SR1 can potentially contribute to formation of the bars, although this is now in the range 0.063-2mm for both the bars and banks. The 3rd coupling (Figure A4) shows a lower value of 74.34% potentially contributing to bar formation, with both banks and bar occurring in the range 0.063-4.75mm. These figures thus suggest that the contribution to bar formation in the 1st and 2nd couplings is most significant from the banks that are eroding immediately upstream of the bars, whilst the bars in the 3rd coupling may also be receiving material from further upstream in the GSR.

GSR2 & SR2

Table 2b (Figures A5 & A6) shows that at the GSR-scale, 67.14% and 60.2% of material from the upstream banks and tributary over the size ranges 0.063-4.75mm and 0.063-4mm respectively can potentially contribute to formation of the non-habitat bars in SR2, which themselves have a grain size range of 0.063-16mm. When looking at the immediate coupling between bar and bank within SR2 (Table 2a) only 51.09% (0.063-4.75mm) of the material can possibly contribute to bar formation. Material may therefore be travelling from several eroding bank locations within the GSR. Furthermore, these figures show that the bar sediments in the range 4.75-16mm are being derived from a source other than the banks or tributary, although their contribution to the mass of the bar is <1% and they are therefore not particularly significant.

GSR2 & SR3

The non-habitat bars in SR3 again occur in the range 0.063-16mm (Table 2b, Figure A7). The upstream banks and tributary at the GSR-scale could possibly contribute 84.14% (0.063-4.75mm) and 60.2% (0.063-4mm) respectively. At the sampling reach-scale (Table 2a) the non-habitat bars in the 1st coupling (Figure A8) have a grain size range of 0.063-16mm to which the upstream banks potentially contribute a maximum of 50.52% of their material over the same range. For the 2nd coupling (Figure A9) the non-habitat bar is composed of sediments in the range 0.063-2mm and the upstream banks can contribute up to 31.75% of their material over the same size range. These results thus suggest that the non-habitat bars are closely associated with the sediments in the banks that are eroding in their immediate vicinity.

GSR2 & SR4

The habitat bar and non-habitat bar in SR4 (Figure A10) could only be compared to potential sources of sediment at the GSR-scale since there were none within the designated sampling reach. Table 2b shows that 99.5% of the material in the habitat bar occurs in the range 0.063-4.75mm. The relative contributions of the upstream banks and tributary are 74.2% (0.063-4mm) and 54.7% (0.063-4.75mm) respectively. These figures suggest that both the banks and tributary contribute to bar formation although it is not possible from this analysis to discern the absolute contribution of each. 70.8% of the non-habitat bar occurs in the range 0.063-16mm, with the relative contribution from the upstream bank the same as above and from tributary being 80.36% over the range 0.063-16mm. This also suggests that both the banks and the tributary contribute to bar formation although the absolute proportions are not known.

However, since the proportion of non-habitat bar sediments between 4 and 16mm is much less than 1% it is possible that the tributary does not contribute very much.

GSR3 & SR5

At the GSR-scale the non-habitat bars are composed 86.17% of sediments in the range 0.063-4.75mm. The potential contribution from the upstream banks is 80.87% in the range 0.063-4mm (Table 2b, Figure A11). At the sampling reach-scale 61.64% of the non-habitat bar material falls in the range 0.063-4mm, to which the possible upstream bank sources can contribute a maximum of 85.14% over the same range (Figure A12). Because the upstream banks can contribute such similar proportions over the same grain size range at the two different scales of analysis, it is not possible to say over which scale the bar-bank coupling is potentially more significant. It is clear, however, that material of 4.75mm calibre is coming from a source other than the banks in this GSR.

GSR4 & SR6

Table 2b shows that 96.22% of the non-habitat bar material at the GSR-scale falls in the range 0.063-22.4mm, whilst the 72.42% of the upstream bank material that can possibly contribute to bar formation occurs in the range 0.063-4.75mm. Again, however, it is much less than 1% of the bar material that occurs in the range 4.75-22.4mm (Figure A13) and so this is relatively unimportant. At the sampling reach-scale 94.7% of the non-habitat bar material falls in the range 0.063-2mm, while 85.82% of the upstream bank material occurs over the same range. At the sampling reach-scale this suggests that the bank is a significant contributor of material to the bar but that at the GSR-scale material from further upstream makes some contribution.

GSR4 & GSR5

Two GSRs are compared here since the habitat bar in question, WP197, (Figure A15) is located outside a sampling reach and at the very upstream limit of GSR5 (see Table 1 above). It is thus compared to the upstream banks in GSR4. Table 2b shows that 50.72% of the bar falls in the range 0.063-4mm and that 64.95% of the bank material falls in the same range. These figures thus suggest that the bar is made up primarily from eroded bank material.

GSR5 & SR7

Table 2b shows that 88.83% of the non-habitat bars in SR7 are composed of materials in the range 0.063-16mm. The upstream banks and tributary can potentially contribute 84.59% (0.063-2mm) and 5.3% (0.063-0.075mm) of their material respectively. Figure A16 shows that only about 2% of the bar material falls in the range 2-16mm and, because the vast majority of the tributary material is finer than 0.063mm, this suggests that the banks are the primary source of sediment for the bar. Table 2a shows that in the 1st coupling in SR7 (Figure A17), 84.21% of the non-habitat bar material is composed of material in the range 0.063-16mm with the only immediate upstream source being the tributary. The 2nd coupling (Figure A18) shows 98.1% of the non-habitat bar to be composed of material in the range 0.063-1mm, with 77.78% of the

potential upstream bank input being in the same range. The figures for the tributary are the same as above. These data suggest that there is a strong coupling between bar and banks at the sampling reach-scale but that there is also some input to the bars from eroding banks within the GSRs. Also there is some other source upstream of GSR5 contributing about 2% of the bars' mass in the range 2-16mm.

GSR5 & SR8

Table 2b (Figure A19) shows that the habitat bar is composed 98.1% of material in the range 0.063-1mm, with the upstream banks and first upstream tributary (the Poplar River) potentially contributing up to 65.97% and 88.43% respectively of their material in the same range. The second upstream tributary can contribute up to 5.3% of its material over the range 0.063-0.075mm. The non-habitat bars are composed 82.88% of material in the range 0.063-8mm, although <1% of this material is actually coarser than 1mm. The upstream banks and Poplar River can potentially contribute up to 66.11% (0.063-4mm) and 88.46% (0.063-2mm) respectively of their material, with the second tributary potentially contributing the same as above. The 1st coupling at the sampling reach-scale (Table 2a, Figure A20) is between non-habitat bars that have 74.95% of their material in the range 0.063-8mm and Poplar River, which can potentially contribute 88.46% of its material in the range 0.063-2mm. The 2nd coupling (Figure A21) compares the habitat bar (98.1% from 0.063-1mm) and non-habitat bars (98.2% over the same range) to the upstream banks and the Poplar River, which can potentially contribute 45.45% and 88.43% of their sediments, again over the same range. The data from both the GSR- and SR-scale analysis thus suggest that the upstream banks and Poplar River are the prime contributors to both the habitat and non-habitat bars, although it is not possible to say which is the most significant. Nor is it possible to say whether the bar-bank couplings are more important at the SR-scale or GSR-scale.

GSR5 & SR9

Table 2b shows that 98.5% of the habitat bar is composed of material in the range 0.063-2mm. Over the same range the upstream banks, the Poplar River and the upstream arroyo can potentially contribute up to 68.43%, 88.46% and 21.3% respectively of their material to the bar. The non-habitat bars are composed 98.03% of material in the range 0.063-4.75mm, although <1% of these sediments are coarser than 1mm (Figure A22). The upstream bank, the Poplar River and upstream arroyo can potentially contribute up to 68.45% (0.063-4mm), 88.46% (0.063-2mm) and 24.8% (0.063-4mm) of their sediments to these bars. Table 2a shows that at the 1st SR-scale coupling the non-habitat bars and island are composed 98.24% of material in the range 0.063-4.75mm, with just under 50% being coarser than 0.25mm (Figure A23). 86.3% of the material in the upstream bank occurs in the range 0.063-0.025mm. In the 2nd coupling the non-habitat bar is composed 97.4% of material in the range 0.063-2mm, whilst 97.9% of the sediments in the upstream banks occur in the same range (Table 2a, Figure A24). Similarly for the 3rd coupling, the habitat bar is made up 98.5% of material in the range 0.063-2mm with 91.87% of the sediments in the upstream banks being of the same range (Table 2a, Figure A24). These data suggest that for the 2nd and 3rd couplings there is a strong linkage between the habitat and non-habitat bars and the banks eroding in the immediate upstream vicinity, whilst in the case of the 1st coupling the figures suggest that just under 50% of the non-habitat bar

and island material is derived from sources further upstream than the banks eroding immediately upstream.

GSR5 & SR10

Table 2b (Figure A26) shows that 97.47% of the non-habitat bar material occurs in the range 0.063-2mm, with 66.53% of the upstream bank material also falling within this range. In the absence of any other potential sources of sediment in GSR5, these figures suggest that most of the bar material comes from the eroding banks within GSR5.

GSR6 & SR11

Table 2b (Figure A27) shows that 94.03% of the non-habitat bars are composed of materials in the range 0.063-4mm, whilst 52.42% and 37.95% of the upstream bank and tributary sediments that can potentially contribute to these bars also fall in the same range. In the 1st coupling at the sampling reach-scale, 97.8% of the non-habitat bar is made up of material in the range 0.063-2mm with 29.3% of the upstream bank material occuring in the same range (Table 2a, Figure A28). In the 2nd coupling 90.3% of the non-habitat bar is made up of sediments in the range 0.063-4mm, with 45.53% and 37.95% of the material in the upstream banks and upstream tributary respectively being in the same range (Table 2a, Figure A29). These figures thus suggest a strong link between the bars and their potential sediment sources at the sampling reach-scale.

GSR6 & SR12

Table 2b (Figure A30) shows that 96.76% of the non-habitat bars are made of materials in the range 0.063-4mm. 61.39% and 58% of the upstream banks and tributary (the Big Muddy Creek) sediments also occur in the same range. At the sampling reach-scale 96.7% of the bar materials fall in the range 0.063-4mm, as does 67.13% of the upstream banks and 58.52% of the Big Muddy Creek sediments (Table 2a, Figure A31). These figures suggest a strong relationship between the bars and their potential sources of sediment immediately upstream, but also that there is some contribution to their composition from the eroding bank sources further upstream within GSR6.

GSR7 & SR13

Table 2b (Figure A34) shows that 98.3% of the habitat bar material and 85.17% of the non-habitat bar material falls within the range 0.063-2mm. 60.54% of the upstream banks also fall within the same range. At the sampling reach-scale Table 2a shows that for the 1st coupling, the habitat bar is composed 97.3% of material in the range 0.063-2mm whilst 42.2% of the upstream banks are composed of materials in the range 0.063-1mm. Examination of Figure A33, however, shows that <1% of the bar material is coarser than 0.5mm, whilst only about 1% of the bank sample is coarser than 0.24mm. The 2nd coupling (Figure A34) shows that 97.3% of the non-habitat bar falls in the range 0.063-2mm, whilst 63.8% of the material in the upstream bank occurs in the same range. These figures thus suggest that there is a strong link between the bars and their immediate potential sources of sediment upstream, but also

that there is some potential contribution from eroding banks further upstream in GSR7, especially in the case of the 1st SR-scale coupling.

GSR7 & SR14

Table 2b (Figure A35) shows that 91.92% of the non-habitat bar sediments occur in the range 0.063-4mm, whilst 69.73% and 49.57% respectively of the upstream bank and upstream arroyo sediments also fall within this range. At the sampling reach-scale (Table 2a, Figure A36), 91.92% of the habitat bars are composed of sediments in the range 0.063-4mm, with 85.2% of the upstream bank material also falling within this range. These data suggest that both the banks and the arroyo contribute material to the bars, although it is not possible to state the absolute quantities involved. Nor is it possible to say whether the bar-bank coupling is strongest at the SR-scale or the GSR-scale.

GSR7&8 and SR15

Table 2b (Figure A37) shows that 90.03% of the habitat bar is composed of sediments in the range 0.063-4.75mm, whilst 70.7% and 49.74% of the upstream banks and upstream arroyo respectively also fall within this range. The non-habitat bar is composed 97.7% of materials in the range 0.063-1mm, with the upstream banks and upstream arroyo having respectively 69.43% and 45.37% of their materials within this range. At the sampling reach-scale, Table 2a (Figure A38) shows that 90.03% of the habitat bar is composed of sediments in the range 0.063-4.75mm and 78.19% of the material in the upstream banks occurs in the range 0.063-4mm. These figures thus suggest that material is contributed to the habitat and non-habitat bars from sources within the sampling reach and from further upstream in GSRs7&8. As before, it is not possible to clarify the absolute amounts from either location.

Table 2a: Fort Peck Reach - The fraction of the grain size distribution found in banks and tributaries that Can possibly contribute to bar and island formation, along with the size range over which this fraction occurs

Sampling Reach-Scale Analysis					
	Habitat bars	**Non-habitat bars & islands**	**Upstream banks**	**Upstream tributary**	**Upstream arroyo**
SR1 (1st coupling)		57.30% (0.063-2mm)	98.73% (0.063-2mm)	33.46% (0.063-2mm)	
SR1 (2nd coupling)		38.40% (0.063-2mm)	97.89% (0.063-2mm)	33.46% (0.063-2mm)	
SR1 (3rd coupling)		80.25% (0.063-4.75mm)	74.34% (0.063-4.75mm)	34.73% (0.063-4.75mm)	55.07% (0.063-4.75mm)
SR2		86.79% (0.063-16mm)	51.09% (0.063-4.75mm)		
SR3 (1st coupling)		96.37% (0.063-16mm)	50.52% (0.063-16mm)		
SR3 (2nd coupling)		70.50% (0.063-2mm)	31.75% (0.063-2mm)		
SR5		61.64% (0.063-4mm)	85.14% (0.063-4mm)		
SR6		94.70% (0.063-2mm)	85.82% (0.063-2mm)		
SR7 (1st coupling)		84.21% (0.063-16mm)		5.30% (0.063-0.075mm)	
SR7 (2nd coupling)		98.10% (0.063-1mm)	77.78% (0.063-1mm)	5.30% (0.063-0.075mm)	
SR8 (1st coupling)		74.95% (0.063-8mm)		88.46% (0.063-2mm)	
SR8 (2nd coupling)	98.10% (0.063-1mm)	98.20% (0.063-1mm)	45.45% (0.063-1mm)	88.43% (0.063-1mm)	
SR9 (1st coupling)		98.24% (0.063-4.75mm)	86.30% (0.063-0.025mm)		
SR9 (2nd coupling)		97.40% (0.063-2mm)	97.90% (0.063-2mm)		
SR9 (3rd coupling)	98.50% (0.063-2mm)		91.87% (0.063-2mm)		
SR11 (1st coupling)		97.80% (0.063-2mm)	29.30% (0.063-2mm)		
SR11 (2nd coupling)		90.30% (0.063-4mm)	45.53% (0.063-4mm)	37.95% (0.063-4mm)	
SR12		96.70% (0.063-4mm)	67.13% (0.063-4mm)	58.52% (0.063-4mm)	
SR13 (1st coupling)	98.30% (0.063-2mm)		42.20% (0.063-1mm)		
SR13 (2nd coupling)		97.30% (0.063-2mm)	63.80% (0.063-2mm)		
SR14		91.92% (0.063-4mm)	85.20% (0.063-4mm)		
SR15	90.03% (0.063-4.75mm)		78.19% (0.063-4mm)		

Table 2b: Fort Peck Reach - The fraction of the grain size distribution found in banks, tributaries and arroyos that can possibly contribute to bar and island formation, along with the size range over which this fraction occurs.

Geomorphically Similar Reach-Scale Analysis						
	Habitat bars	Non-habitat bars & islands	Upstream banks	Upstream tributary 1	Upstream tributary 2	Upstream arroyos
GSR1 & SR1		67.28% (0.063-4.75mm)	83.82% (0.063-4.75mm)	34.73% (0.063-4.75mm)		55.07 (0.063-4.75mm)
GSR2 & SR2		86.79% (0.063-16mm)	67.14% (0.063-4.75mm)	60.20% (0.063-4mm)		
GSR2 & SR3		87.74% (0.063-16mm)	84.14% (0.063-5.6mm)	60.20% (0.063-4mm)		
GSR2 & SR4 (1st)	99.50% (0.063-4.75mm)		74.20% (0.063-4mm)	54.70% (0.063-4.75mm)		
GSR2 & SR4 (2nd)		70.80% (0.063-16mm)	74.20% (0.063-4mm)	80.36% (0.063-16mm)		
GSR3 & SR5		86.17% (0.063-4.75mm)	80.87% (0.063-4mm)			
GSR4 & SR6		96.22% (0.063-22.4mm)	72.42% (0.063-4.75mm)			
GSR4 & GSR5	50.72% (0.063-4mm)		64.95% (0.063-4mm)			
GSR5 & SR7		88.83% (0.063-16mm)	84.59% (0.063-2mm)	5.30% (0.063-0.075mm)		
GSR5 & SR8 (1st)	98.10% (0.063-1mm)		65.97% (0.063-1mm)	88.43% (0.063-1mm)	5.30% (0.063-0.075mm)	
GSR5 & SR8 (2nd)		82.88% (0.063-8mm)	66.11% (0.063-4mm)	88.46% (0.063-2mm)	5.30% (0.063-0.075mm)	
GSR5 & SR9 (1st)	98.50% (0.063-2mm)		68.43% (0.063-2mm)	88.46% (0.063-2mm)	5.30% (0.063-0.075mm)	21.30% (0.063-2mm)
GSR5 & SR9 (2nd)		98.03% (0.063-4.75mm)	68.45% (0.063-4mm)	88.46% (0.063-2mm)	5.30% (0.063-0.075mm)	24.80% (0.063-4mm)
GSR5 & SR10		97.47% (0.063-2mm)	66.53% (0.063-2mm)			
GSR6 & SR11		94.03% (0.063-4mm)	52.42% (0.063-4mm)	37.95% (0.063-4mm)		
GSR6 & SR12		96.76% (0.063-4mm)	61.39% (0.063-4mm)	58% (0.063-4mm)		
GSR7 & SR13	98.30% (0.063-2mm)	85.17% (0.063-2mm)	60.54% (0.063-2mm)			
GSR7 & SR14		91.92% (0.063-4mm)	69.73% (0.063-4mm)			49.57% (0.063-4mm)
GSR7&8 & SR15 (1st)	90.03% (0.063-4.75mm)		70.70% (0.063-4.75mm)			49.74% (0.063-4.75mm)
GSR7&8 & SR15 (2nd)		97.70% (0.063-1mm)	69.43% (0.063-1mm)			45.37% (0.063-1mm)

Garrison Reach

GSR1 & SR1

Table 3 shows that 99.33% of the material in the habitat bar is composed of sediments in the range 0.063-4.75mm, whilst 88.93% of the material in the banks is of the same range (Figure A39). 98.74% of the non-habitat bars are composed of materials in the range 0.063-32mm, with about 35% of these sediments being coarser than 1mm and about 12% coarser than 10mm (Figure A40). The upstream banks are composed 87.85% of material in the range 0.063-4.75mm. Table 3 also provides the data for the sampling reach-scale analyses. The 1st coupling in SR1 shows that 99.33% of the habitat bar material falls in the range 0.063-4.75mm, with 74.47% of the upstream bank material occuring in the range 0.063-4mm. In both cases, <3% of the sediments are coarser than 0.5mm (Figure A41). In the 2nd coupling, 99.5% of the non-habitat bar material occurs in the range 0.063-32mm, with about 78% of the material coarser than 0.5mm and around 24% coarser than 10mm (Figure 42). The associated upstream banks have 78.12% of their sediments in the range 0.063-4.75mm but with only about 2% coarser than 0.5mm. The 3rd coupling (Figure A43) shows that 97.98% of the non-habitat bar is in the range 0.063-4.75mm and that 78.94% of the upstream bank material also falls in the same range. These results all suggest that the habitat and non-habitat bars are strongly dependent on sediments found within the banks and, furthermore, that there is a strong bar-bank relationship at the sampling reach-scale. The 2nd coupling is the exception to this rule, since about 76% of the material in the non-habitat bar is coarser than the sediments found in the corresponding upstream sections of eroding bank.

GSR1&2 and SR2

Table 3 (Figure A44) shows that 97.28% of the non-habitat bar material occurs in the range 0.063-4mm. Similarly, 85.75% and 94.24% of the upstream banks and tributary (the Knife River) sediments respectively fall in the same range. At the sampling reach-scale the figures for the non-habitat bar and Knife River sediments are the same as above, whilst 60.81% of the upstream banks are composed of materials also in the range 0.063-4mm. This suggests a strong relationship between the bar and upstream banks and the Knife River, although it is not possible to say if the bar is more strongly related to the bank sediments at the SR-scale or the GSR-scale.

GSR2 & SR3

Table 3 (Figure A46) shows that 99.23% of the habitat bars are composed of sediments in the range 0.063-4mm. 74.55% of the upstream bank materials and 95.24% of the Knife River sediments also fall within this range. 70.2% of the second tributary sediments occur in the range 0.063-2mm. Figure A47 and Table 3 show a strong 1st coupling at the sampling each-scale. 99.3% of the habitat bar material and 97.88% of the upstream bank sediments both occur in the range 0.063-2mm. The 2nd coupling also shows a strong relationship between the bar, bank and tributary. The habitat bar has 99.17% of its material in the range 0.063-2mm, whilst 86.43% of the upstream bank material and 70.2% of the upstream tributary sediments also occur in the same range. These data suggest that the upstream banks and both tributaries can

contribute sediments to the habitat bars, although it is not possible at present to say which of these potential sources is the most significant.

GSR2 & SR4

Table 3 shows that 96.34% of the habitat bar sediments occur in the range 0.063-16mm. 83.06% of the upstream tributary sediments also fall within this range, whilst 74.84% of the upstream bank material occurs in the range 0.063-4.75mm. As well as showing a strong qualitative relationship between all three samples, however, Figure A49 also shows that <3% of any of these samples is coarser than 1mm. Thus both the upstream banks and tributaries could be contributing sediments to the habitat bars, although it is not possible to state which is the more important source.

GSR3&4 and SR5

Table 3 shows that 58.95% of the habitat bar and 94.92% of the non-habitat bars are made up of materials in the range 0.063-4mm, whilst the upstream banks are composed 67.62% of materials in the same range. Figure A50 shows a strong degree of similarity between the three plots and it is thus reasonable to assume that the banks probably contribute the majority of the sediments to the habitat and non-habitat bars.

GSR4&5 and SR6

Table 3 (Figure A51) shows that 95.63% of the habitat bar is composed of material in the range 0.063-0.5mm, whilst 51.78%, 9.98% and 47.5% of the upstream banks, tributary and arroyo sediments respectively also fall within the same range. Table 3 also shows that 94.16% of the non-habitat bar and island are composed of materials in the range 0.063-4mm, whilst 54.68%, 25.75% and 68.55% of the upstream banks, tributary and arroyo sediments also fall within this range. The 1st coupling at the sampling reach-scale shows that 95.63% of the habitat bar is composed of material in the range 0.063-0.5mm and that 82.27% of the upstream banks are in the same range. The 2nd coupling shows that 94.16% of the non-habitat bars are composed of materials in the range 0.063-4mm, whilst 55.86% of the upstream banks sediments and 79.5% of the upstream arroyo sediments occur in the same range. These data, along with the visual evidence of Figures A52 and A53, suggest that the bars are more closely related to the sediments from the banks and arroyo than to those from the tributary (Figure A51). And of these two possible sources it is more probable that the banks contribute a greater proportion of sediment to the bars than the arroyo, although it is not possible at this stage to quantify the amounts of material involved.

GSR5 & SR7

Table 3 shows that 98.7% of the habitat bar material and 76.52% of the non-habitat bar material occurs in the 0.063-4mm range, as does 39.12% of the upstream bank sediments. Along with the visual evidence of Figure A54 these figures suggest that the banks contribute a significant proportion of sediment to the downstream bars.

Table 3: Garrison Reach - The fraction of the grain size distribution found in banks tributaries and arroyos that can possibly contribute to bar and island formation, along with the size range over which this fraction occurs

Sampling Reach-Scale Analysis						
	Habitat bars	Non-habitat bars & islands	Upstream banks	Upstream tributary 1	Upstream tributary 2	Upstream arroyos
SR1 (1st coupling)	99.33% (0.063-4.75mm)		74.47% (0.063-4mm)			
SR1 (2nd coupling)		99.50% (0.063-32mm)	78.12% (0.063-4.75mm)			
SR1 (3rd coupling)		97.98% (0.063-4.75mm)	78.94% (0.063-4.75mm)			
SR2		97.28% (0.063-4mm)	60.81% (0.063-4mm)	95.24% (0.063-4mm)		
SR3 (1st coupling)	99.30% (0.063-2mm)		97.88% (0.063-2mm)			
SR3 (2nd coupling)	99.17% (0.063-2mm)		86.43% (0.063-2mm)	70.20% (0.063-2mm)		
SR6 (1st coupling)	95.63% (0.063-0.5mm)		82.27% (0.063-0.5mm)			
SR6 (2nd coupling)		94.16% (0.063-4mm)	55.86% (0.063-4mm)			79.50% (0.063-4mm)
Geomorphically Similar Reach-Scale Analysis						
	Habitat bars	Non-habitat bars & islands	Upstream banks	Upstream tributary 1	Upstream tributary 2	Upstream arroyos
GSR1 & SR1 (1st coupling)	99.33% (0.063-4.75mm)		88.93% (0.063-4.75mm)			
GSR1 & SR1 (2nd coupling)		98.74% (0.063-32mm)	87.85% (0.063-4.75mm)			
GSR1&2 & SR2		97.28% (0.063-4mm)	85.75% (0.063-4mm)	95.24% (0.063-4mm)		
GSR2 & SR3	99.23% (0.063-4mm)		74.55% (0.063-4mm)	95.24% (0.063-4mm)	70.20% (0.063-2mm)	
GSR2 & SR4	96.34% (0.063-16mm)		74.84% (0.063-4.75mm)	83.06% (0.063-16mm)		
GSR3&4 & SR5	58.95% (0.063-4mm)	94.92% (0.063-4mm)	67.62% (0.063-4mm)			
GSR4 &5 & SR6 (1st)	95.63% (0.063-0.5mm)		51.78% (0.063-0.5mm)	9.98% (0.063-0.5mm)		47.50% (0.063-0.5mm)
GSR4 &5 & SR6 (2nd)		94.16% (0.063-4mm)	54.68% (0.063-4mm)	25.75% (0.063-4mm)		68.55% (0.063-4mm)
GSR5 & SR7	98.70% (0.063-4mm)	76.52% (0.063-4mm)	39.12% (0.063-4mm)			

Fort Randall Reach

SR1

Although SR1 is located at the downstream end of GSR1, there are no potential sources of sediment upstream in the GSR against which the bar and island in SR1 can be compared. Analysis is thus restricted to the sampling reach-scale. So saying, Table 4 shows that 99.01% of the non-habitat bar and island are composed of sediments in the range 0.063-22.4mm, whilst 4.19% of the sediments in the upstream eroding bank are in the range 0.075mm. Figure A55 shows that the vast majority of the bar and island material is between 0.1mm and 1mm in diametre, so it is clear that a source other than the eroding bank is providing the material. This may have been a previously eroding, and now stabilised, section of bank or, given the proximity of the reach to Fort Randall Dam, it may be the material that has been scoured from the bed of the Missouri River by the sediment-starved flows being released from the dam.

GSR2&3 and SR2

Table 4 shows that 99.46% of the habitat bar material occurs over the range 0.063-8mm, whilst 20.19% of the sediments in the upstream banks occurs over the range 0.063-4mm. At the sampling reach-scale, Table 4 shows that the same proportion of habitat bar material occurs over the same range of grain sizes, whilst 52.93% of the upstream bank occurs in the range 0.063-4mm. Examination of Figures A56 and A57 shows that in both the above cases less than about 2% of any of the samples are coarser than 1mm. Combined with the above data, this semi-qualitative assessment suggests that the banks are a significant source of the materials found in the habitat bars.

GSR4 & SR3

Table 4 shows that 88.75% of the materials in the non-habitat islands and bar are composed of sediments in the range 0.063-16mm, whilst 66.78% of the sediments in the upstream banks occur in the same range. At the sampling reach-scale, the same proportion of non-habitat island and bar sediments occur over the same range as above, whilst 62.89% of the upstream arroyo sediments also fall within the range 0.063-16mm. Examination of Figures A58 and A59, however, shows that there is a much greater similarity between the grain size distributions of the islands and bar with the upstream banks than with the arroyos. Unfortunately, it is not possible to quantify in absolute terms the contribution of each potential source.

GSR4&5 and SR4

Table 4 shows that 99.29% of the habitat bar material occurs in the range 0.063-0.5mm, whilst 33.35% of the upstream bank material and 14.82% of the arroyo material also occurs over the same range. 90.73% of the material in the non-habitat bars and islands occurs in the 0.063-16mm range, whilst 39.03% of the upstream bank material occurs from 0.063-4.75mm. At the sampling reach-scale, 99.29% of the

habitat bar material occurs in the range 0.063-0.5mm, whilst only 0.4% of the upstream bank material lies within the same range. 86.39% of the material in the non-habitat bars and islands occurs in the range 0.063-16mm. These data suggest that the upstream banks nearest to the majority of the habitat and non-habitat bars and islands contribute virtually nothing to their composition and that it is the eroding banks upstream of SR4, in GSRs 4 and 5, along with the upstream arroyo, that contribute most of the material. Examination of Figures A60 and A61 supports this assertion.

GSR6 & SR5

Table 4 shows that 95.47% of the sediments in the non-habitat bars fall in the range 0.063-22.4mm, whilst 41.83% of the material in the upstream bank and 94.65% of the material in the tributary delta bars occur in the range 0.063-4mm. The tributary delta bars are taken to represent the sediments being deposited in the Missouri River by Ponca Creek, since it was not possible to access the tributary itself for sampling purposes. Examination of Figure A62 shows that in all three cases, less than about 5% of the sediments are coarser than 0.5mm and so it is fairly safe to assume that the non-habitat bars are probably composed of sediments from both the upstream eroding banks and Ponca Creek, although the absolute contribution from each source is not known.

Downstream of GSR6 & SR6

As with the case above, the tributary delta bar is taken to represent the material being deposited by the tributary of the Missouri River, this time the Niobrara River. Table 4 (Figure A63) shows that 89.21% of the non-habitat island and bar are composed of sediments in the range 0.063-16mm, whilst 99.23% of the tributary bar sediments occur in this range. It is thus probable that the island and bar are almost entirely the product of Niobrara River sediments.

Table 4: Fort Randall Reach - The fraction of the grain size distribution found in banks and arroyos that can possibly contribute to bar and island formation, along with the size range over which this fraction occurs.

Sampling Reach-Scale Analysis					
	Habitat bars	**Non-habitat bars & islands**	**Upstream banks**	**Upstream arroyos**	**Tributary delta bars**
SR1		99.01% (0.063-22.4mm)	4.19% (0.063-0.075mm)		
SR2	99.46% (0.063-8mm)		52.93% (0.063-4mm)		
SR3		88.75% (0.063-16mm)		62.89% (0.063-16mm)	
SR4	99.29% (0.063-0.5mm)	86.39% (0.063-16mm)	0.40% (0.063-0.5mm)		
Geomorphically Similar Reach-Scale Analysis					
	Habitat bars	**Non-habitat bars & islands**	**Upstream banks**	**Upstream arroyos**	**Tributary delta bars**
GSR2&3 & SR2	99.46% (0.063-8mm)		20.19% (0.063-4mm)		
GSR4 & SR3		88.75% (0.063-16mm)	66.78% (0.063-16mm)		
GSR4&5 & SR4 (1st)	99.29% (0.063-0.5mm)		33.35% (0.063-0.5mm)	14.82% (0.063-0.5mm)	
GSR6 & SR5		95.47% (0.063-22.4mm)	41.83% (0.063-4mm)		94.65% (0.063-4mm)
Downstream of GSR6 & SR6		89.21% (0.063-16mm)			99.23% (0.063-16mm)

Gavins Point Reach

GSR1 & SR1

At both the GSR-scale and the SR-scale, Table 5 shows that 99.56% of the material in the habitat bars and 99.36% of the material in the non-habitat bar falls in the range 0.063-16mm. At the GSR-scale 85.66% of the upstream bank sediments occur in the same range, whilst at the SR-scale 86.5% of the upstream bank sediments also occur in the same range. These data, along with their visual representation in Figures A64 and A65, suggest that in all probability the material in these bars has its origin in the upstream banks, although it is not possible to say whether the banks in the sampling reach contribute more than those further upstream in GSR1.

GSR1 & SR2

The comparisons in SR2 are rather more complex than usual since a non-habitat bar and island have been examined separately due to their different grain size

distributions. At both the GSR-scale and the SR-scale, Table 5 shows that 99.61% of the habitat bar is composed of materials in the range 0.063-8mm, whilst 28.46% of the upstream tributary sediments also occupy this range. At the GSR-scale 84.48% of the upstream bank material falls within this same range, whilst at the SR-scale 82.28% of the upstream bank material also falls within this range. These data, along with inspection of Figures A66 and A68, suggest that both the banks and the tributary contribute to the material in the habitat bar, although it is not possible to say which contributes the most despite the two Figures appearing to show that it is the upstream banks that do so.

Table 5 also shows that 99.06% of a non-habitat bar is composed of material in the range 0.063-8mm at both the GSR-scale and the SR-scale. The upstream tributary can potentially contribute up to 28.46% in the same range and also at both scales of comparison. The difference is that the upstream bank sources of sediment only operate at the GSR-scale, with 84.42% of these sediments in the range 0.063-8mm potentially contributing to the bar. In a similar fashion, 74.07% of the sediment in a non-habitat island is composed of materials in the range 0.063-42mm at both the GSR-scale and the SR-scale, whilst 93.62% of the sediments from the upstream tributary can potentially contribute to this island over the same size range and at both scales of comparison. 85.58% of the material in the upstream banks at the GSR-scale can potentially contribute to the island in the range 0.063-32mm. These data, along with an examination of Figures A67 and A69, suggest that the sediments in the upstream banks contribute more to the non-habitat bar, whilst the sediments of the upstream tributary contribute more to the non-habitat island. Given the nature of the data, however, it is not possible to make such a statement with any conviction since it is impossible to quantify the absolute contributions from each potential source to each potential sink.

GSR2 & SR3

Table 5 shows that 99.5% of the habitat bar sediments occur in the range 0.063-5.6mm at both the GSR-scale and the SR-scale, with 82.13% of the upstream bank sediments at the GSR-scale also falling within this range and 94.32% of the upstream bank sediments at the SR-scale occurring in the range 0.063-4mm. 95.73% of the non-habitat bar is composed of sediments in the range 0.063-16mm at both the GSR-scale and the SR-scale, whilst 88.71% of the upstream bank sediments fall within this range at the GSR-scale and 95.05% of the upstream bank sediments occur from 0.063-5.6mm at the SR-scale. These data, along with Figures A70 to A73, all suggest that the upstream banks contribute significantly to the composition of the habitat and non-habitat bars, although it is not possible to tell whether the relationship is more significant at the SR-scale or the GSR-scale.

GSR2 & SR4

Along with Figure A74, Table 5 suggests that a significant proportion of the non-habitat bar material comes from the upstream eroding banks. It can be seen that 96.08% of the sediments in the bar occur in the range 0.063-5.6mm, whilst 87.88% of the sediments in the upstream banks also occur in the same range. Figure A74 shows that the two grain size distribution curves match very closely.

GSR2&3 and SR5

Table 5 shows that 97.51% of the material in the non-habitat bars is composed of sediments in the range 0.063-5.6mm, whilst 89.78% of the upstream bank sediments also occur in the same range. At the sampling reach-scale, the 1st coupling shows that 99.25% of the non-habitat bar is comnposed of material in the range 0.063-2mm, with 92.02% of the upstream bank sediments also falling in the same range. The 2nd coupling shows that 95.76%of the non-habitat bar is in the range 0.063-5.6mm and that 88.99% of the upstream bank sediments are in the range 0.063-4mm. These data, along with an examination of Figures A75 to A77, suggest that the banks contribute a significant proportion of the material found in the bars. Figures A76 and A77 seem to suggest that the bar-bank coupling is slightly stronger at the SR-scale than at the GSR-scale, although it is not possible to ascertain the absolute contributions from the banks in the sampling reach and those further upstream in GSRs 2 and 3.

Table 5: Gavins Point Reach - The fraction of the grain size distribution found in banks and tributaries that can possibly contribute to bar and island formation, along with the size range over which this fraction occurs.

Sampling Reach-Scale Analysis				
	Habitat bars	**Non-habitat bars & islands**	**Upstream banks**	**Upstream tributary**
SR1	99.56% (0.063-16mm)	99.36% (0.063-16mm)	86.50% (0.063-16mm)	
SR2 (1st coupling)	99.61% (0.063-8mm)		82.28% (0.063-8mm)	28.46% (0.063-8mm)
SR2 (2nd coupling - 1st)		99.06% (0.063-8mm)		28.46% (0.063-8mm)
SR2 (2nd coupling - 2nd)		74.07% (0.063-42mm)		93.62% (0.063-42mm)
SR3 (1st coupling)	99.50% (0.063-5.6mm)		94.39% (0.063-4mm)	
SR3 (2nd coupling)		95.73% (0.063-16mm)	95.05% (0.063-5.6mm)	
SR5 (1st coupling)		99.25% (0.063-2mm)	92.02% (0.063-2mm)	
SR5 (2nd coupling)		95.76% (0.063-5.6mm)	88.99% (0.063-4mm)	
Geomorphically Similar Reach-Scale Analysis				
	Habitat bars	**Non-habitat bars & islands**	**Upstream banks**	**Upstream tributary**
GSR1 & SR1	99.56% (0.063-16mm)	99.36% (0.063-16mm)	85.66% (0.063-16mm)	
GSR1 & SR2 (1st coupling)	99.61% (0.063-8mm)		84.48% (0.063-8mm)	28.46% (0.063-8mm)
GSR1 & SR2 (2nd coupling - 1st)		99.06% (0.063-8mm)	84.42% (0.063-8mm)	28.46% (0.063-8mm)
GSR1 & SR2 (2nd coupling - 2nd)		74.07% (0.063-42mm)	85.58% (0.063-32mm)	93.62% (0.063-42mm)
GSR2 & SR3 (1st coupling)	99.50% (0.063-5.6mm)		82.13% (0.063-5.6mm)	
GSR2 & SR3 (2nd coupling)		95.73% (0.063-16mm)	88.71% (0.063-16mm)	
GSR2 & SR4		96.08% (0.063-5.6mm)	87.88% (0.063-5.6mm)	
GSR2&3 & SR5		97.51% (0.063-5.6mm)	89.78% (0.063-5.6mm)	

Summary of Results

Fort Peck Reach

Of the 16 Geomorphically Similar Reach and Sampling Reach comparisons examined in this reach, all of them were found to suggest that the bank sediments could potentially contribute a significant amount of material to the habitat and non-habitat bars and islands. And of these, seven were shown to imply a strong degree of linkage between the bar or island and the bank sources in the immediate upstream vicinity. It should be borne in mind that because we have not been comparing absolute amounts of material, even a relatively small percentage value for a bank grain size range could still equate to a very large tonnage of bank material – easily enough to account for the formation of a bar or island. Furthermore, in five of the comparisons, tributaries or arroyos were found to potentially account for a significant proportions of the bar and island material.

Garrison Reach

All seven of the GSR and SR comparisons showed that bank material could potentially contribute a significant proportion of material to the bars and islands. Of these, one suggested a particularly strong bar-bank coupling at the sampling reach-scale and four suggested that both banks, tributaries and arroyos could contribute material to the bars and islands.

Fort Randall Reach

Of the six GSR and SR relationships examined, four suggested that banks could contribute significantly to the bar and island material. Two of these also showed that an arroyo and tributary could contribute significantly to the depositional features also. One comparison showed that the bars were probably composed entirely of material from a tributary.

Gavins Point Reach

Of the five GSR and SR relationships examined, all five showed that banks could potentially contribute a significant amount of material to the bars and islands. In addition, one of these showed that a tributary was also a potentially significant source of bar and island material.

Conclusions

Although it is not possible to say categorically that the habitat and non-habitat bars and islands are made up largely of sediments from the upstream eroding banks, the evidence presented in this report strongly suggests that this is the case. In each of the four main study reaches, numerous strong correlations were found between the bar and island sediments and those in the banks. Furthermore, the evidence also suggests that in each of the reaches, tributaries and arroyos make a significant, albeit less so than the banks, contribution to the material in the bars and islands.

These findings are the first step towards developing a comprehensive sediment budget for the Upper Missouri River. In order to complete the budget it will be necessary to compute some absolute values for the amounts of sediment being moved and stored in the system. The figures in this report provide the proportions of material being provided by the various potential sediment sources. It will be necessary to combine these with erosion rate data to in order to obtain the absolute amounts. These data will be provided once the banklines and in-channel features of the Missouri River have been digitised and combined with figures describing bank, bar and island heights. This task is currently scheduled to be completed in the next phase of the study.

Part VII -

Appendix A: Grain Size Plots

Figure A1: Fort Peck Reach - Comparison of non-habitat bars in Sampling Reach 1 with potential upstream bank, tributary and arroyo sources of sediment in Geomorphically Similar Reach 1

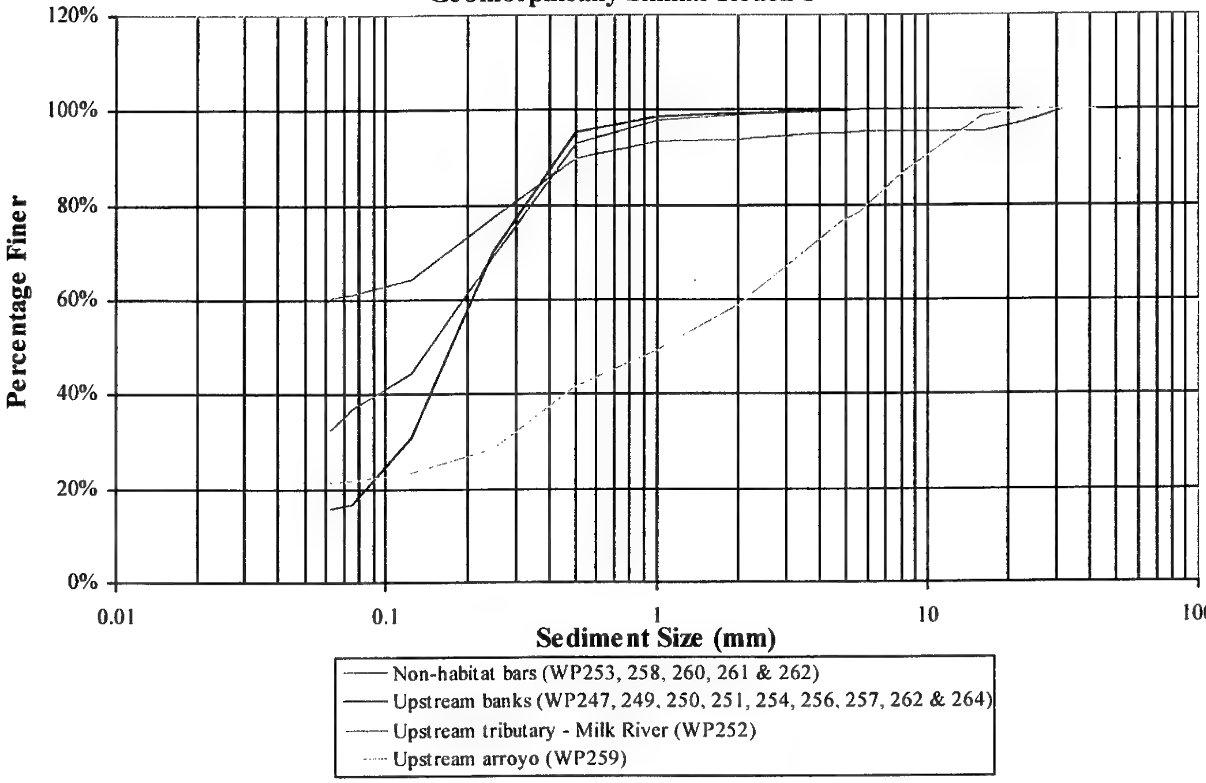

Figure A2: Fort Peck Reach - First comparison of non-habitat bar in Sampling Reach 1 with potential upstream bank and tributary sources of sediment

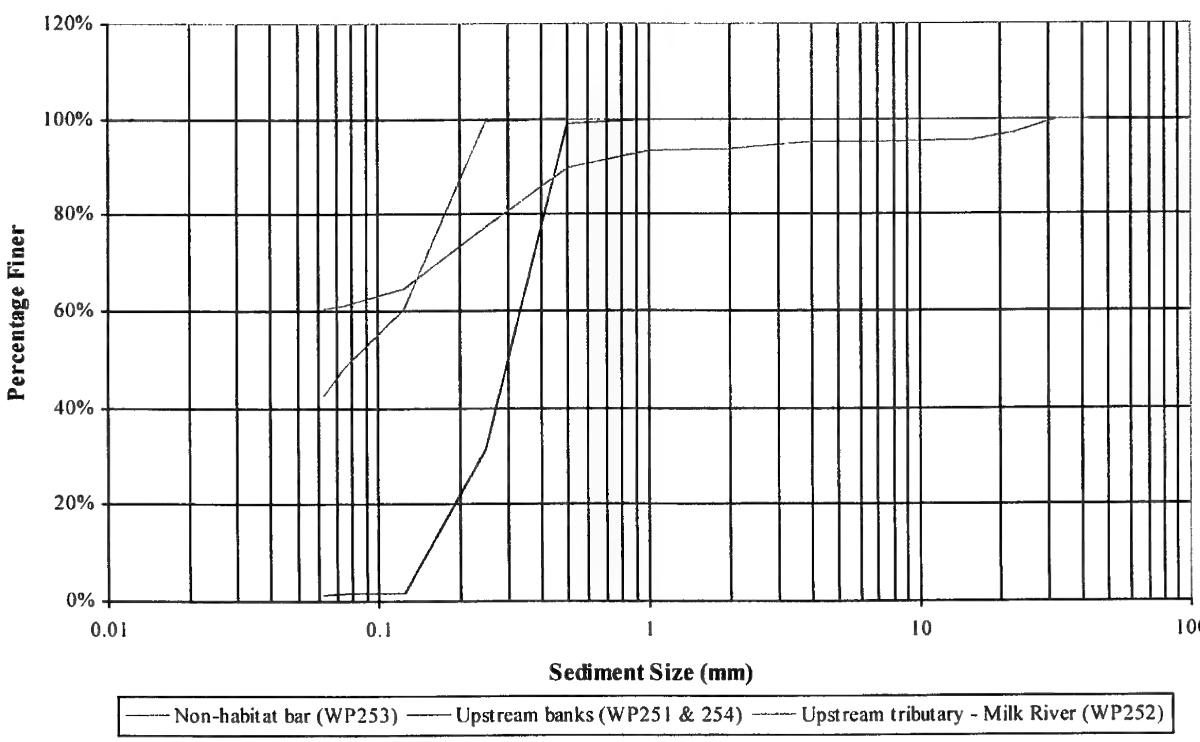

Figure A3: Fort Peck Reach - Second comparison of non-habitat bar in Sampling Reach 1 with potential upstream bank and tributary sources of sediment

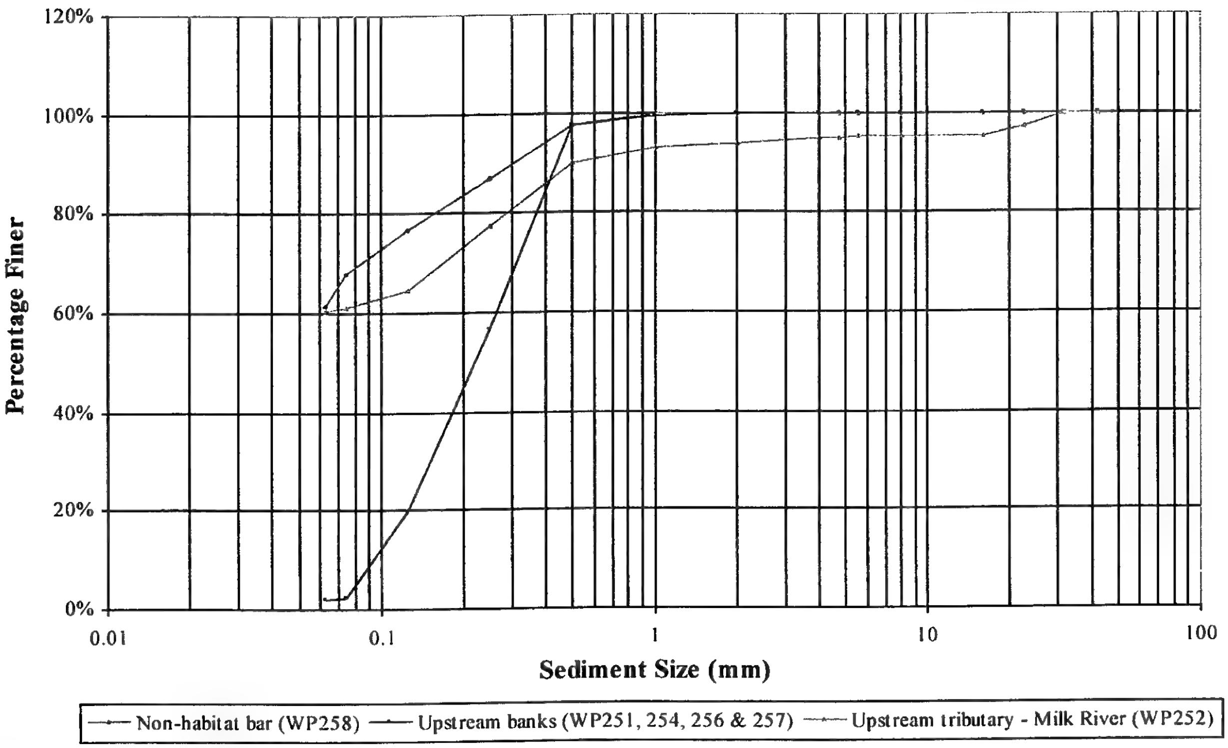

Figure A4: Fort Peck Reach - Third comparison of non-habitat bars in Sampling Reach 1 with potential upstream bank, tributary and arroyo sources of sediment

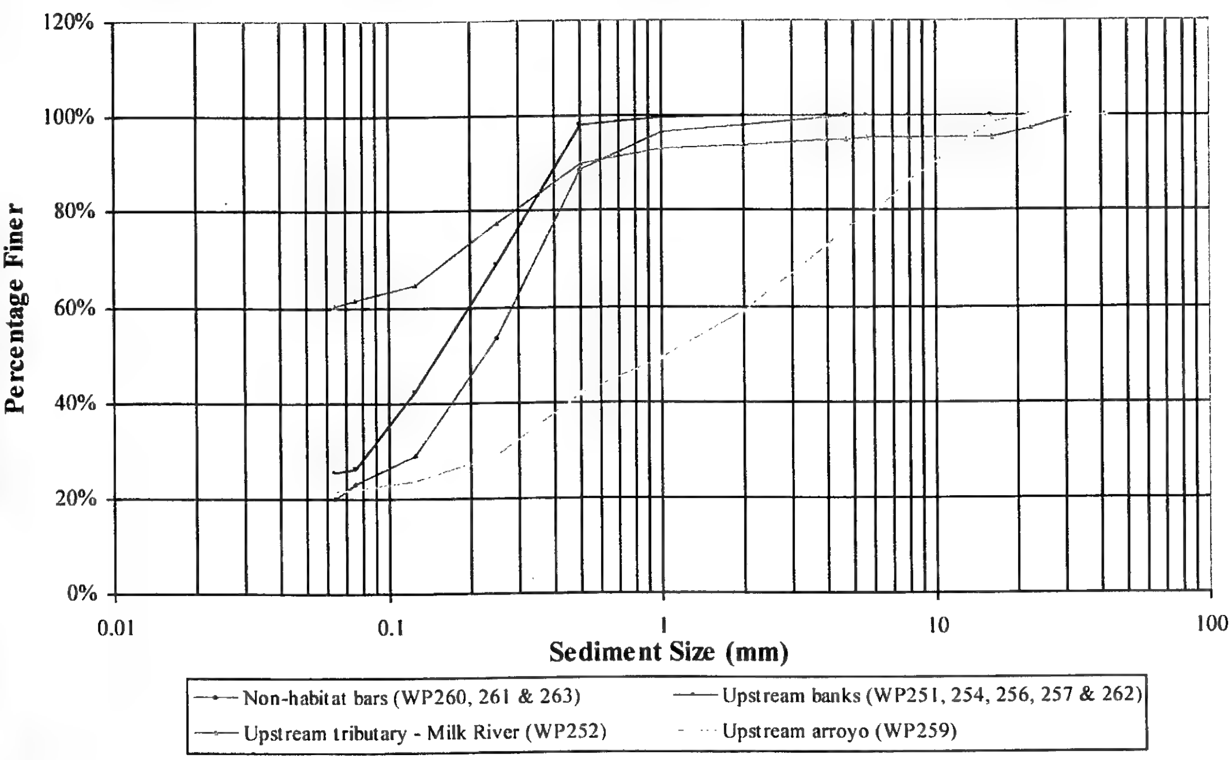

Figure A5: Fort Peck Reach - Comparison of non-habitat bars in Sampling Reach 2 with potential upstream bank and tributary sources of sediment in Geomorphically Similar Reach 2

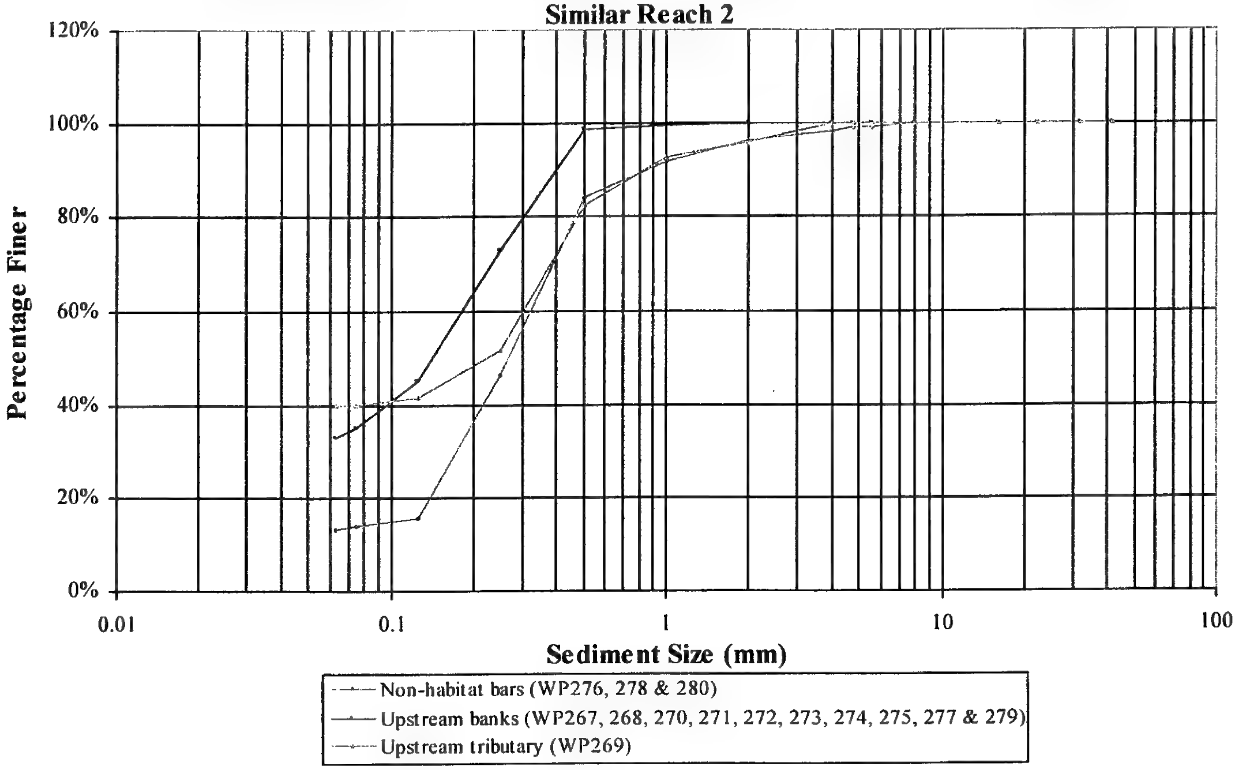

Figure A6: Fort Peck Reach - Comparison of non-habitat bars in Sampling Reach 2 with potential upstream bank sources of sediment

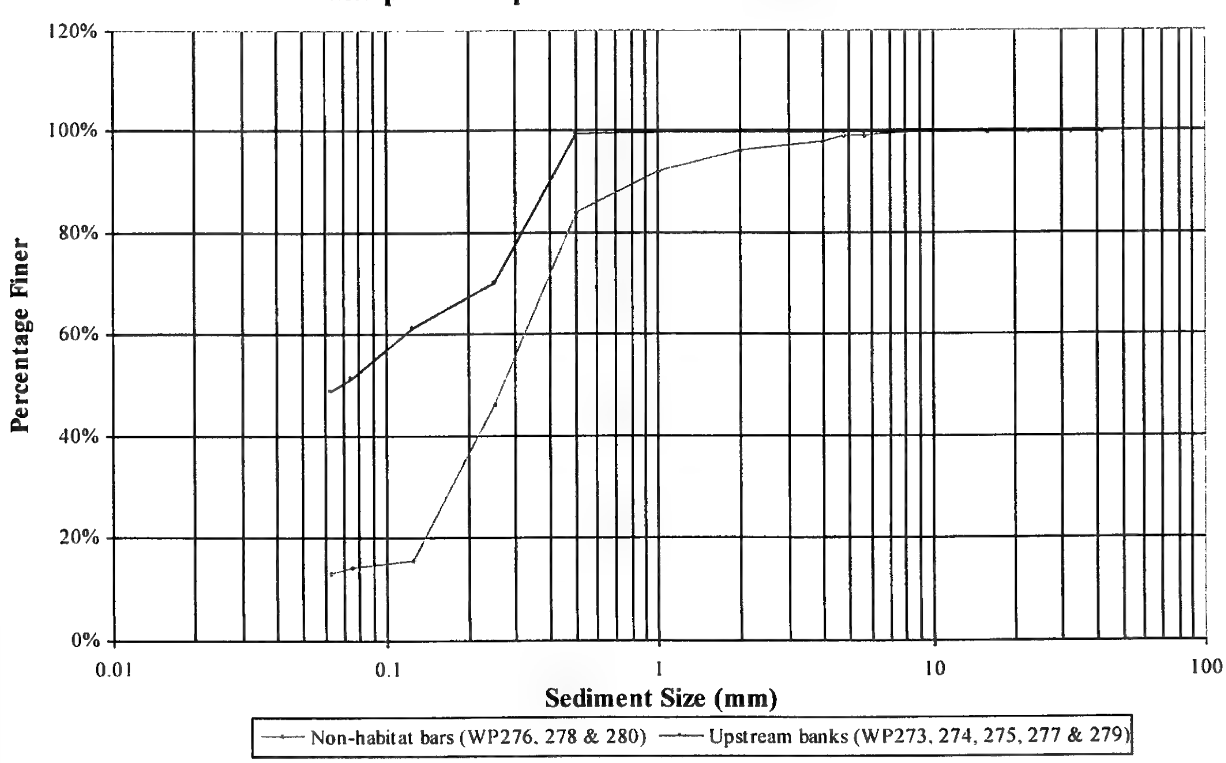

Figure A7: Fort Peck Reach - Comparison of non-habitat bars in Sampling Reach 3 with potential upstream bank, tributary and arroyo sources of sediment in Geomorphically Similar Reach 2

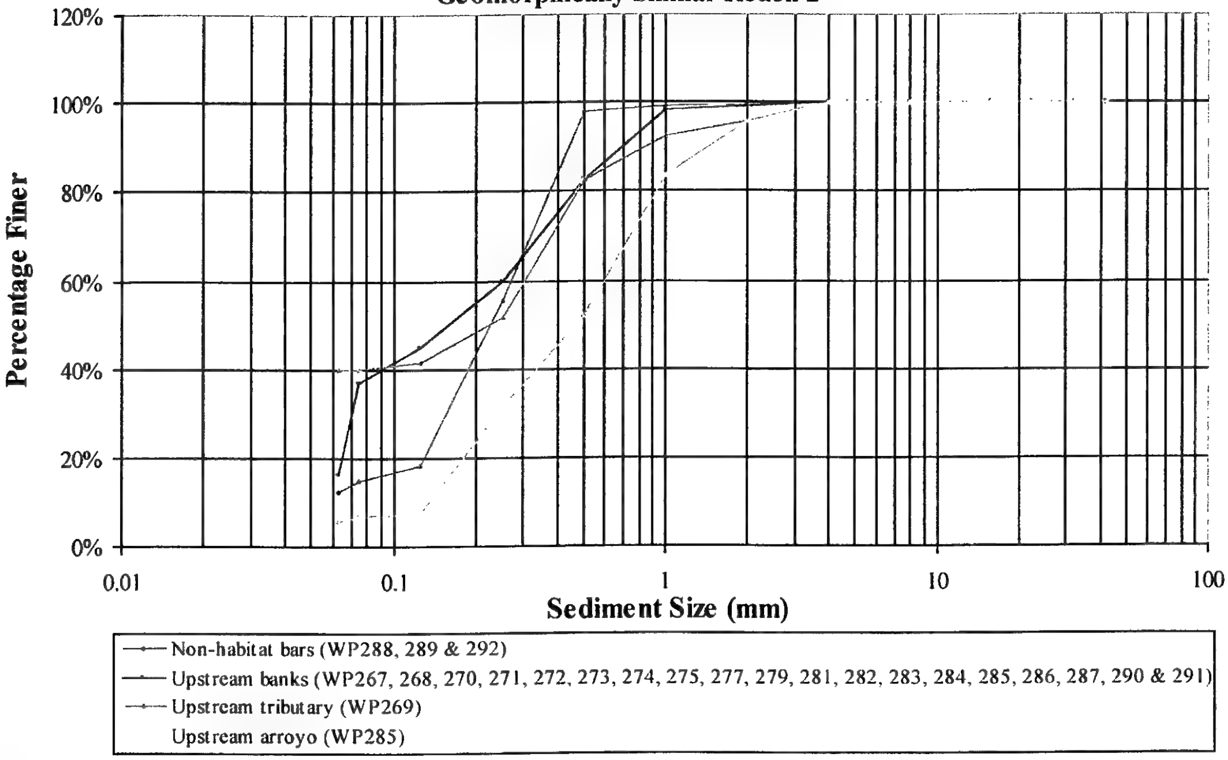

Figure A8: Fort Peck Reach - First comparison of non-habitat bars in Sampling Reach 3 with potential upstream bank sources of sediment

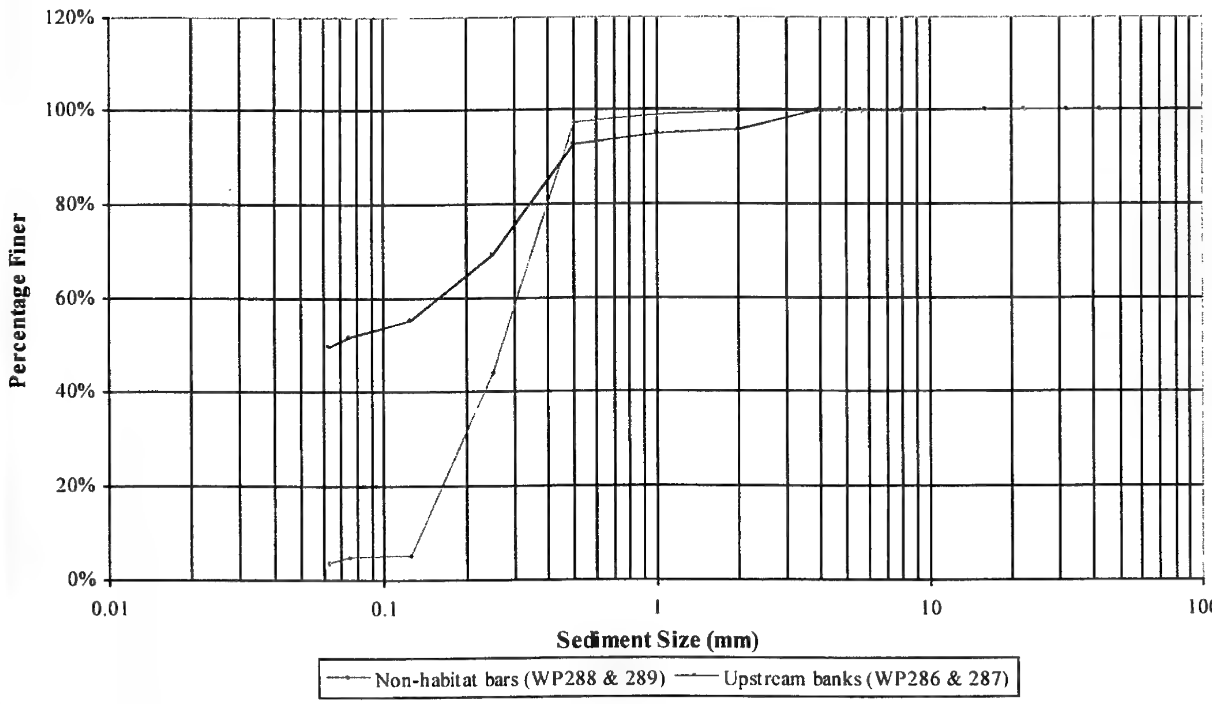

Figure A9: Fort Peck Reach - Second comparison of non-habitat bar in Sampling Reach 3 with potential upstream bank sources of sediment

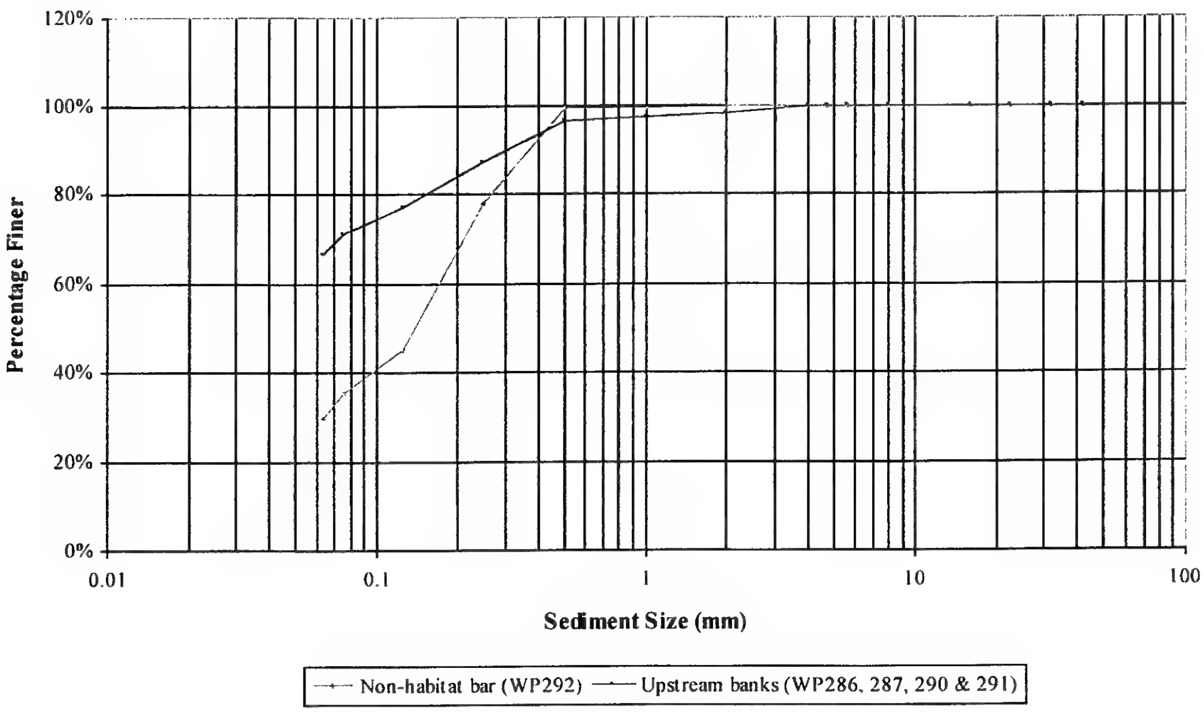

Figure A10: Fort Peck Reach - Comparison of non-habitat bar and habitat bar in Sampling Reach 4 with potential upstream bank and tributary sources of sediment in Geomorphically Similar Reach 2

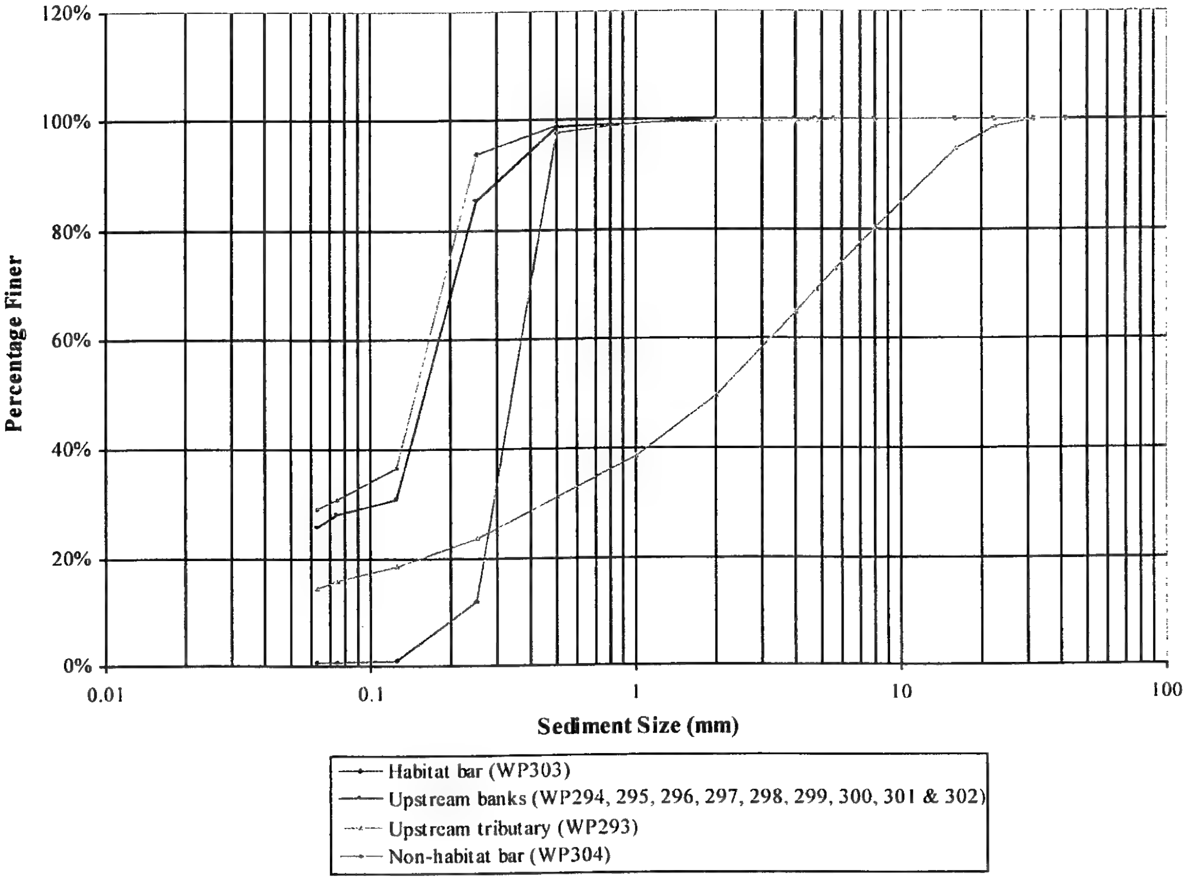

Figure A11: Fort Peck Reach - Comparison of non-habitat bars in Sampling Reach 5 with potential upstream bank sources of sediment in Geomorphically Similar Reach 3

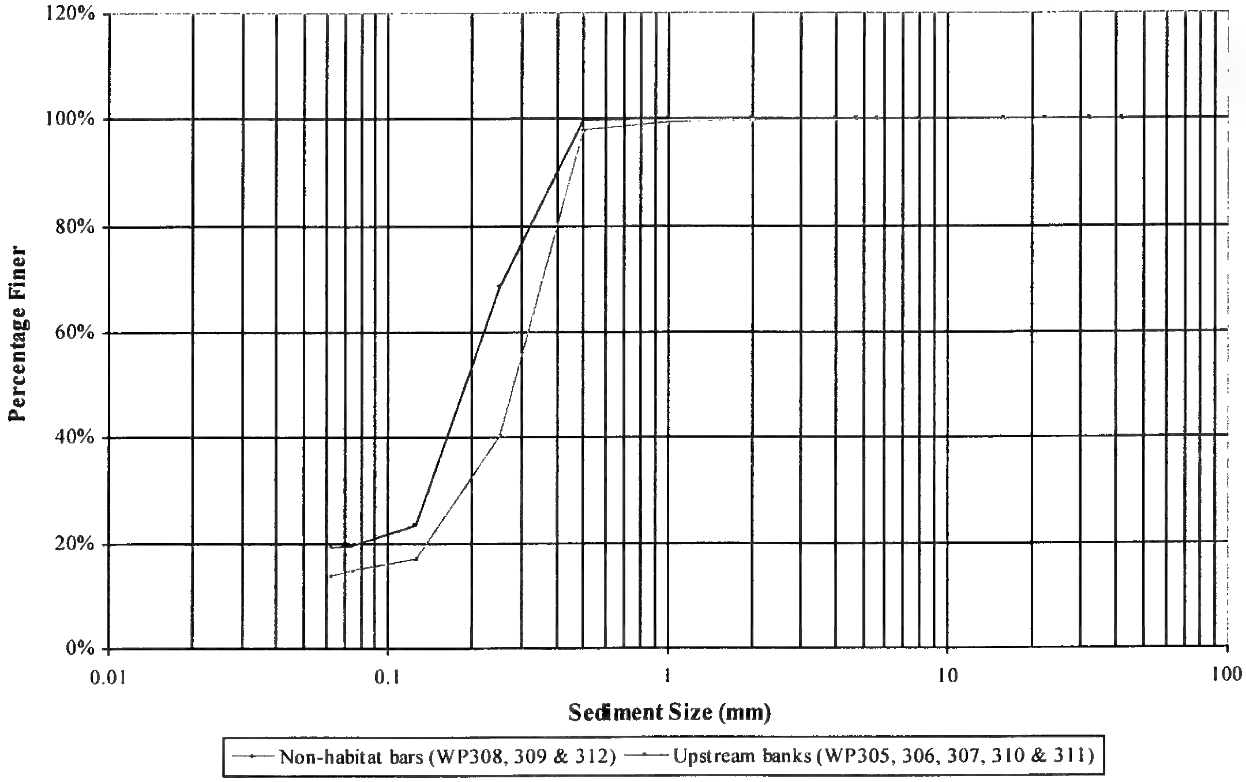

Figure A12: Fort Peck Reach - Comparison of non-habitat bar in Sampling Reach 5 with potential upstream bank sources of sediment

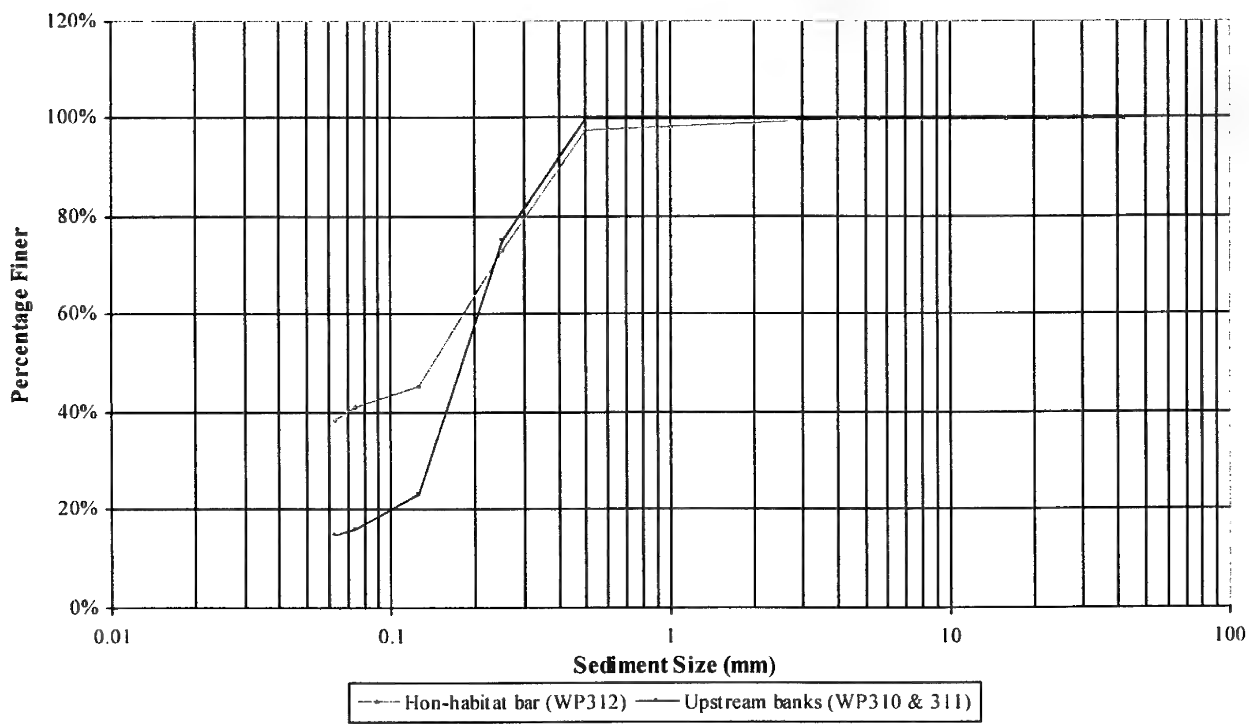

Figure A13: Fort Peck Reach - Comparison of non-habitat bars in Sampling Reach 6 with potential upstream bank sources of sediment in Geomorphically Similar Reach 4

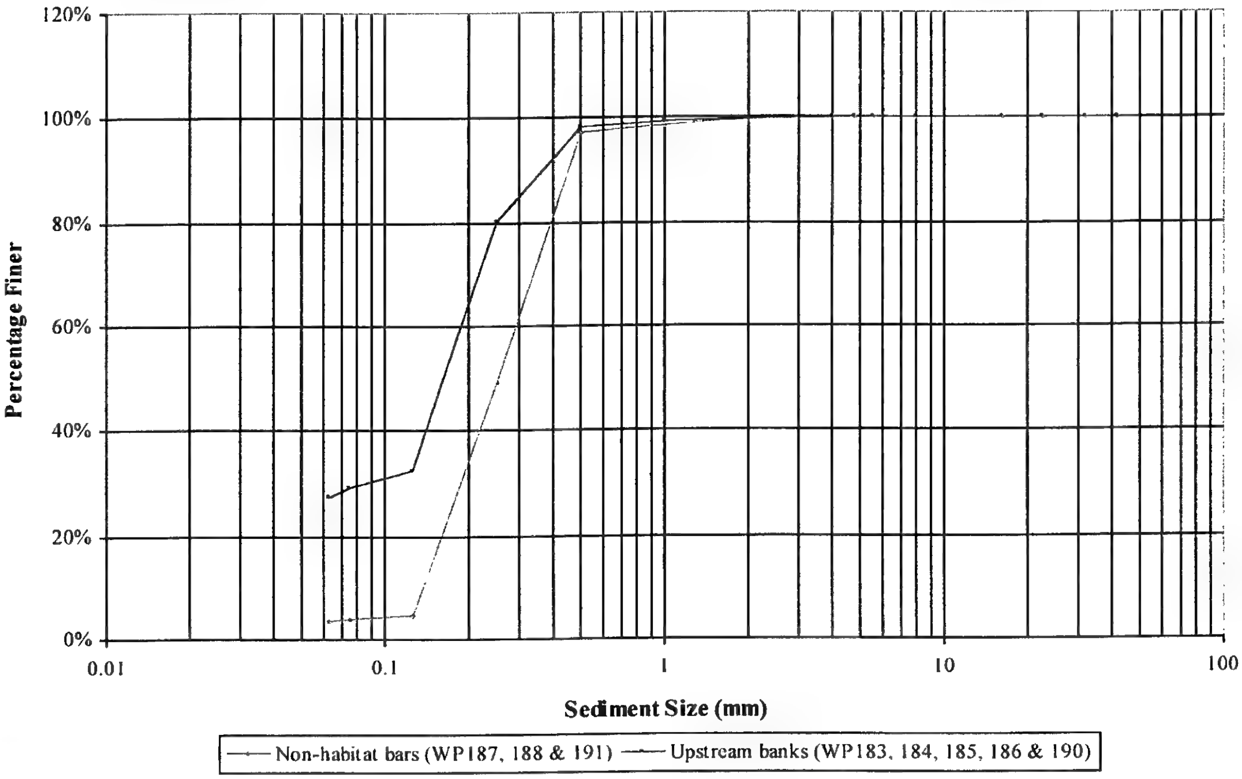

Figure A14: Fort Peck Reach - Comparison of non-habitat bar in Sampling Reach 6 with potential upstream bank sources of sediment

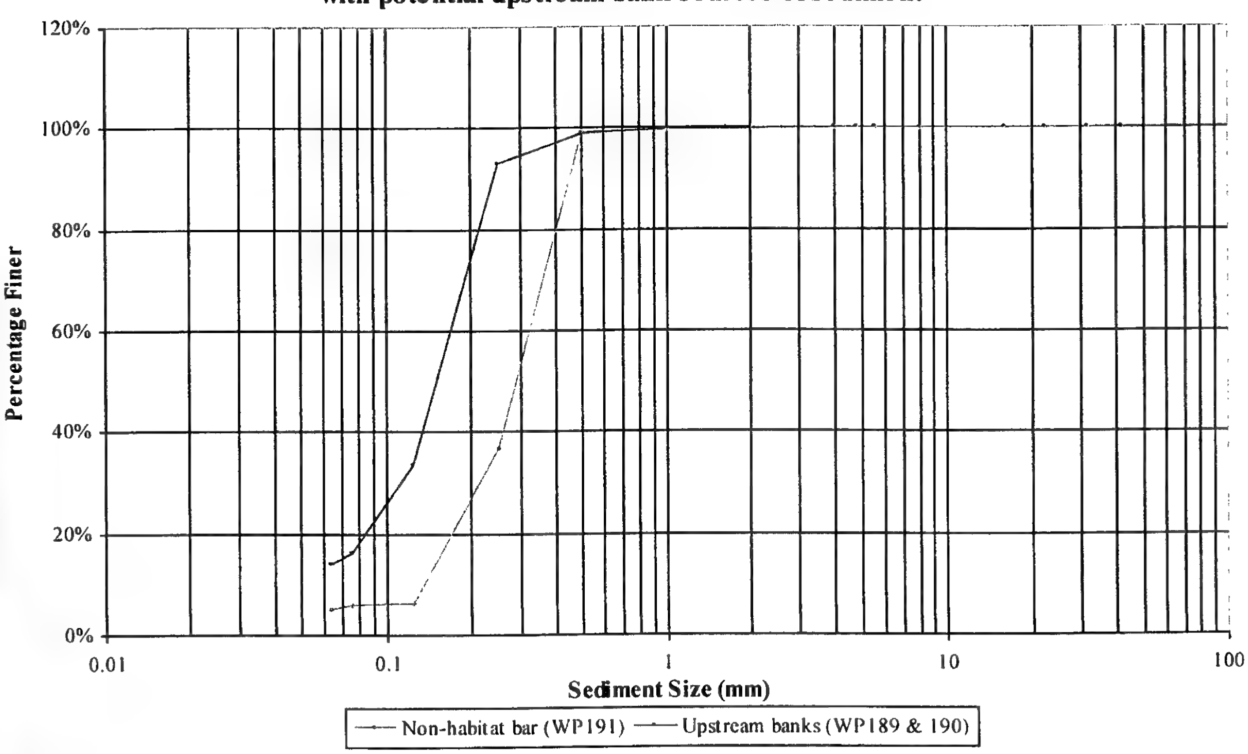

Figure A15: Fort Peck Reach - Comparison of habitat bar in Geomorphically Similar Reach 5 with potential upstream bank sources of sediment in Geomorphically Similar Reach 4

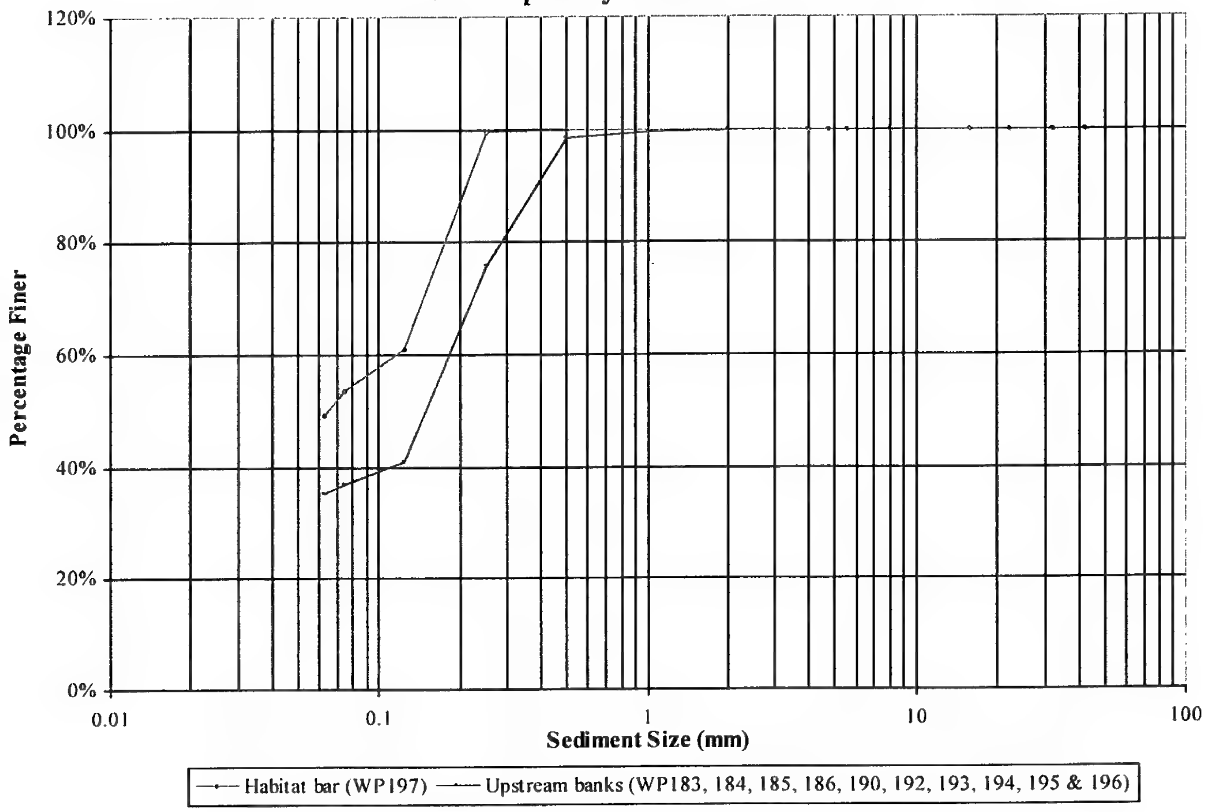

Figure A16: Fort Peck Reach - Comparison of non-habitat bars in Sampling Reach 7 with potential upstream bank and tributary sources of sediment in Geomorphically Similar Reach 5

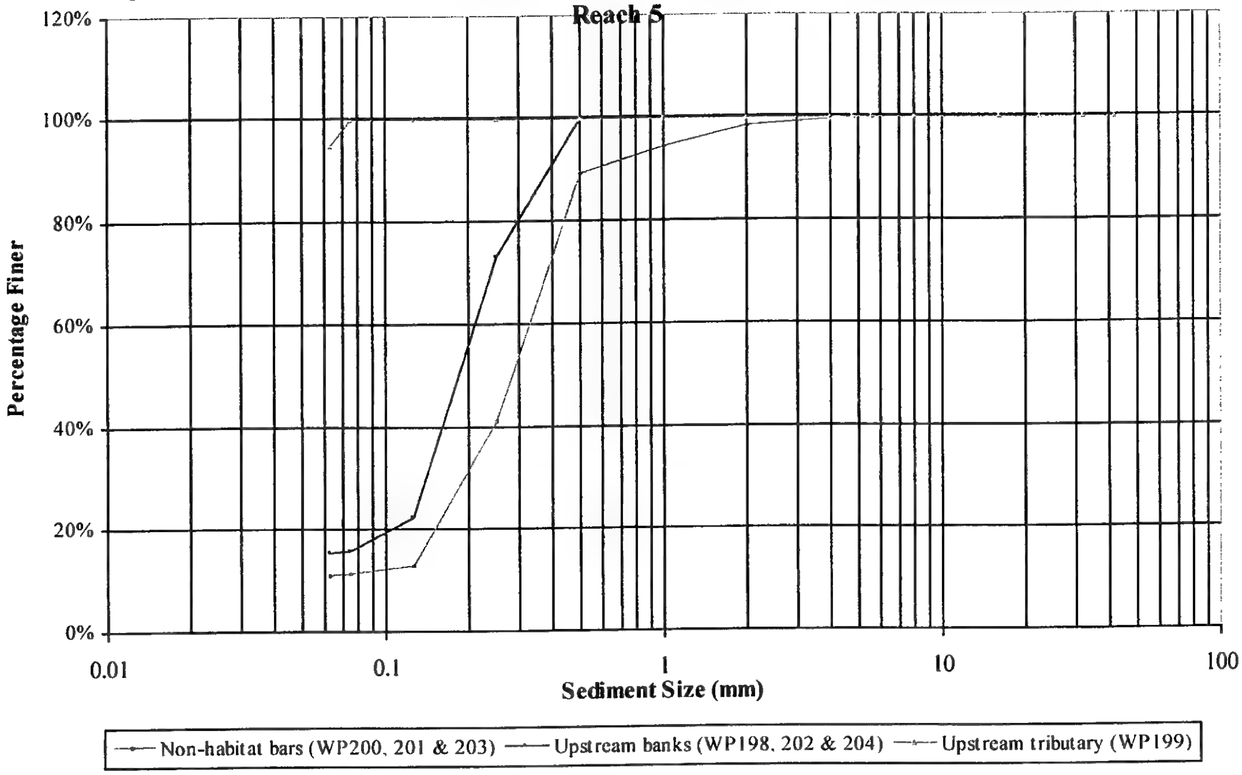

Figure A17: Fort Peck Reach - First comparison of non-habitat bars in Sampling Reach 7 with potential upstream tributary source of sediment

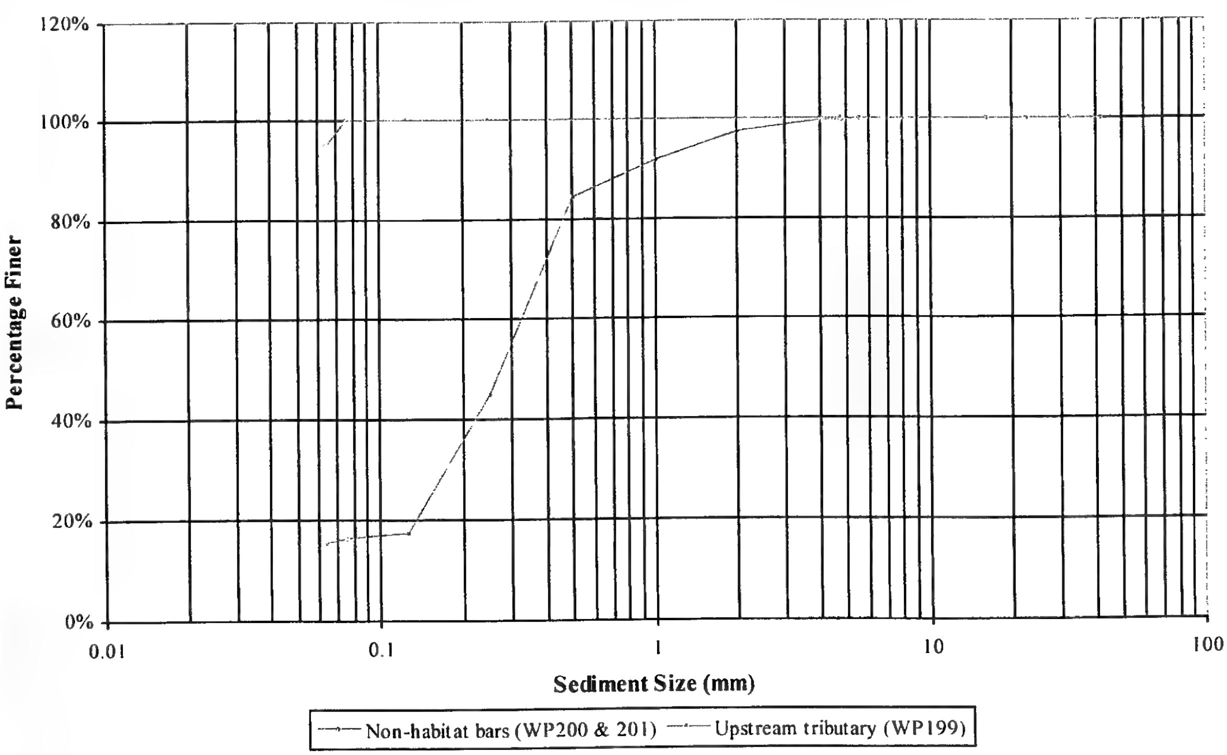

Figure A18: Fort Peck Reach - Second comparison of non-habitat bar in Sampling Reach 7 with potential upstream bank and tributary sources of sediment

Figure A19: Fort Peck Reach - Comparison of habitat bar and non-habitat bars in Sampling Reach 8 with potential upstream bank and tributary sources of sediment in Geomorphically Similar Reach 5

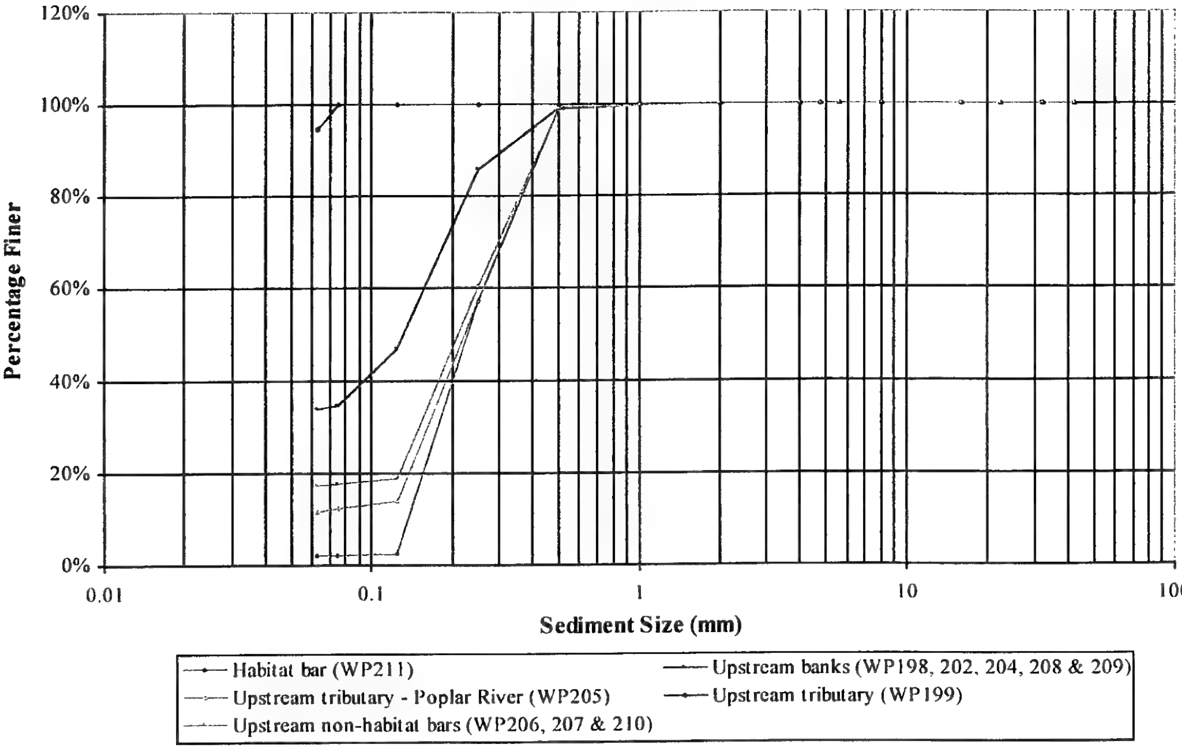

Figure A20: Fort Peck Reach - First comparison of non-habitat bars in Sampling Reach 8 with potential upstream tributary source of sediment

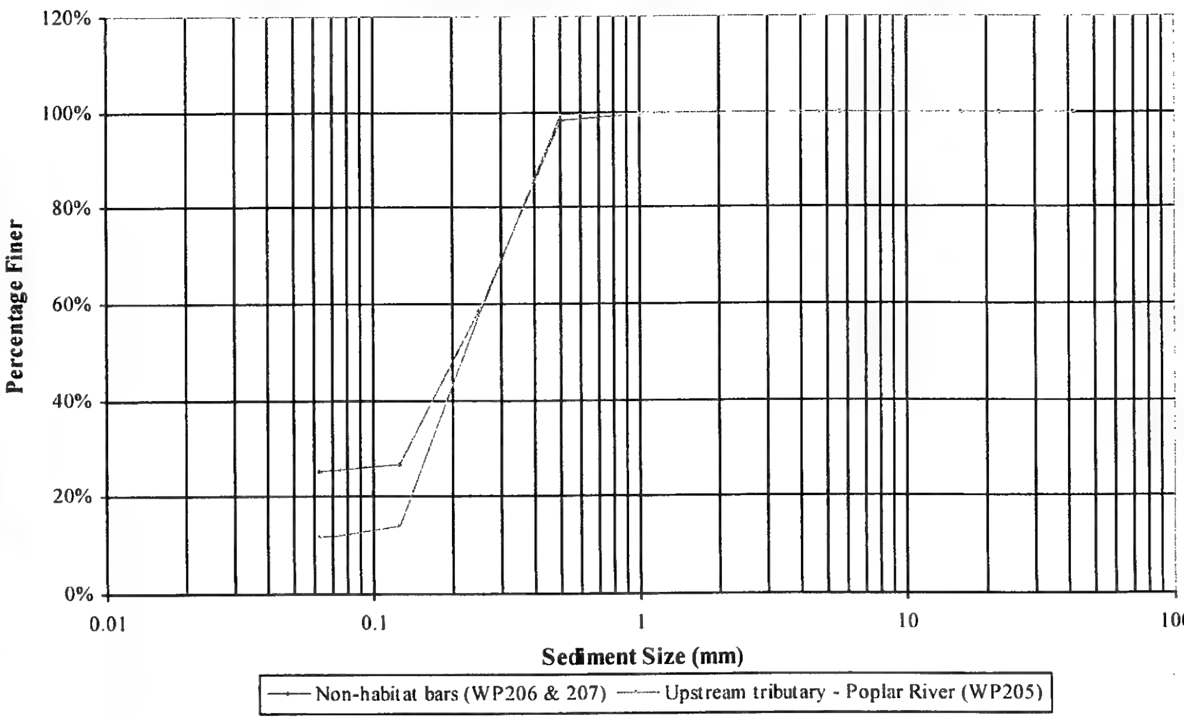

Figure A21: Fort Peck Reach - Second comparison of a habitat bar and a non-habitat bar in Sampling Reach 8 with potential upstream bank and tributary sources of sediment

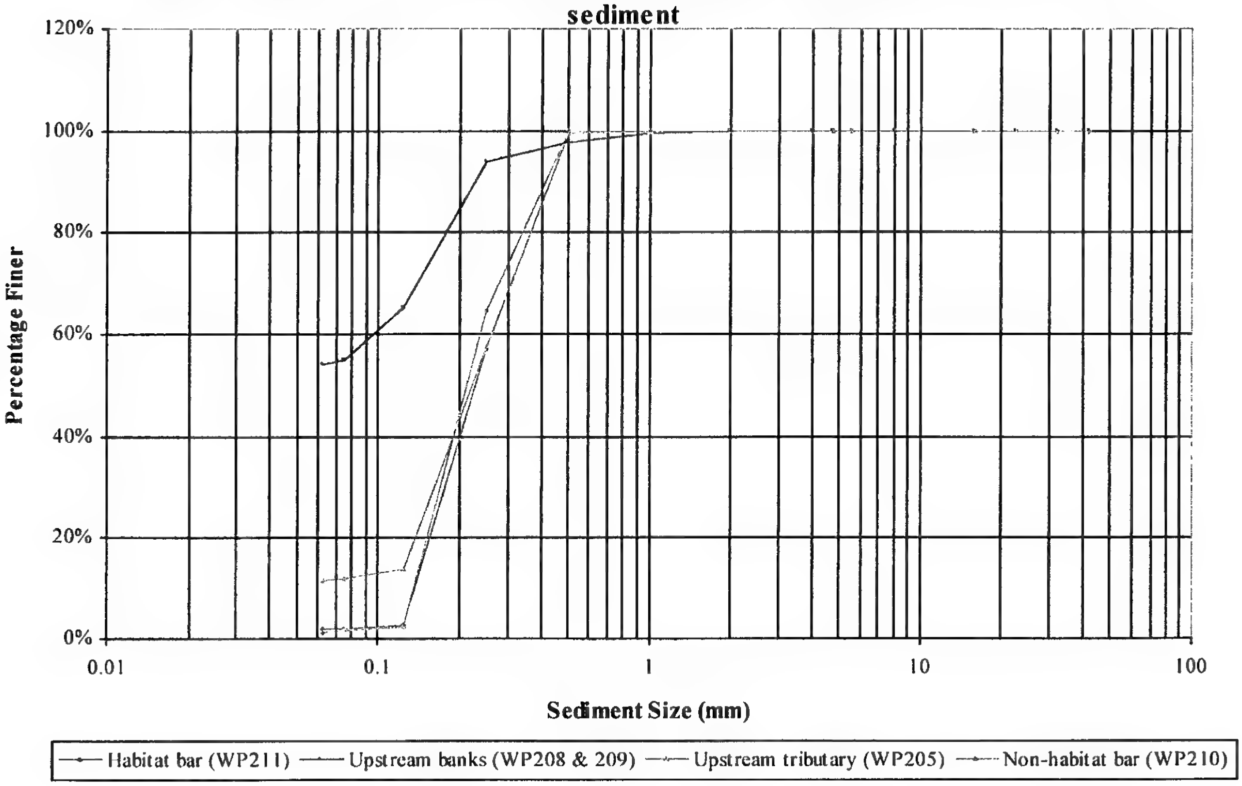

Figure A22: Fort Peck Reach - Comparison of habitat bar and non-habitat bars and island in Sampling Reach 9 with potential upstream bank, tributary and arroyo sources of sediment in Geomorphically Similar Reach 5

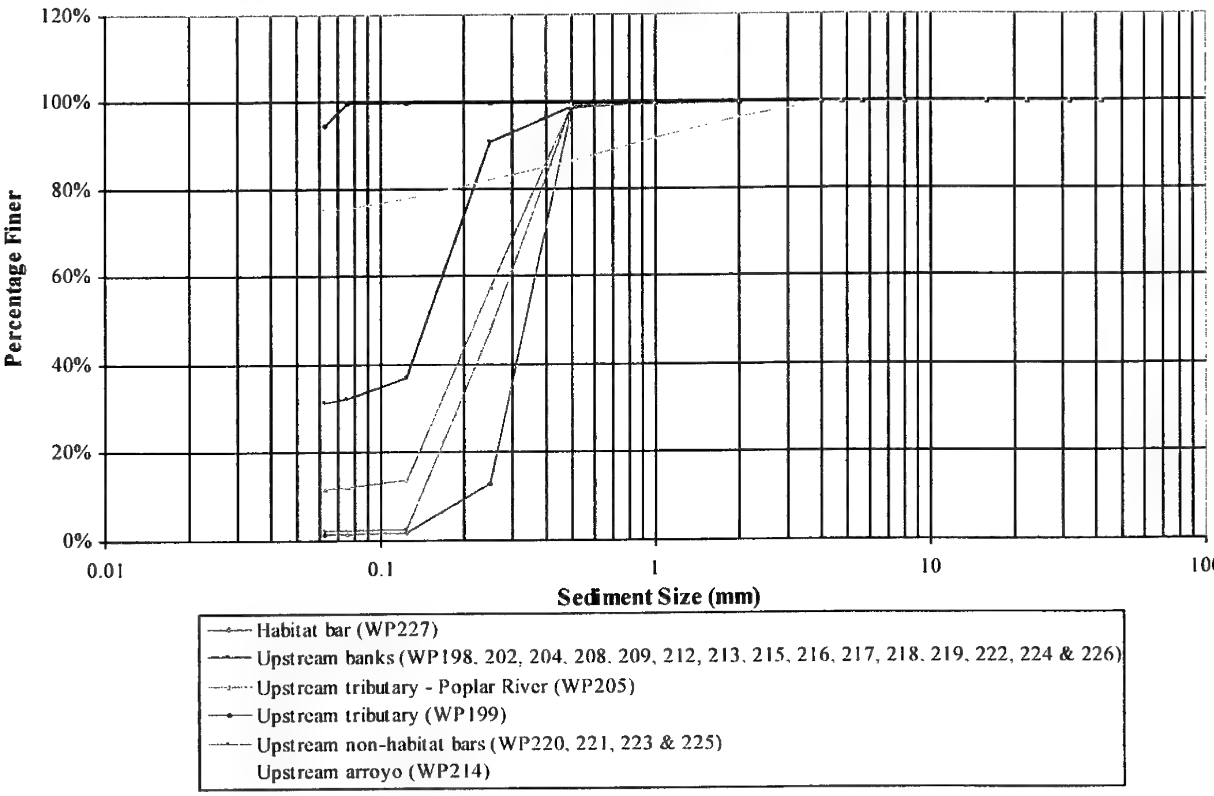

Figure A23: Fort Peck Reach - First comparison of non-habitat bars and Island in Sampling Reach 9 with potential upstream bank sources of sediment

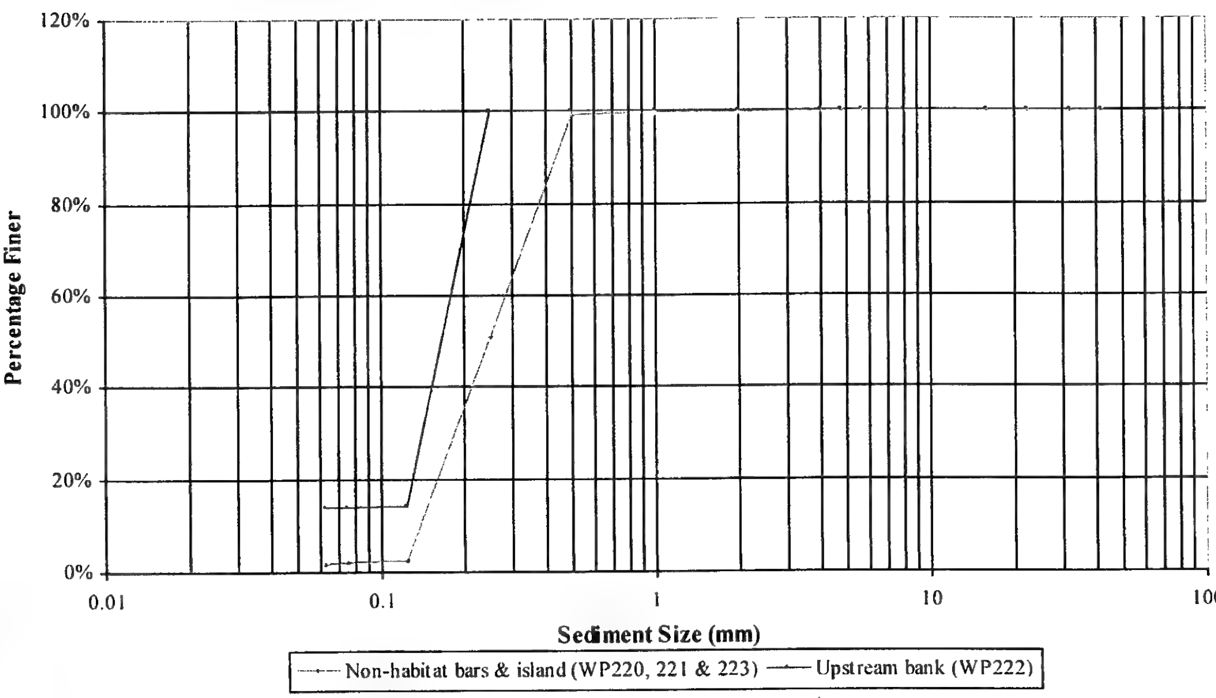

Figure A24: Fort Peck Reach - Second comparison of non-habitat bar in Sampling Reach 9 with potential upstream bank sources of sediment

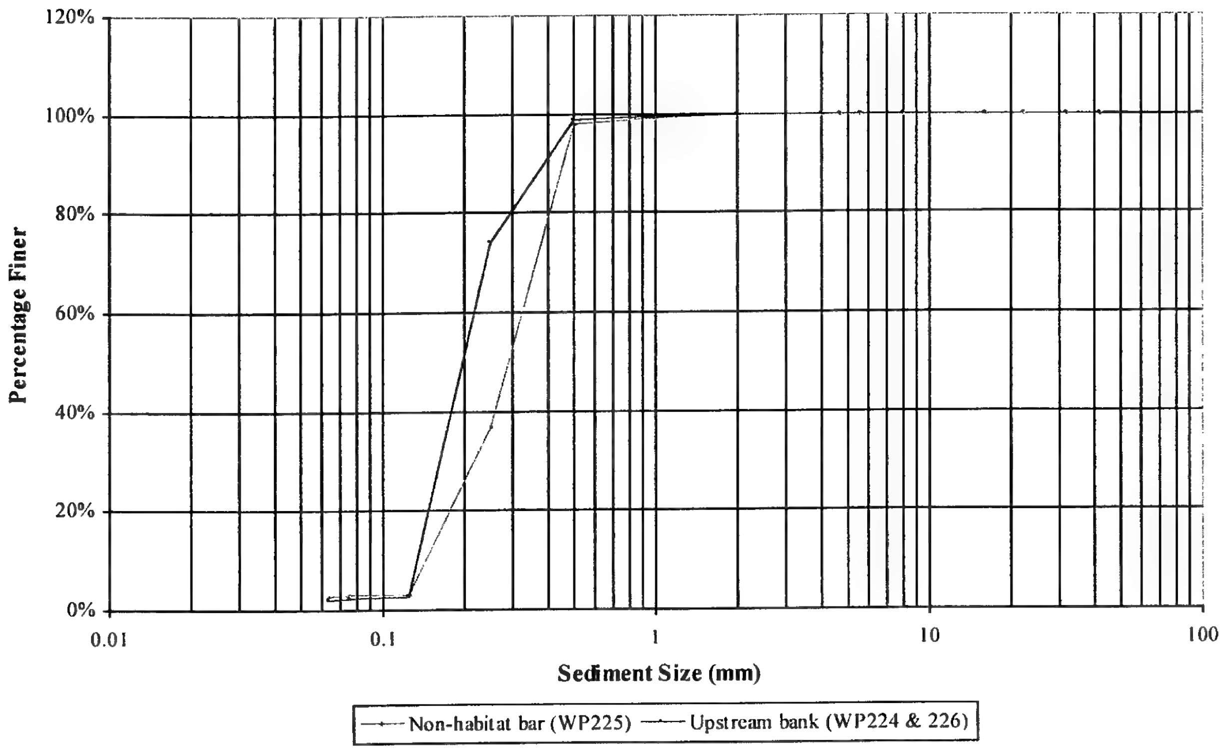

Figure A25: Fort Peck Reach - Third comparison of habitat bar in Sampling Reach 9 with potential upstream bank sources of sediment

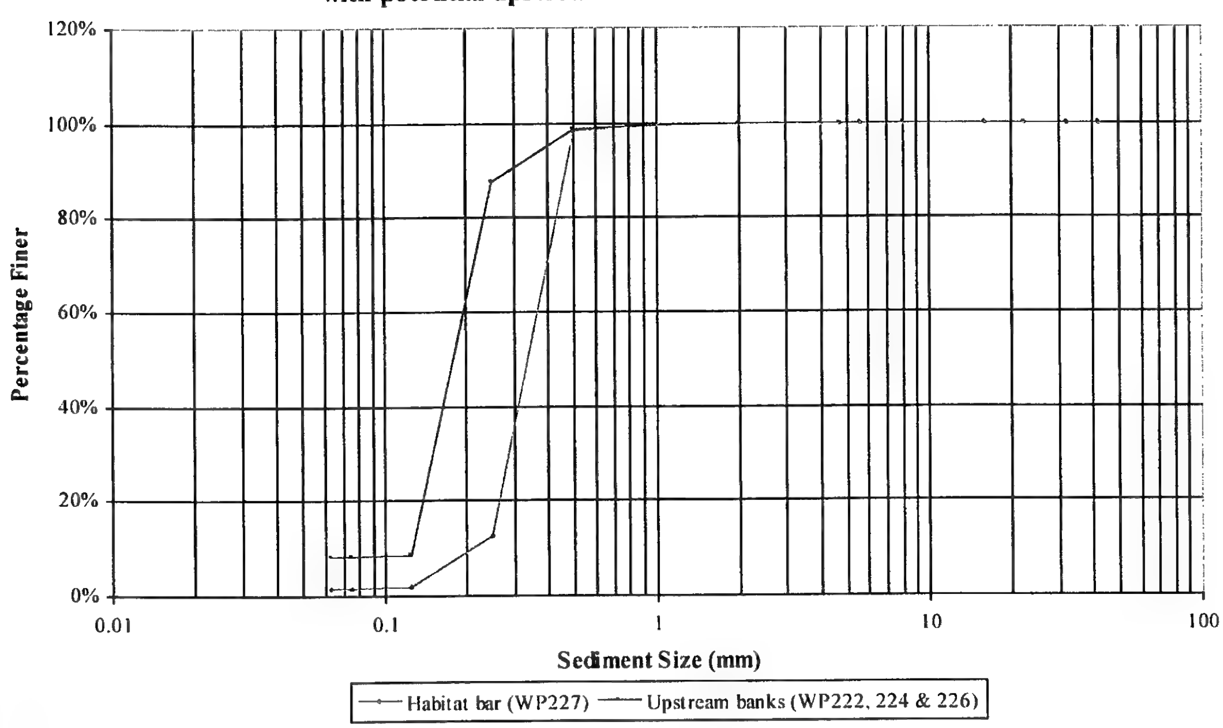

Figure A26: Fort Peck Reach - Comparison of non-habitat bars in Sampling Reach 10 with potential upstream bank sources of sediment in Geomorphically Similar Reach 5

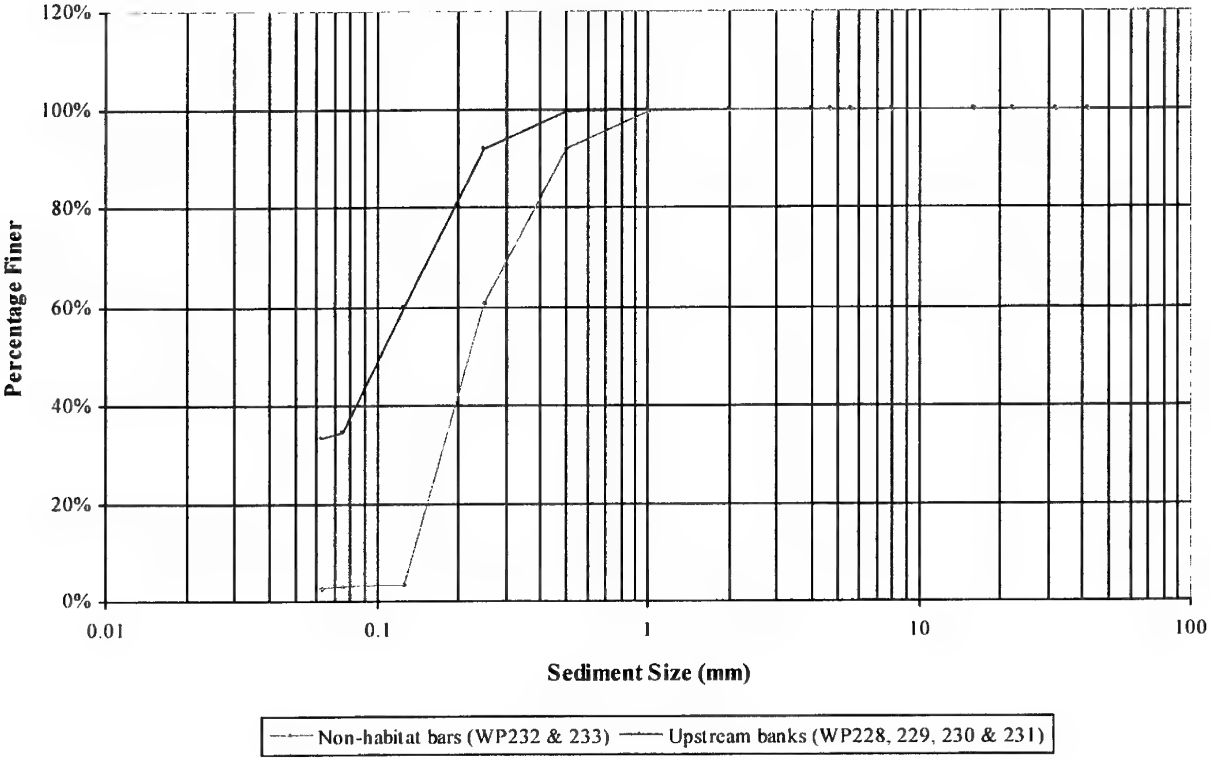

Figure A27: Fort Peck Reach - Comparison of non-habitat bars in Sampling Reach 11 with potential upstream bank and tributary sources of sediment in Geomorphically Similar Reach 6

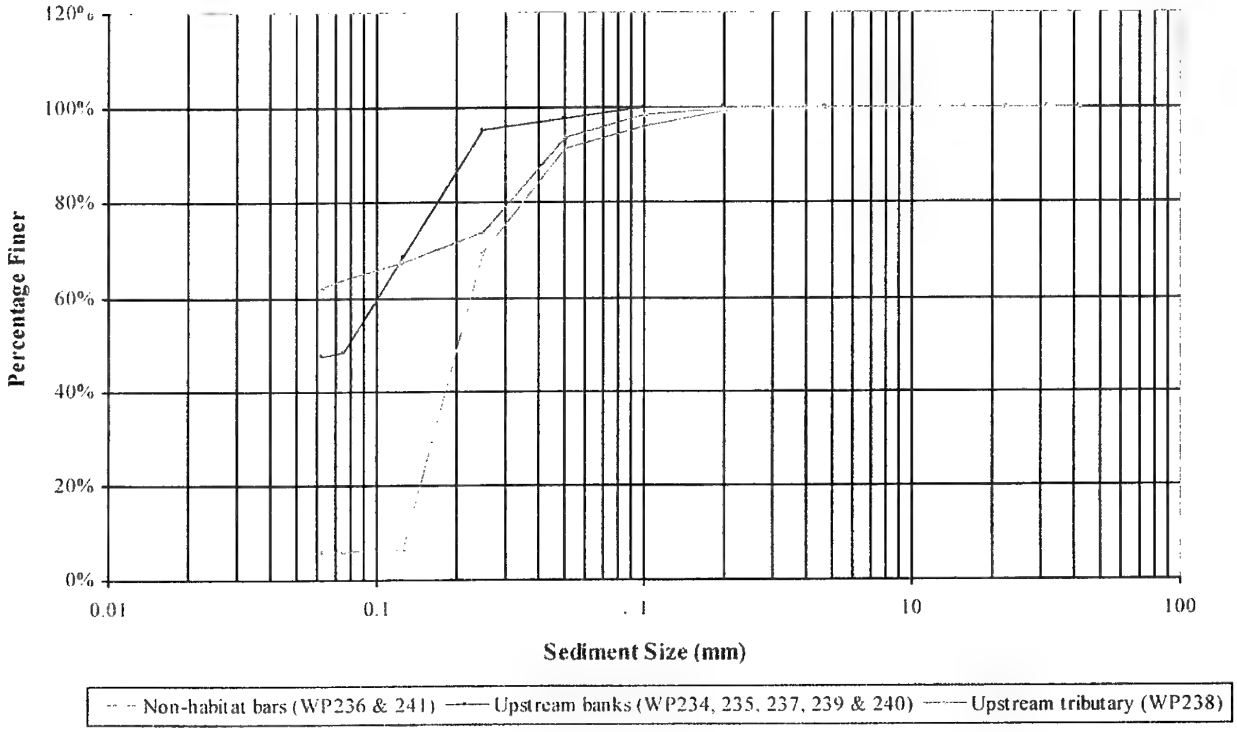

Figure A28: Fort Peck Reach - First comparison of non-habitat bar in Sampling Reach 11 with potential upstream bank source of sediment

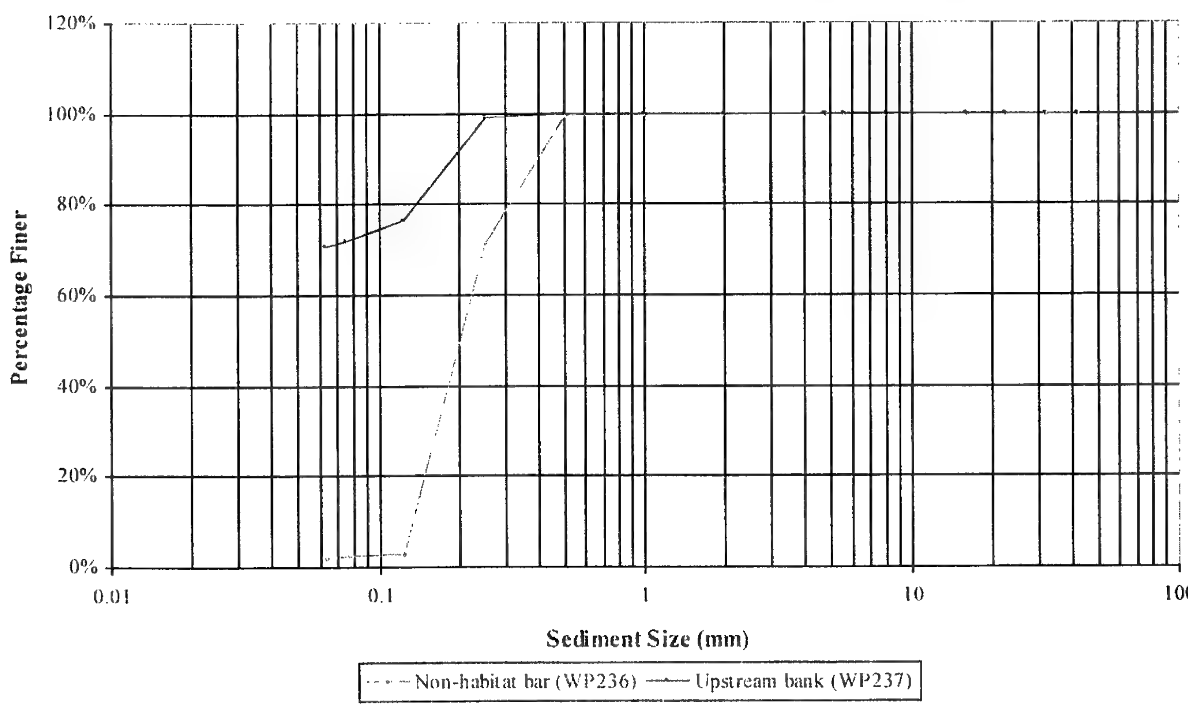

Figure A29: Fort Peck Reach - Second comparison of non-habitat bar in Sampling Reach 11 with potential upstream bank and tributary sources of sediment

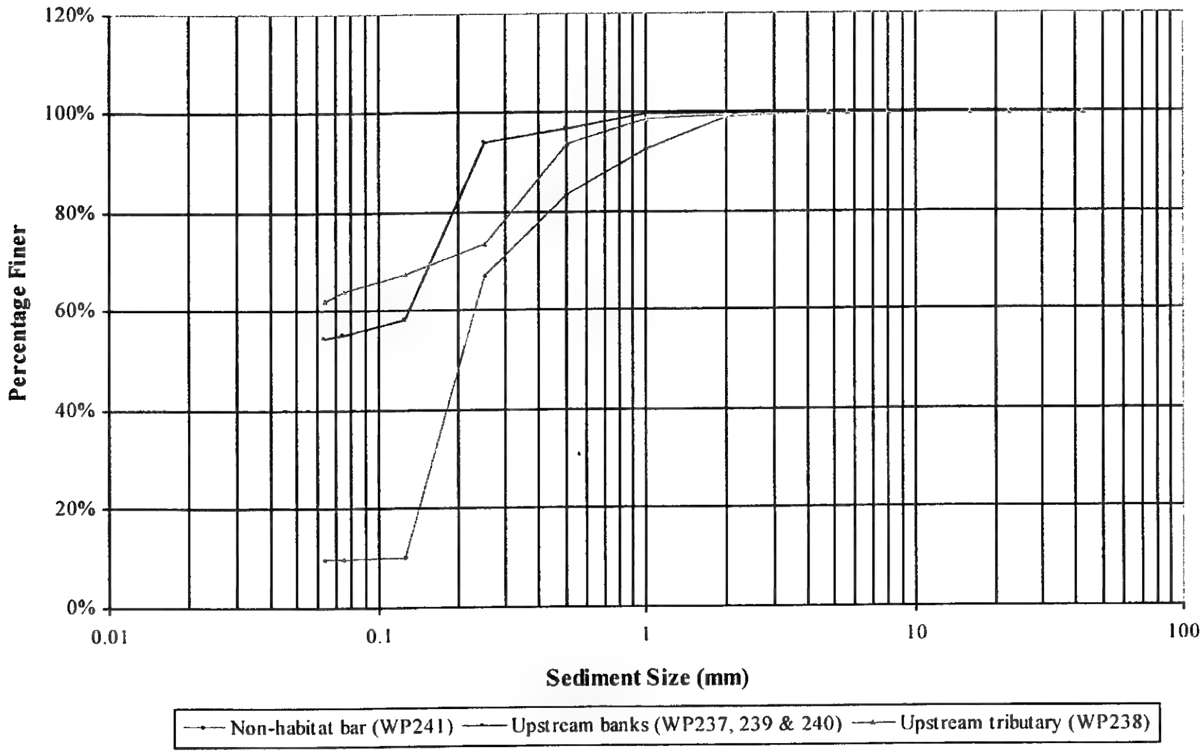

Figure A30: Fort Peck Reach - Comparison of non-habitat bars in Sampling Reach 12 with potential upstream bank and tributary sources of sediment in Geomorphically Similar Reach 6

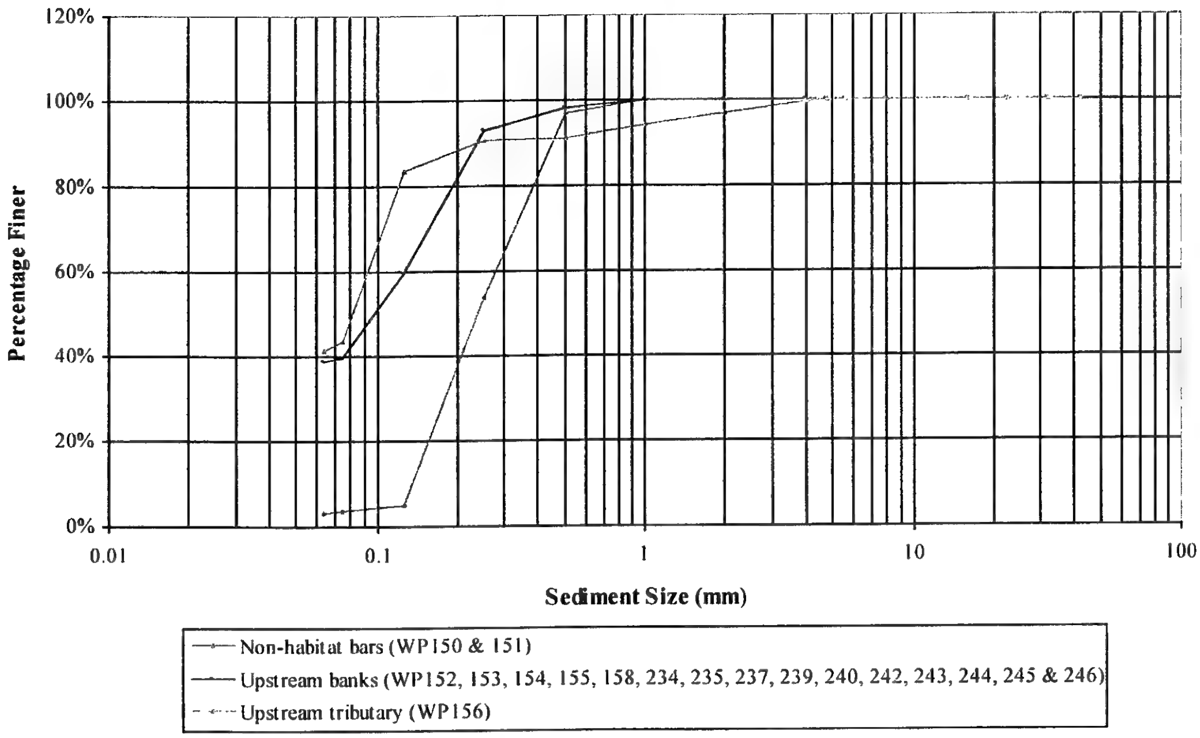

Figure A31: Fort Peck Reach - Comparison of non-habitat bars in Sampling Reach 12 with potential upstream bank and tributary sources of sediment

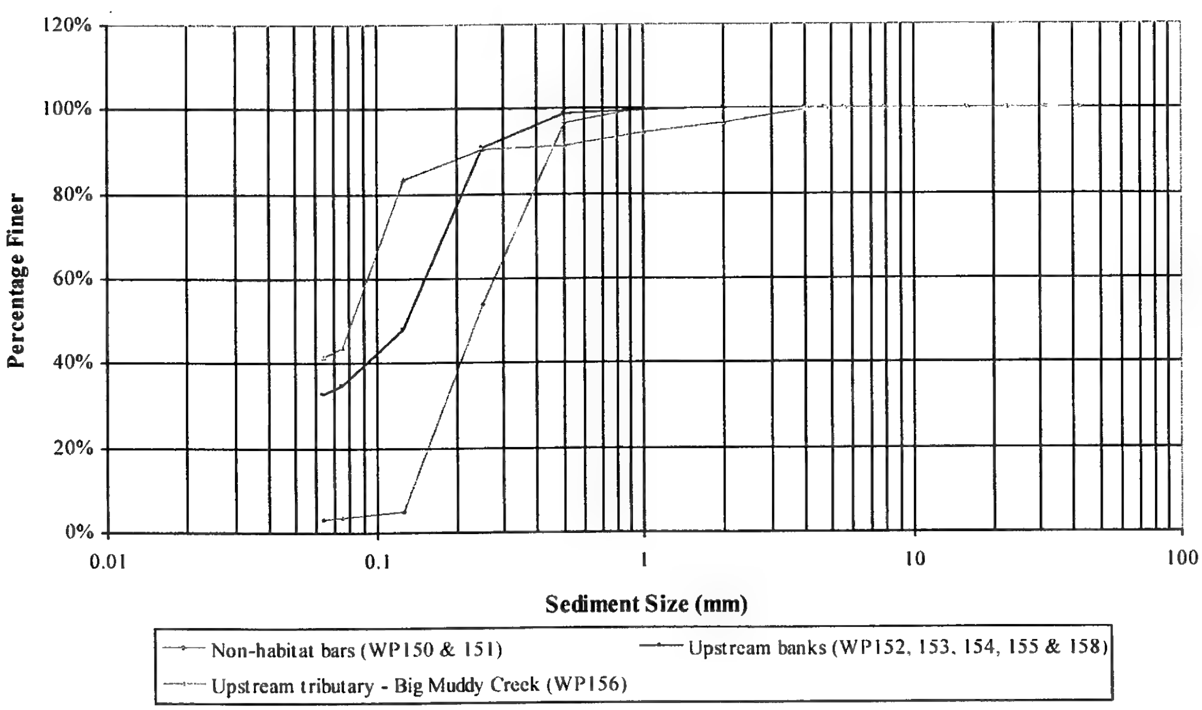

Figure A32: Fort Peck Reach - Comparison of habitat and non-habitat bars in Sampling Reach 13 with potential upstream bank sources of sediment in Geomorphically Similar Reach 7

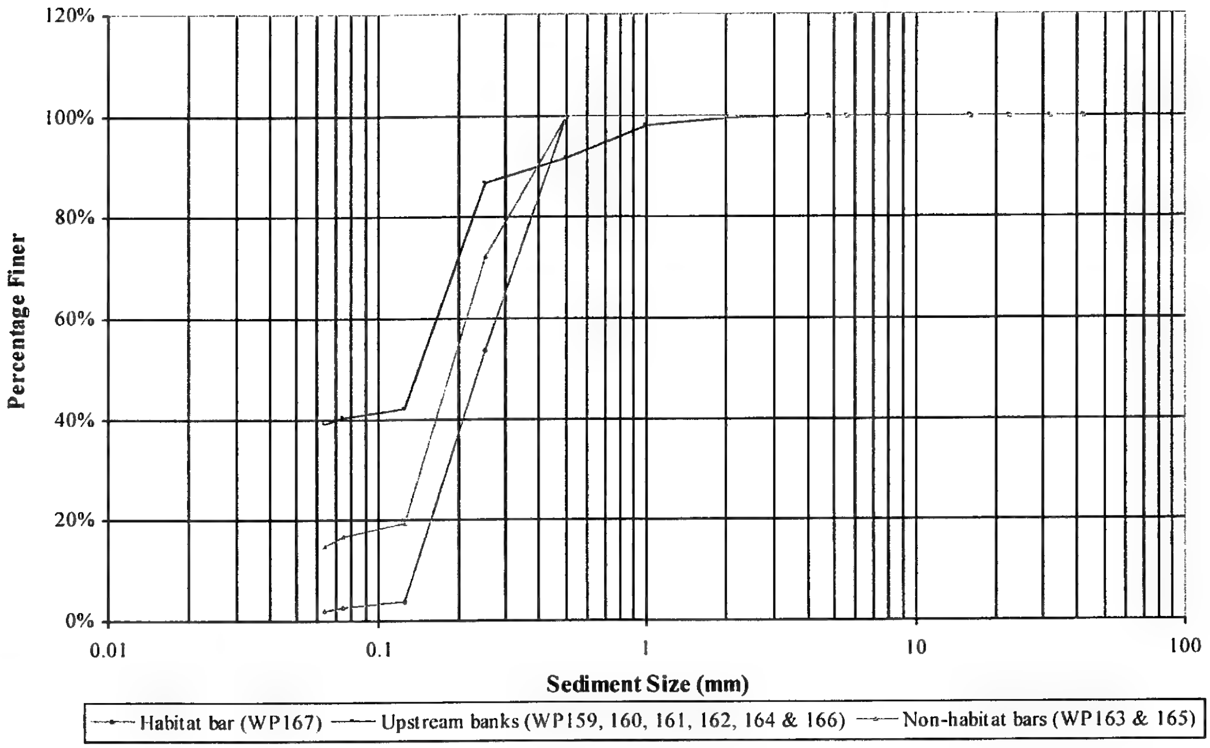

Figure A33: Fort Peck Reach - First comparison of habitat bar in Sampling Reach 13 with potential upstream bank sources of sediment

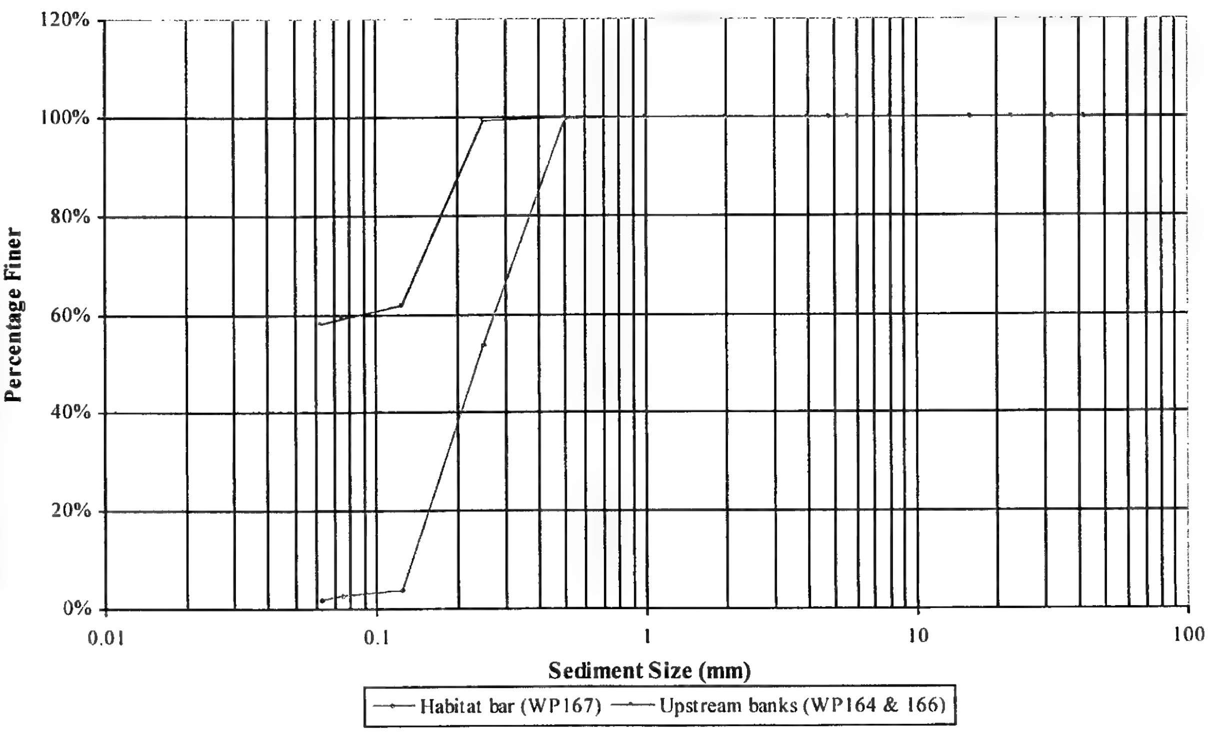

Figure A34: Fort Peck Reach - Second comparison of non-habitat bar in Sampling Reach 13 with potential upstream bank source of sediment

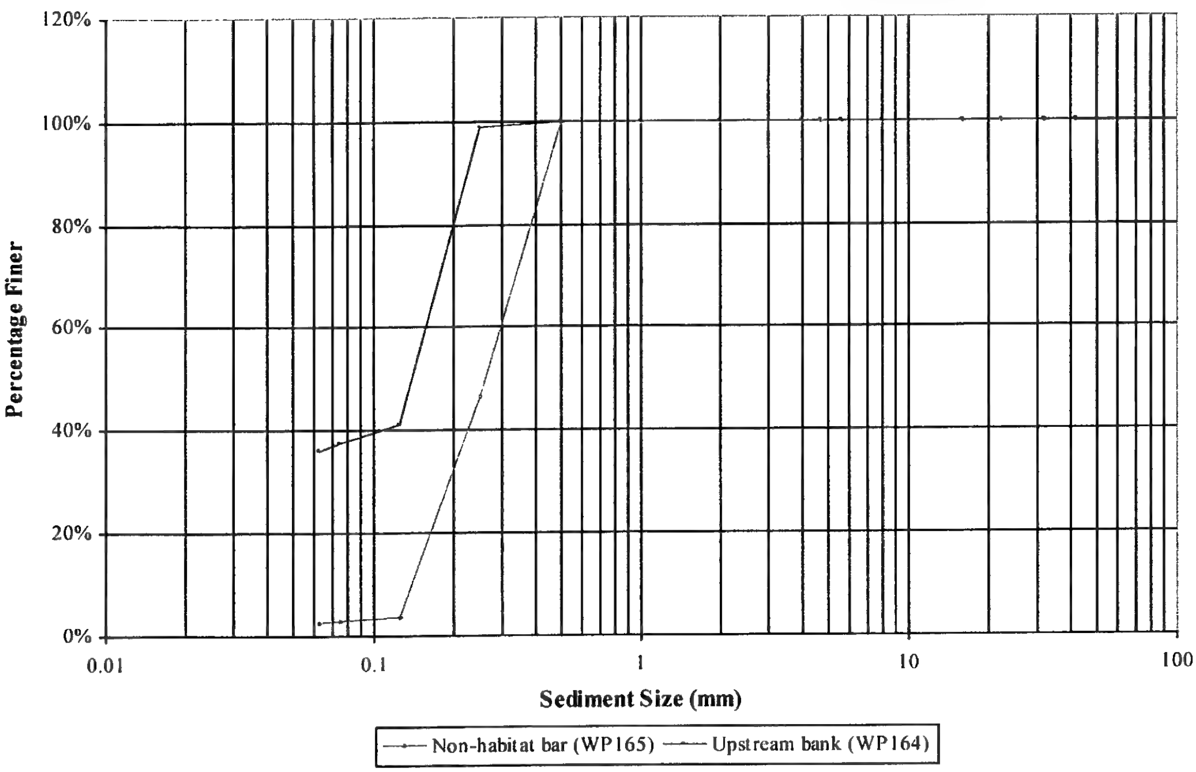

Figure A35: Fort Peck Reach - Comparison of non-habitat bars in Sampling Reach 14 with potential upstream bank and arroyo sources of sediment in Geomorphically Similar Reach 7

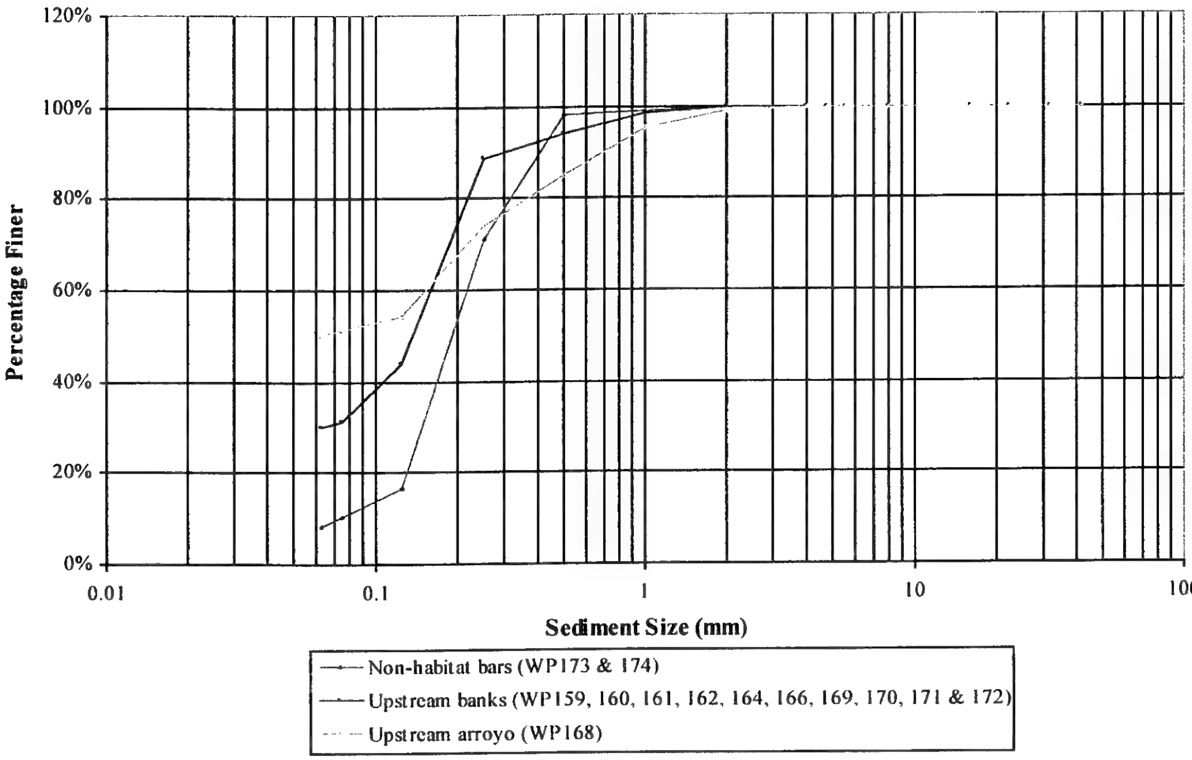

Figure A36: Fort Peck Reach - Comparison of non-habitat bars in Sampling Reach 14 with potential upstream bank sources of sediment

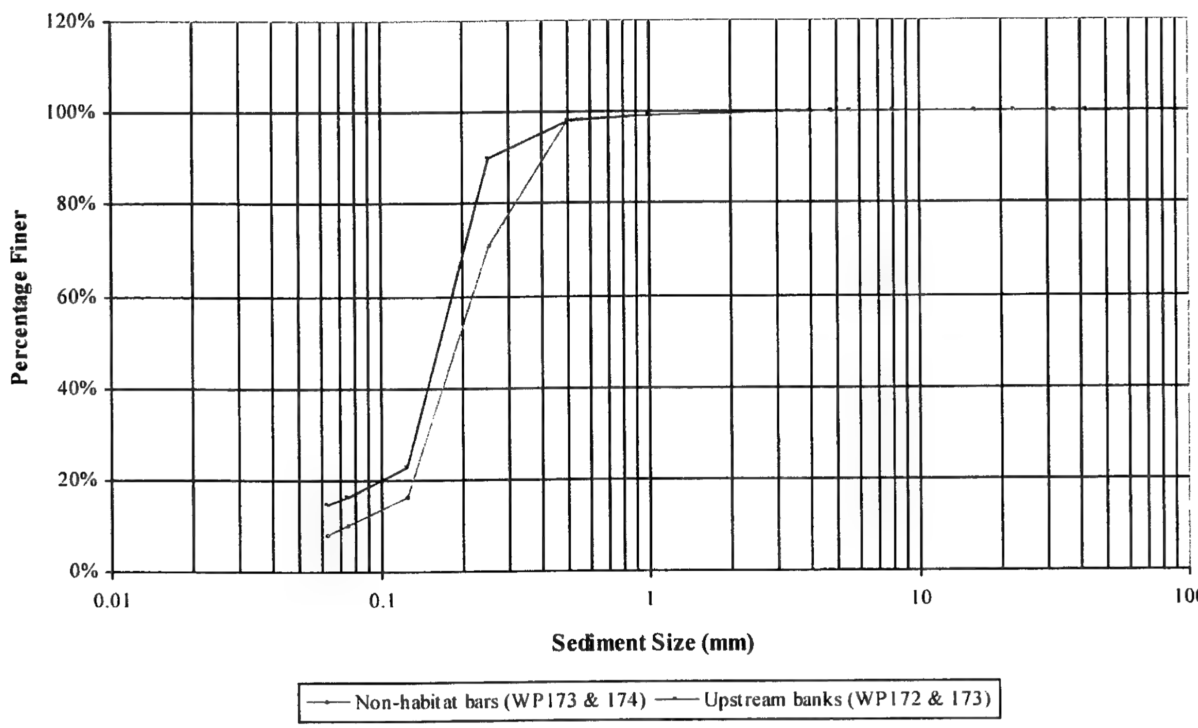

Figure A37: Fort Peck Reach - Comparison of habitat and non-habitat bars in Sampling Reach 15 with potential upstream bank and arroyo sources of sediment in Geomorphically Similar Reaches 7 and 8

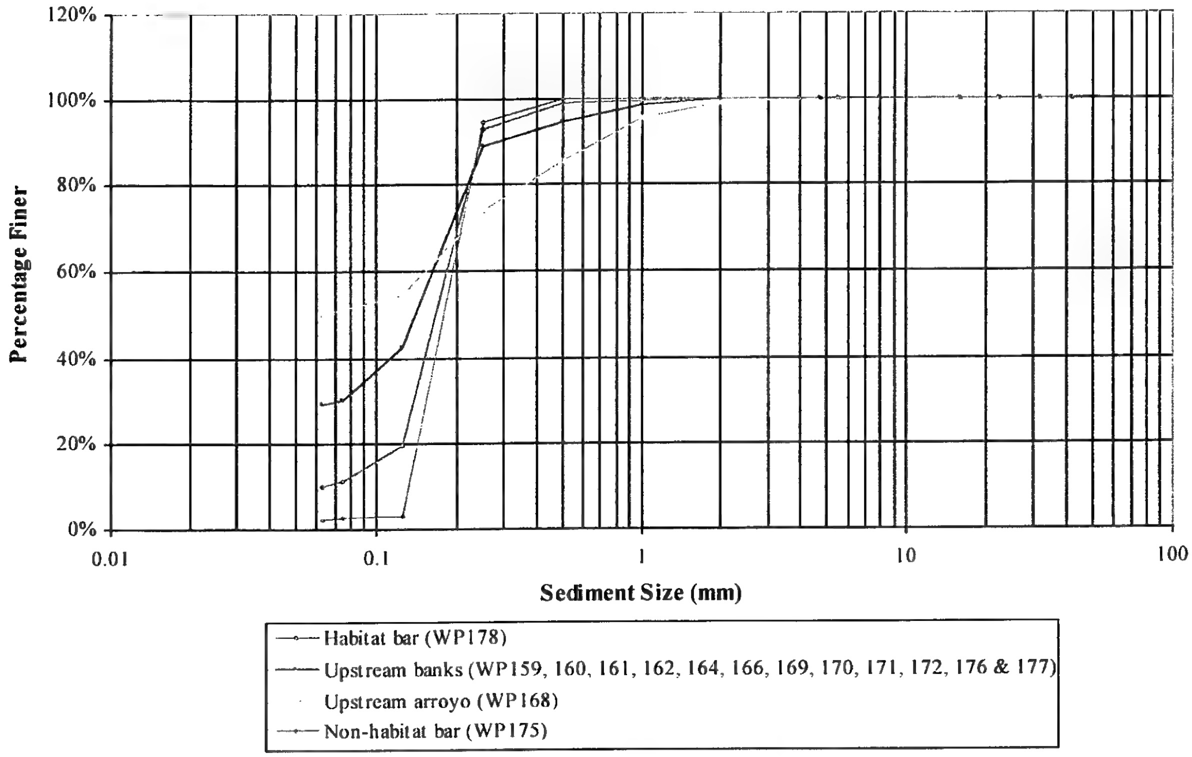

Figure A38: Fort Peck Reach - Comparison of habitat bar in Sampling Reach 15 with potential upstream bank sources of sediment

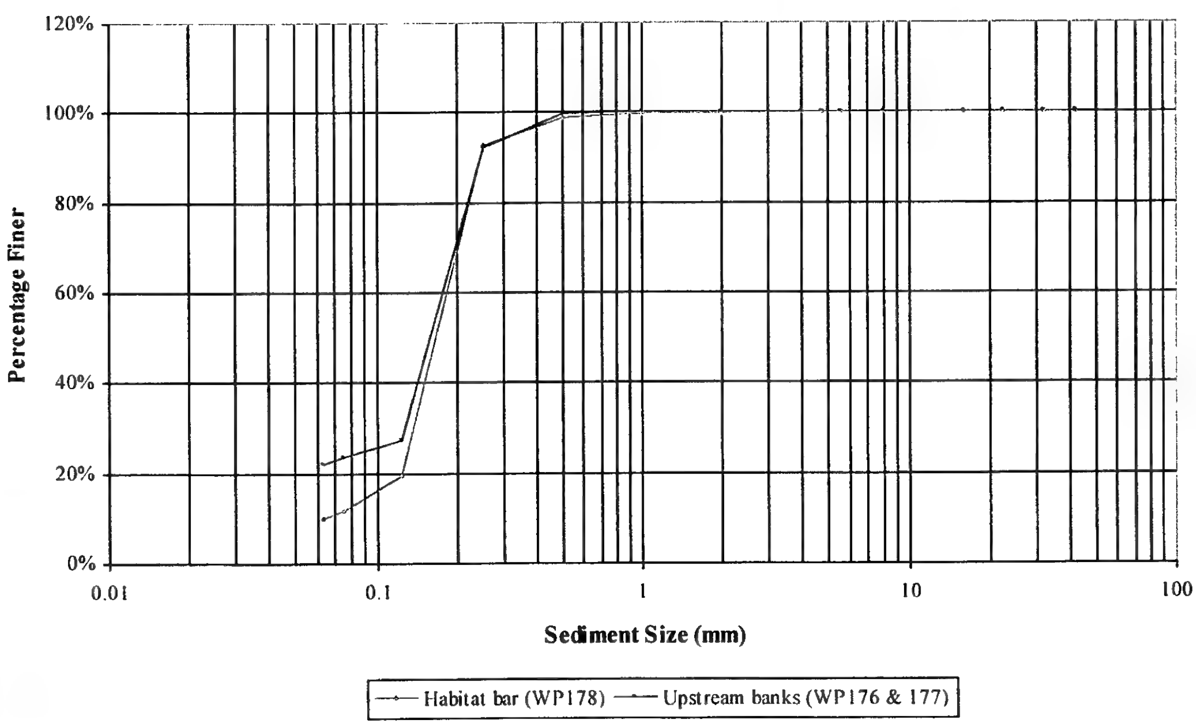

Figure A39: Garrison Reach - Comparison of habitat bar in Sampling Reach 1 with potential upstream bank sources of sediment in Geomorphically Similar Reach 1

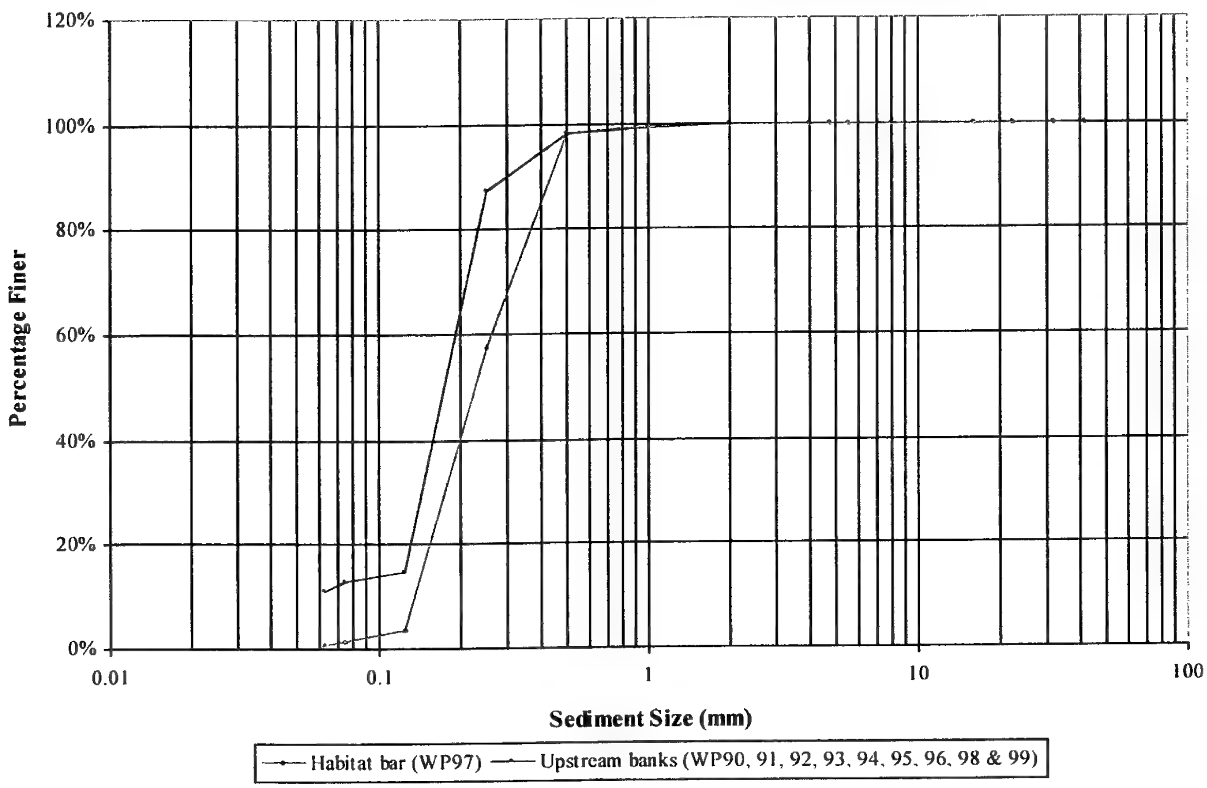

Figure A40: Garrison Reach - Comparison of non-habitat bars in Sampling Reach 1 with potential upstream bank sources of sediment in Geomorphically Similar Reach 1

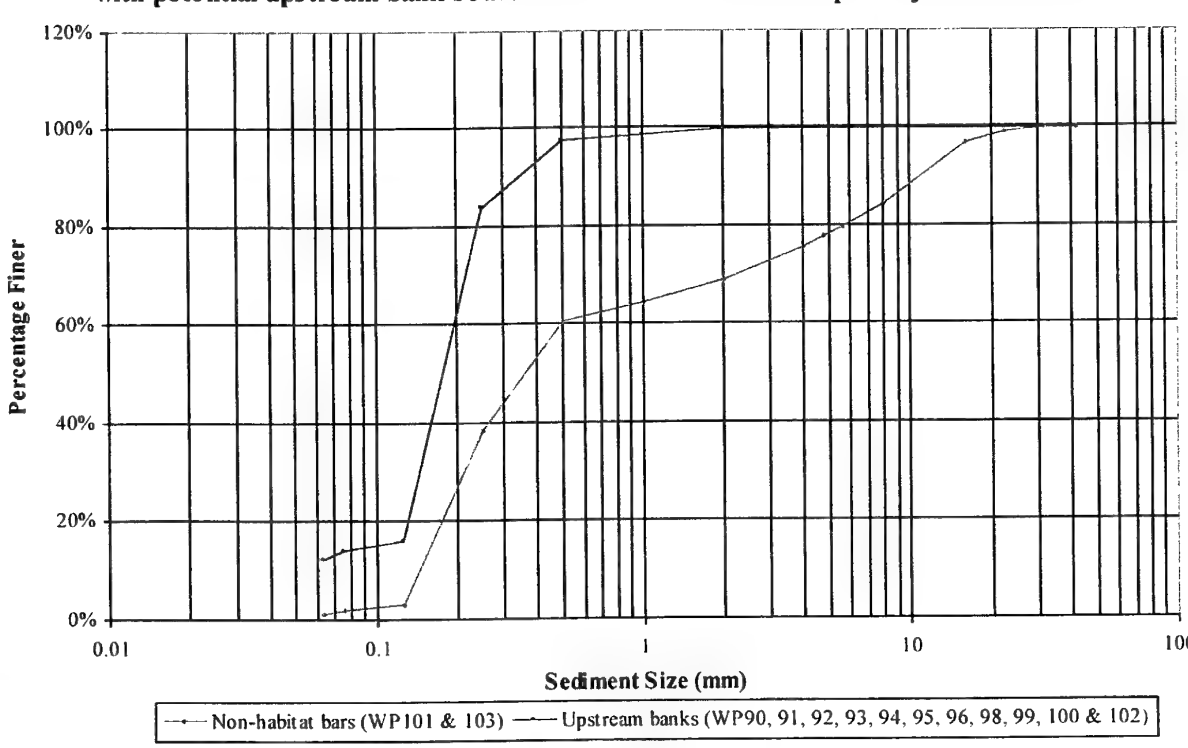

Figure A41: Garrison Reach - Comparison of habitat bar in Sampling Reach 1 with potential upstream bank sources of sediment

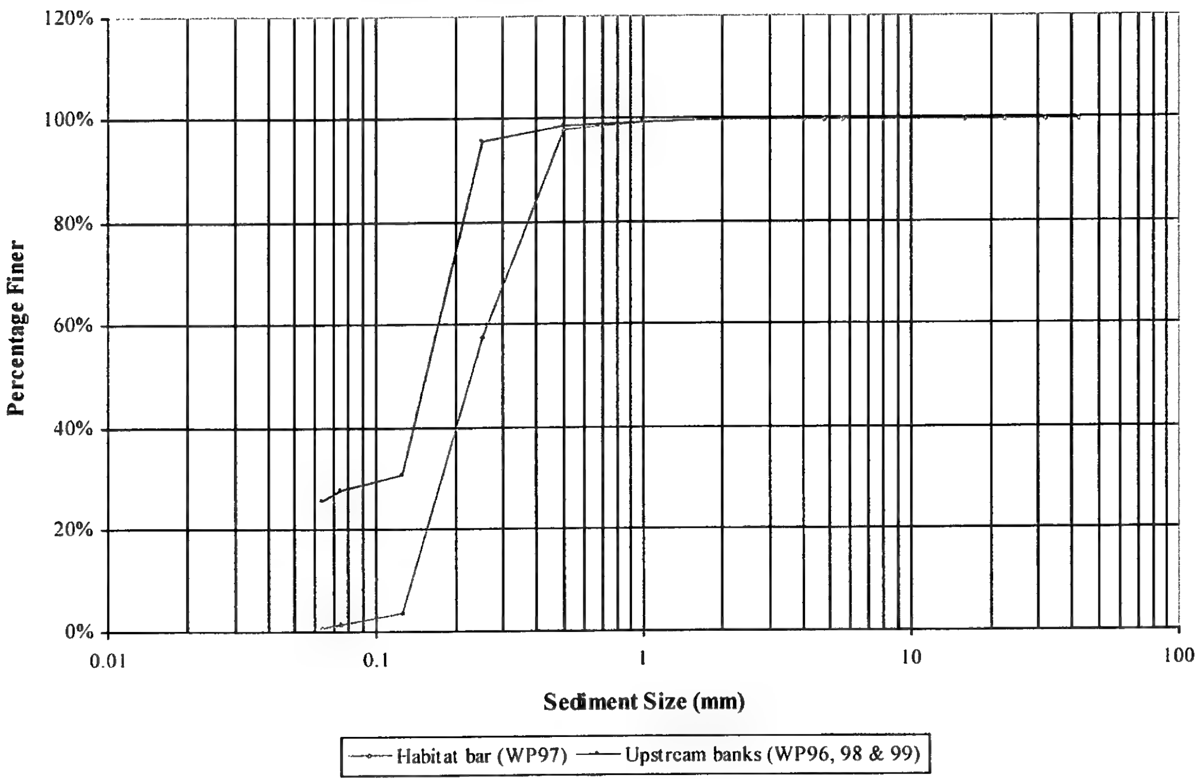

Figure A42: Garrison Reach - Comparison of non-habitat bar in Sampling Reach 1 with potential upstream bank sources of sediment

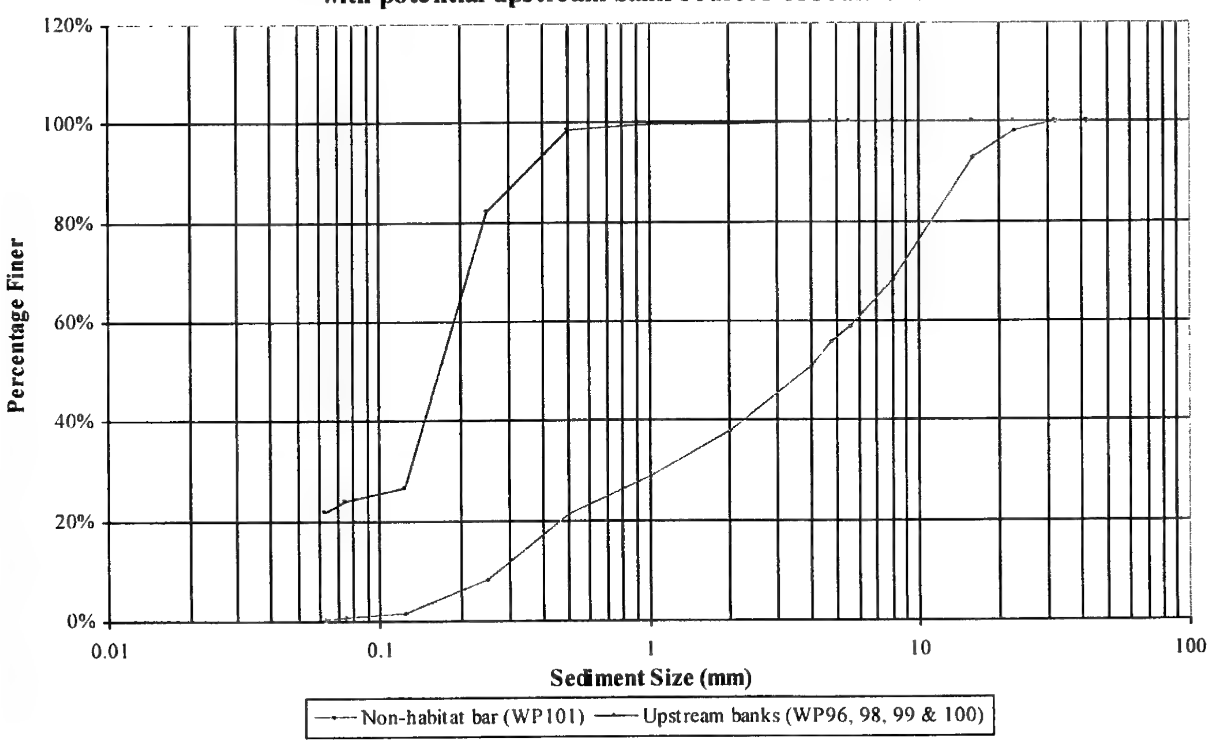

Figure A43: Garrison Reach - Comparison of non-habitat bar in Sampling Reach 1 with potential upstream bank sources of sediment

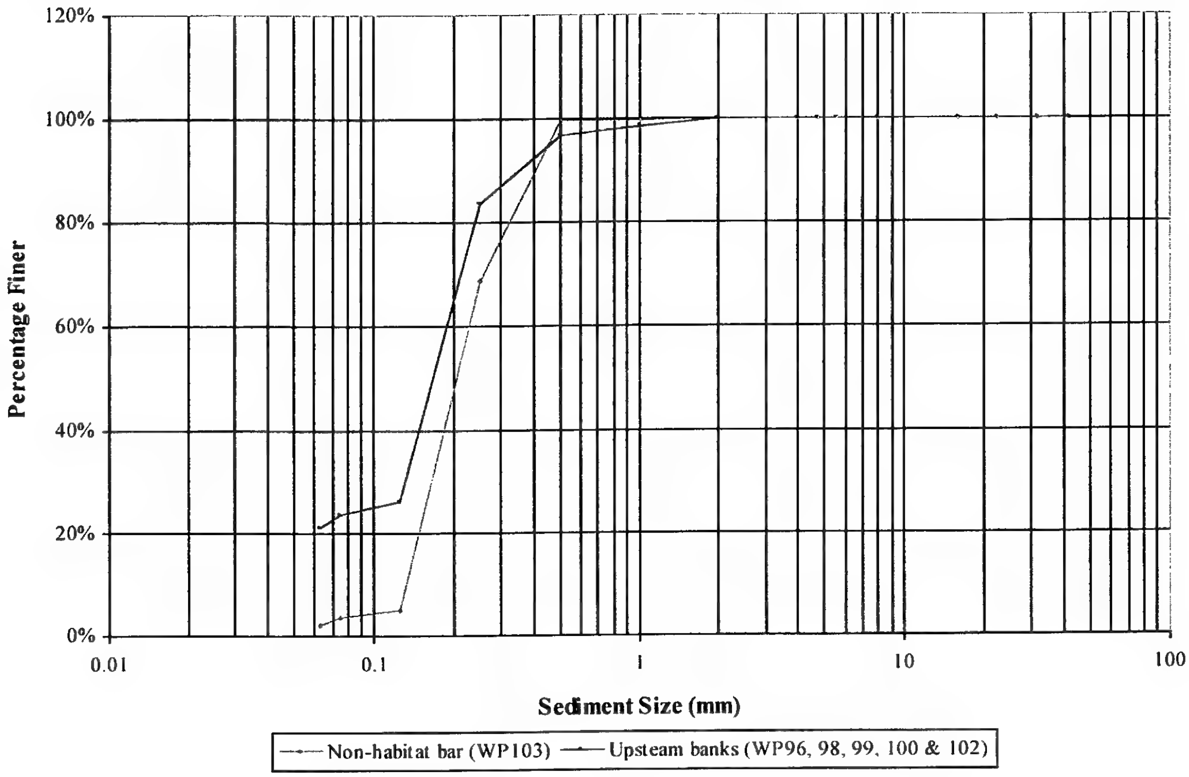

Figure A44: Garrison Reach - Comparison of non-habitat bar in Sampling Reach 2 with potential upstream bank and tributary sources of sediment in Geomorphically Similar Reaches 1 and 2

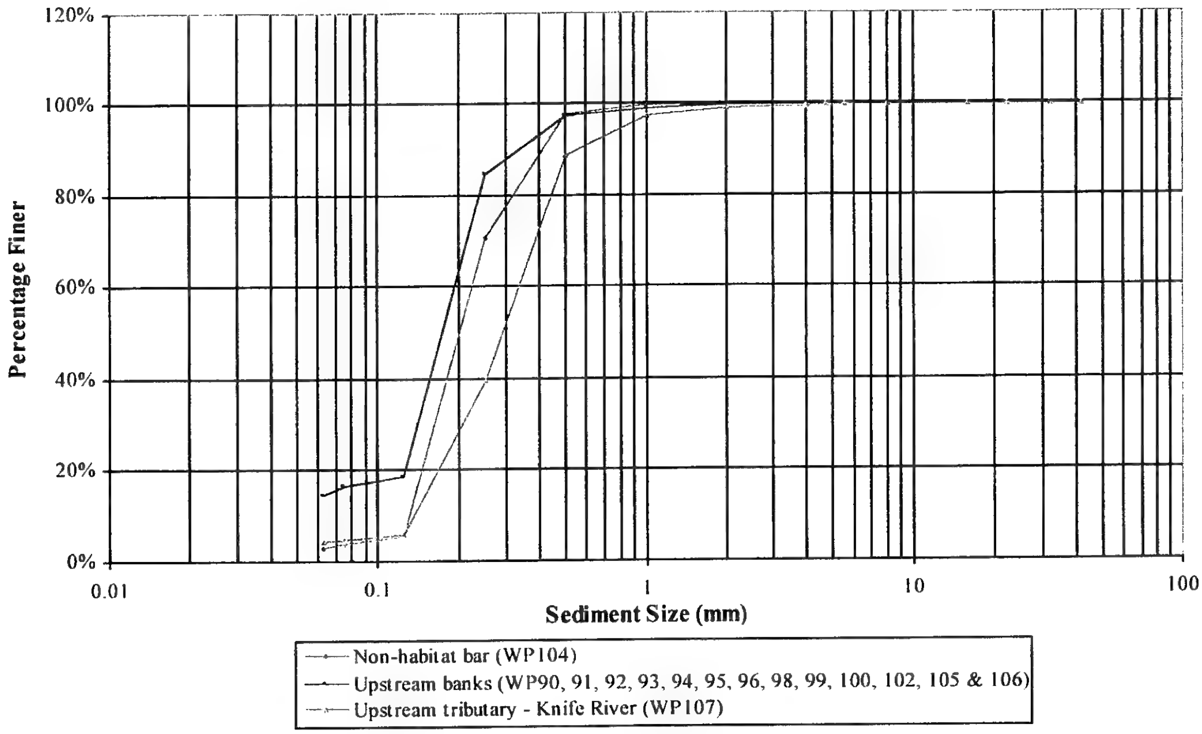

Figure A45: Garrison Reach - Comparison of non-habitat bar in Sampling Reach 2 with potential upstream bank and tributary sources of sediment

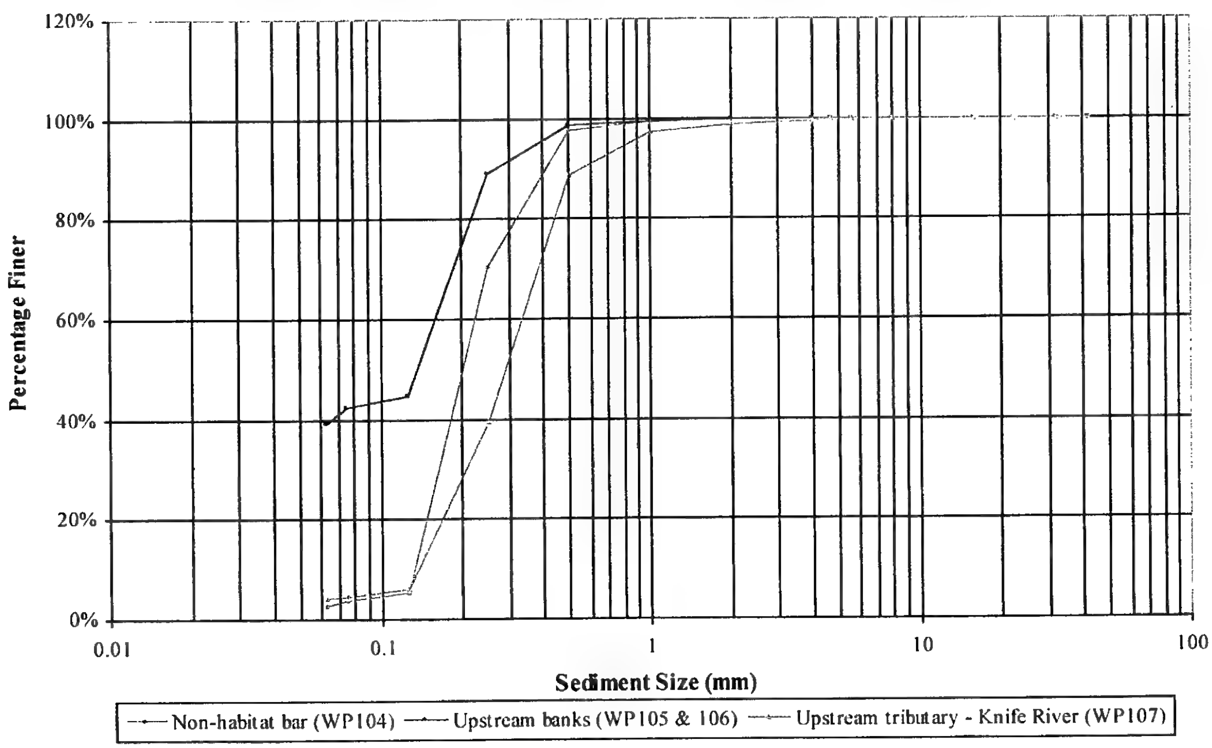

Figure A46: Garrison Reach - Comparison of habitat bars in Sampling Reach 3 with potential upstream bank and tributary sources of sediment in Geomorphically Similar Reach 2

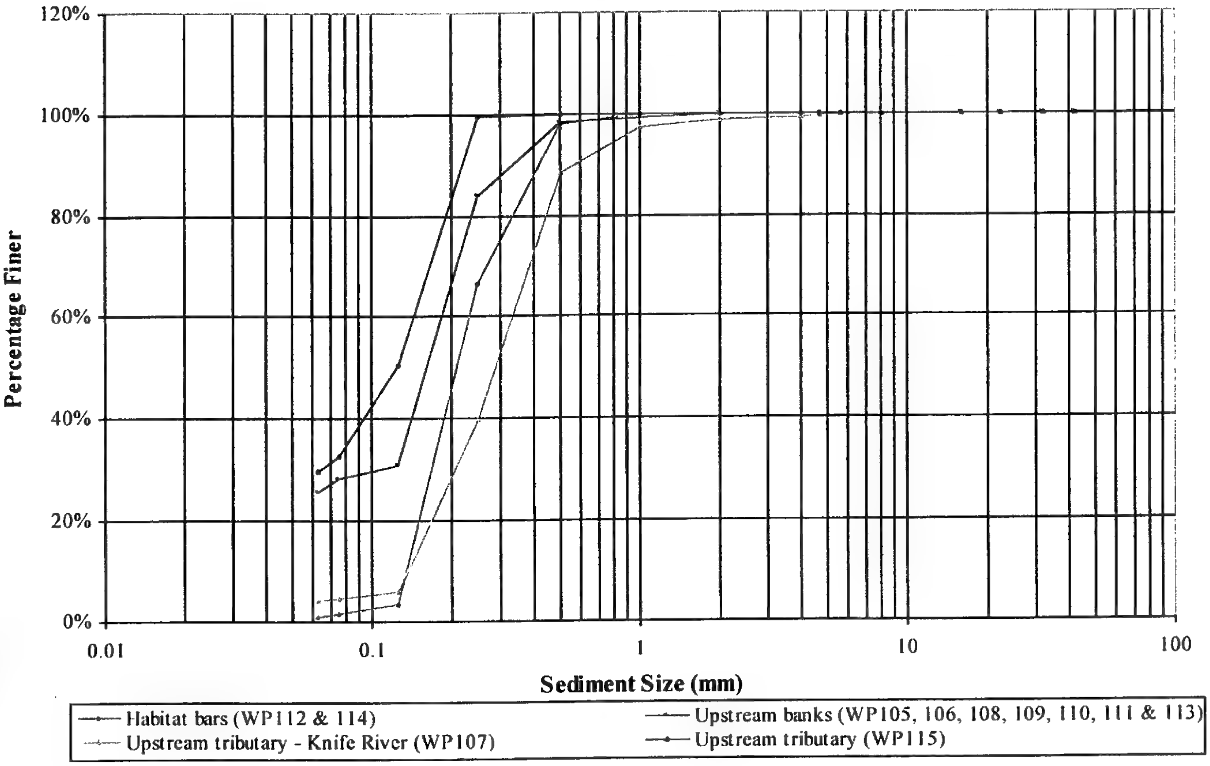

Figure A47: Garrison Reach - First comparison of habitat bar in Sampling Reach 3 with potential upstream bank sources of sediment

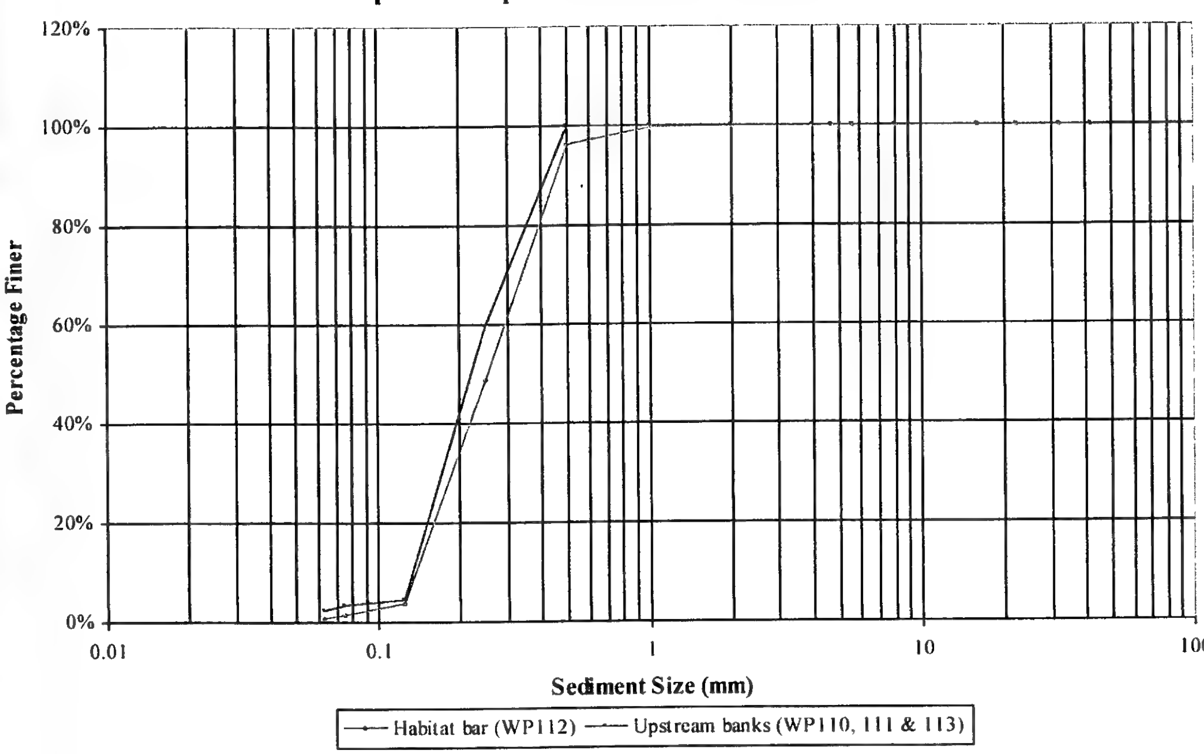

Figure A48: Garrison Reach - Second comparison of habitat bar in Sampling Reach 3 with potential upstream bank and tributary sources of sediment

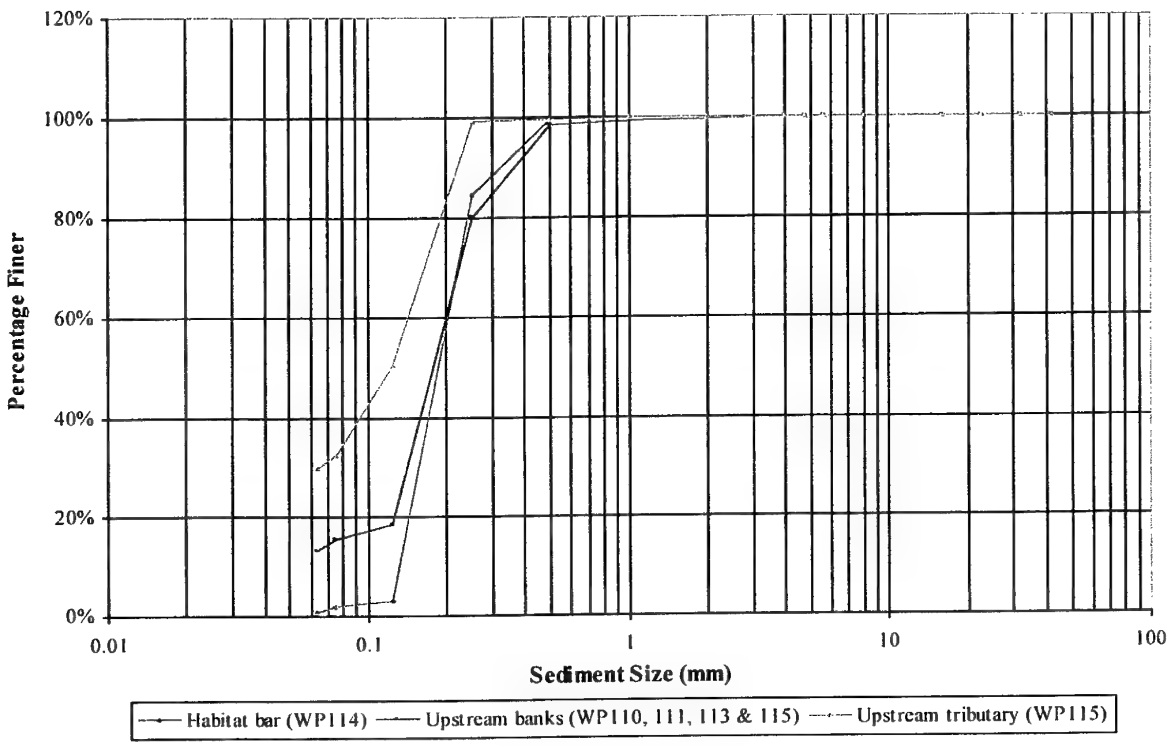

Figure A49: Garrison Reach - Comparison of habitat bars in Sampling Reach 4 with potential upstream bank and tributary sources of sediment in Geomorphically Similar Reach 2

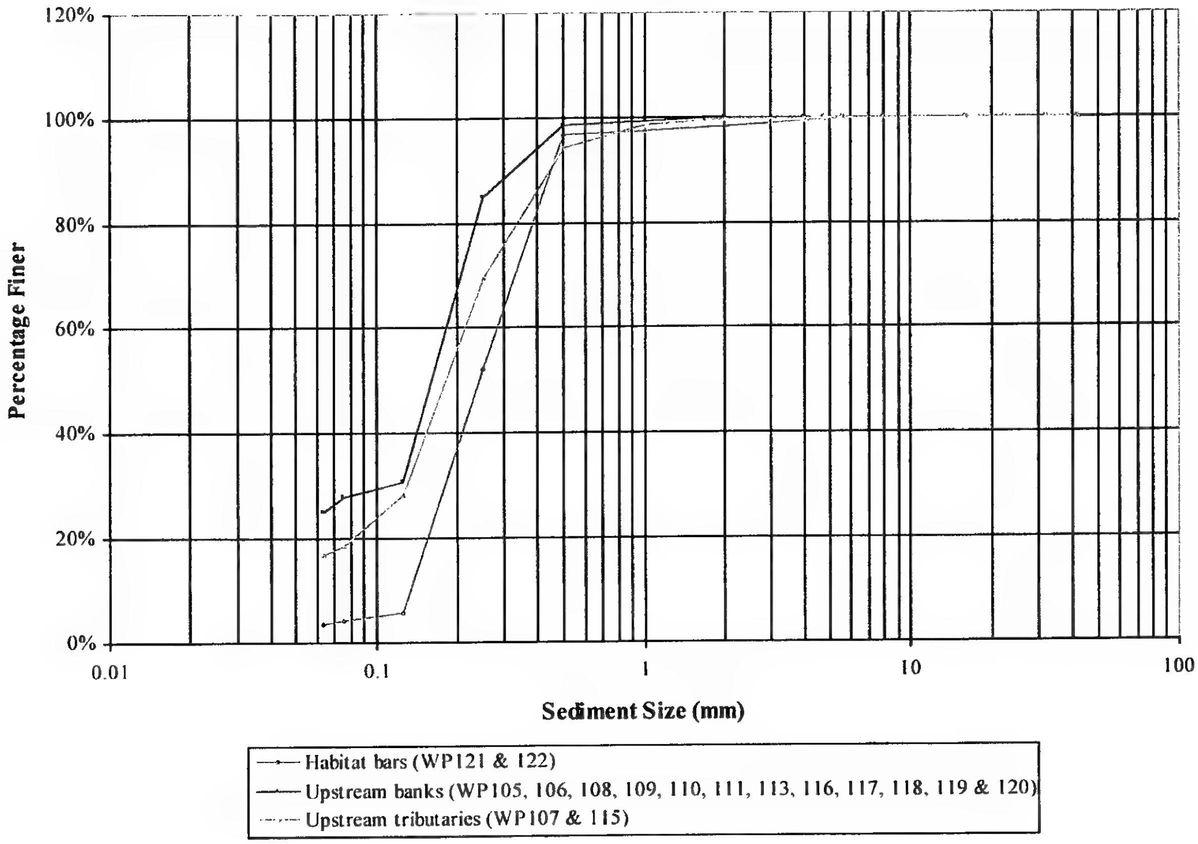

Figure A50: Garrison Reach - Comparison of habitat bar and non-habitat bars in Sampling Reach 5 with potential upstream bank sources of sediment in Geomorphically Similar Reaches 3 and 4

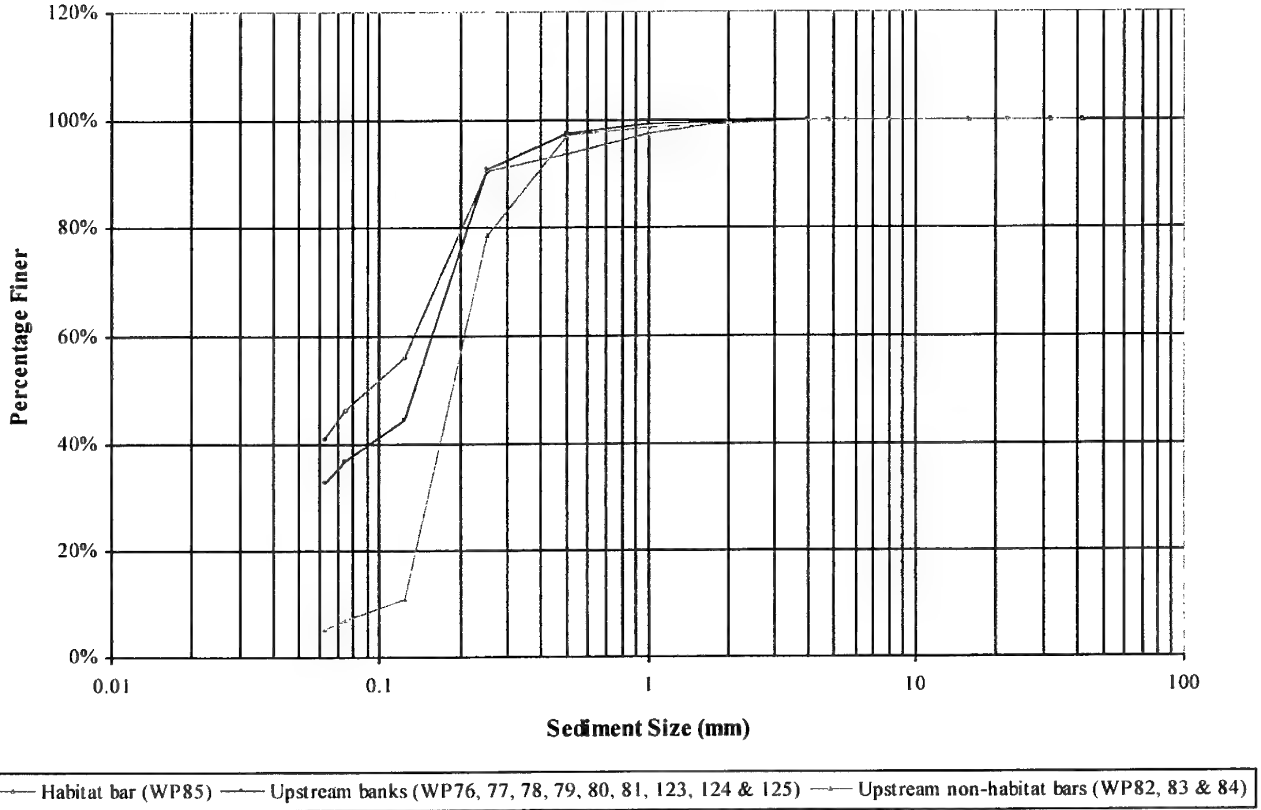

Figure A51: Garrison Reach - Comparison of habitat bar and non-habitat bar and island in Sampling Reach 6 with potential upstream bank, tributary and arroyo sources of sediment in Geomorphically Similar Reaches 4 and 5

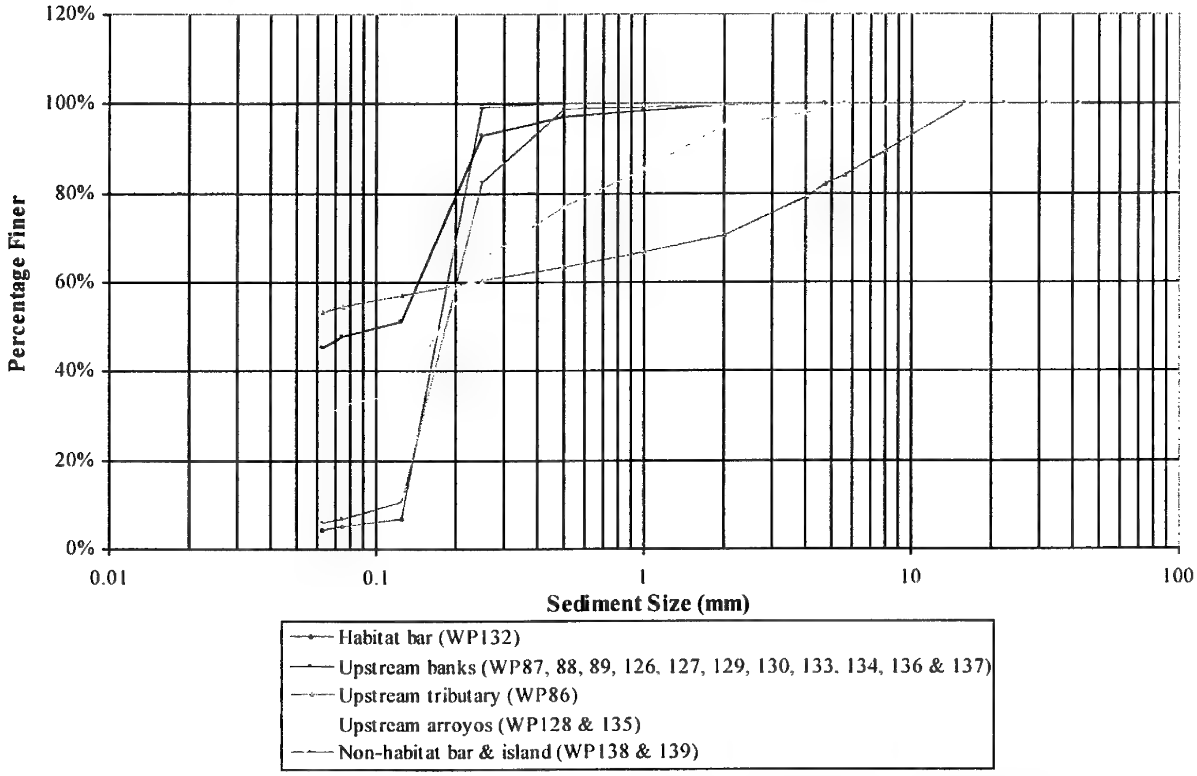

Figure A52: Garrison Reach - First comparison of habitat bar in Sampling Reach 6 with potential upstream bank source of sediment

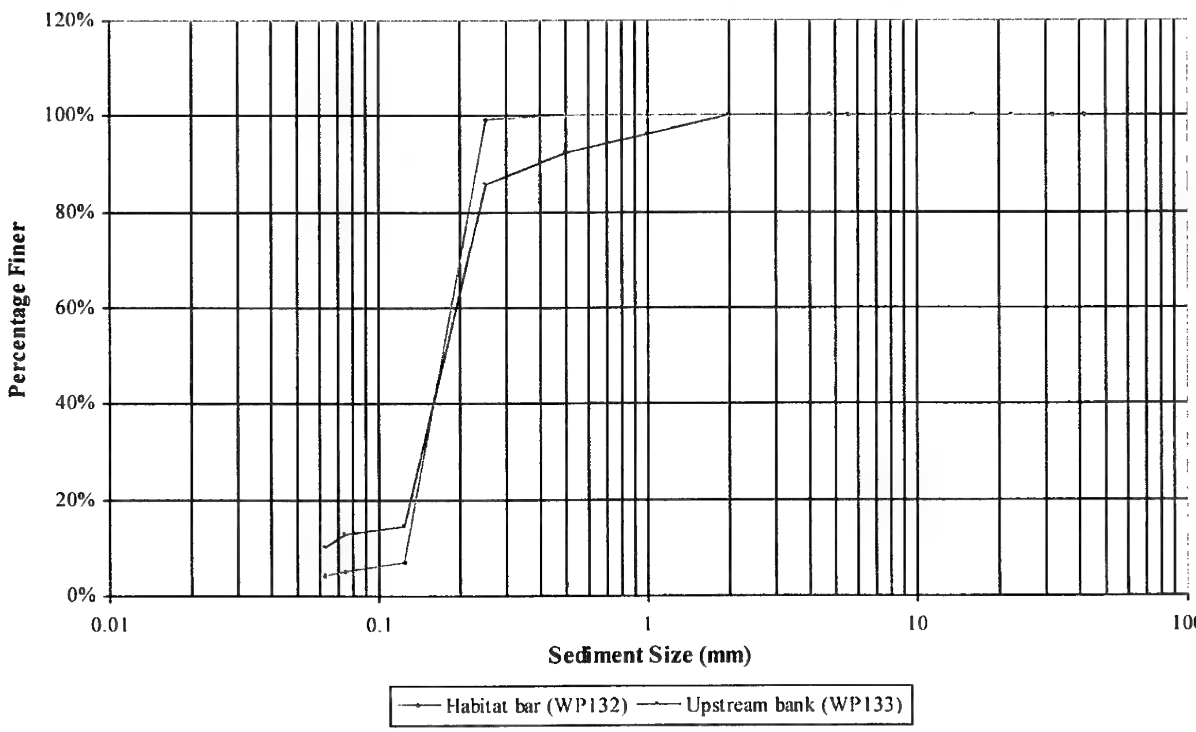

Figure A53: Garrison Reach - Second comparison of non-habitat bars in Sampling Reach 6 with potential upstream bank and arroyo sources of sediment

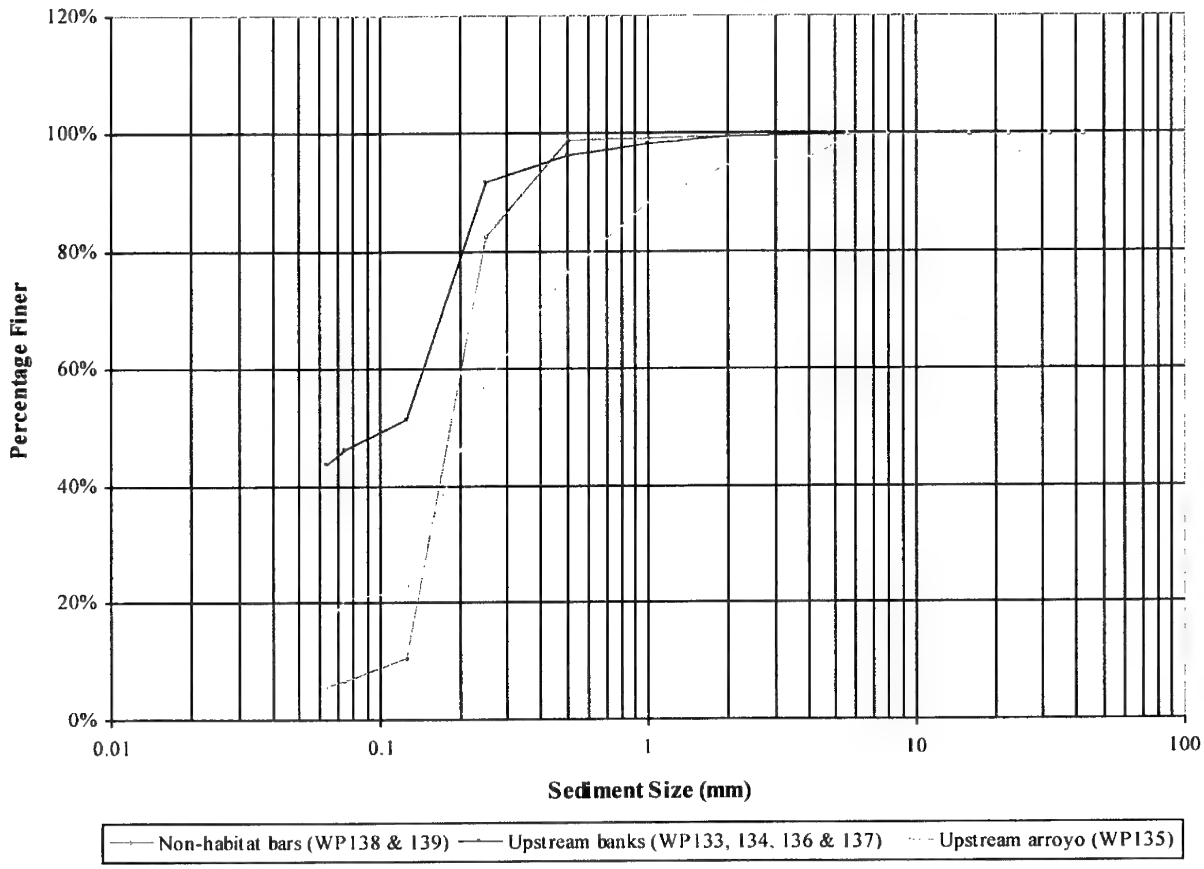

Figure A54: Garrison Reach - Comparison of habitat bar and non-habitat island in Sampling Reach 7 with potential upstream bank sources of sediment in Geomorphically Similar Reaches 4 and 5

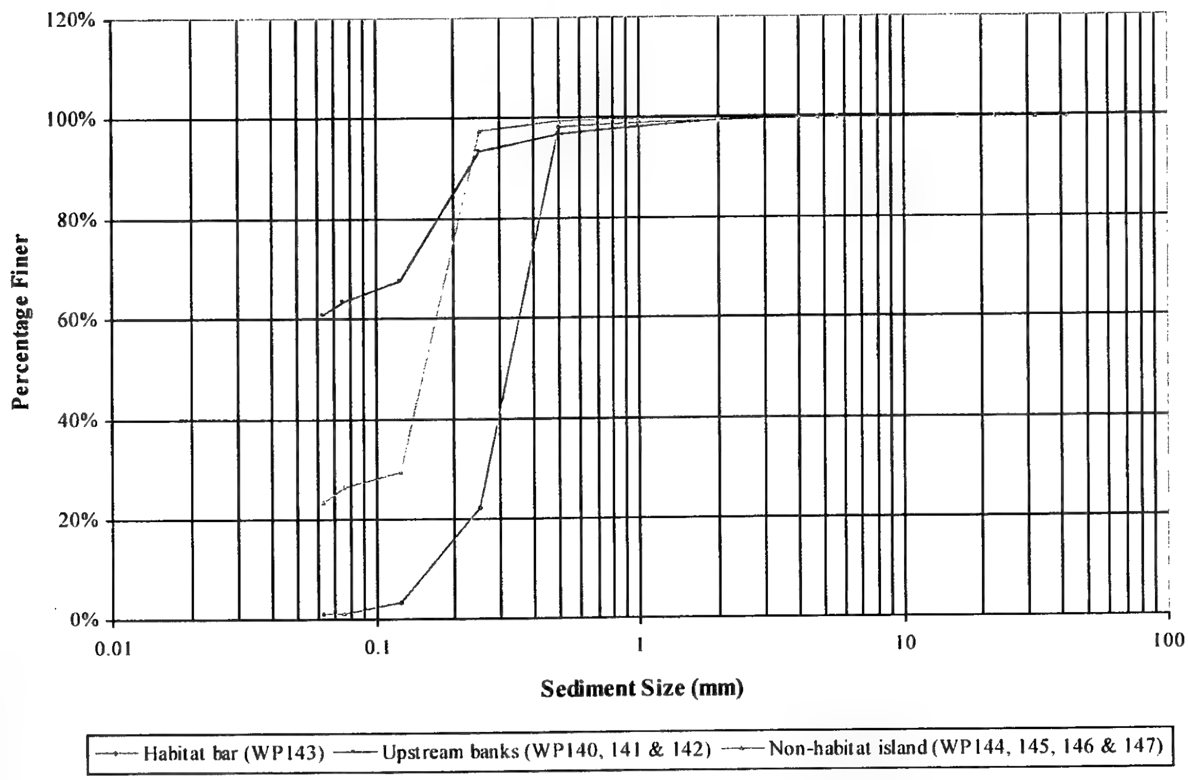

Figure A55: Fort Randall Reach - Comparison of non-habitat bar and island in Sampling Reach 1 with potential upstream bank source of sediment

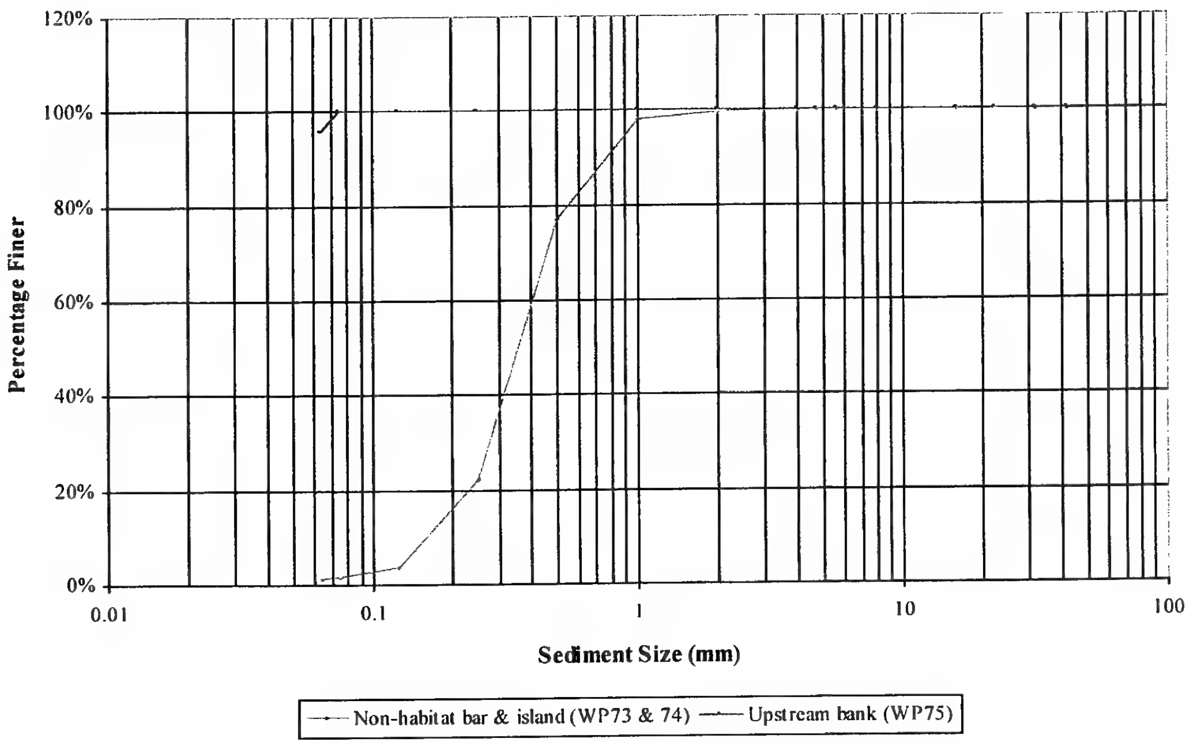

Figure A56: Fort Randall Reach - Comparison of habitat bars in Sampling Reach 2 with potential bank sources of sediment in Geomorphically Similar Reaches 2 and 3

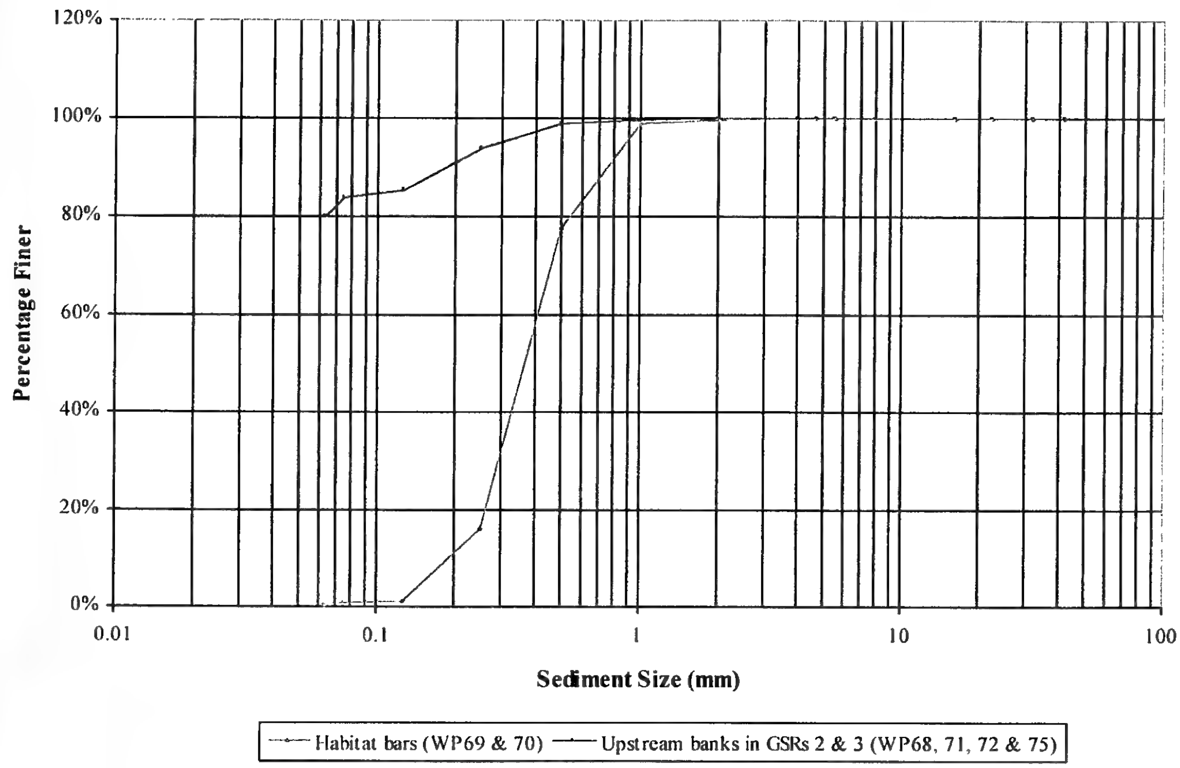

Figure A57: Fort Randall Reach - Comparison of habitat bars in Sampling Reach 2 with potential upstream bank source of sediment

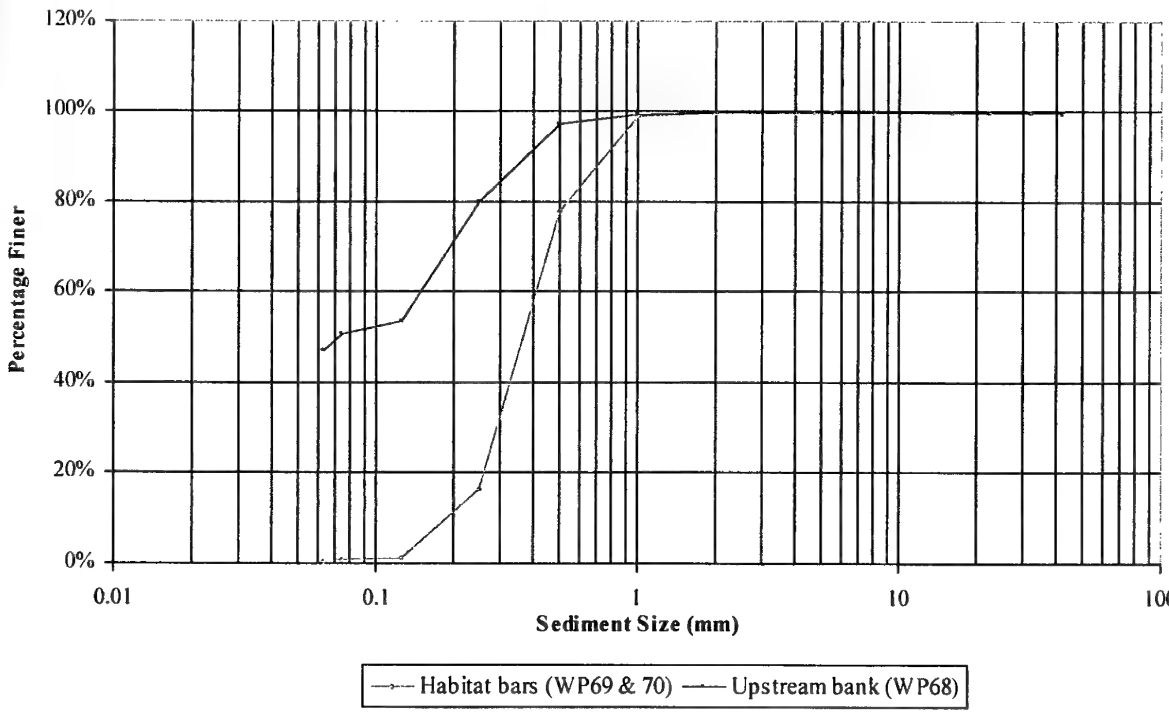

Figure A58: Fort Randall Reach - Comparison of non-habitat islands & bars in Sampling Reach 3 with potential bank sources of sediment in Geomorphically Similar Reach 4

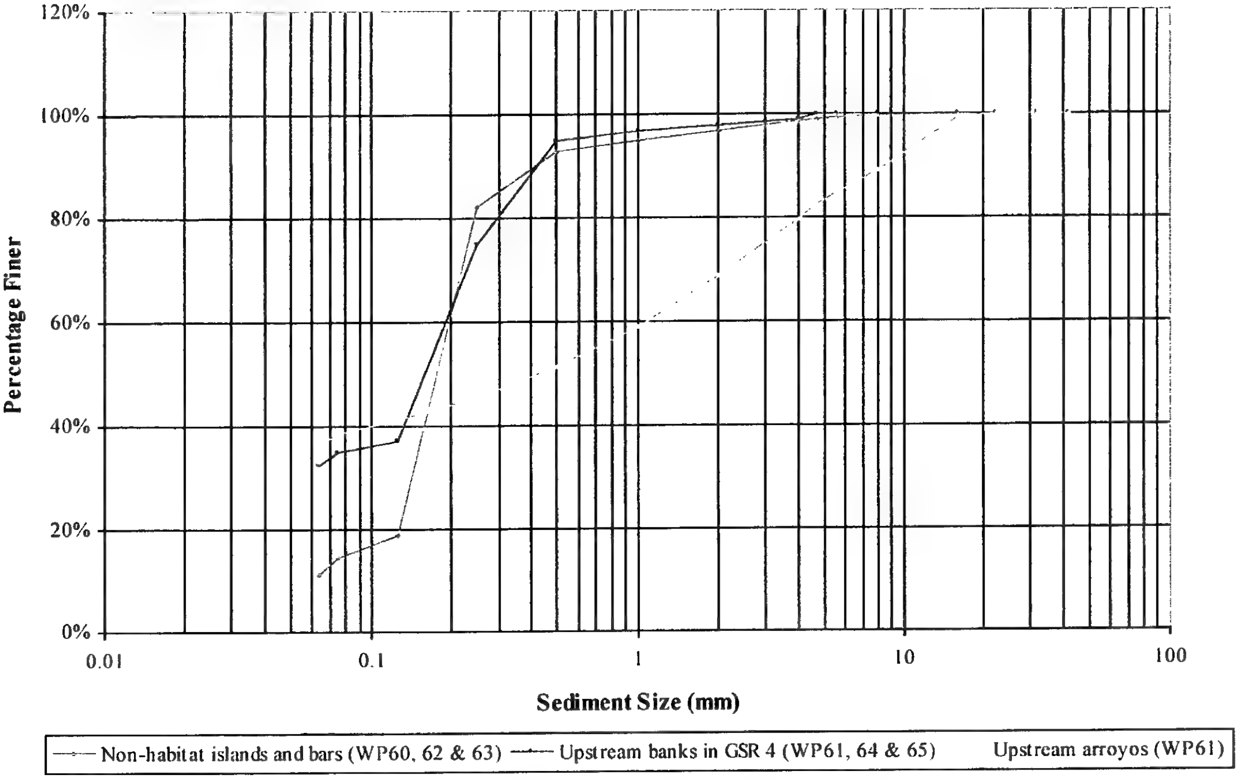

Figure A59: Fort Randall Reach - Comparison of non-habitat islands and bar in Sampling Reach 3 with potential upstream arroyo sources of sediment

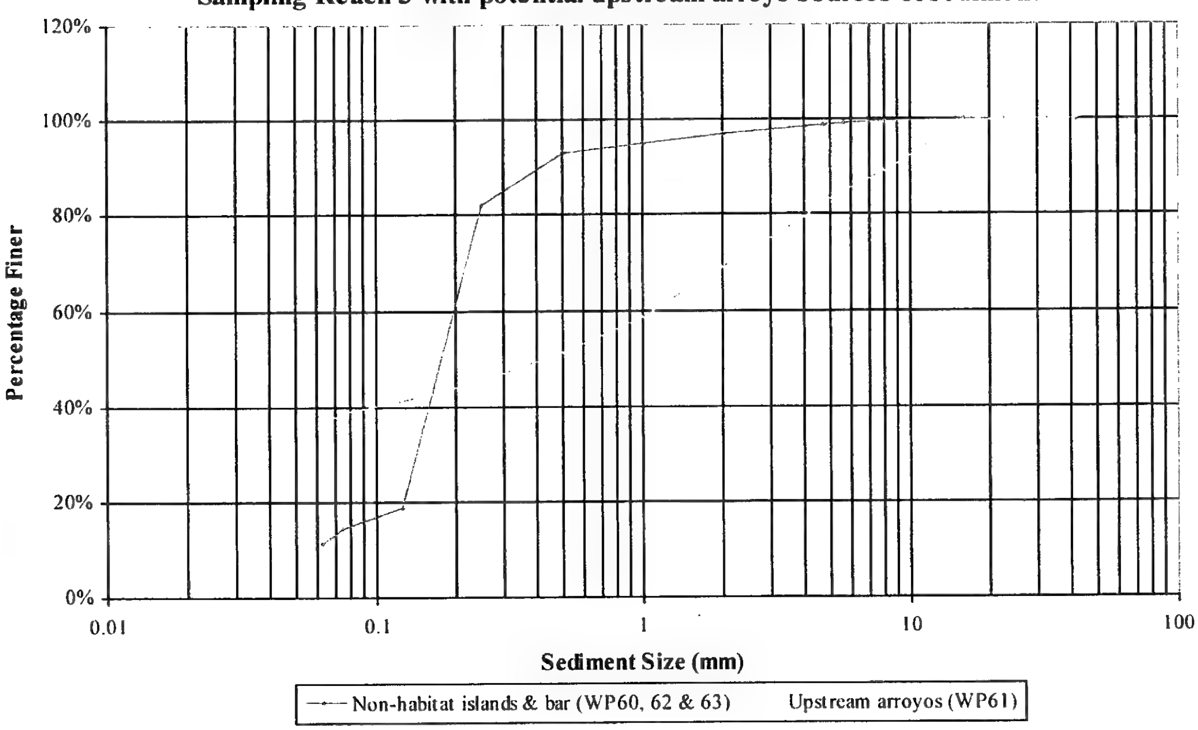

Figure A60: Fort Randall Reach - Comparison of habitat bar in Sampling Reach 4 with potential sediment sources from upstream banks, bars, islands and arroyos in Geomorphically Similar Reaches 4 and 5

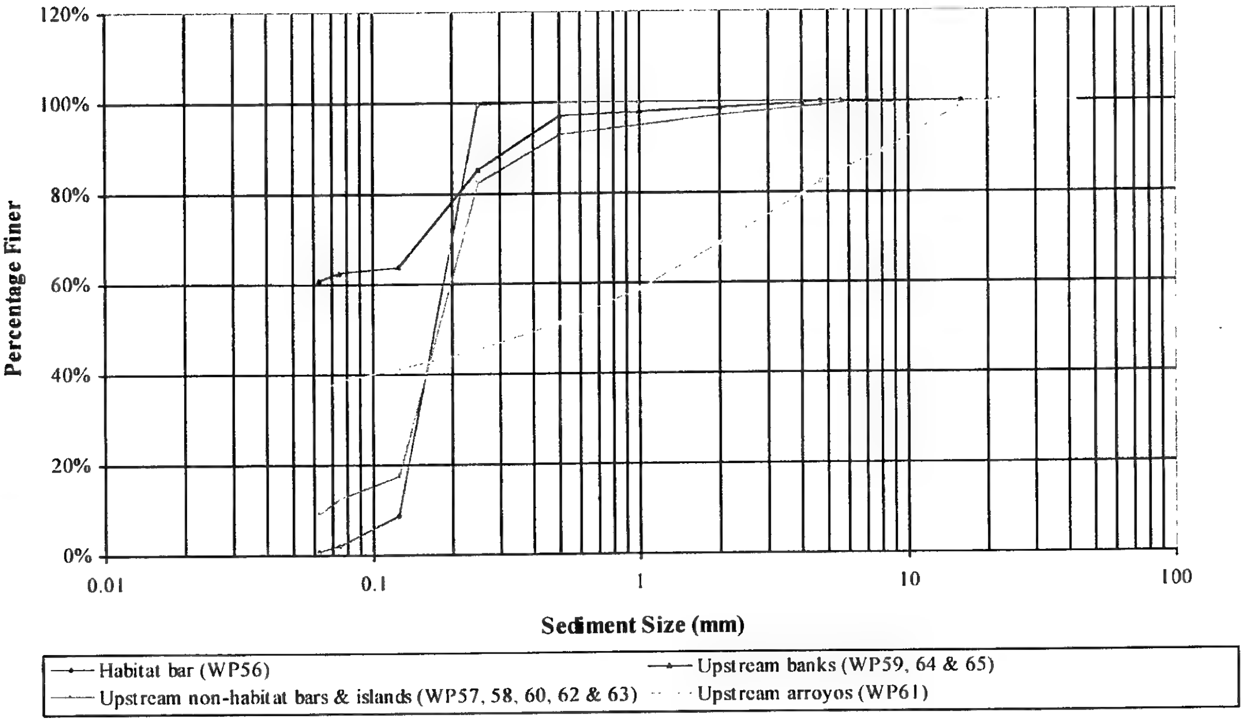

Figure A61: Fort Randall Reach - Comparison of habitat bar and non-habitat bars in Sampling Reach 4 with a potential upstream bank source of sediment

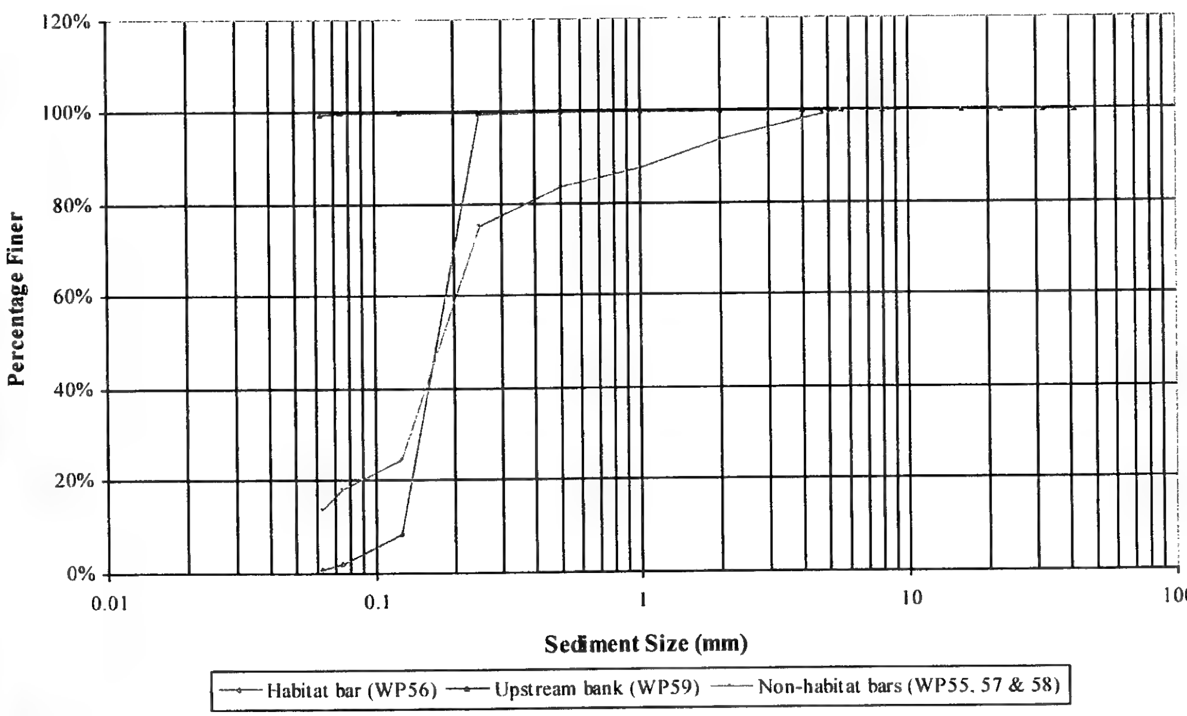

Figure A62: Fort Randall Reach - Comparison of non-habitat bars in Sampling Reach 5 with potential bank and tributary sources of sediment in Geomorphically Similar Reach 6

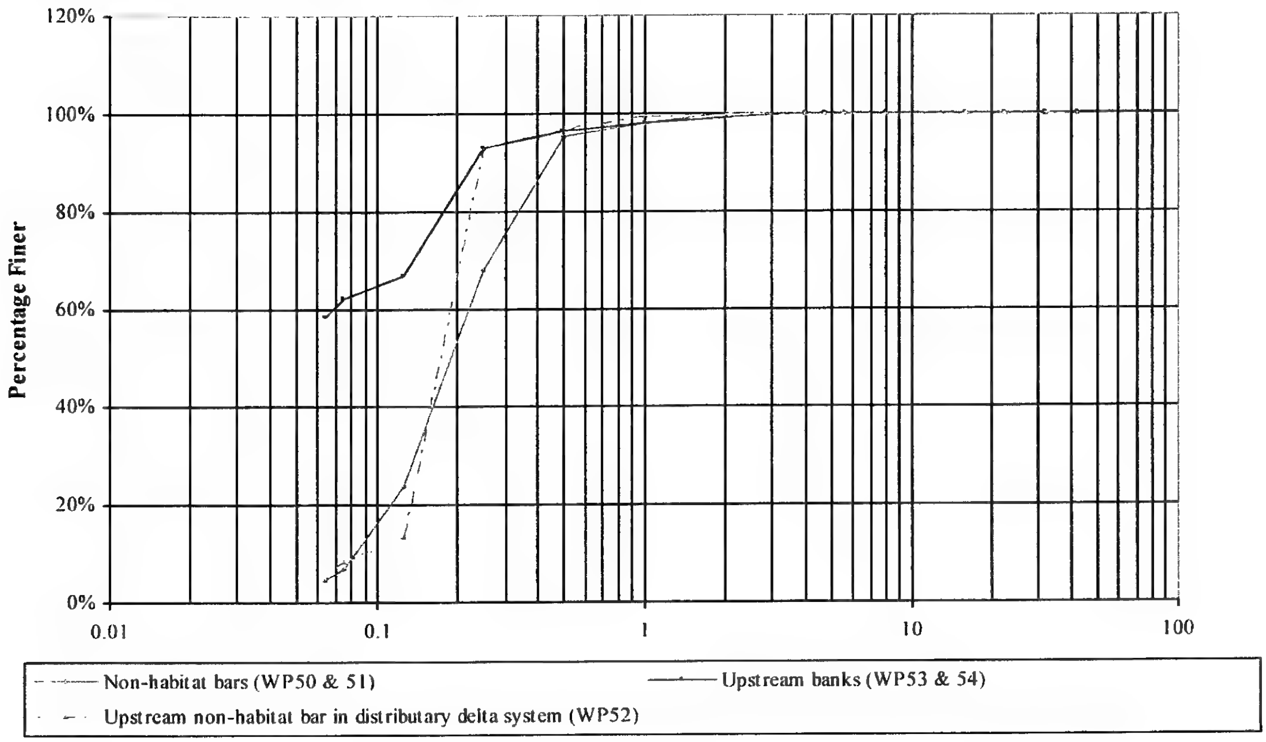

Figure A63: Fort Randall Reach - Comparison of non-habitat island & bar in Sampling Reach 6 with a potential sediment source from an upstream tributary, downstream of Geomorphically Similar Reach 6

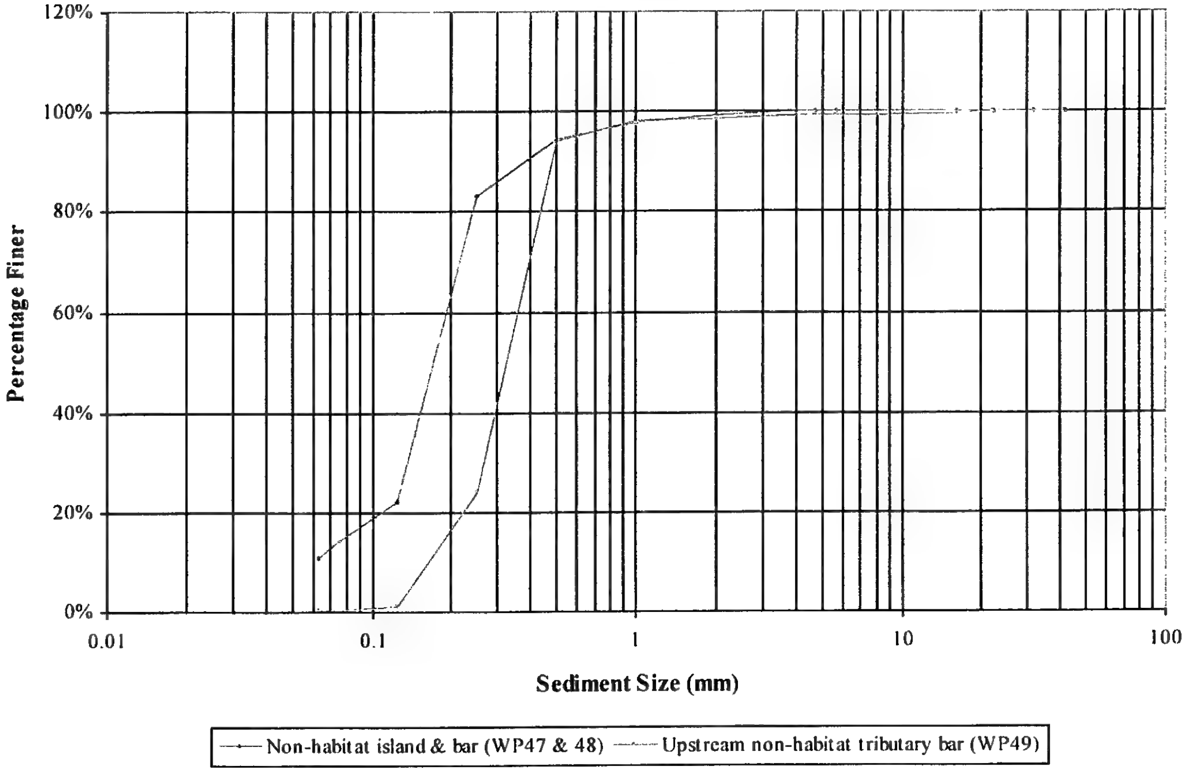

Figure A64: Gavins Point Reach - Comparison of habitat bars and non-habitat bar in Sampling Reach 1 with potential upstream bank sources of sediment in Geomorphically Similar Reach 1

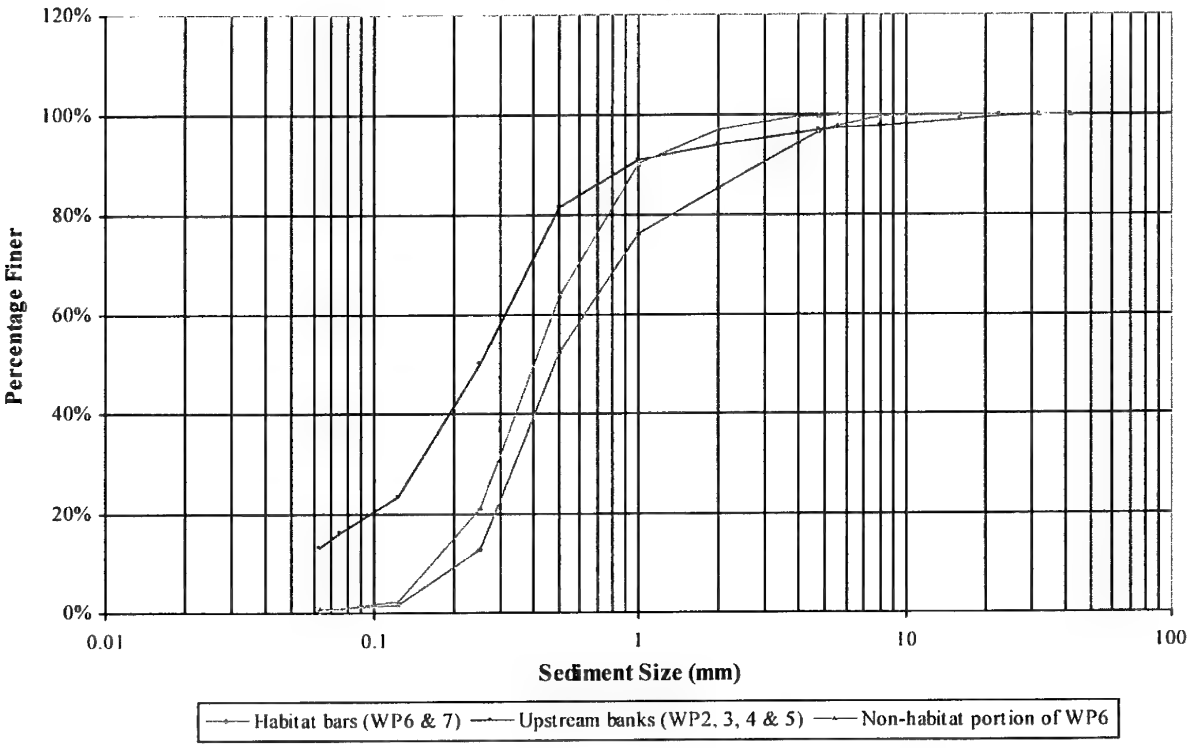

Figure A65: Gavins Point Reach - Comparison of habitat bars and non-habitat bar in Sampling Reach 1 with potential upstream bank sources of sediment

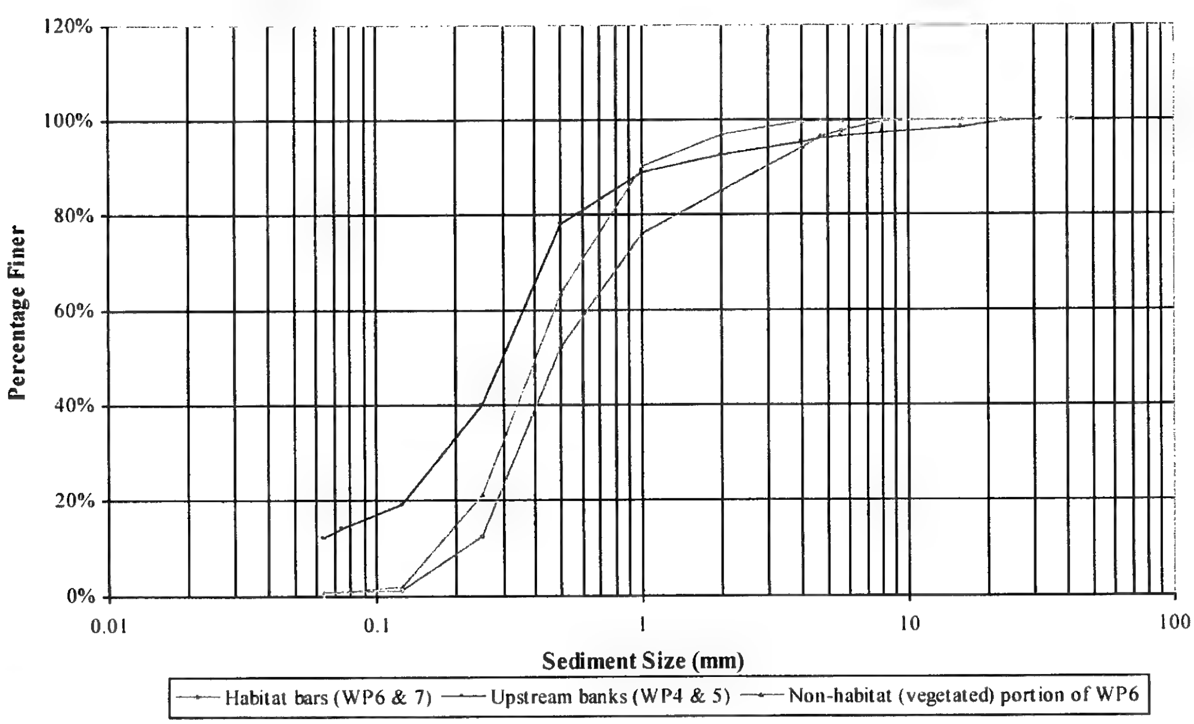

Figure A66: Gavins Point Reach - Comparison of habitat bar in Sampling Reach 2 with potential upstream bank and tributary sources of sediment in Geomorphically Similar Reach 1

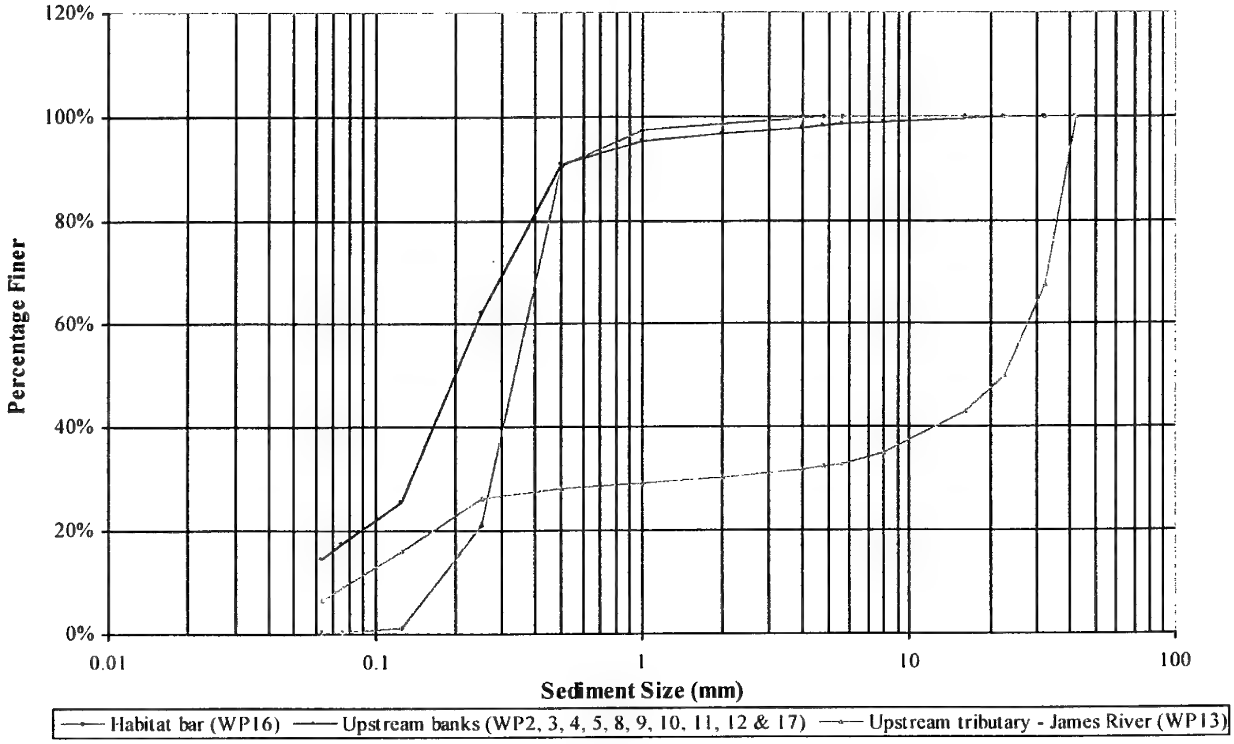

Figure A67: Gavins Point Reach - Comparison of non-habitat bar and island in Sampling Reach 2 with potential upstream bank and tributary sources of sediment in Geomorphically Similar Reach 1

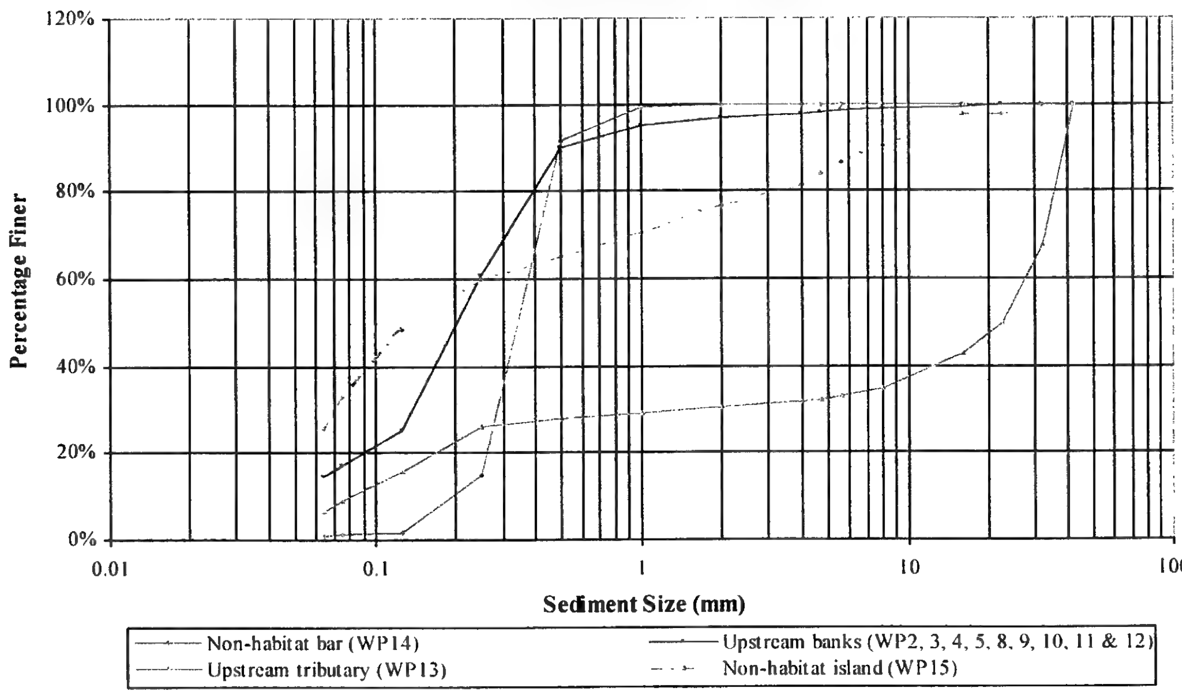

Figure A68: Gavins Point Reach - First comparison of habitat bar in Sampling Reach 2 with potential upstream bank and tributary sources of sediment

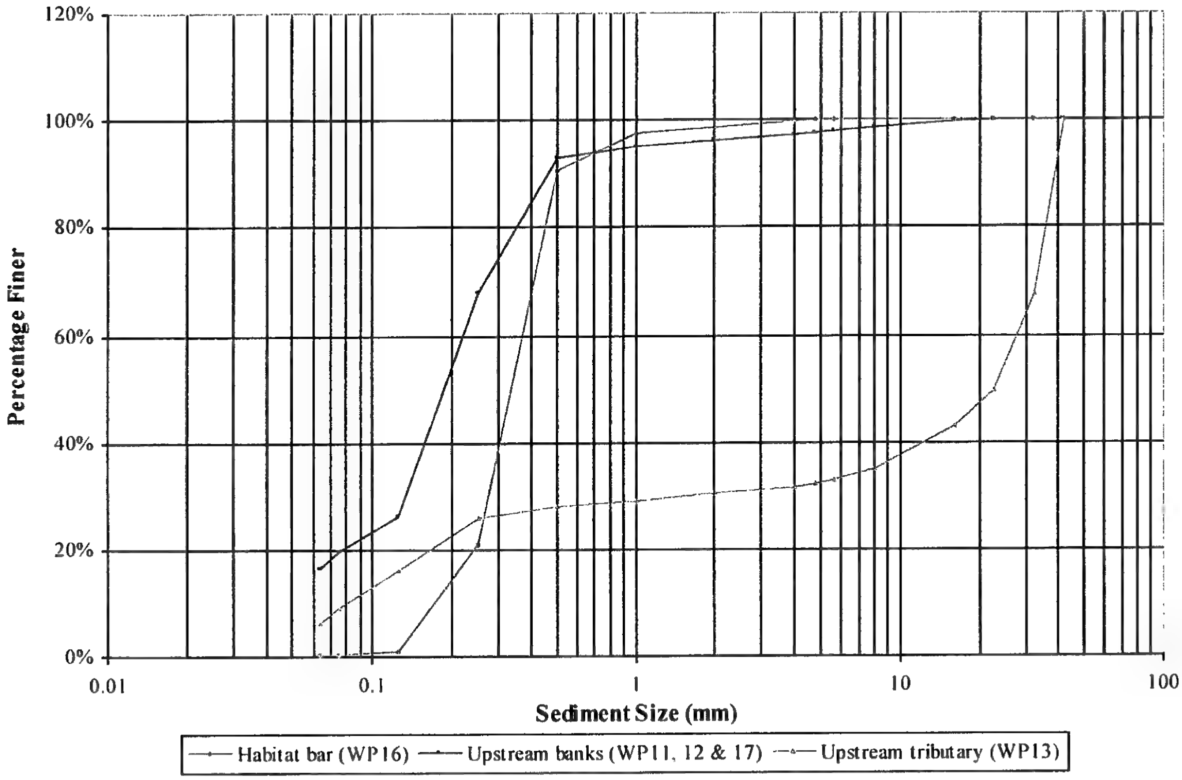

Figure A69: Gavins Point Reach - Second comparison of non-habitat bar and island in Sampling Reach 2 with a potential upstream tributary source of sediment

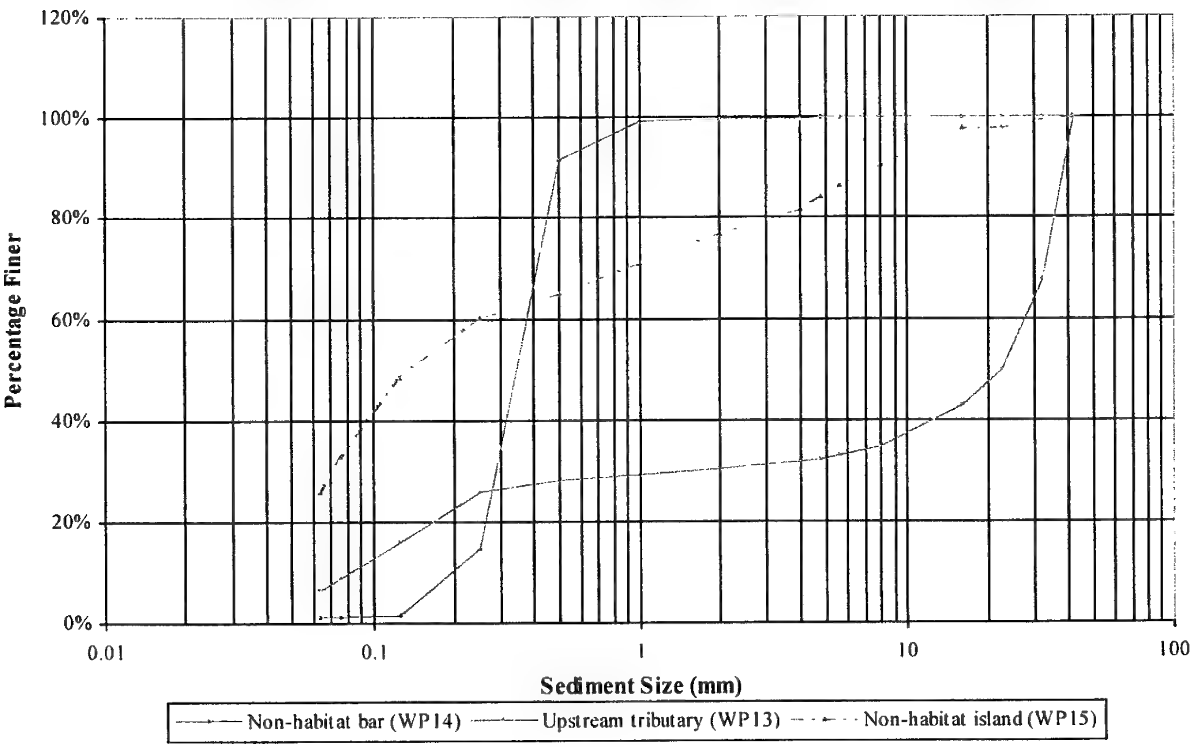

Figure A70: Gavins Point Reach - Comparison of habitat bar in Sampling Reach 3 with potential upstream bank sources of sediment in Geomorphically Similar Reach 2

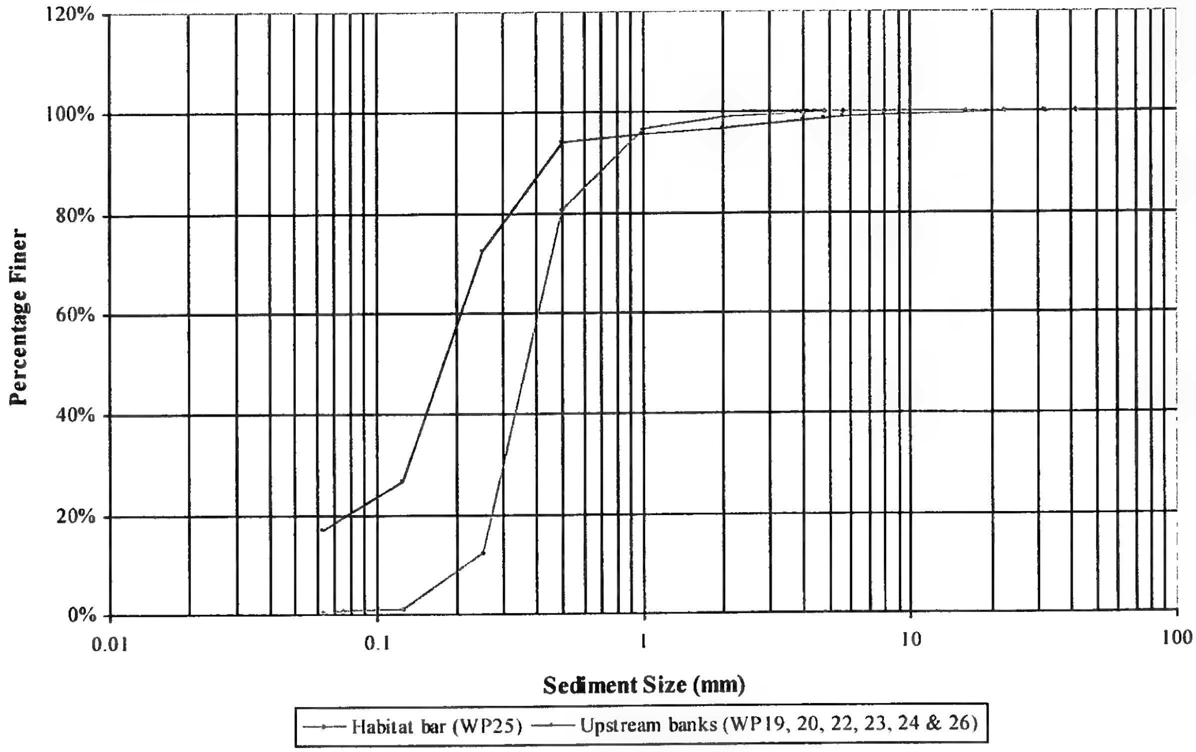

Figure A71: Gavins Point Reach - Comparison of non-habitat bar in Sampling Reach 3 with potential upstream bank sources of sediment in Geomorphically Similar Reach 2

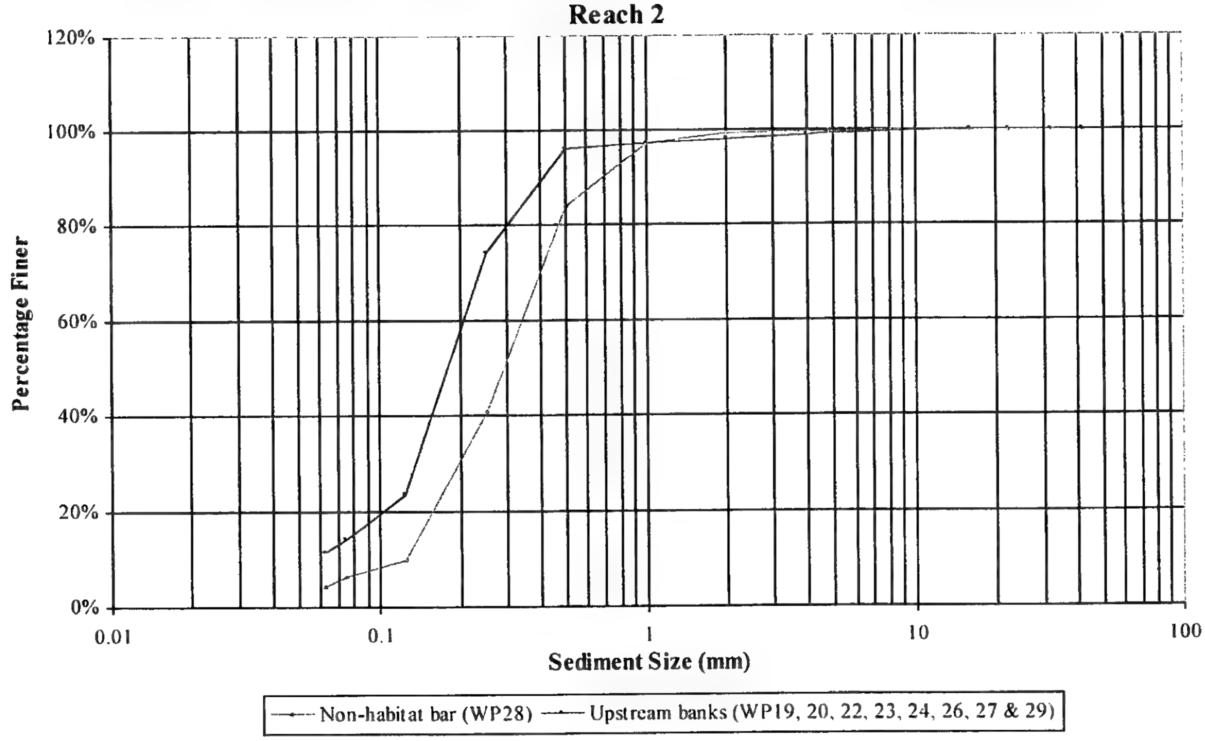

Figure A72: Gavins Point Reach - First comparison of habitat bar in Sampling Reach 3 with potential upstream bank sources of sediment

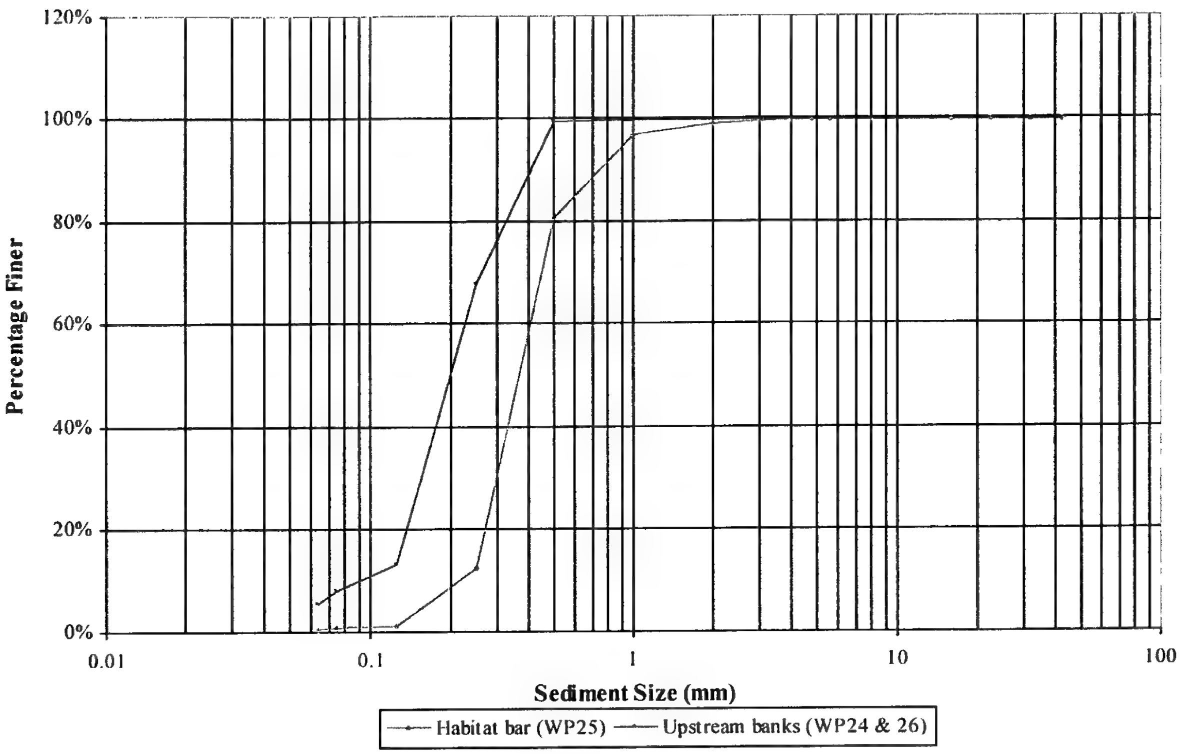

Figure A73: Gavins Point Reach - Second comparison of non-habitat bar in Sampling Reach 3 with potential upstream bank sources of sediment

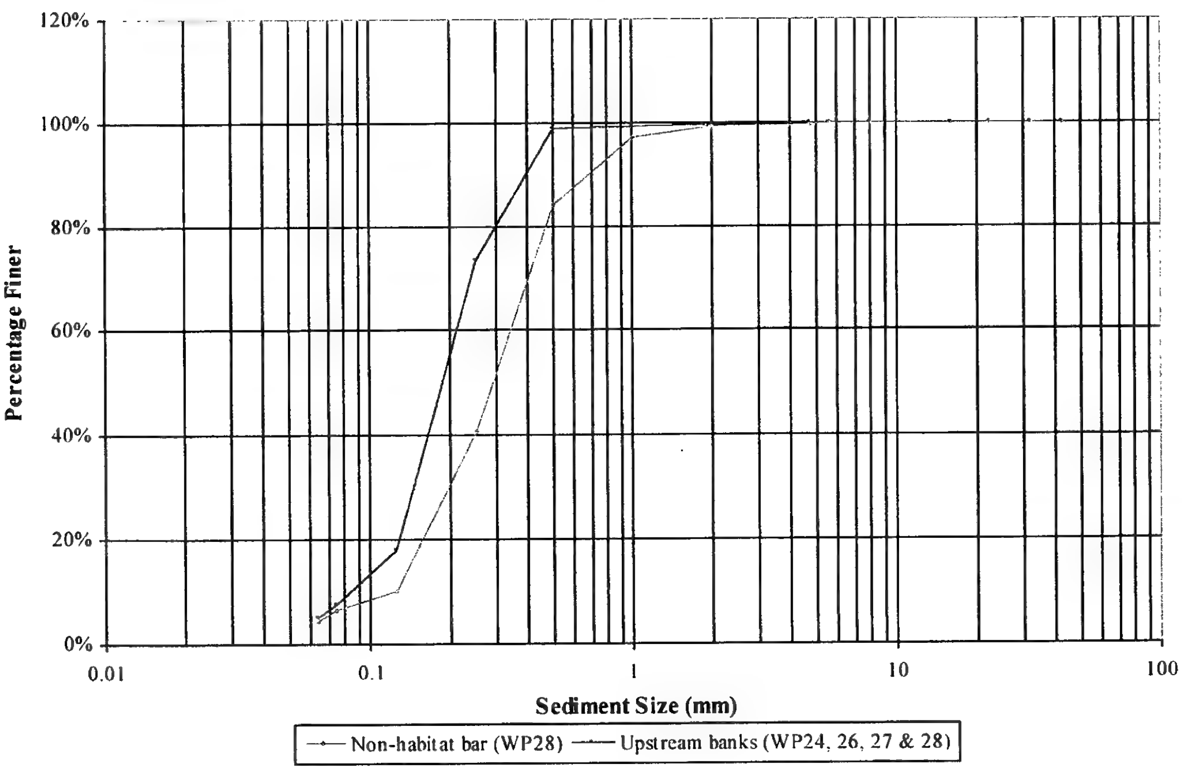

Figure A74: Gavins Point Reach - Comparison of non-habitat bar in Sampling Reach 4 with potential upstream bank sources of sediment in Geomorphically Similar Reach 2

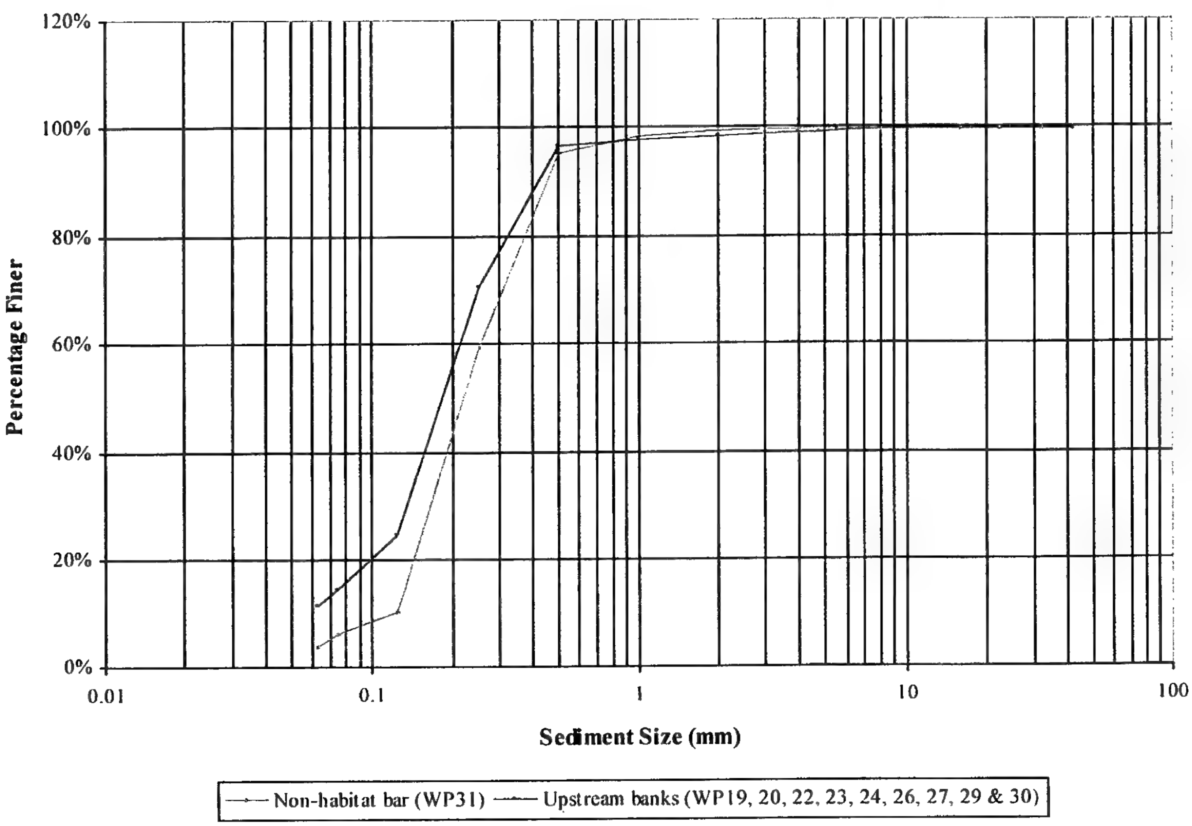

Figure A75: Gavins Point Reach - Comparison of non-habitat bars in Sampling Reach 5 with potential upstream bank sources of sediment in Geomorphically Similar Reaches 2 and 3

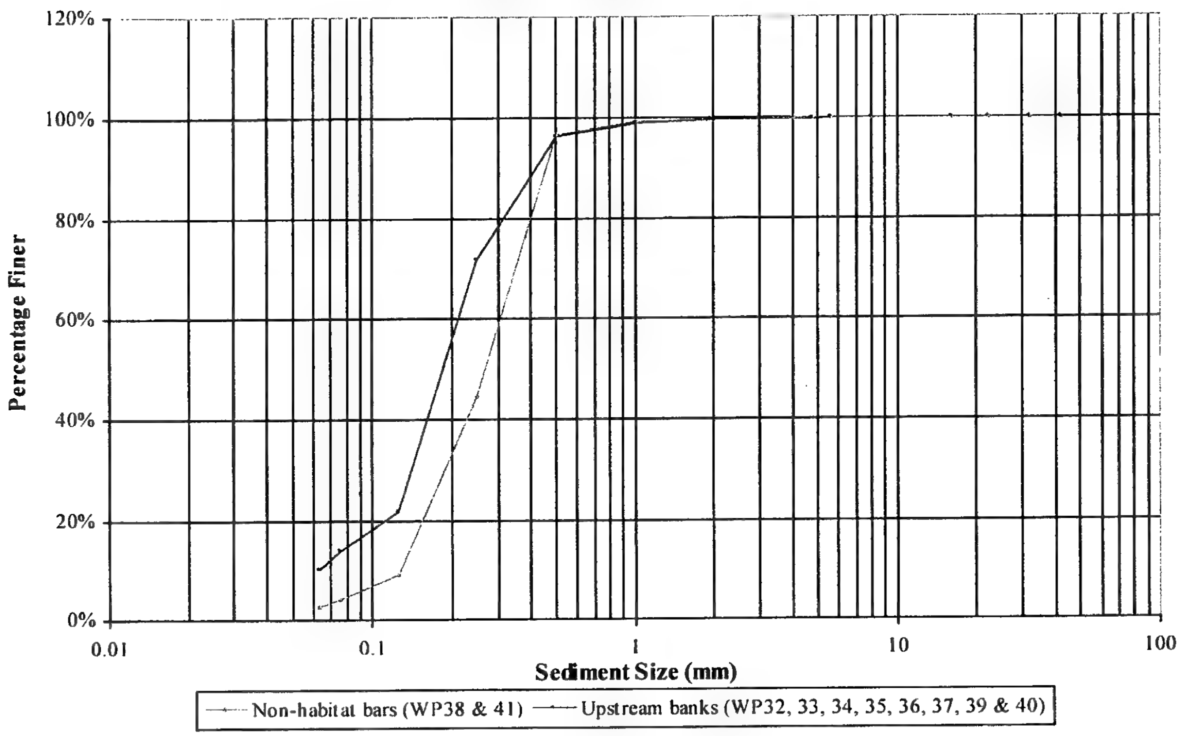

Figure A76: Gavins Point Reach - First comparison of non-habitat bar in Sampling Reach 5 with potential upstream bank sources of sediment

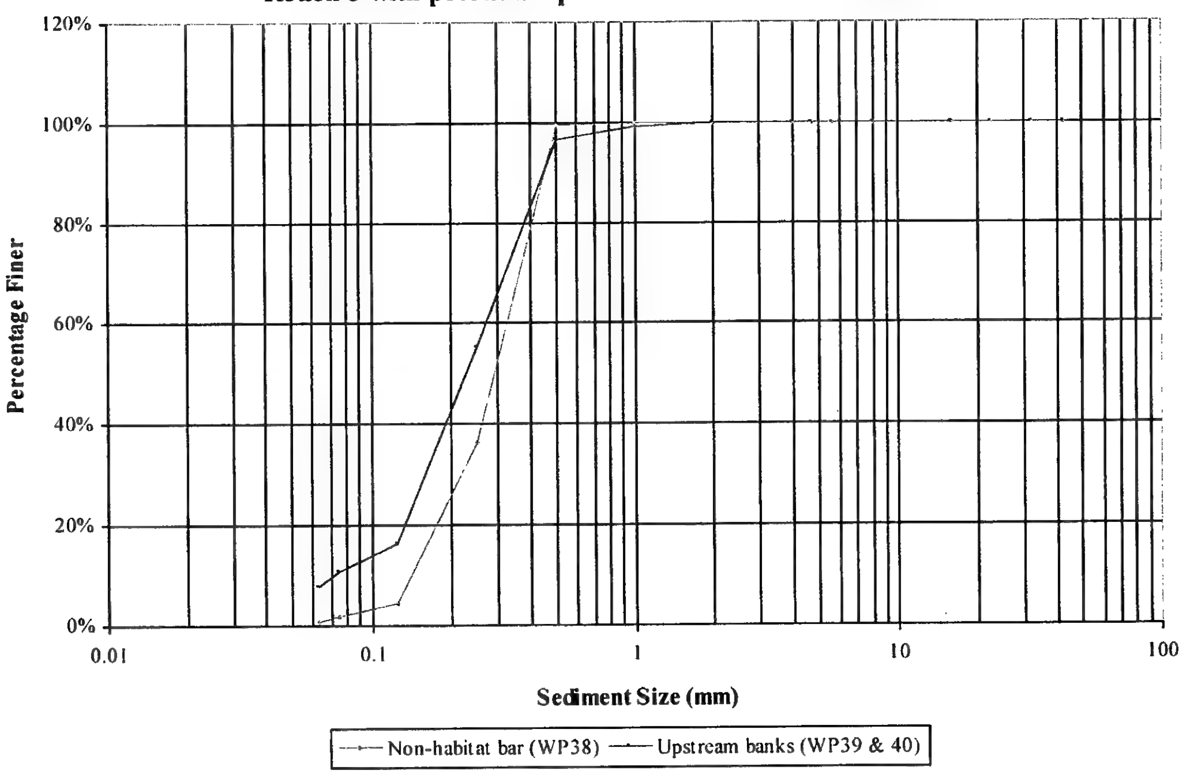

Figure A77: Gavins Point Reach - Second comparison of non-habitat bar in Sampling Reach 5 with potential upstream bank sources of sediment

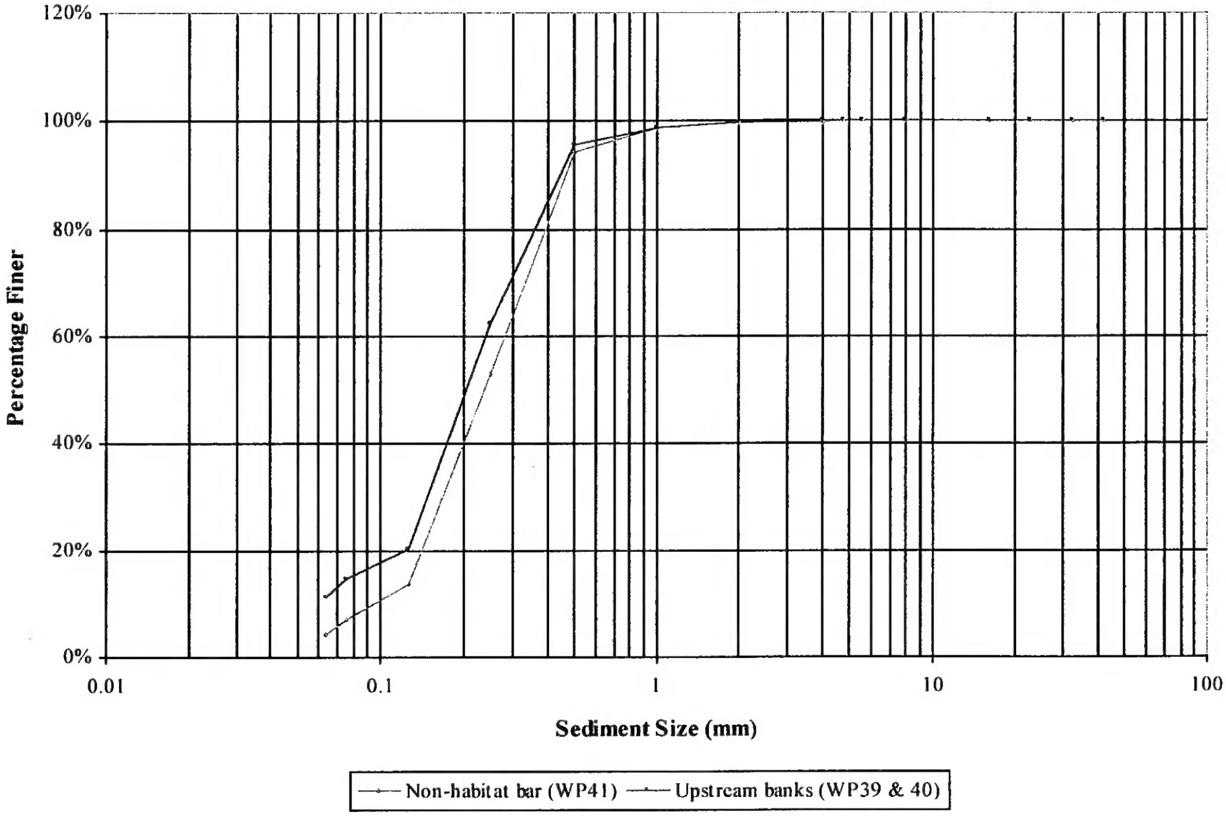

Figure B1: Fort Peck Reach - Comparison of the grain size distributions of habitat and non-habitat bars and islands

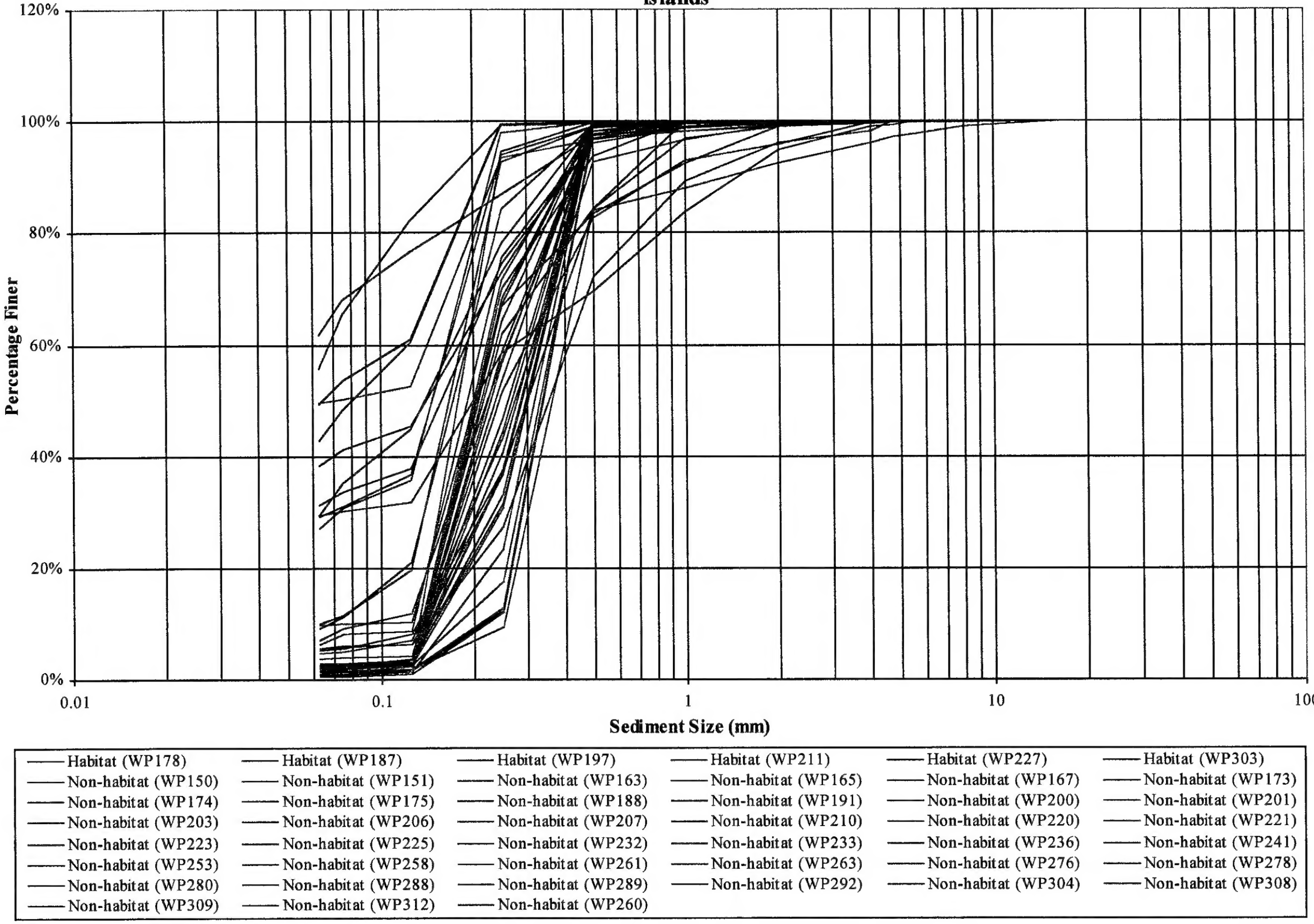

Figure B2: Garrison Reach - Comparison of the grain size distributions of habitat and non-habitat bars and islands

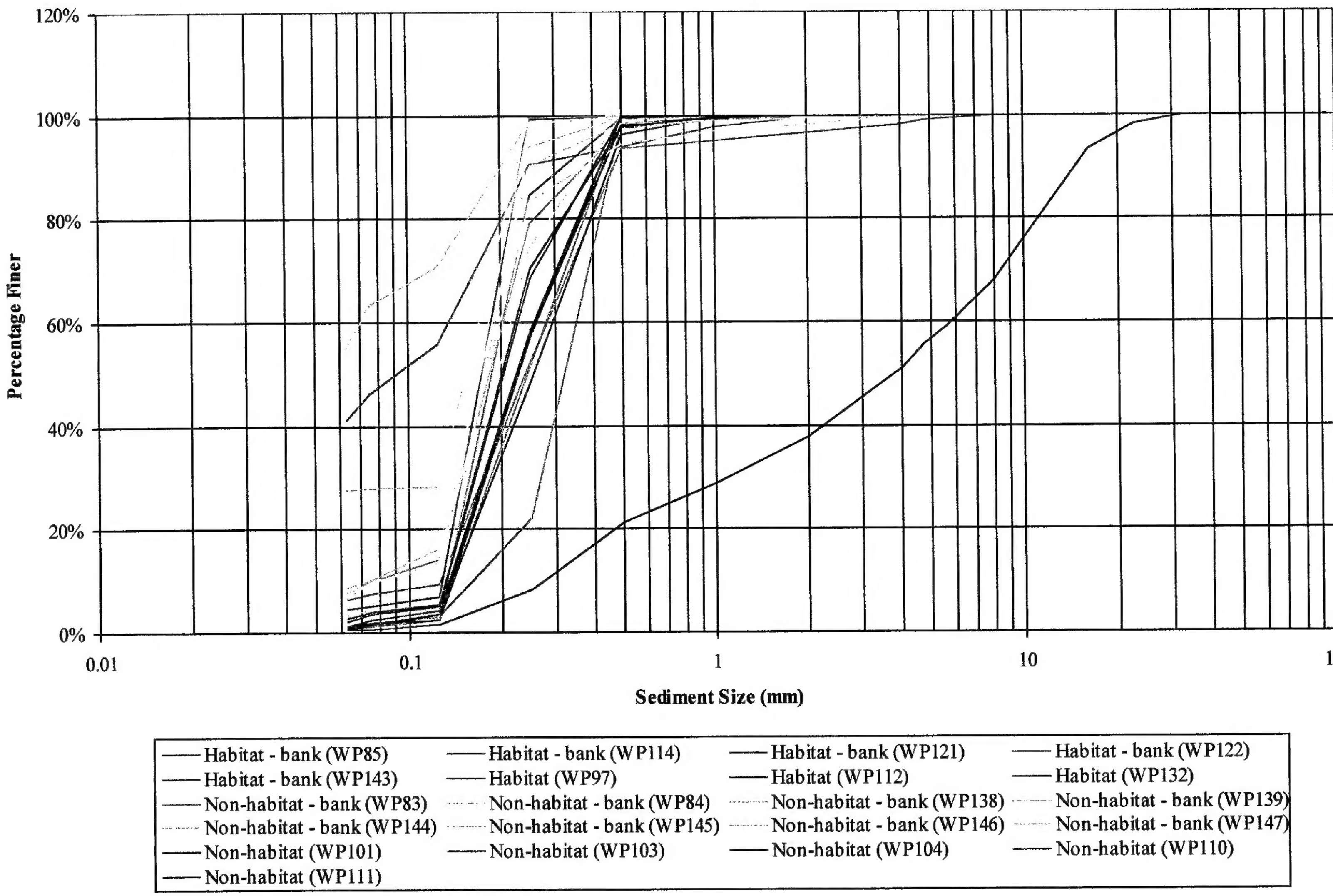

Figure B3: Fort Randall Reach - Comparison of the grain size distributions for habitat and non-habitat bars and islands

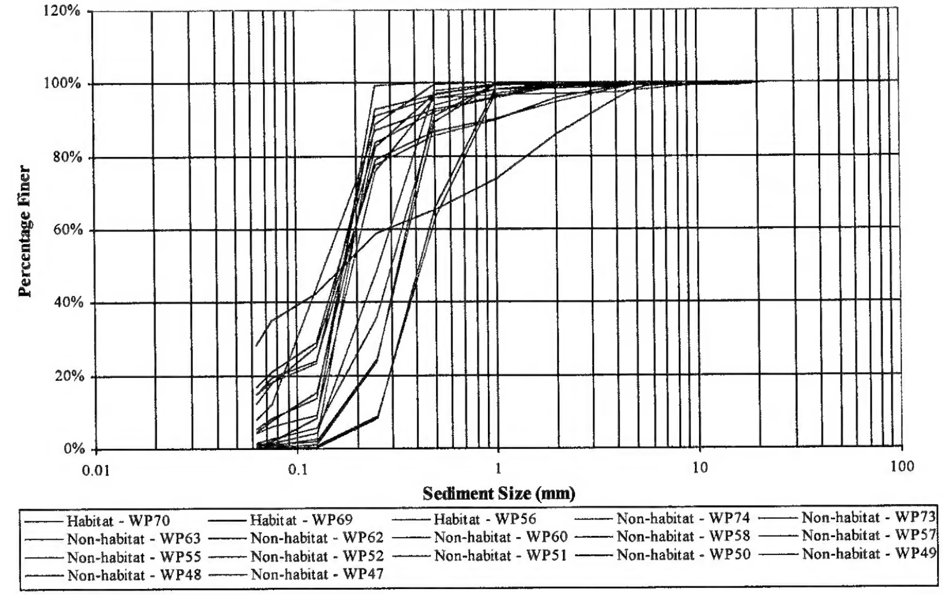

Figure B4: Gavins Point Reach - Comparison of the grain size distributions of habitat and non-habitat bars and islands